

1994

Enhancement of granulation and start-up in the anaerobic sequencing batch reactor

Randall Anthony Wirtz
Iowa State University

Follow this and additional works at: <https://lib.dr.iastate.edu/rtd>

 Part of the [Chemical Engineering Commons](#), and the [Civil Engineering Commons](#)

Recommended Citation

Wirtz, Randall Anthony, "Enhancement of granulation and start-up in the anaerobic sequencing batch reactor" (1994). *Retrospective Theses and Dissertations*. 10523.
<https://lib.dr.iastate.edu/rtd/10523>

This Dissertation is brought to you for free and open access by the Iowa State University Capstones, Theses and Dissertations at Iowa State University Digital Repository. It has been accepted for inclusion in Retrospective Theses and Dissertations by an authorized administrator of Iowa State University Digital Repository. For more information, please contact digirep@iastate.edu.

INFORMATION TO USERS

This manuscript has been reproduced from the microfilm master. UMI films the text directly from the original or copy submitted. Thus, some thesis and dissertation copies are in typewriter face, while others may be from any type of computer printer.

The quality of this reproduction is dependent upon the quality of the copy submitted. Broken or indistinct print, colored or poor quality illustrations and photographs, print bleedthrough, substandard margins, and improper alignment can adversely affect reproduction.

In the unlikely event that the author did not send UMI a complete manuscript and there are missing pages, these will be noted. Also, if unauthorized copyright material had to be removed, a note will indicate the deletion.

Oversize materials (e.g., maps, drawings, charts) are reproduced by sectioning the original, beginning at the upper left-hand corner and continuing from left to right in equal sections with small overlaps. Each original is also photographed in one exposure and is included in reduced form at the back of the book.

Photographs included in the original manuscript have been reproduced xerographically in this copy. Higher quality 6" x 9" black and white photographic prints are available for any photographs or illustrations appearing in this copy for an additional charge. Contact UMI directly to order.

U·M·I

University Microfilms International
A Bell & Howell Information Company
300 North Zeeb Road, Ann Arbor, MI 48106-1346 USA
313/761-4700 800/521-0600



Order Number 9503608

**Enhancement of granulation and start-up in the anaerobic
sequencing batch reactor**

Wirtz, Randall Anthony, Ph.D.

Iowa State University, 1994

U·M·I
300 N. Zeeb Rd.
Ann Arbor, MI 48106



Enhancement of granulation and start-up in the
anaerobic sequencing batch reactor

by

Randall Anthony Wirtz

A Dissertation Submitted to the
Graduate Faculty in Partial Fulfillment of the
Requirements for the Degree of
DOCTOR OF PHILOSOPHY

Department: Civil and Construction Engineering
Major: Civil Engineering (Environmental Engineering)

Approved:

Signature was redacted for privacy.

~~In Charge of Major Work~~

Signature was redacted for privacy.

For the Major Department

Signature was redacted for privacy.

For the Graduate College

Iowa State University
Ames, Iowa

1994

*To Kalla Kaye: thank you for your love, support,
encouragement, and patience.*

TABLE OF CONTENTS

	Page
LIST OF TABLES	vii
LIST OF FIGURES	xii
LIST OF ABBREVIATIONS	xvii
ACKNOWLEDGEMENTS	xx
INTRODUCTION	1
Background	1
Objectives and Scope	3
LITERATURE REVIEW	6
Origins of Life	6
Historical Perspectives of Anaerobic Bacteria	7
The Anaerobic Bacteria	10
Anaerobes and Oxygen	11
Physiology of Anaerobes	14
Hydrolytic/Fermentative Bacteria	17
Acetogenic Bacteria	20
Acetogenic Dehydrogenations	21
Acetogenic Hydrogenations	23
Methanogenic Bacteria	25
General Background	25
Biochemistry of Methanogens	28
Interplay among the Anaerobic Bacteria	41
Anaerobic Wastewater Treatment	44
Anaerobic versus Aerobic Treatment	44
Environmental/Operational Parameters in Anaerobic Treatment	46
Environmental Parameters	47
Operational Parameters	54
Early Research	58
High-Rate Anaerobic Treatment	60
The Anaerobic Contact Process	60
The Anaerobic Filter	61
The Hybrid Anaerobic Filter	64
The Expanded-Bed Anaerobic Reactor	65

The Upflow Anaerobic Sludge Blanket Reactor	68
The Anaerobic Sequencing Batch Reactor	70
The Phenomenon of Granulation	81
Theory of Bacterial Adhesion and Aggregation	81
General Characteristics of Granules in Anaerobic Systems	83
Granulation in the ASBR	85
First Report of Granulation	85
Further Studies with Granular Biomass in the ASBR	87
Granulation in the UASB and Expanded-Bed Processes	89
Granule Microbiology and Morphology	90
Granule Chemical Composition	95
Activity of Granular Biomass	97
Modeling the Granulation Process	100
Effect of Substrate and Temperature	104
Effect of Chemical Enhancement	106
Effect of Physical Enhancement	113
EXPERIMENTAL SETUP	115
Anaerobic Sequencing Batch Reactor Design	115
Gas/Foam Separation System	118
Biogas Recirculation System	119
Biogas Collection and Measurement System	121
Substrate Feed and Effluent Decant Systems	123
Coagulant Feed System	124
EXPERIMENTAL PROCEDURES	125
Substrate Feed Preparation	125
Biological Seeding of the ASBR	130
ASBR Start-up and Operation	132
ASBR Mixing	135
Granulation Enhancement	136
Attachment Matrices	136
Coagulant Addition	138
EXPERIMENTAL TESTING	141
Chemical Oxygen Demand	142
Volatile Fatty Acids	145
Effluent Suspended Solids	147
Mixed Liquor Suspended Solids	149
Hydrogen Ion Concentration	151
Alkalinity	151

Ammonia Concentration	153
Biogas Production and Composition	155
Automated Image Analysis	159
Specific Methanogenic Activity	160
Scanning and Transmission Electron Microscopy	163
Elemental Analysis of Biomass	164
RESULTS AND DISCUSSION	166
Sucrose Experiments	167
Control Study	167
Operational Performance	168
Solids and Granulation	170
Powdered Activated Carbon Enhancement Study	175
Operational Performance	175
Solids and Granulation	179
PAC Effect	181
Granular Activated Carbon Enhancement Study	181
Operational Performance	182
Solids and Granulation	185
GAC Effect	185
Garnet Enhancement Study	187
Operational Performance	187
Solids and Granulation	191
Garnet Effect	193
Silica Sand Enhancement Study	193
Cationic Polymer Enhancement Study	194
Operational Performance	198
Solids and Granulation	202
Cationic Polymer Effect	203
PolyDADM Enhancement Study	206
Operational Performance	206
Solids and Granulation	210
PolyDADM Effect	212
Ferric Chloride Enhancement Study	213
Operational Performance	213
Solids and Granulation	215
Ferric Chloride Effect	218
Beef/Glucose Experiments	218
Control Study	219
Operational Performance	219
Solids and Granulation	221

Cationic Polymer Enhancement Study	225
Operational Performance	225
Solids and Granulation	228
Cationic Polymer Effect	231
Summary of Enhancement Results	231
Specific Methanogenic Activity Experiments	234
Background and Theory	234
Specific Methanogenic Activity Results	237
Sucrose Tests	237
Acetate Tests	239
Electron Microscopy	242
Granule Surface	243
Granule Structure and Arrangement	249
Granule Elemental Analysis	254
CONCLUSIONS AND RECOMMENDATIONS	256
APPLICATIONS	261
Background	261
Economics	261
Cationic Polymer	262
PAC and GAC	263
REFERENCES	266
APPENDIX: EXPERIMENTAL DATA TABLES	285

LIST OF TABLES

	Page
Table 1. Examples of anaerobic respiration.	16
Table 2. Proton-reducing reactions by the acetogenic bacteria [14, 27, 143, 168].	23
Table 3. The methanogenic bacteria [12].	26
Table 4. Methanogenic substrates [12].	27
Table 5. Important reactions by the methanogens [12, 168].	27
Table 6. Effects of alkali and alkaline-earth metals on anaerobic digestion [95].	52
Table 7. Bacterial counts in granules from UASB reactors [31, 33].	91
Table 8. General composition of granules [31].	96
Table 9. Granule chemical composition [32, 33].	96
Table 10. Specific methanogenic activity of various biomass [32, 87].	99
Table 11. Substrates suitable for granule formation.	105
Table 12. Solubility products of metal salts [98].	111
Table 13. Sucrose feed mixture.	126
Table 14. Beef extract and glucose feed mixture.	127
Table 15. Composition of the beef extract soup base.	128
Table 16. Nutrient (NPK) solution.	128
Table 17. Trace metal solution.	129
Table 18. Ames municipal water analysis.	131
Table 19. ASBR cycle time for 48 and 24-hr HRTs.	133

Table 20.	Attachment matrices utilized for granulation enhancement.	138
Table 21.	Polymer characteristics.	139
Table 22.	Coagulants utilized for granulation enhancement.	139
Table 23.	Operational parameters routinely tested.	141
Table 24.	Reagents used in the COD test.	144
Table 25.	Gas chromatography analysis setup.	158
Table 26.	Elemental analysis of granules.	165
Table 27.	Start-up and granulation summary.	232
Table 28.	Summary of specific methanogenic activity experiments.	238
Table 29.	Chemical composition of granular and initial seed biomass.	255
Table 30.	COD data for the sucrose control test.	286
Table 31.	Biogas data for the sucrose control test.	287
Table 32.	Volatile acids data for the sucrose control test.	291
Table 33.	Particle size analysis for the sucrose control test.	291
Table 34.	Alkalinity and pH data for the sucrose control test.	292
Table 35.	Solids data for the sucrose control test.	293
Table 36.	COD data for the sucrose+PAC test.	294
Table 37.	Biogas data for the sucrose+PAC test.	296
Table 38.	Volatile acids data for the sucrose+PAC test.	303
Table 39.	Particle size analysis for the sucrose+PAC test.	304
Table 40.	Alkalinity and pH data for the sucrose+PAC test.	305

Table 41.	Solids data for the sucrose+PAC test.	307
Table 42.	COD data for the sucrose+GAC test.	309
Table 43.	Biogas data for the sucrose+GAC test.	310
Table 44.	Volatile acids data for the sucrose+GAC test.	315
Table 45.	Particle size analysis for the sucrose+GAC test.	315
Table 46.	Alkalinity and pH data for the sucrose+GAC test.	316
Table 47.	Solids data for the sucrose+GAC test.	317
Table 48.	COD data for the sucrose+garnet test.	318
Table 49.	Biogas data for the sucrose+garnet test.	319
Table 50.	Volatile acids data for the sucrose+garnet test.	323
Table 51.	Particle size analysis for the sucrose+garnet test.	323
Table 52.	Alkalinity and pH data for the sucrose+garnet test.	324
Table 53.	Solids data for the sucrose+garnet test.	325
Table 54.	COD data for the sucrose+sand test.	326
Table 55.	Biogas data for the sucrose+sand test.	327
Table 56.	Volatile acids data for the sucrose+sand test.	329
Table 57.	Alkalinity and pH data for the sucrose+sand test.	329
Table 58.	Solids data for the sucrose+sand test.	330
Table 59.	COD data for the sucrose+cationic polymer test.	331
Table 60.	Biogas data for the sucrose+cationic polymer test.	332
Table 61.	Volatile acids data for the sucrose+cationic polymer test.	336

Table 62.	Particle size analysis for the sucrose+cationic polymer test.	336
Table 63.	Alkalinity and pH data for the sucrose+cationic polymer test.	337
Table 64.	Solids data for the sucrose+cationic polymer test.	338
Table 65.	COD data for the sucrose+polyDADM test.	339
Table 66.	Biogas data for the sucrose+polyDADM test.	340
Table 67.	Volatile acids data for the sucrose+polyDADM test.	344
Table 68.	Particle size analysis for the sucrose+polyDADM test.	344
Table 69.	Alkalinity and pH data for the sucrose+polyDADM test.	345
Table 70.	Solids data for the sucrose+polyDADM test.	346
Table 71.	COD data for the sucrose+ferric chloride test.	347
Table 72.	Biogas data for the sucrose+ferric chloride test.	348
Table 73.	Volatile acids data for the sucrose+ferric chloride test.	350
Table 74.	Particle size analysis for the sucrose+ferric chloride test.	350
Table 75.	Alkalinity and pH data for the sucrose+ferric chloride test.	350
Table 76.	Solids data for the sucrose+ferric chloride test.	351
Table 77.	COD data for the beef/glucose control test.	352
Table 78.	Biogas data for the beef/glucose control test.	353
Table 79.	Volatile acids data for the beef/glucose control test.	356
Table 80.	Particle size analysis for the beef/glucose control test.	356
Table 81.	Alkalinity and pH data for the beef/glucose control test.	357
Table 82.	Solids data for the beef/glucose control test.	358

Table 83.	COD data for the beef/glucose control test.	359
Table 84.	Biogas data for the beef/glucose control test.	360
Table 85.	Volatile acids data for the beef/glucose control test.	363
Table 86.	Particle size analysis for the beef/glucose control test.	363
Table 87.	Alkalinity and pH data for the beef/glucose control test.	364
Table 88.	Solids data for the beef/glucose control test.	365
Table 89.	SMA test with the PAC-enhanced ASBR, day 158.	366
Table 90.	SMA test with the PAC-enhanced ASBR, day 169.	369
Table 91.	SMA test with the PAC-enhanced ASBR, day 228.	373
Table 92.	SMA test with the PAC-enhanced ASBR, day 283.	375
Table 93.	SMA test with the GAC-enhanced ASBR, day 65.	377
Table 94.	SMA test with the GAC-enhanced ASBR, day 76.	380
Table 95.	SMA test with the GAC-enhanced ASBR, day 93.	383
Table 96.	SMA test with the GAC-enhanced ASBR, day 113.	385
Table 97.	SMA test with the GAC-enhanced ASBR, day 135.	387
Table 98.	SMA test with the GAC-enhanced ASBR, day 190.	389
Table 99.	SMA test with the GAC-enhanced ASBR, day 195.	391
Table 100.	SMA test with the garnet-enhanced ASBR, day 83.	393

LIST OF FIGURES

	Page
Figure 1. Simplified pathways for polysaccharide fermentation by the acidogenic bacteria [14].	18
Figure 2. Biochemistry of carbon dioxide utilization by methanogens.	34
Figure 3. Biochemistry of methyl compound utilization by methanogens.	35
Figure 4. Biochemistry of acetate utilization by methanogens.	36
Figure 5. Substrate and intermediate product flow among anaerobic bacteria.	42
Figure 6. The anaerobic contact process.	61
Figure 7. The anaerobic filter.	62
Figure 8. The hybrid anaerobic filter.	65
Figure 9. The anaerobic expanded-bed (fluidized-bed) reactor.	66
Figure 10. The upflow anaerobic sludge blanket reactor.	69
Figure 11. The anaerobic sequencing batch reactor.	71
Figure 12. The phases of the anaerobic sequencing batch reactor.	72
Figure 13. Graphical representation of the Monod function.	74
Figure 14. Theoretical substrate concentration and F/M ratio over time in the ASBR.	75
Figure 15. Anaerobic sequencing batch reactor setup.	116
Figure 16. Schematic of the top cover of the ASBR.	117
Figure 17. ASBR biogas recirculation diffuser system.	120
Figure 18. COD removal for the sucrose control study.	169

Figure 19. Methane production for the sucrose control study.	169
Figure 20. Volatile acids data for the sucrose control study.	171
Figure 21. Alkalinity and pH data for the sucrose control study.	171
Figure 22. MLSS and SRT for the sucrose control study.	173
Figure 23. Average particle size data for the sucrose control study.	173
Figure 24. COD removal for the PAC-enhanced sucrose study.	177
Figure 25. Methane production for the PAC-enhanced sucrose study.	177
Figure 26. Volatile acids data for the PAC-enhanced sucrose study.	178
Figure 27. Alkalinity and pH data for the PAC-enhanced sucrose study.	178
Figure 28. MLSS and SRT for the PAC-enhanced sucrose study.	180
Figure 29. Average particle size data for the PAC-enhanced sucrose study.	180
Figure 30. COD removal for the GAC-enhanced sucrose study.	183
Figure 31. Methane production for the GAC-enhanced sucrose study.	183
Figure 32. Volatile acids data for the GAC-enhanced sucrose study.	184
Figure 33. Alkalinity and pH data for the GAC-enhanced sucrose study.	184
Figure 34. MLSS and SRT for the GAC-enhanced sucrose study.	186
Figure 35. Average particle size data for the GAC-enhanced sucrose study.	186
Figure 36. COD removal for the garnet-enhanced sucrose study.	189
Figure 37. Methane production for the garnet-enhanced sucrose study.	189
Figure 38. Volatile acids data for the garnet-enhanced sucrose study.	190
Figure 39. Alkalinity and pH data for the garnet-enhanced sucrose study.	190

Figure 40. MLSS and SRT for the garnet-enhanced sucrose study.	192
Figure 41. Average particle size data for the garnet-enhanced sucrose study.	192
Figure 42. COD removal for the silica sand-enhanced sucrose study.	195
Figure 43. Methane production for the silica sand-enhanced sucrose study.	195
Figure 44. Volatile acids data for the silica sand-enhanced sucrose study.	196
Figure 45. Alkalinity and pH data for the silica sand-enhanced sucrose study.	196
Figure 46. MLSS and SRT for the silica sand-enhanced sucrose study.	197
Figure 47. COD removal for the cationic polymer-enhanced sucrose study.	199
Figure 48. Methane production for the cationic polymer-enhanced sucrose study.	199
Figure 49. Volatile acids data for the cationic polymer-enhanced sucrose study.	200
Figure 50. Alkalinity and pH data for the cationic polymer-enhanced sucrose study.	200
Figure 51. MLSS and SRT for the cationic polymer-enhanced sucrose study.	204
Figure 52. Average particle size data for the cationic polymer-enhanced sucrose study.	204
Figure 53. COD removal for the polyDADM-enhanced sucrose study.	207
Figure 54. Methane production for the polyDADM-enhanced sucrose study.	207
Figure 55. Volatile acids data for the polyDADM-enhanced sucrose study.	208
Figure 56. Alkalinity and pH data for the polyDADM-enhanced sucrose study.	208
Figure 57. MLSS and SRT for the polyDADM-enhanced sucrose study.	211
Figure 58. Average particle size data for the polyDADM-enhanced sucrose study.	211
Figure 59. COD removal for the ferric chloride-enhanced sucrose study.	214

Figure 60. Methane production for the ferric chloride-enhanced sucrose study.	214
Figure 61. Volatile acids data for the ferric chloride-enhanced sucrose study.	216
Figure 62. Alkalinity and pH data for the ferric chloride-enhanced sucrose study.	216
Figure 63. MLSS and SRT for the ferric chloride-enhanced sucrose study.	217
Figure 64. Average particle size data for the ferric chloride-enhanced sucrose study.	217
Figure 65. COD removal for the beef/glucose control study.	220
Figure 66. Methane production for the beef/glucose control study.	220
Figure 67. Volatile acids data for the beef/glucose control study.	222
Figure 68. Alkalinity and pH data for the beef/glucose control study.	222
Figure 69. MLSS and SRT for the beef/glucose control study.	223
Figure 70. Average particle size data for the beef/glucose control study.	223
Figure 71. COD removal for the cationic polymer-enhanced beef/glucose study.	226
Figure 72. Methane production for the cationic polymer-enhanced beef/glucose study.	226
Figure 73. Volatile acids data for the cationic polymer-enhanced beef/glucose study.	227
Figure 74. Alkalinity and pH data for the cationic polymer-enhanced beef/glucose study.	227
Figure 75. MLSS and SRT for the cationic polymer-enhanced beef/glucose study.	229
Figure 76. Average particle size data for the cationic polymer-enhanced beef/glucose study.	229
Figure 77. Idealized granule exhibiting a layered structure.	235

Figure 78. Idealized granule exhibiting a non-layered structure.	235
Figure 79. SMA over the course of the GAC enhanced study.	240
Figure 80. SMA comparison of granular and non-granular biomass.	240
Figure 81. SMA comparison of GAC granules fed acetate and sucrose.	241
Figure 82. SEM images of granule surface.	245
Figure 83. SEM images of granule surface.	248
Figure 84. Images of granule interior.	252

LIST OF ABBREVIATIONS

AIA	automated image analysis
ALK	alkalinity (bicarbonate)
B	boron
BOD	biochemical oxygen demand
BOD ₅	five-day biochemical oxygen demand
BOD _u	ultimate biochemical oxygen demand
Ca	calcium
COD	chemical oxygen demand
cm	centimeters
Cu	copper
°C	degrees Celsius
FAS	ferrous ammonium sulfate
Fe	iron
ft	feet
g	gram
gal	gallon
GC	gas chromatography
g/L/day	grams per liter per day
hr	hour

hrs	hours
HRT	hydraulic retention time
in	inch or inches
k	specific substrate removal rate
k_m	maximum specific substrate removal rate
K	potassium
K_m	half saturation constant
K_s	solubility product
kg	kilogram
L	liter
lb	pound
m	meters
M	biomass concentration
Mg	magnesium
mgal	million gallons
mgd	million gallons per day
mg/L	milligram per liter
min	minute
mL	milliliter
MLSS	mixed liquor suspended solids
mm	millimeters

mol	mole or moles
Na	sodium
Ni	nickel
OLR	organic loading rate
P	phosphorous
S	sulfur or sulfide
SEM	scanning electron microscopy
SRT	solids retention time
SS	suspended solids
STP	standard temperature and pressure
TEM	transition electron microscopy
TKN	total Kjeldahl nitrogen
TOC	total organic carbon
TS	total solids
TSS	total suspended solids
VA	volatile acids
VFA	volatile fatty acids
VS	volatile solids
VSS	volatile suspended solids
Zn	zinc
μ	specific biomass growth rate or 10^{-6}

ACKNOWLEDGMENTS

The author wishes to express his sincere thanks and appreciation to the many individuals who had a part in this research. The list of course begins with my major professor, Dr. Richard R. Dague. Dr. Dague provided knowledge, guidance and assistance (not to mention the funding) throughout this research and served as an extremely positive role model for all of the graduate students that worked for him. He is a credit to his profession.

The graduate committee members also are to be thanked for their time and their input into this research. The members are Dr. T. Al Austin, CCE; Dr. LaDon C. Jones, CCE; Dr. Robert E. Andrews, MIPM; and Dr. James A. Thomas, B&B. A special note of thanks also goes out to Dr. Say-Kee Ong, who filled in for Dr. Jones for the final dissertation defense.

The author would also like to thank the secretaries of the Civil and Construction Engineering Department. Without their dedication little would get accomplished in a reasonable amount of time.

The Analytical Laboratory Service and the Bessey Microscopy Facility at Iowa State University performed much of the technical and analytical work for this research. Thank you for your service, promptness, and professional insight.

Finally, the author would like to thank the U.S. Department of Agriculture for their financial support of this research through the Iowa Biotechnology Byproducts Consortium.

INTRODUCTION

Background

High-rate anaerobic wastewater treatment has been practiced in varying degrees for approximately forty years. The first systems were developed in the 1950s and were suspended-growth reactors with sludge recycle to maintain the solids retention time (SRT) independent of the liquid detention time. Attached-growth reactors were developed in the 1960s and maintained long SRTs by physically holding the biomass inside the reactor with rock or plastic media. Several variations of these systems were developed in the 1970s and 1980s and are described later in this document. One of the most recent developments in high-rate anaerobic waste treatment is the anaerobic sequencing batch reactor (ASBR), developed by Richard R. Dague and graduate students at Iowa State University. A U.S. Patent (No. 5,185,079) for the ASBR was issued in February of 1993.

Initial experiments with the ASBR were conducted in 1989 and 1990 by Habben [47] and Pidaparti [113]. Since that time, the ASBR has been applied at laboratory scale to several different wastewaters, including starch wastewaters, furfuraldehyde wastewaters, landfill leachate, and swine wastes. Additionally, fundamental research has been conducted on a number of operational aspects of the ASBR. Past research has been aimed at defining appropriate height to width ratios, mixing requirements, and operating temperatures. Further details concerning ASBR research is found in the literature review section of this document. The ASBR has also been demonstrated at pilot-scale for a starch wastewater. A full-scale ASBR for treating swine waste is in the design phase.

Traditionally, one of the most significant problems with anaerobic processes has been start-up. The systems have normally taken several months (sometimes years) to reach stable operation at their design conditions. This has been one of the biggest deterrents to using anaerobic treatment processes at full-scale. Industries, with little knowledge of anaerobic systems, felt that the systems were slow and took a long time to treat wastes to the desired degree. What was really the case, however, was that the microbes were "slow growing," which is not equivalent to "slow working." Although anaerobic systems may require relatively long start-up times due to their slow growth, once a sufficient consortia of bacteria has been established, the specific removal rates (per unit biomass) are comparable to those of aerobic systems.

Because of the requirement for long start-up periods before design load could be realized in anaerobic systems (including the ASBR), it was decided to study methods of operation that would decrease the start-up period. By decreasing the start-up time, industry may be more apt to consider anaerobic treatment systems for their wastewater, since most industries do not want to wait a half year or longer to have a treatment system be effective.

It was also decided to study the phenomenon of granulation in the ASBR, which was first observed by Sung and Dague [142] in a previous study. Granulation is the agglomeration of individual biomass particles into discrete pellets, or granules, some of which may grow to 5 or 6 mm in diameter. Granular biomass has several distinct advantages over flocculent (dispersed) biomass, which will be detailed later. The

important point is that the development of a granular biomass is beneficial to the treatment system, and the earlier it is developed the better. It was expected that optimum conditions for these two objectives, a short start-up period and the formation of granules, would be identical. That is, when granulation developed, the system would be mature and able to handle higher chemical oxygen demand (COD) loading rates. Conversely, when the system became mature enough to handle higher loading rates, it would be in the process of granulation. These statements were hypotheses, and definitely not absolute. Therefore, it was decided to study these phenomena in some detail.

Objectives and Scope

The selected topic for study was a fairly broad, ill-defined area for two main reasons: (1) there are many factors which contribute to the start-up efficiency and granulation of biomass in anaerobic reactors, and (2) granulation had only been observed once in an ASBR, and it required approximately 300 days to achieve granulation in that study [145]. Obviously, if granulation was to be studied in any detail, it would have to be achieved in a much shorter time frame than 10 months, otherwise the researcher would be limited to only a few experiments (or research would have to be conducted for several years). Therefore, it was necessary to find methods of enhancing granulation in the ASBR during the start-up period. Considerable research has been conducted on granulation in another type of anaerobic reactor, the upflow anaerobic sludge blanket reactor (UASB). The UASB is a continuous-flow reactor, the kinetics of which are completely different

from the ASBR, which is a batch system. However, it was plausible that the mechanisms involved in granulation in the reactor may also play a role in granulation in the ASBR. Parameters studied for granulation enhancement in the UASB included chemical enhancement (calcium, phosphorous, others), hydraulic and COD loading rates, and physical enhancement with a biomass support matrix, such as granular activated carbon. Each of these topics are covered in more detail in the literature review section.

Physical enhancement of granulation in the ASBR was selected for this study. Attachment matrices, including powdered activated carbon (PAC), granular activated carbon (GAC), garnet, and silica sand were chosen as representative matrices to which biomass may attach and form granules. It was later decided to also study the effect of adding polymers to the ASBR to aid in granulation of the biomass. Three coagulants were selected based on preliminary data: a cationic polymer, a polyquaternary amine polymer, and ferric chloride. The use of these enhancement materials is described in the procedures section of this document.

The objectives of this study were many, but the main goals were as shown below:

1. Start-up of the ASBR from municipal digester biosolids was desired within a minimum time, consistent with the following:
 - a. the biomass settles well with a relatively clear supernatant
 - b. the hydraulic retention time (HRT) of the ASBR is 1 day or less
 - c. the COD loading rate is 4 g COD/L of reactor/day or more

- d. COD removal efficiency of the ASBR is 70% or better, and is increasing
 - e. methane production correlates well with COD reduction
2. Granulation of the biomass, starting from municipal digester biosolids, was desired within a minimum time, consistent with the following:
 - a. the biomass settles well with a relatively clear supernatant
 - b. the overall average biomass particle size is increasing over time
 - c. the ASBR is able to handle increasingly higher COD loading rates with little decrease in COD removal efficiency
 3. It was desired to achieve maximum COD loading rates (greater than 10 g COD/L/day) with 90% + COD removal efficiency; previously maximum loading rates achieved in the ASBR were in the range of 10 to 12 g/L/day.
 4. It was desired to characterize the granular biomass with the following criteria and methods:
 - a. average particle size
 - b. specific methanogenic activity
 - c. scanning and transmission electron microscopy for granule morphology

Many other minor points were studied in varying degrees of detail and are presented in the results section.

LITERATURE REVIEW

Origins of Life

Anaerobic biochemical processes have been around since the origins of life. It is believed that the first organisms that could actually be defined as "living" originated in the seas and oceans of the young earth, some 3.5 billion years ago [12]. Since earth's atmosphere had little, if any, free oxygen at that time, the first microorganisms were necessarily anaerobic. It is generally believed that the first simple microorganisms carried out simple fermentations for energy production. The next likely step in evolution was probably the development of more complicated membrane systems and electron transport systems, which would have enabled the microorganisms to carry out electron transport phosphorylation. This step would have enabled the microbes to utilize a large variety of non-fermentable organic compounds as electron donors, and also would have made possible lithotrophy, which is energy production from the oxidation of inorganic compounds [12].

One probable early electron acceptor utilized by microbes was CO_2 , which could have been reduced to methane by early methanogenic bacteria. Another group of bacteria which developed early were the sulfate-reducing bacteria, which used sulfate as an electron acceptor to produce hydrogen sulfide (H_2S). The sulfate reducers possess a primitive type of cytochrome, which may have eventually lead to the more complex cytochromes of the phototrophic microorganisms. The first phototrophs were anaerobic, using light energy for

ATP (adenosine triphosphate) synthesis, similarly to the modern-day purple or green sulfur bacteria [12].

The next advancement of life was probably the evolution of a second light reaction, which made photosynthesis possible. These organisms were capable of using the energy of light to power the incorporation of CO₂ into cell material, using water as an electron donor and producing free molecular oxygen as a byproduct. Over time, the oxidizing atmosphere that we observe today was formed and a much wider range of organisms began to evolve. The relatively new aerobic organisms were capable of using oxygen as a terminal electron acceptor, which greatly increased the amount of energy that could be obtained from a given biochemical oxidation of organic compounds over that which can be obtained anaerobically [12]. The obvious advantages of aerobic life lead to the significant evolution of aerobic organisms. However, anaerobic life was maintained in the reducing environments of earth, such as in the muds of swamps and seas and many other places.

Historical Perspectives of Anaerobic Bacteria

The discovery of anaerobic life is generally credited to Pasteur in 1861, when he observed that living cells existed that could grow without air, and were actually inhibited by free molecular oxygen [23, 59]. Pasteur was the first to discover that many species were able to carry out aerobic respiration when free oxygen was present, and switch to anaerobic fermentative pathways in the absence of free oxygen (facultative anaerobes). He also was the first to study strict anaerobic organisms, namely a butyric acid-fermenting

species of the genus *Clostridium*. He deduced their toxicity to oxygen by microscopic observations of the microbes in a drop of fluid. Pasteur noted that the cells near the surface of the droplet quickly lost their motility, while the microbes within the droplet maintained their motility for a considerable period of time. By passing air through a reaction vessel containing active *Clostridia* undergoing fermentation reactions, he observed a dramatic decrease in the fermentation rate, which further strengthened his belief that oxygen was toxic to these organisms. Pasteur also noted the extremely low growth yields of yeast fermenting sugar anaerobically, as compared to the same yeast growing aerobically on the sugar [23].

Further study of anaerobic bacteria was difficult due to the difficulty of culturing them at the time. Anaerobic techniques were not yet available, and it took another century until reliable and effective anaerobic culturing techniques were devised. Although the study of all anaerobic bacteria was difficult during the late 1800s and through the first half of the twentieth century, study of the methanogens was especially difficult owing to their extreme inhibition by low free oxygen levels. A brief history of methanogenic bacteria study follows here.

The earliest observation of methanogenic anaerobic life reportedly dates back to 1776 when Volta described methane evolution from aquatic muds, although at that point scientists were not aware that the gas was biological in its origin (much less anaerobic). A century later, Béchamp demonstrated that the gas had a biological origin using an ethanol-based media inoculated with rabbit feces [168]. During the latter 1800s and early 1900s,

researchers deduced that methane was produced through the anaerobic breakdown of relatively simple organic compounds, although cultures of the bacteria were not produced owing to the limited anaerobic culturing techniques available at the time.

It was not until the 1930s that Barker reported the isolation of the first "pure" culture of a methanogen, *Methanobacillus omelianskii*. This organism was reported to oxidize ethanol to acetate, with the simultaneous reduction of bicarbonate to methane. It was later (1967) proven by Bryant et al. that *M. omelianskii* actually consisted of the association of two different microorganisms: an "S" organisms which oxidized ethanol to acetate and hydrogen ions, and *Methanobacterium bryantii*, which utilized the hydrogen produced by the "S" organisms to reduce bicarbonate to methane [168].

The first truly pure methanogenic culture is credited to Schnell in 1947, whose cultures were able to convert the methyl groups of acetate and methanol to methane. In the 1960s, Hungate introduced a new method for cultivating strict anaerobes, termed the "roll-tube" technique. This contribution significantly advanced studies on methanogenesis and allowed researchers to isolate several new species of methanogens in pure culture. It was not until after these advancements that scientists discovered the unique biochemistry involved in methanogenesis. These advances ultimately lead to the separation of methanogens (and several other bacteria groups) into their own phylogenic kingdom, the Archaeobacteria. The newly revised "ancestral tree" now consists of Eukaryota, Eubacteria (other prokaryotes), and Archaeobacteria [12, 168].

In 1976, there were nine confirmed species of methanogens. By 1984, the number of methanogenic species had increased to 29. As of 1991, there were 51 species of methanogens isolated in pure culture [12, 168]. It is thus evident that the methanogens are a fairly diverse group of bacteria, although they all share common biochemical pathways and a relatively limited substrate requirement. Methanogenic bacteria are discussed in more detail in a later section.

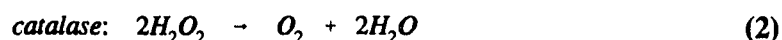
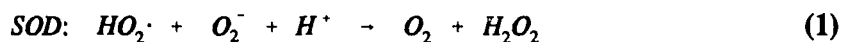
The Anaerobic Bacteria

In a well-engineered anaerobic system employed to produce methane from a relatively complex substrate (e.g., proteins, carbohydrates, and fats), a consortium of bacteria develops, with the end-products from one group of bacteria used as the substrates of another group of bacteria. In broad terms, there are generally three major groups of bacteria present in anaerobic systems that produce methane: the fermentative/hydrolytic acidogenic bacteria, the acetogenic bacteria, and the methanogenic bacteria. Each of these groups also contain additional subgroups, with distinct differences in specific substrates used and products formed. Other anaerobic organisms are also normally present in varying degrees, depending on the environmental and nutritional conditions of the system. These other anaerobes include the sulfate-reducing bacteria and several others. For the purpose of this document, discussion will be focused on the three major groups of bacteria, with some discussion on the competing reactions of the other bacteria.

The following discussion is centered on the main characteristics and biochemical mechanisms of the major groups of anaerobic bacteria involved in methane production. The first two sections discuss anaerobic bacteria in a general manner, and the next three sections discuss each group individually. The final section is devoted to discussion of the interplay among the three groups.

Anaerobes and Oxygen

The ability to grow in the absence of free oxygen, along with the sensitivity to its presence, was the characteristic feature of obligate anaerobes observed by Pasteur when he first describe them in 1861. However, since that time it has been realized that the extreme sensitivity to oxygen displayed by obligate anaerobes is relative in that oxygen is potentially toxic to all living cells [59]. The toxicity of oxygen is not due to molecular oxygen, O_2 , but rather to the reduced forms of oxygen, including hydrogen peroxide (H_2O_2), superoxide anion (O_2^-), and hydroxy radical ($\bullet OH$). In most aerobic organisms, superoxide dismutase (SOD) converts the superoxide anion to oxygen and hydrogen peroxide, and catalase converts hydrogen peroxide to oxygen and water by the following equations:



The hydroxy radical, however, has such high reaction rates that it can react with crucial macromolecules within the cell and disrupt normal cell function in both aerobes and anaerobes. A typical reaction with a molecule, RH, is shown below in Equation 3. The radical formed in the reaction will then undergo a reaction with another molecule, and propagation of subsequent reactions will continue until the radical is quenched by an appropriate molecule, such as vitamin E in lipid membranes.



In normally growing aerobic organisms, the built-in defense mechanisms of catalase, SOD, and quenching molecules are sufficient to protect the cells from reduced forms of oxygen [59, 172].

Strict anaerobic bacteria, by definition, are always inhibited or killed by the presence of free oxygen. There is, however, a wide range of oxygen resistance in anaerobic bacteria. Additionally, it has been shown that many anaerobes contain defense systems similar to the aerobic bacteria, including catalase and SOD, and that some oxygen-tolerant species do not contain these seemingly essential enzymes. It is, therefore, inconclusive at this point as to the mechanisms involved in oxygen toxicity in anaerobic organisms. Several factors important in the degree of toxicity to oxygen are outlined below [59].

- (1) *Rate of oxygen reduction.* This relates to the rate of oxygen uptake. As more oxygen is taken up and reduced, the probability of damage to the cell increases. Therefore, the phase of growth is important in that rapidly growing cells will take up more oxygen, which increases chances of toxicity. An extreme example of this are spores of clostridia, whose dormancy makes them oxygen stable, even though growing cells of clostridia are oxygen sensitive.
- (2) *Mode of oxygen reduction.* Some anaerobes have been shown to reduce molecular oxygen to water by NADH oxidases. Although this is a detoxification mechanism, the NADH consumed in the reaction is no longer available for reduction of metabolites.
- (3) *Protective enzymes.* Many anaerobes possess catalase, SOD, and other peroxidases which maintain low levels of O_2^- and H_2O_2 .
- (4) *Cell composition.* Probable macromolecules damaged by oxygen include DNA, cell membranes, and ferredoxins. Differences in composition or concentration of reactive sites on these molecules could explain the differences in oxygen sensitivity of various anaerobes.
- (5) *Repair mechanisms.* It has been shown in *Escherichia coli* that decreased resistance to hydrogen peroxide is correlated with a loss of DNA repair systems, rather than with a loss of SOD or catalase. It is possible that this observation could be extended to strict anaerobic bacteria as well.

Physiology of Anaerobes

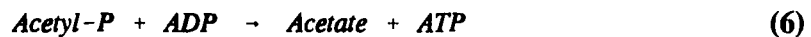
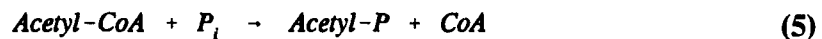
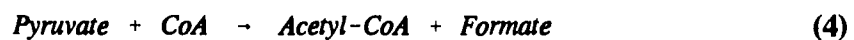
The physiology and other characteristics of several groups of anaerobic bacteria are presented in more detail in the following sections. However, a general overview of anaerobic bacteria physiology is instructive at this point. As earlier stated, anaerobic bacteria are sensitive to oxygen, and are unable to use free molecular oxygen for respiratory or metabolic purposes. Rather, anaerobic bacteria use less oxidized compounds as final electron acceptors, which results in less energy produced per mass of substrate oxidized as compared to aerobic oxidation of the same substrate [59]. In general, anaerobes use three main mechanisms to produce energy for biosynthetic purposes: photophosphorylation, substrate-level phosphorylation (fermentation), and electron transport linked phosphorylation (anaerobic respiration). In aerobic organisms, the energy production mechanism is termed oxidative phosphorylation. Oxidative phosphorylation produces a high yield of ATP because the reducing equivalent produced (NADH) is oxidized by oxygen as the final electron acceptor, which represents a redox potential change of 1130 mV. Anaerobes cannot use oxygen for their final electron acceptor, and, therefore, must use a less-oxidized electron acceptor to oxidize NADH. The change in redox potential of this reaction is normally considerably less than 1130 mV, and so represents a lower energy production than in oxidative phosphorylation, everything else being equal.

Photophosphorylation is not described here because the nature of this study did not include phototrophic organisms. In substrate-level phosphorylation (SLP), or

fermentation, electrons are removed from an organic substrate (electron donor) [59]. The removed electrons are transferred to an intermediate, often NAD^+ , and subsequently to another organic compound (electron acceptor), which becomes the end-product of the fermentation. ATP production in fermentations arises from two distinct enzymatic processes [59]:

- (1) Formation of an energy-rich covalently bonded intermediate by a dehydrogenase or lyase reaction. The intermediates formed are acid anhydrides or thioesters.
- (2) Transfer of the energy from the intermediate to ATP by a kinase reaction.

These steps are demonstrated in their basic form in Equations 4, 5, and 6, for the fermentation of pyruvate to acetate with the subsequent production of ATP. The first reaction involves the enzyme pyruvate:formate lyase which yields acetyl-CoA and formate, and the second reaction involves a kinase reaction to form acetate and ATP. P_i in the equations represents inorganic phosphorous, and CoA is coenzyme A.



Electron transport linked phosphorylation (anaerobic respiration), on the other hand, involves electron transport chains similar in function to those of aerobic organisms, with the most significant difference being the final electron acceptor. As noted, oxygen is used by aerobic organisms, whereas less oxidized molecules are used in anaerobic respiration. Examples of terminal electron acceptors in anaerobic respiration are listed in Table 1.

Table 1. Examples of anaerobic respiration.

Microorganisms	Final electron acceptor	Product
Methanogens	CO ₂	CH ₄
Sulfate reducers	SO ₄ ²⁻	H ₂ S
Other anaerobes	NO ₃ ⁻	NO ₂ ⁻
	NO ₂ ⁻	N ₂
	fumarate	succinate

The electron carrier molecules involved in anaerobic respiration are similar to those utilized by aerobic oxidative phosphorylation [59]. Electrons are removed from the substrate molecule (oxidation of substrate) by a reducing compound, such as NAD⁺ (to form NADH + H⁺), and the electrons are transported in succession to a number of electron carrier molecules until they finally reach the terminal electron acceptor, such as nitrate, sulfate, or carbon dioxide. ATP production is accomplished by a number of ATPases through proton gradients and other mechanisms [12, 59, 172].

Hydrolytic/Fermentative Bacteria

In the majority of cases, the incoming substrate to an anaerobic reactor (or into an anaerobic ecosystem) is fairly complex, consisting of polymers, such as polysaccharides, proteins, lipids, nucleic acids, or a combination of these. The hydrolytic/fermentative bacteria attack these compounds with extracellular hydrolases, thus converting them to monomers and oligomers of the respective starting compounds. The organisms then convert these smaller molecules to organic acids, alcohols, CO_2 , H_2 , NH_4^+ , and S^{2-} [14, 20a, 27, 45, 47, 50, 137, 168]. These bacteria, hereafter referred to as the acidogens, include obligate anaerobes such as *Clostridium*, *Bacteroides*, and *Ruminococcus* species and facultative anaerobes such as *E. coli* and *Bacillus* sp [27]. There are many other bacteria species and genera that facilitate the hydrolysis of complex polymeric substrates, but a comprehensive review of this subject is beyond the scope of this document.

The various mechanisms and pathways utilized by the acidogenic bacteria are complex and diverse. However, the basic overall mechanisms are hydrolysis of complex molecules, transport of some of the products of hydrolysis into the cell, and fermentation of the transported products to organic acids and other compounds previously mentioned. A simplified diagram of the overall fermentation of a polysaccharide to end-products is presented in Figure 1 [14].

In a well-functioning anaerobic system in which the hydrogen produced by the acidogens (Figure 1) is removed by the other groups of bacteria (see following sections), the products resulting from the work of the acidogenic bacteria will be in a relatively

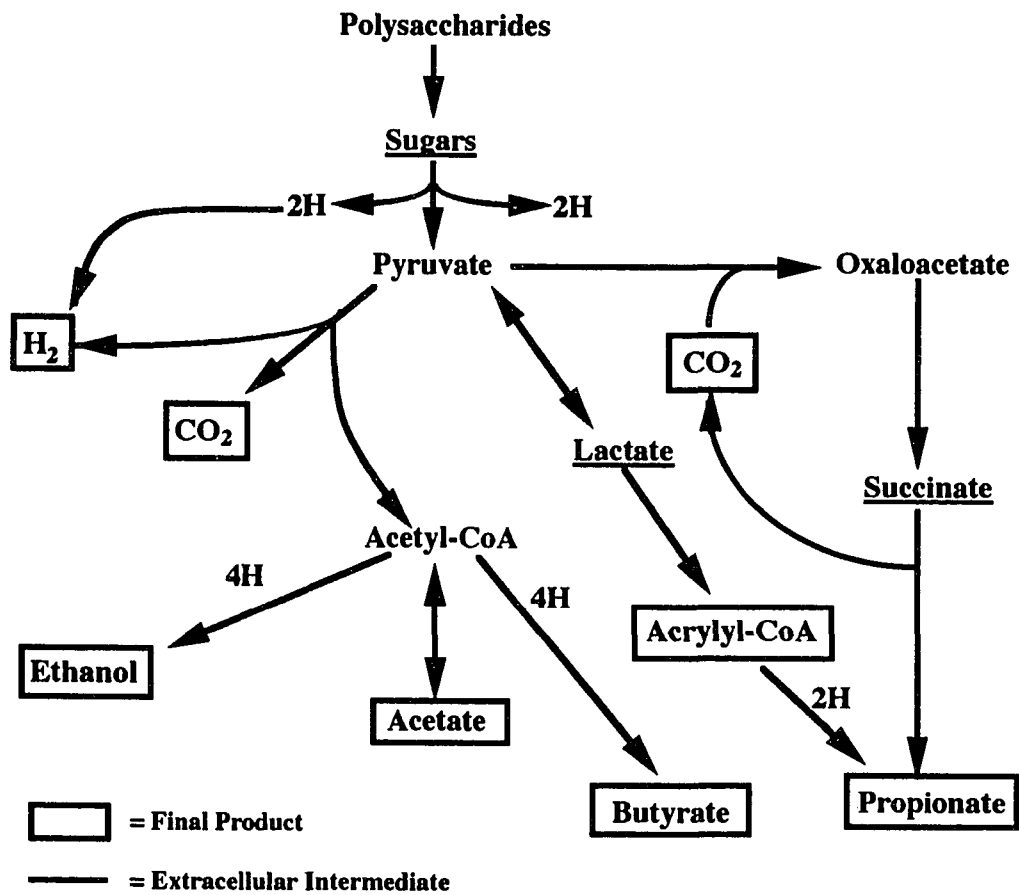


Figure 1. Simplified pathways for polysaccharide fermentation by the acidogenic bacteria [14].

oxidized state, such as acetate and CO_2 . However, in systems that are not removing the hydrogen produced by the acidogens, more reduced products will be formed, such as propionate, butyrate, valerate, ethanol, and lactate. This phenomenon can mainly be attributed to the mechanism involved in removing hydrogen ions from the system by various hydrogenases to form H_2 . The result of H_2 formation is the oxidation of NADH to NAD^+ , which is then available to oxidize other compounds. If most of the NAD^+/NADH molecules are in the reduced form, the oxidizing power of the microbes is limited, resulting in more reduced products of fermentation [14, 143].

Lipids and proteins are also hydrolyzed by the acidogens to their respective end-products [14, 168]. Lipids are generally split into free fatty acids, glycerol, galactose, and other non-fatty acid products. The non-fatty acid moieties are fermented to additional acids, CO_2 , and H_2 . Unsaturated fatty acids are hydrogenated to form saturated fatty acids. Protein degradation by acidogenic bacteria is an important component of the nitrogen and sulfur cycles in nature. Proteolytic bacteria hydrolyse peptide bonds in protein, resulting in the production of peptides and free amino acids. Fermentation of the hydrolysis products results in the production of short-chain and branched-chain fatty acids, ammonia, and CO_2 .

Factors important for proper function of the acidogenic bacteria include, pH, and substrate solubility and complexity [14, 20a, 168]. Temperature is also important, but since most studies on hydrolysis have been conducted with rumen bacteria at ambient rumen temperatures, the effect of temperature is not well documented. The solubility of

the substrate is important in that more soluble molecules generally undergo hydrolysis more readily than do insoluble polymeric molecules. However, in the case of proteins this is not always the case. The number of sulfide bridges in a protein is also important, and, generally, as the number of S-S bridges increases, the rate of hydrolysis decreases [168]. The pH of the system has been shown to have a significant effect on the rate of hydrolysis and solubilization of large polymers. Although the optimum pH for many enzymes (cell-free) is 5 or lower, the optimum pH for most hydrolytic bacteria is considerable higher, in the range of 5.6 to 8 [20a, 137, 168]. Chyi [20a] conducted anaerobic solubilization experiments with cellulose and determined an optimum pH (based on percent cellulose solubilized) of between 5.2 and 6.0. Further observations determined that the rate limiting step in the overall conversion of cellulose to volatile acids was the hydrolysis step, and not the fermentation reactions.

Acetogenic Bacteria

The acetogenic bacteria are a diverse group of bacteria responsible for conversion of the products from the acidogens (fatty acids, alcohols, CO₂, H₂, ethanol, etc.) into acetate, CO₂, and H₂, plus other minor compounds [14, 27, 93, 168]. In general terms, there are two basic groups of anaerobic acetogenic bacteria [168]: the proton-reducing acetogens which use hydrogen as their electron sink to form molecular hydrogen (acetogenic dehydrogenation), and the hydrogen-utilizing acetogens which use hydrogen in the reduction of more oxidized molecules to form acetate (acetogenic hydrogenation).

These groups of bacteria, although sharing acetate as the end-product of their metabolic reactions, are obviously distinct from each other in their overall effect on anaerobic digestion, and are, therefore, discussed separately in the following paragraphs.

Acetogenic Dehydrogenations

Dehydrogenations are those reactions in which the oxidation of the substrate is coupled to the reduction of protons, resulting in the formation of molecular hydrogen (H_2) and acetate (or a longer-chain fatty acid [168]). These reactions are growth supporting for two major groups of bacteria: the fermentative bacteria, which produce hydrogen and acetate, propionate, butyrate, and longer-chain fatty acids (previously discussed); and the obligate proton-reducing bacteria, which produce hydrogen and acetate as major end-products.

One major distinction between these two groups of bacteria is that the fermentative bacteria, in addition to reducing protons, are also able to use other organic electron sinks. Although the energy available from a given reaction is maximal when hydrogen is the final electron acceptor, the fermentative bacteria are still able to derive energy and grow when other electron sinks are utilized by forming more reduced end-products (e.g., propionate rather than acetate production). However, the obligate-proton reducing bacteria are limited to the use of protons as an electron acceptor. Therefore, the removal of hydrogen from the environment by other bacterial groups is essential to maintain thermodynamically favorable conditions for the obligate proton reducers [168]. Numerous recent studies have examined

the thermodynamics of such reactions [27, 47, 151, 168, 170], especially those of the propionate and butyrate oxidizing bacteria. It has been found that the energy produced by such reactions yield a very small amount of energy, and at elevated hydrogen partial pressures, acetate and hydrogen production from propionate and butyrate are endogonic. It is generally believed that hydrogen partial pressures must be maintained below 10^{-3} and 10^{-4} atm, respectively, for exothermic oxidation of butyrate and propionate [14, 27, 45, 52, 54, 63, 107, 143, 164].

Anaerobic oxidation of propionate results in the production of acetate, CO_2 , and H_2 , and, under standard conditions, this reaction has a standard free energy of approximately +76 kJ/reaction (Table 2). Under normal digester operation, exothermic propionate oxidation is only possible when hydrogen partial pressures are extremely low, as previously stated [14, 47, 91, 168]. Common propionate-oxidizing bacteria found in anaerobic systems include *Syntrophobacter wolinii* and *Desulfobulbus propionicus* [63]. One mole of butyrate is oxidized to two moles of acetate plus hydrogen and has a standard free energy of 53 kJ/reaction (thought to be a β -oxidation reaction). Bacteria capable of butyrate oxidation to acetate include *Syntrophomonas wolfei*, *Syntrophomonas sapovorans*, and *Clostridium bryantii* [143].

Other substrates for the obligate proton reducing bacteria include higher-chained fatty acids, benzoate, and ethanol. The higher chained-fatty acids are thought to be degraded to acetate (plus propionate for some) through β -oxidation. *S. wolfei* has been determined to be one of the most active higher-chain fatty acid oxidizing organisms in

many anaerobic digesters. Ethanol is degraded to acetate through a number of biochemical mechanisms, but in conjunction with proton reduction, the main products are acetate and hydrogen (*Pelobacter carbinolicus*). Benzoate is oxidized by *Syntrophus buswellii* to acetate and hydrogen (Table 2) [168].

Table 2. Proton-reducing reactions by the acetogenic bacteria [14, 27, 143, 168].

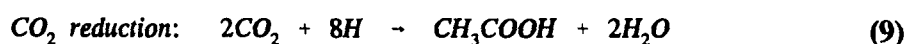
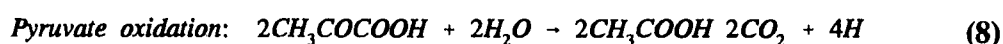
Reaction	ΔG° (kJ/reaction) standard conditions	$\Delta G'$ (kJ/reaction) digester conditions ^a
$\text{CH}_3\text{CH}_2\text{COO}^- + 3\text{H}_2\text{O} \rightarrow \text{CH}_3\text{COO}^- + \text{HCO}_3^- + \text{H}^+ + 3\text{H}_2$	+76.1	-8.4
$\text{CH}_3\text{CH}_2\text{CH}_2\text{COO}^- + 2\text{H}_2\text{O} \rightarrow 2\text{CH}_3\text{COO}^- + \text{H}^+ + 2\text{H}_2$	+48.1	-29.2
$\text{CH}_3\text{CH}_2\text{OH} + \text{H}_2\text{O} \rightarrow \text{CH}_3\text{COO}^- + \text{H}^+ + 2\text{H}_2$	+9.6	-49.8
$\text{C}_7\text{H}_5\text{O}_2^- + 7\text{H}_2\text{O} \rightarrow 3\text{CH}_3\text{COO}^- + \text{HCO}_3^- + 3\text{H}^+ + 3\text{H}_2$	+53.0	-10.7

^a Digester conditions: $\text{H}_2 = 10^{-3}$ atm, $\text{CO}_2 = 0.5$ atm, $\text{HCO}_3^- = 60$ mM, pH = 7.0, propionate = butyrate = ethanol = acetate = 1 mM, temperature = 37°C.

Acetogenic Hydrogenations

This group of bacteria (generally referred to as the homoacetogens) includes mixotrophs that utilize carbon dioxide as the terminal electron acceptor to produce acetate as the sole product of anaerobic respiration. Many of the homoacetogenic bacteria are capable of deriving the electrons necessary for the reduction of CO_2 to acetate from hydrogen, C-1 compounds, or multi-carbon compounds (hexoses, lactate, glycerate) [12, 86, 168]. A subgroup of the homoacetogens are some of the hydrolytic/fermentative bacteria previously described, which ferment glucose and other hexoses to acetate. Many of the bacteria of this group are metabolically quite adaptable to changing environments.

These bacteria, such as *Acetobacterium woodii*, *Clostridium thermoaceticum*, and *Clostridium acetium*, can grow both organotrophically and lithotrophically by carrying out homoacetogenic fermentations of hexoses or through the reduction of CO₂ with H₂ to produce acetate, respectively [12, 168]. The glucose fermentations of the homoacetogenic bacteria utilize the glycolytic pathway to produce two moles of pyruvate and 2 moles of NADH (equivalent of 4H) from one mole of glucose. The two pyruvates are then oxidized to two acetates and two CO₂, with the loss of 4 additional protons. These two molecules of CO₂ are then reduced using the eight electrons produced from glycolysis and pyruvate oxidation to produce acetate. Starting from one mole of glucose, three moles of acetate are produced by the reactions shown in Equations 7-10 (charges and cofactors are left out of some reactions for brevity).



Many of the homoacetogens are capable of performing all of the reactions 7 through 10, whereas others utilize only one or two of these pathways. Other bacteria can use lactate, glycerate, and other substrates in homoacetogenic reactions [12, 168].

Methanogenic Bacteria

General Background

The methanogenic bacteria utilize the end-products of the other groups of bacteria (mainly acetate, H_2 , and CO_2) to form methane and CO_2 . It is in this stage of anaerobic decomposition that waste stabilization actually occurs to a significant extent [23, 93, 168]. The energy contained (COD-basis) in the methane produced by the methanogens normally represents over 90% of the initial "energy" of the original substrate, and, therefore, represents the majority of stabilization of a given organic waste material. Without the methanogens, organic matter could not be anaerobically stabilized to any significant extent. Additionally, the large concentrations of acids produced in the first two stages of anaerobic degradation tend to lower the pH of the system, which would inhibit the methanogens and other bacterial consortia if they were not stabilized to methane and carbon dioxide.

As previously stated, there were 51 reported species of methanogens as of 1991, grouped into eighteen genera and eight major groups. Table 3 lists the known methanogens along with their characteristics. The substrates utilized by methanogenic bacteria consist of approximately 10 simple compounds, and are listed in Table 4 below.

The most common biochemical reactions involved in methane formation are listed in Table 5. Of the substrates listed, $H_2 + CO_2$ and formate are utilized by the most methanogenic bacterial species. However, it has been estimated that approximately 70% of the methane formed in nature is via acetate cleavage to methane and carbon dioxide. This is despite the fact that the free energy associated with acetate cleavage is extremely

Table 3. The methanogenic bacteria [12].

Genus	Morphology	Number of species	Substrates for methanogenesis
GROUP I			
<i>Methanobacterium</i>	long rods	8	H ₂ + CO ₂ , formate
<i>Methanobrevibacter</i>	short rods	3	H ₂ + CO ₂ , formate
GROUP II			
<i>Methanothermus</i>	rods	2	H ₂ + CO ₂ , reduces S ⁰
GROUP III			
<i>Methanococcus</i>	irregular cocci	5	H ₂ + CO ₂ , formate
GROUP IV			
<i>Methanomicrobium</i>	short rods	2	H ₂ + CO ₂ , formate
<i>Methanogenium</i>	irregular cocci	3	H ₂ + CO ₂ , formate
<i>Methanospirillum</i>	spirilla	1	H ₂ + CO ₂ , formate
GROUP V			
<i>Methanoplanus</i>	plate-shaped	2	H ₂ + CO ₂ , formate
<i>Methanosphaera</i>	cocci	1	CH ₃ OH + H ₂
GROUP VI			
<i>Methanosarcina</i>	irregular cocci	5	H ₂ + CO ₂ , formate, CH ₃ OH, methylamines, acetate
<i>Methanolobus</i>	irregular cocci	3	CH ₃ OH, methylamines
<i>Methanoculleus</i>	irregular cocci	4	H ₂ + CO ₂ , formate, alcohols
<i>Methanococcoides</i>	irregular cocci	1	CH ₃ OH, methylamines
<i>Methanohalophilus</i>	irregular cocci	3	CH ₃ OH, methylamines, methyl sulfides
<i>Methanotherix</i>	rods/filaments	3	acetate
<i>Methanosaeta</i>	rods/filaments	1	acetate
GROUP VII			
<i>Methanopyrus</i>	rods in chains	1	H ₂ + CO ₂
GROUP VIII			
<i>Methanocorpusculum</i>	irregular cocci	3	H ₂ + CO ₂ , formate, alcohols

Table 4. Methanogenic substrates [12].

CO₂-Type Substrates	
Carbon dioxide + hydrogen	CO ₂ + H ₂
Formate	HCOOH
Carbon monoxide	CO
Methyl Substrates	
Methanol	CH ₃ OH
Methylamine	CH ₃ NH ₃ ⁺
Dimethylamine	(CH ₃) ₂ NH ₂ ⁺
Trimethylamine	(CH ₃) ₃ NH ⁺
Methylmercaptan	CH ₃ SH
Dimethylsulfide	(CH ₃) ₂ S
Acetoclastic Substrate	
Acetate	CH ₃ COOH

Table 5. Important reactions by methanogens [12, 168].

Reaction	ΔG (kJ/mol CH ₄)
1. $4\text{H}_2 + \text{CO}_2 \rightarrow \text{CH}_4 + 2\text{H}_2\text{O}$	-130
2. $4\text{HCOO}^- + 2\text{H}^+ \rightarrow \text{CH}_4 + \text{CO}_2 + 2\text{HCO}_3^-$	-127
3. $4\text{CO} + 2\text{H}_2\text{O} \rightarrow \text{CH}_4 + 3\text{CO}_2$	-186
4. $4\text{CH}_3\text{OH} \rightarrow 3\text{CH}_4 + \text{CO}_2 + 2\text{H}_2\text{O}$	-103
5. $4\text{CH}_3\text{NH}_3^+ + 2\text{H}_2\text{O} \rightarrow 3\text{CH}_4 + \text{CO}_2 + 4\text{NH}_4^+$	-74
6. $\text{CH}_3\text{COO}^- + \text{H}^+ \rightarrow \text{CH}_4 + \text{CO}_2$	-32
7. $(\text{CH}_3)_2\text{S} + \text{H}_2\text{O} \rightarrow 1.5\text{CH}_4 + 0.5\text{CO}_2 + \text{H}_2\text{S}$	-74

low. Additionally, only three genera of methanogens, *Methanosarcina*, *Methanotherix*, and *Methanosaeta*, have bacterial species capable of utilizing acetate to produce methane and carbon dioxide [12, 68, 93]. These observations demonstrate the importance of maintaining a suitable environment for the acetoclastic methanogens. It is also important to note that for some methanogenic species, the substrate serves as both the energy and sole carbon source, whereas other methanogens grow only when supplemented with additional carbon sources. For example, only three genera are capable of splitting acetate into methane and carbon dioxide (energy production), but several other groups of methanogens require acetate for biosynthetic purposes [168].

Another important function of the methanogens is maintenance of low hydrogen partial pressure in the anaerobic environment. The implications of this statement are two-fold: (1) by maintaining a low hydrogen partial pressure (i.e., less than 10^{-5} atm), the thermodynamics of the acidogenic and acetogenic bacteria will be favorable (energy yielding); and (2) by maintaining a low hydrogen ion concentration, the pH of the anaerobic environment will be maintained within the optimum range (6.5-7.5) for the methanogens. This second point will be discussed in a later section [23, 47, 93, 168].

Biochemistry of the Methanogens

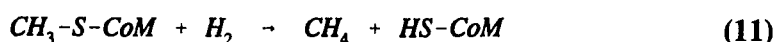
Because of the importance of the methanogenic bacteria to the overall function of an anaerobic environment, a general overview of their biochemistry is presented here. Schematic diagrams of methane production, energy production, and biosynthesis from

CO₂, methanol, and acetate are presented in Figures 2, 3, and 4, respectively, below. The pertinent enzymes, coenzymes, and cofactors are indicated where appropriate [12, 168].

Each of these systems is discussed in this section.

Coenzymes and Cofactors. One interesting characteristic of the methanogens is the presence of several unique coenzymes. The list of unique coenzymes involved in methanogenesis is long, and a complete description of all of the coenzymes is beyond the scope of this document. A few of the more important coenzymes are discussed below:

Coenzyme M, or 2-mercaptoethanesulfonic acid (HS-CH₂CH₂SO₃⁻), is involved in the terminal step of methane production in all known methanogens. Methane is produced through the reduction of 2-(methylthio)ethanesulfonic acid to produce methane and reduced CoM:



Despite the importance of CoM for the production of methane, not all methanogens are able to synthesize CoM, and thus require it as a growth factor. One methanogen of this type is *Methanobrevibacter ruminantium*, found in the gut of rumen animals. CoM is supplied to *M. ruminantium* by several methanogens which secrete CoM [12, 168]. Several other enzymes and cofactors are unique to the methanogens and are described here [12, 112, 168, 170].

Coenzyme F₄₂₀ is a flavin derivative, similar in structure to the common flavin coenzyme, flavin mononucleotide (FMN). *Coenzyme F₄₂₀*, however, is a two electron carrier, rather than a one or two carrier, which is a common characteristic of many flavin coenzymes. It interacts with the hydrogenases and NADP⁺ reductases of methanogens, and also plays a role in methanogenesis as an electron donor in at least one of the steps of carbon dioxide reduction. An interesting property of *coenzyme F₄₂₀* is its ability to absorb light at 420 nm and fluoresce blue-green in the oxidized state. This feature presents a useful method of methanogenic identification [12, 170].

Coenzyme F₄₃₀ is a nickel-containing tetrapyrrole and plays a crucial part in the final step of methanogenesis as part of the methyl reductase system. The nickel requirement of most methanogens is mainly due to *coenzyme F₄₃₀*, which is found in abundance in methanogens [12, 170].

Methanofuran is a low molecular weight coenzyme that interacts in the first step of methanogenesis from CO₂. Carbon dioxide is initially reduced to the formyl level and is bound by the amino side chain of a furan ring. The formyl group is subsequently transferred to a second coenzyme [12].

Methanopterin is a methanogenic coenzyme resembling the vitamin folic acid, and serves as the C-1 carrier during the reduction of CO_2 to CH_4 . The reduced form, tetrahydromethanopterin, is the active form of the coenzyme. Methanopterin also has the property of fluorescence after light absorption at 342 nm [12, 170].

HS-HTP, or 7-mercaptoheptanoylthreonine phosphate, is a cofactor involved in the final step of methanogenesis catalyzed by the methyl reductase system. The sulfhydryl active group serves as the electron donor in this final step, resulting in a disulfide linkage between CoM and HS-HTP (CoM-S-S-HTP) [12].

Enzymes. The specific enzymes involved in all of the steps of methanogenesis and biosynthesis are complex, and a detailed description is not presented here. However, a general discussion of the properties and types of enzymes important in methanogens follows. The general types of enzymes utilized by methanogens during methane production include hydrogenases, reductases, dehydrogenases, and transferases. Obviously, many other enzyme types can be found in methanogens, but those listed are especially important in the common methanogenic pathways and are discussed below [12, 112, 125, 168, 172].

Hydrogenases bind H_2 and split it into protons, which then may be used for ATP production or serve as reducing equivalents in reduction reactions [12]. The hydrogenase

active in methanogenesis from CO_2 catalyzes the addition of hydrogen (reduction) to at least two of intermediates involved.

Generally speaking, a reductase, or oxidoreductase, catalyzes a reaction in which a molecule is reduced through the addition of electrons, with the simultaneous oxidation of an electron donating molecule [172]. The methyl reductase system of methanogens is the most obvious example of this type of enzyme. The methyl group of CoM-S-CH_3 is reduced to methane, with the concomitant generation of a disulfide of CoM-S-S-HTP (HS-HTP is oxidized) [12, 112, 125, 168, 170].

Transferases catalyze the transfer of a functional group from one molecule to another [172]. It is generally accepted that there are two main transferases involved in methanogenesis from methyl substrates, such as methanol (CH_3OH). These are generically termed methyltransferase I and II. Methyltransferase I transfers the methyl group from methanol to a vitamin B_{12} derivative, and methyltransferase II transfers the same methyl group from B_{12} to CoM to form methyl CoM [170]. The methanopterins do not possess transferase activity, but they do act as C-1 carriers for most of the reductive steps during CO_2 reduction to methane [12, 168, 170].

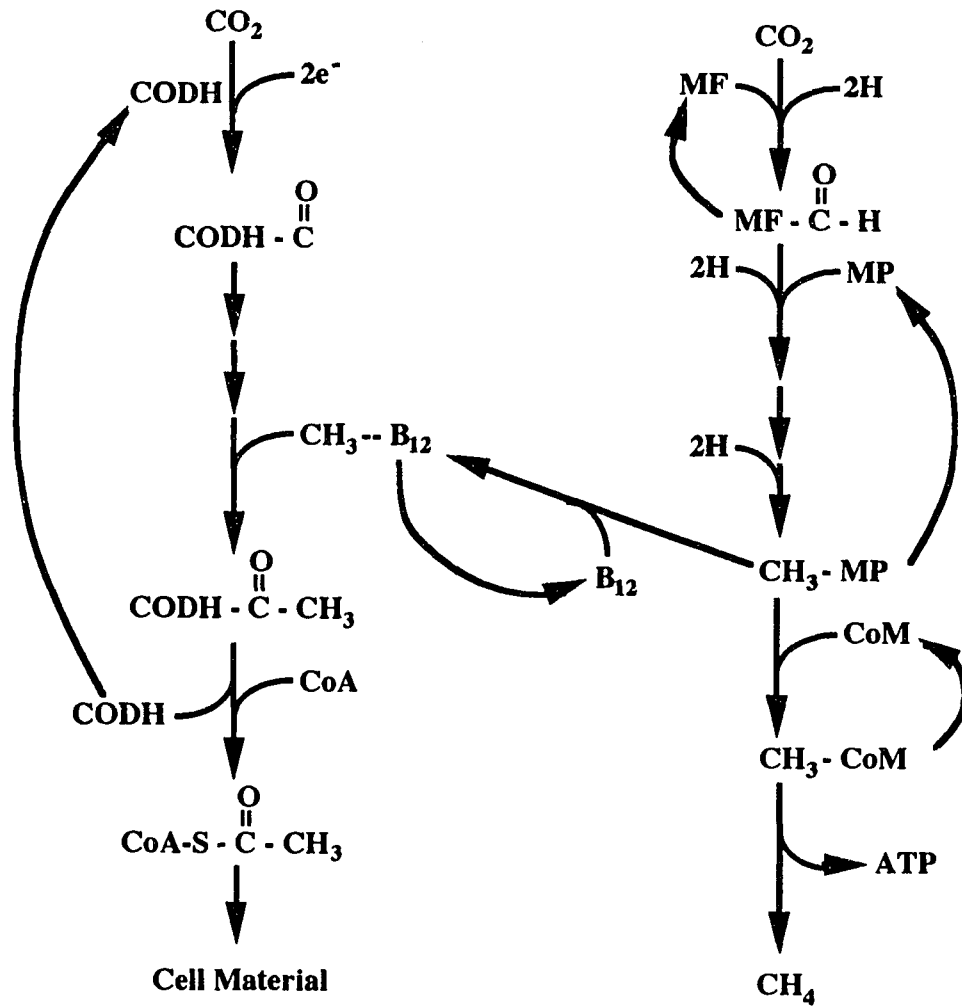
Generally, dehydrogenases catalyze the removal of hydrogen from (oxidation) of molecules [12, 172]. There are several dehydrogenases involved in methanogenesis, including CO dehydrogenase, which oxidizes carbon monoxide to carbon dioxide, and formate dehydrogenase, which oxidizes formate to carbon dioxide [168, 170].

Methanogenesis. Different pathways are involved in methanogenesis from the three main substrate types, which are carbon dioxide (including formate and carbon monoxide), methyl substrates (including methanol and methylamines), and acetate. Certain segments of the pathways are common to all three substrates, but there are some differences which are presented here.

Carbon dioxide is activated by methanofuran and reduced to the formyl level. The formyl group is transferred to tetrahydromethanopterin and dehydrated to the methylene level. The methylene group is subsequently reduced to a methyl group, which is transferred to CoM to form methyl-CoM. The methyl group is then reduced to methane by methyl reductase (Figure 2) [12, 168].

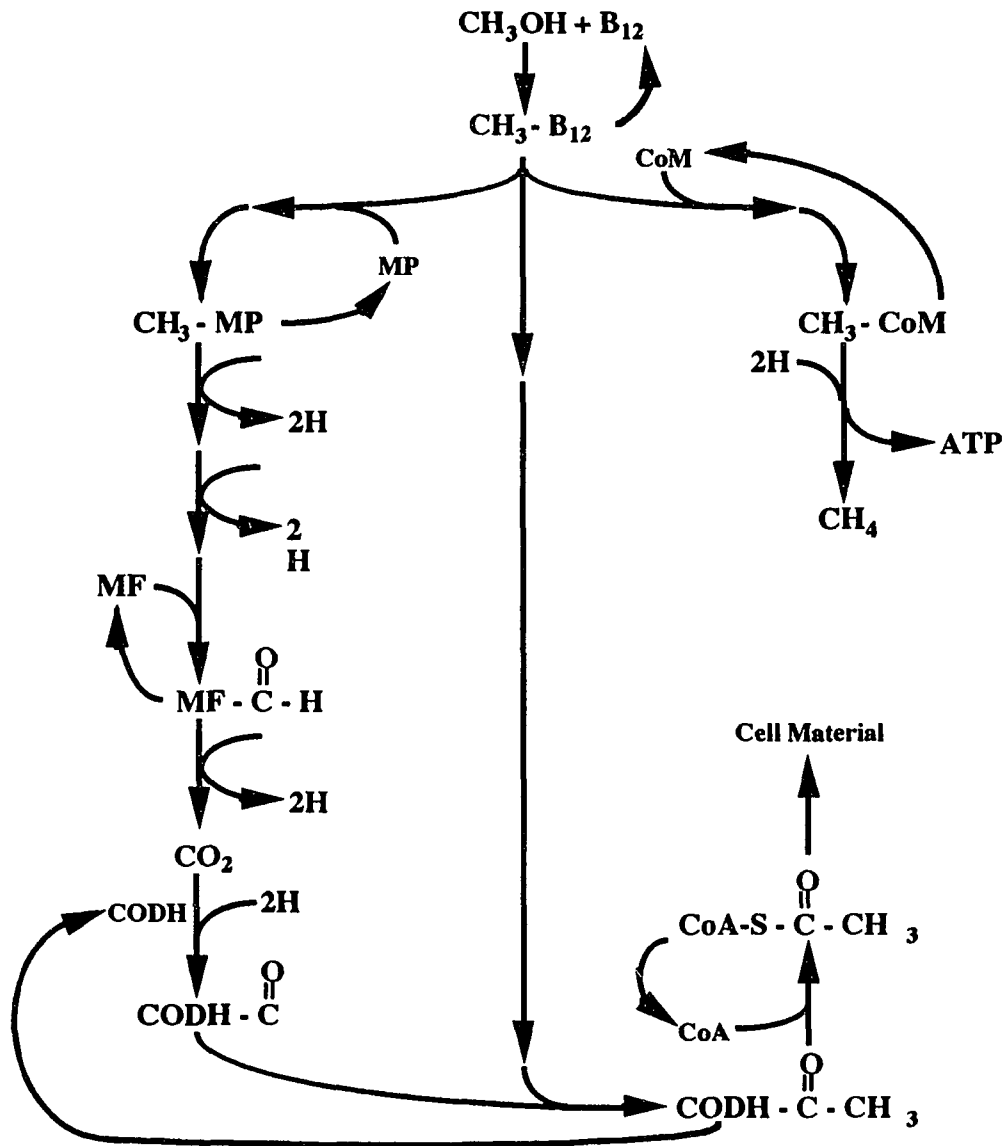
Methyl substrates donate their methyl groups to a vitamin B₁₂ protein to form methyl-B₁₂, which then transfers the methyl group to CoM. Reducing equivalents for the reduction of methyl-CoM are derived from the oxidation of other methanol molecules to CO₂ (Figure 3) [12, 168].

Acetoclastic methanogenesis is tied to reactions of the acetyl-CoA pathway (see below). Acetate is activated to acetyl-CoA which interacts with CO dehydrogenase. This results in the transfer of the methyl group of acetate to a vitamin B₁₂ enzyme of the acetyl-CoA pathway. The methyl group is subsequently transferred to tetrahydromethanopterin and then to CoM to form methyl-CoM. Methyl-CoM is then reduced to methane with electrons generated from the oxidation of CO to CO₂ by CO dehydrogenase (Figure 4) [12].



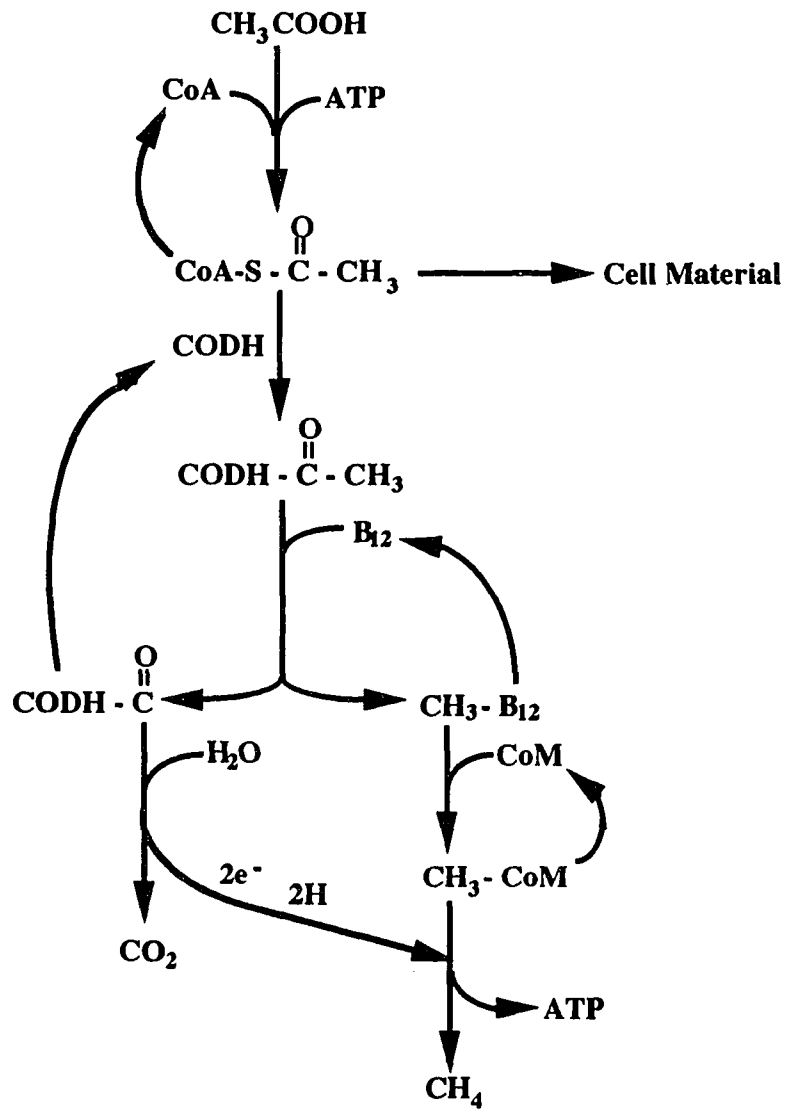
MF = methanofuran
MP = tetrahydromethanopterin
CoM = coenzyme M
CoA = coenzyme A
B₁₂ = vitamin B₁₂
CODH = carbon monoxide dehydrogenase

Figure 2. Biochemistry of carbon dioxide utilization by methanogens.



MF = methanofuran
MP = tetrahydromethanopterin
CoM = coenzyme M
CoA = coenzyme A
B₁₂ = vitamin B₁₂
CODH = carbon monoxide dehydrogenase

Figure 3. Biochemistry of methyl compound utilization by methanogens.



<p> MF = methanofuran MP = tetrahydromethanopterin CoM = coenzyme M CoA = coenzyme A B₁₂ = vitamin B₁₂ CODH = carbon monoxide dehydrogenase </p>

Figure 4. Biochemistry of acetate utilization by methanogens.

Although several strains of methanogens utilize CO₂, H₂, and methyl substrates for methanogenesis, only a few are able to convert acetate to methane and carbon dioxide. These are limited to species of the genera *Methanotherix*, *Methanosarcina*, and *Methanosaeta* (Table 4). *Methanotherix* and *Methanosarcina* have especially been implicated as the major acetate-utilizing bacteria involved in methanogenesis in most anaerobic systems. The literature cites the three most important species of these genera as *Methanosarcina barkeri*, *Methanotherix concilii*, and *Methanotherix soehngenii* [70, 76, 88, 90, 110, 168, 169].

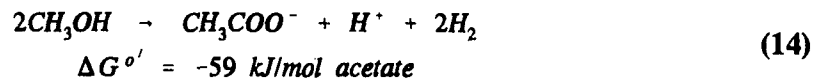
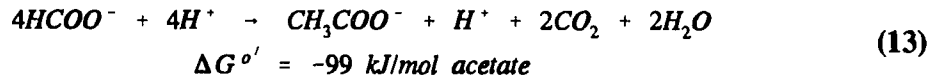
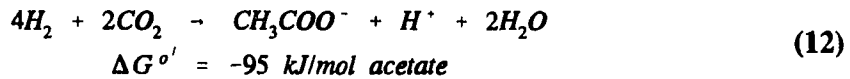
Energy Production. Based on experimental evidence, current theory predicts that many methanogenic bacteria conserve energy by electron transport phosphorylation [168]. Through this process, a proton motive force is generated, consisting of membrane potential (inside negative, outside positive) and an pH gradient (inside alkaline, outside acidic). In addition, a few strains have been isolated that apparently conserve energy through substrate-level phosphorylation [168].

Proton dependent ATPases have been demonstrated in most methanogens, although a few strains have been shown to contain sodium dependent ATPases (especially those that convert methanol to methane). Generally, the terminal step of methanogenesis is the energy conservation step. The conversion of methyl-CoM is linked to a proton pump that pumps H⁺ produced in this step to the outside of the cytoplasmic membrane, thus establishing a proton gradient and a membrane potential. Membrane-bound proton-

translocating ATPases then dissipate the proton motive force and produce ATP from ADP and P_i in a fashion that is similar to ATP production in other eubacteria and eukaryotes [12, 112, 141, 168]. Through thermodynamic considerations, it is generally accepted that the minimum standard free energy of formation of 1 mole of ATP from ADP and P_i is approximately 31.8 kJ/mol. The conversion of CO_2 to CH_4 ($\Delta G^{\circ} = -130.4$ kJ/mol), methanol to CH_4 ($\Delta G^{\circ} = -103$ kJ/mol) and of formate to CH_4 ($\Delta G^{\circ} = -119.5$ kJ/mol) will yield a maximum of 3 mole of ATP per mole CH_4 produced. The conversion of acetate to CH_4 ($\Delta G^{\circ} = -32.5$ kJ/mol), on the other hand may yield a maximum of only one mole of ATP per mol methane produced [168].

It is this low production of ATP that is responsible for the low growth rates of methanogens, especially those that utilize acetate as their methanogenic substrate. For example, under optimum defined conditions (pH = 7.0, all growth factors and nutrients provided in excess), doubling times for *Methanotherx concilii*, *Methanotherx soehngeni*, and *Methanosarcina barkeri* have been estimated as 3.4 days, 6.7 days, and 3.1 days, respectively. Further, it is estimated that under normal environmental conditions, these doubling times are considerably longer [70, 90, 110].

Biosynthesis. Methanogenic bacteria synthesize cellular carbon starting from activated acetate (acetyl-CoA) and CO_2 . Acetate may be taken in directly by the cell when sufficient acetate concentration exists in the environment, or it may be synthesized from single- carbon molecules by the following exergonic reactions:



The energy produced is conserved by the formation of the activated acetyl-CoA, rather than acetate [168].

When acetate is unavailable in the environment, acetyl-CoA can be formed from one-carbon compounds (e.g., CO_2) through the reduction of two molecules of CO_2 . The methyl group of acetate is produced by the reduction of CO_2 following the methanogenic pathway for methane formation previously discussed. The carboxyl group of acetate results from the reduction of CO_2 by the action of CO dehydrogenase, to produce a carbonyl moiety. The condensation of the methyl group, the carbonyl moiety, and coenzyme A then (mechanism not fully known), with the production of acetyl-CoA. The formation of acetyl-CoA from methanol and acetate has already been described. From this discussion, it is obvious that methanogenesis and acetate formation are tightly coupled processes in that they have common intermediates and utilize common enzymes. This results in an energy savings to the methanogens. However, even though the pathways share common intermediates, the large majority (99%) of the intermediate products are directed towards methane production for energy production [12, 168].

Ammonium ions are used to satisfy the majority of the nitrogen requirement for methanogens. However, some methanogens have the ability to fix molecular N_2 into cellular nitrogen under limiting ammonia concentrations. Additionally, other methanogens are not capable of synthesizing all required amino acids. Glutamate accounts for over half of the soluble amino acid pool in several methanogens, which serves as the main precursor of the other nitrogen-containing compounds. Formation of other amino acids proceeds through the action of glutamate-pyruvate transaminase and glutamate-oxaloacetate transaminase, which connect the various amino acids through a type of tricarboxylic acid cycle [168].

The sulfur requirements for methanogens is supplied by reduced forms of sulfur, such as sulfide or cysteine. The precise metabolic pathways used for sulfur assimilation is not presently clear. Sulfhydryl groups serve as important active sites in many methanogenic enzymes and coenzymes, one of which is coenzyme M (which also contains an oxidized sulfur atom) [168]. Elemental sulfur is also an inhibitor of methanogenesis. In methanogenic pure cultures growing on hydrogen, the addition of elemental sulfur inhibited methane formation and resulted in H_2S formation [168].

Trace elements required by methanogens include cobalt, iron, molybdenum, nickel, magnesium, and potassium. The growth of a few methanogens is also stimulated by tungsten and selenium. The great majority of the trace metal requirement is utilized in the synthesis of enzymes, coenzymes, and cofactors [168].

Interplay among the Anaerobic Bacteria

The previous sections discussed each major group of bacteria in anaerobic environments as individual, or separate, entities. In actual environments, however, all groups of bacteria work together to fully stabilize organic material within their environment. In fact, the various groups depend on the other groups to provide utilizable substrates, to degrade metabolic end-products, and to maintain appropriate conditions (e.g., pH) in the environment. Figure 5 depicts the flow of substrates and end-products among the various groups of bacteria.

The hydrolytic/fermentative bacteria depend on the acetogenic bacteria to degrade the fatty acids (except acetate) that are produced during fermentation of polymeric substrates. Additionally, the homoacetogenic and methanogenic bacteria utilize H_2 produced by the fermentative bacteria. Each of these processes improves the thermodynamic conditions for the hydrolytic/fermentative bacteria, thereby increasing the energy yield derived from fermentations [47, 81, 93, 168, 170].

The acetogenic bacteria rely on the fermentative bacteria for their carbon and energy source in the form of fatty acids (3 carbons or longer). As mentioned, the homoacetogenic bacteria also utilize hydrogen produced in the fermentations. The end-products of acetogenesis (acetate, CO_2 , H_2) is utilized by the methanogens for energy and synthesis [47, 81, 93, 168, 170].

Methanogenic bacteria scavenge the H_2 produced by both of the other groups of bacteria, and also utilize CO_2 , formate, acetate, and methanol for growth and energy. The

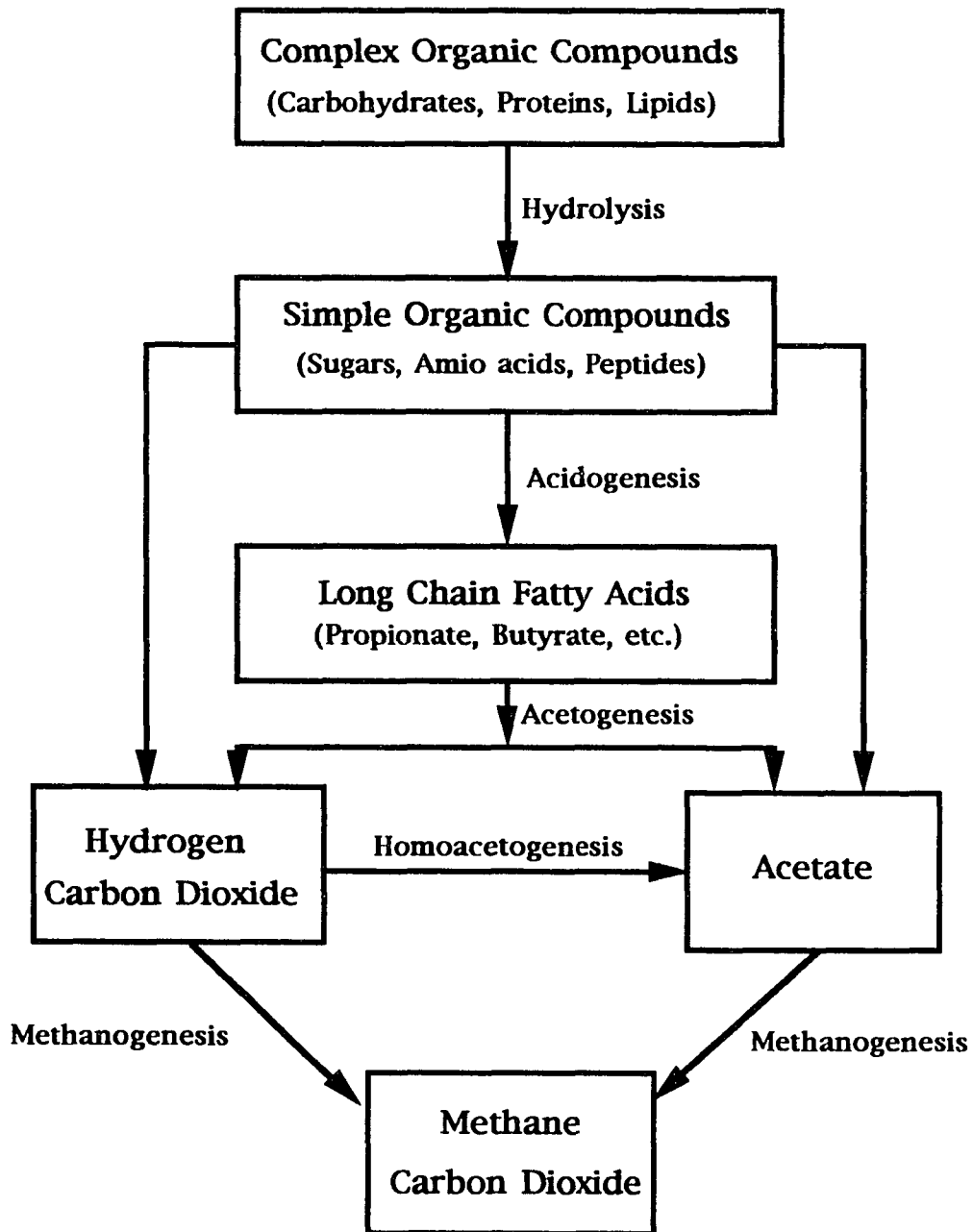


Figure 5. Substrate and intermediate product flow among anaerobic bacteria.

H_2 -consumption is especially beneficial to the propionate and butyrate-oxidizing acetogens, since the standard free energy change for propionate and butyrate oxidation is positive under high hydrogen partial pressure. However, in the presence of methanogens, which utilize H_2 in methanogenesis, the free energy is negative enough to allow energy production from the oxidation of propionate and butyrate. In some environments, methanogenic production of CO_2 may also provide this starting material for the homoacetogenic bacteria, which convert two equivalent of CO_2 to acetate. In addition, by stabilizing the acetate produced by the fermentative and acetogenic bacteria, a proper pH is maintained in the system so that none of the bacteria in the system become inhibited by low pH [23, 47, 81, 93, 168, 170].

There are also instances of substrate competition between groups or classes of bacteria. One example of this is competition between methanogens and homoacetogens for H_2 and CO_2 . Methanogens convert these compounds to methane, whereas homoacetogens convert them to acetate. In most systems, methanogens are generally able to out-compete the homoacetogens for CO_2 and H_2 . Under these conditions, the homoacetogens, which are capable of heterotrophic metabolism as well as autotrophic, utilize organic compounds for carbon and energy [168].

A second example of competition for substrates is the well-documented case between the methanogens and the sulfate-reducing bacteria (SRB) [108, 168]. In the absence of sulfate, some SRB species actually provide substrates (H_2 , acetate) to the methanogens. However, in the presence of sulfate, the SRB generally out-compete the

methanogens for H_2 and acetate. This is especially significant at high sulfate and low H_2 or acetate concentrations. The SRB have lower K_m values for both H_2 and acetate, and, therefore, have a higher affinity for these substrates than do the methanogens, especially under limiting conditions of H_2 or acetate [108, 168].

Anaerobic Wastewater Treatment

Anaerobic versus Aerobic Treatment

There are generally two biological treatment methods for waste stabilization: aerobic and anaerobic treatment. Aerobic treatment has been widely used for low-strength, domestic wastewater treatment and also for many industrial wastes. Aerobic bacteria, because of the high energy yield characteristic of the oxidative phosphorylation pathways utilized by aerobes, grow very rapidly as compared to the anaerobic bacteria, which gain a much smaller amount of energy from degradation of a given waste material. Aerobic bacteria convert some (approximately 1/3 to 1/2) of the waste material to CO_2 and water, with the remaining energy directed towards cell synthesis. The result of this process is the production of large quantities of biomass which must be further stabilized (usually through anaerobic digestion) before disposal. Additionally, by definition, aerobic organisms require molecular oxygen to grow and reproduce. The addition of oxygen to the aerobic wastewater treatment system, such as an activated sludge system, results in significant operating costs.

Anaerobic microorganisms, however, require no oxygen, and are, in fact, inhibited or killed by free oxygen. Therefore, there is no requirement for oxygen addition in anaerobic waste treatment. Also, since anaerobic microbes reproduce at relatively low rates (most of the energy of the reactions is lost as methane), the biomass production rate is low, which further results in lower biomass disposal costs. Another advantage is that nutrient requirements are lower for anaerobic bacteria, owing to their lower reproduction rates. An additional benefit to anaerobic treatment is the production of methane, which contains most (about 90-95%) of the energy of the original waste compound. That is, a significant portion of the energy of a waste can be captured in the form of methane, which can then be used to produce electricity or burned to release heat [23, 93].

There are, however, a few disadvantages to anaerobic waste treatment when compared to aerobic processes. The first is the general requirement for higher operating temperature for efficient anaerobic waste stabilization. Although there has been and still is considerable investigation into anaerobic stabilization at lower temperatures, most anaerobic systems are designed to operate at or near 35°C. However, many, if not most, anaerobic systems produce more than sufficient methane which can be burned and utilized for heating the anaerobic reactor. A second disadvantage often cited for anaerobic systems is the slow growth rates of the methanogenic bacteria, resulting in long start-up periods of anaerobic systems. This phenomenon has traditionally been confused with low substrate removal rates. It can not be emphasized enough that these two rates are distinct from each other. Anaerobic substrate removal rates are similar to aerobic rates. The underlying

principal behind the slow methanogenic growth rates is that the methanogens derive very little energy through methanogenesis, and, therefore, require long time periods to reproduce [23, 93]. That notwithstanding, the long start-up period for anaerobic systems is a significant problem and possibly the most significant deterrent to the widespread use of anaerobic technologies. Many industries are simply not willing to wait for several months or even years for their waste treatment system to reach design loads.

The problem of long start-up periods, therefore, was selected as one of the items to be addressed in this research. That is, methods of decreasing the time required to achieve stable anaerobic degradation of a given wastewater were to be examined in this research. The methods employed are outlined in a later section.

Environmental/Operational Parameters in Anaerobic Treatment

The parameters affecting anaerobic digestion can be broadly classified as environmental and operational. Due to the relatively slow growth rates of anaerobic, and especially methanogenic, bacteria, a longer time is required for these microbes to adjust to changing conditions within the anaerobic reactor [94]. It is, therefore, desirable to maintain near optimum environmental and operational conditions in a given anaerobic waste treatment system. The following paragraphs discuss the important environmental and operational parameters to efficient anaerobic waste treatment.

Environmental Parameters

The main environmental parameters that effect anaerobic digestion are temperature, pH, alkalinity and volatile acids concentrations, substrate and nutrient availability, and the presence of toxic or inhibitory compounds. Each of these parameters has an intimate effect on the overall efficiency of a given anaerobic waste treatment system, and are discussed in detail.

Temperature. Anaerobic digestion is greatly affected by the temperature at which the process is carried out. As early as the 1930's, Rudolfs and Heukelekian reported on noticeable differences in the rate of digestion at different temperatures (thermophilic and non-thermophilic). It is generally accepted that the organisms responsible for digestion at thermophilic temperatures (50 to 70°C) are different from those responsible for digestion at lower temperatures, such as the mesophilic range (28 to 35°C). McCarty [94] and several other researchers also found the presence of two distinct temperature ranges, similar to those given. More recently, psychrophilic (10 to 20°C) has been investigated for several wastes. It has become apparent that anaerobic digestion may be carried out within a number of temperature ranges.

Temperature affects the rates at which digestion is carried out, rather than the total degree of digestion that is achieved. Pidaparti and Dague [25] and Dague [23a] reported similar total COD and volatile solids destruction at temperatures of both 35°C and 25°C. However, since the rates of degradation are slower at lower temperatures, the digestion

process must be allowed to operate at longer detention times or the biomass population must increase in order to obtain the same degree of stabilization at lower temperatures.

A general rule of thumb is that microbial metabolism rates (and thus, rates of digestion) approximately double for each 10°C rise in temperature. This can be shown mathematically by applying Equation 15 below, which is a common temperature correction equation applied in the wastewater industry.

$$k_T = k_{20} \theta^{T-20} \quad (15)$$

where, k_T = rate at the given temperature, T°C, 1/time
 k_{20} = rate at 20°C, 1/time
 T = given temperature, °C
 θ = a constant that is specific for the given biological process

For many biological processes, θ is equal to 1.07. By applying Equation 15 at a temperature of 30°C, the ratio of k_{30}/k_{20} is equal to 1.97, essentially 2. Therefore, Equation 15 predicts that biological rates will be twice as fast at 30°C as they are at 20°C.

Hydrogen Ion Concentration. The hydrogen ion concentration (pH = $-\log[H^+]$) in an anaerobic reactor has a major effect on the performance of the system. McCarty [94] suggested a range for pH of 6.6 to 7.6 with an optimum between 7.0 to 7.2. Other reports have indicated that methanogenesis is possible at pH values as low as 6 to 6.2 and as high as 8.1 to 8.5 [59, 137a, 168]. However, the optimum pH is still quoted as being 7.0. During the course of the research presented in this document, pH values as low

as 6.4 and as high as 7.8 have been observed for short periods of time with little effect on methanogenesis. Since the methanogens are the most important organisms in an anaerobic system, it is important that the pH be maintained at a level that is not inhibitory to them, i.e. at pH near neutral. This range of pH has been shown to be the optimum for the anaerobic process as a whole, not just for the methanogenic organisms.

Alkalinity and Volatile Acids. The alkalinity of a system is a measure of its capacity to neutralize strong acids without a significant decrease in pH. In most wastewater applications operating near neutral pH, the main component of alkalinity is the bicarbonate ion, although carbonate, hydroxyl, phosphate, and borate species also contribute to alkalinity to varying degrees. Bicarbonate is mainly produced by the formation of ammonium bicarbonate from CO_2 and NH_3 during anaerobic degradation of complex substrates (e.g., protein) by the following reaction:



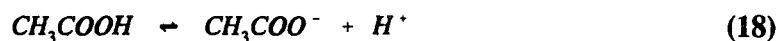
The ammonium bicarbonate dissociates to NH_4^+ and HCO_3^- . The bicarbonate ion provides a buffer to decreases in pH through the carbonic acid/bicarbonate system, as shown in Equation 17.



Examination of Equation 17 shows that the carbonic acid-bicarbonate system is directly influenced by the pH of the reactor and vice versa. Therefore, as acid (H^+) is added to the system, bicarbonate is used to produce carbonic acid (which is also in equilibrium with carbon dioxide and water), but the pH of the system will not decrease significantly until the majority of the bicarbonate is gone. Additionally, ammonium is in equilibrium with ammonia and protons. However, the pK_a of the NH_4^+/NH_3 system is approximately 8.95 at $35^\circ C$, and, therefore, provides little buffer capacity in most treatment systems [53].

Many wastewaters do not contain sufficient alkalinity to maintain proper pH levels over the course of treatment. In these applications, it is usually necessary to add alkalinity to ensure maintenance of appropriate pH. Common alkaline compounds used for this are ammonia, lime, sodium bicarbonate, and sodium hydroxide [23, 94, 96].

Volatile organic acids are produced through the degradation of more complex molecules by the acidogenic and acetogenic bacteria. If the volatile acid (acetic, propionic, butyric) concentration increase to high levels, the pH of the system may be depressed due to the equilibrium established between the acids and their respective salts. Equation 18 represents the H^+ produced by acetic acid ionization.



Since the pK_a of most of the volatile acids is less than 4, most of the acid will be present in the ionized form, thus producing H^+ with a subsequent decrease in pH unless sufficient alkalinity exists to neutralize the acid. A high volatile acids concentration in conjunction

with low pH (< 6.5) is a prevalent problem with improperly operated anaerobic systems, and is commonly known as a "stuck" digester. In order to relieve this condition, the pH must be raised to non-inhibitory levels with an alkaline material, often lime. The methanogens may then function properly to remove the acids and produce methane. It has been noted that it is the low pH, rather than high volatile acids concentration, that inhibits proper anaerobic digestion; therefore, the pH is the single most important environmental parameter for efficient anaerobic treatment [23, 94, 96].

Nutrient and Trace Element Availability. Although anaerobic bacteria grow at a relatively slow rate, they do require nutrients (nitrogen, phosphorous, sulfur, potassium, sodium, and others) and trace elements (iron, nickel, copper, zinc, and other metals) in small quantities for efficient growth and methanogenesis [106, 142, 148, 149]. Nitrogen and sulfur are incorporated into cellular material, such as proteins, and phosphorous plays an important role in the high energy phosphorous bonds in which chemical energy is stored as ATP and other energy-storage molecules. Sodium and potassium are mainly used to maintain the ionic strength of the cytoplasm at appropriate levels, as well as playing a role in ATP production in some ATPases [18, 19, 59, 65, 168].

Heavy metals are incorporated into the various enzymes, coenzymes, and cofactors of the anaerobic bacteria. Often, the heavy metals are important constituents of the active sites on enzymes and coenzymes [18, 19, 65, 106, 168, 172]. The nutrients and trace

elements listed here are necessary in low concentrations, and in a properly operated system are not the limiting compounds. However, care must be taken so that the concentrations of these compounds are not high enough to cause inhibition, as presented below [95].

Toxic or Inhibitory Compounds. Many organic and inorganic materials may be toxic to anaerobic organisms. Often, at low concentrations, these same materials may be stimulatory to the microorganisms, but as the concentration of the material increases, it becomes inhibitory and finally toxic. The alkali and alkaline-earth metals are examples of compounds that exhibit this phenomenon [95, 121]. McCarty [95] reported on the effects of several alkali and alkaline-earth metals on anaerobic digestion. His summary is presented in Table 6.

Ammonia, although necessary for cellular biosynthesis, can be toxic at higher concentrations. As earlier stated, ammonia is in equilibrium with ammonium, and the pK_a of the system is 8.95 at 35°C (Equation 19). Therefore, at a pH of 7.0, it can be

Table 6. Effects of alkali and alkaline-earth metals on anaerobic digestion [95].

Cation	Concentration (mg/L)		
	Stimulatory	Moderately Inhibitory	Strongly Inhibitory
Sodium	100-200	3,500-5,500	8,000
Potassium	200-400	2,500-4,500	12,000
Calcium	100-200	2,500-4,500	8,000
Magnesium	75-150	1,000-1,500	3,000



calculated that the ratio of NH_3 to NH_4^+ is 0.011 ($10^{-8.95}/10^{-7.0}$). Stated differently, 98.9% of the ammonia pool will be in ionic form, which is the less toxic form of the two species. McCarty stated that a total ammonia concentrations of 50 to 200 mg/L was beneficial to anaerobic waste treatment. Total ammonia concentrations of 200 to 1,000 mg/L have no adverse effects, whereas concentrations of 1,500 to 3,000 are inhibitory, especially at high pH values. Greater than 3,000 mg/L of total ammonia was stated to be toxic to the anaerobic system [95].

Parkin et al. [109a] reported on the effects of industrial toxicants to methane fermentation. The study reported on the toxicity of nickel, ammonium, sulfide, and formaldehyde. In all cases, the inhibition to the methanogenic bacteria appeared to be reversible, and acclimation of the biomass to the toxicant occurred, indicating the inhibition to toxicants can be overcome with time. The authors state that a long solids retention time (SRT) is the best safeguard against failures of a treatment system that must handle toxicants.

Heavy metals have also been reported to inhibit methanogenesis. Copper, zinc, and nickel have all been associated with digestion problems due to relatively low concentrations of the soluble metals. Sulfate may also inhibit methanogenesis due to the competing reactions of the sulfate-reducing bacteria [120, 154]. Under normal sulfate concentrations,

though, sulfate is reduced to sulfide with little effect on methanogenesis. Sulfide has also been observed to be inhibitory at low concentrations. However, when heavy metals and sulfides exist together, they combine to form extremely insoluble precipitates of metal sulfides. Additionally, slowly- or non-biodegradable organic compounds and inorganic compounds may inhibit anaerobic digestion if present in high enough concentrations. The best remedies for treatment of such wastewaters is removal of the compound prior to anaerobic treatment, or dilution of the wastewater so that the concentration of the compound is below inhibitory levels [65, 95, 120].

Operational Parameters

Operational parameters are those that are under direct control of the operator. These parameters include solids retention time, organic loading rate, and hydraulic retention time. Control of these parameters defines the loading criteria of the anaerobic system.

Solids Retention Time. The solids retention time (SRT) of an anaerobic system is a reflection of the average time that a solid particle is retained in the system. If the SRT is less than the microbial regeneration time of the slowest growing organism, the proper consortium of anaerobic bacteria may not be maintained in the system [26]. Since the slowest growing anaerobes are the methanogens, SRT control is especially beneficial to these organisms. The SRT of a system is defined as the mass of solids in a system divided

by the mass of solids lost from the system per time. If the biomass inventory (MLSS) of a system is in equilibrium, the SRT may also be defined as the mass of solids in the system divided by the mass of solids produced per time, since the mass produced is equal to the mass lost (Equation 20).

$$SRT = \frac{\text{mass of solids within the system}}{\text{mass of solids lost per time}} \quad (20)$$

The required SRT is dependent on the temperature of the system since, as temperature increases, microbial regeneration times decrease. Therefore, at high temperatures, the required SRT is less than that required at lower temperatures.

Dague et al. [26] reported that the required SRT for stable anaerobic treatment at 35°C is approximately 10 days. Because of increased metabolic rates at higher temperatures, the minimum SRT at a temperature of 55°C is only 2 to 3 days.

The SRT has an effect on the degree of stabilization of the organic content of a waste. As the SRT is increased beyond its minimum, removal rates of organic material increase and gradually plateau as the SRT becomes very long [26]. As the SRT becomes less than 10 days (at 35°C), some of the methanogens will be lost from the system at a rate faster than the rate at which they reproduce. As this situation continues, the concentration of acetic acid begins to increase. As the SRT continues to decrease, longer-chained volatile acids (propionic and butyric) begin to increase in concentration because the hydrogen partial pressure will also rise due to decreased hydrogen removal by the

methanogens. Failure of the anaerobic system is close at this point, and the SRT must be increased to avoid complete failure [23, 26, 96].

Hydraulic Retention Time. The hydraulic retention time (HRT) is the average amount of time that a molecule of water is retained within the reactor. In the case of a completely-mixed reactor, the HRT is equal to the SRT. The HRT is mainly important in that it affects the organic loading rate (described below). From a cost perspective, it is advantageous to operate an anaerobic treatment system for a give wastewater at the minimum possible HRT. This results in a smaller reactor volume and less capital cost. Typical HRTs for municipal digesters range from 15 to 40 days. High-rate anaerobic processes are often operated at HRTs of 48, 24, 12, or even 6 hrs. HRTs less than 3 hours have been reported for anaerobic filters treating domestic strength wastewater [31a].

The HRT also affects the SRT of the system to an extent. If the biomass inventory of a system is the same for two different HRTs, and the concentration of biomass in the effluent from the system is also constant, then the low HRT system will operate at an SRT of one-half of the long-HRT system. This is because more liquid passes through the short-HRT reactor over a given time period, and thus, more solids will be carried out of the system, everything else being equal. For a suspended-growth system in which the solids inventory and effluent solids can be measured directly, the SRT can be calculated in terms of the solids inventory, effluent solids, and HRT (Equation 21):

$$SRT = \frac{(MLSS)(HRT)}{TSS_{eff}} \quad (21)$$

where, SRT = solids retention time, time
 MLSS = mixed liquor suspended solids, mass/volume
 HRT = hydraulic retention time, time
 TSS_{eff} = effluent total suspended solids, mass/volume

Organic Loading Rate. The organic loading rate (OLR) is the mass flux of organic material into the reactor per unit of time, usually reported as mass of organic material per volume of reactor per time (e.g., g/L/day). The OLR is often reported as a COD or BOD loading rate (g COD/L/day or g BOD/L/day), which is defined in terms of the concentration of COD in the influent wastewater and the HRT of the system (Equation 22).

It is generally advantageous for treatment systems to be able to operate at high OLR for best overall economy (smaller reactors). However, the actual OLR employed is determined by the type of waste treated and by the type of reactor used to treat the waste [23, 96].

$$OLR = \frac{COD_i}{HRT} \quad ; \quad OLR = \frac{BOD_i}{HRT} \quad (22)$$

where, OLR = organic loading rate, g COD/L/day
 COD_i = COD concentration of the influent, g COD/L
 BOD_i = BOD concentration of the influent, g BOD/L
 HRT = hydraulic retention time, days

Early Research

Approximately 30 years after Pasteur discovered anaerobic life in 1861, the first anaerobic processes were employed for waste stabilization. Anaerobic bacteria were first applied to waste stabilization in the 1890s in a combined process of clarification (sedimentation) and sludge digestion (the septic tank). Interestingly, the septic tank is still used today in rural areas not serviced by municipal sanitary sewers. Prior to the septic tank, cesspools were utilized for wastewater disposal, which were little more than sedimentation basins in which anaerobic decomposition occurred, although the mechanism of anaerobic treatment was not understood at the time [23].

In 1906, Travis proposed the use two-story tanks to separate sedimentation from solids digestion, and, in 1907, the German Karl Imhoff developed the two-story "Imhoff" tank. This process employed an upper level in which the influent wastewater was clarified by sedimentation, and a lower level in which anaerobic digestion occurred. The Imhoff tank became popular during the first three decades of the 1900s and were installed in over 240 cities throughout Europe and the United States. The most common problems with the Imhoff tank were odors and scum formation [23].

In 1918, John Alvord constructed the first system of separate sludge digestion in the city of Madison, Wisconsin. The system consisted of a clarifier and a separate tank for digestion of the solids. The solids were removed hydraulically from the sedimentation tanks, which alleviated the problem of rising sludge into the settling zone, which was a characteristic problem of the Imhoff tank. Separate sludge digestion was first incorporated

into a wastewater treatment plant in 1923 in Brownsville, Texas. The next major modification to anaerobic digestion processes was the heating of the digestion tanks, which was first practiced in Antigo, Wisconsin, in 1926. Within five years of that date, over 100 plants serving 3.5 million people in the U.S. were practicing heated digestion [23].

Temperature effects on solids digestion were widely researched during the 1930s at temperatures ranging from less than 10°C up to 60°C. Numerous optimum temperatures were cited, but it was noted by several researchers that digestion rates increased at increasing temperatures. Additionally, it was observed that the total stabilization and gas production at different temperatures were similar, but that stabilization required longer time periods at lower temperatures. In the latter 1930s, multi-stage digestion was employed, with the first stage operating at thermophilic temperatures and the second stage at mesophilic temperatures [23].

The first reports of the importance of the solids retention time, rather than the liquid detention time, came about in the 1940s. Schlenz reported on a system that operated at a 60-day solids detention time and a 30-day liquid detention time, which was achieved by transferring a larger volume of the supernatant (rather than the settled sludge) to the second stage digestion unit. A further report of this phenomenon was the application of two stage digestion to a wastewater from a yeast manufacturer. The system operated at approximately a four-day liquid detention time and decreased the five day biochemical oxygen demand (BOD_5) from 5,000 mg/L to 1,100 mg/L. This was one of the first applications of anaerobic treatment to a liquid waste, rather than a sludge [23]. In 1950,

Rawn and Candell reported on a four-stage digestion system which employed the recycling of settled sludge from the fourth to the first stage. Although not stated by the authors, this, in effect, increased the solids retention time (SRT) of the system and the amount of biomass in the digesters [23].

High-Rate Anaerobic Treatment

The Anaerobic Contact Process

The first "high-rate" process for anaerobic treatment appeared in the literature in 1953. Fullen reported on a process that was being studied in Austin, Minnesota, treating a packing house wastewater in which the influent wastewater was mixed with an activated anaerobic sludge at a temperature of 92 to 94°F. The mixed liquor was then taken to a clarification basin and separated from the supernatant by degasification and sedimentation. After sedimentation, the anaerobic biomass was returned to the digester to complete the cycle. The process, which was later called the anaerobic contact process (Figure 6), reduced the BOD₅ of the wastewater by 95% in a liquid detention time of 24 hrs or less. The anaerobic contact process, analogous to the aerobic activated sludge process, could handle more than 0.20 lb BOD₅/ft³/day, which was four times greater than typical activated sludge BOD loading rates. This was attributed to the greater mixed liquor concentrations that could be maintained in the anaerobic contact process: up to 15,000 mg/L as compared to 2,000 to 3,000 in aerobic activated sludge systems. In 1957, this system was applied to sewage wastewater with similar (although poorer) results at temperatures of 4 to 25°C [22,

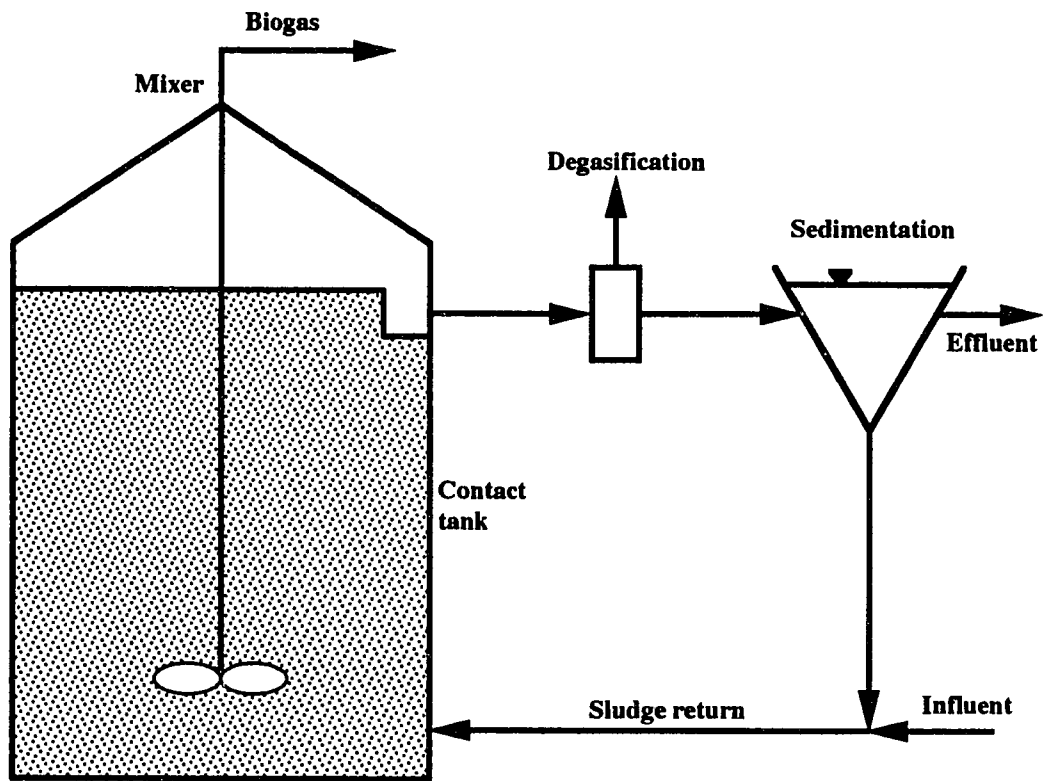


Figure 6. The anaerobic contact process.

23]. Other full-scale installations of the anaerobic contact process have been reported [9, 28].

The Anaerobic Filter

The first reports on the anaerobic filter (Figure 7) were presented by McCarty in 1966 and Young and McCarty in the 1969 [23, 167a]. Their anaerobic filter was packed

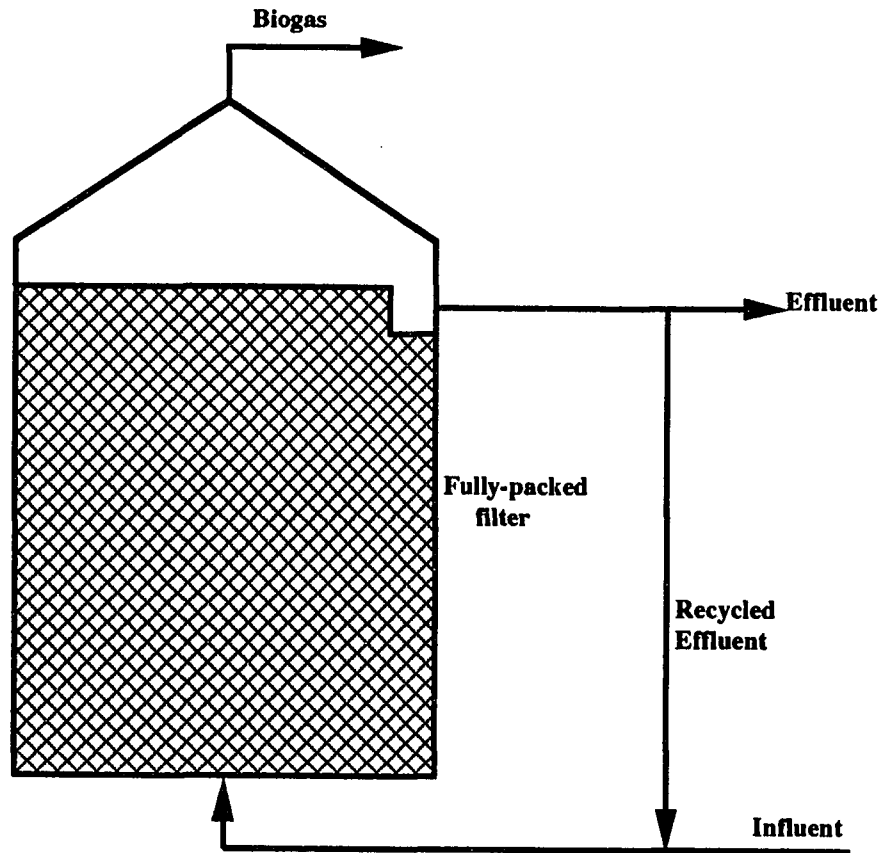


Figure 7. The anaerobic filter.

with quartzite stone media for microbial attachment, similar to the aerobic trickling filters popular for domestic wastewater treatment plants. The typical anaerobic filter operates in an upflow mode, with the influent waste stream entering at the bottom of the filter and exiting at the top. However, some anaerobic filters are operated in a downflow mode, with the influent waste stream entering at the top and the effluent exiting at the bottom. Recycle of the effluent to the influent line may or may not be practiced. The anaerobic

filter was the first of the so-called second-generation anaerobic treatment processes, which allowed the attainment of very long SRTs without the requirement of returning sludge to the reactor. Rather, the biomass attaches to the media and is caught in the interstitial spaces between the attachment media, and is thus retained in the reactor rather than exiting with the liquid effluent.

In Young and McCarty's paper, the authors point out that the anaerobic filter has many advantages over conventional biological treatment processes, including: (1) the anaerobic filter is suited for treatment of soluble wastes, (2) no effluent or solids recycle is required, (3) dilute wastes can be treated efficiently because of the accumulation of high concentrations of biological solids (long solids retention time), and (4) very low volumes of sludge are produced, which reduces sludge disposal costs.

The first anaerobic filters of Young and McCarty were operated at 25°C with the flow introduced at the bottom of the filter and exiting at the top without recycle. The filters consisted of plexiglass columns filled with smooth quartzite stone (1 to 1.5 inches in diameter); the completed filter had a porosity of 0.42. Two separate synthetic substrates were studied: a protein-carbohydrate mixture and a volatile acid mixture (acetic acid and propionic acid). Compared to modern anaerobic filters, the filters were operated at relatively low organic loading rates (0.4 to 3.4 g COD/L/day) with COD removals near or above 90 percent except at the higher loadings. The authors obtained the higher organic loadings by decreasing the hydraulic retention time (HRT) to as low as 4.5 hours (based on the void volume of the filter). Significant washout of biomass occurred at these low

HRTs, resulting in poor COD removal efficiencies [167a]. Hentz and Harremoes [55] presented a comprehensive literature review on waste treatment using anaerobic filters.

The Hybrid Anaerobic Filter

The anaerobic filter became popular during the 1970s because of its loading and hydraulic capacity and its ease of operation. However, plugging of the media over time resulted in channeling of the influent through the filter and decreased organic removal efficiencies. A modification to the anaerobic filter was made by removing the lower portion (one-third to two-thirds) of the attachment media. The new reactor, termed the hybrid anaerobic filter, or the upflow blanket filter (UBF), reduced the chances of plugging by having a suspended growth system in the bottom of the filter (Figure 8). However, the media at the top of the filter was still able to maintain high biomass concentrations within the filter. Additionally, capital costs are reduced because of the smaller amount of filter media required.

Guiot and van den Berg [13] studied a UBF which consisted of an open volume in the bottom two-thirds of the reactor with the top third containing plastic rings as the support media. The authors used a soluble sugar waste as the substrate. The reactors were operated at 27°C. The COD removal efficiencies were above 95% for loads up to 25 g COD/L/day. Similar removal efficiencies were obtained when the HRT was reduced to as low as 3 hours. Droste et al. [10] used a similar UBF to treat domestic strength

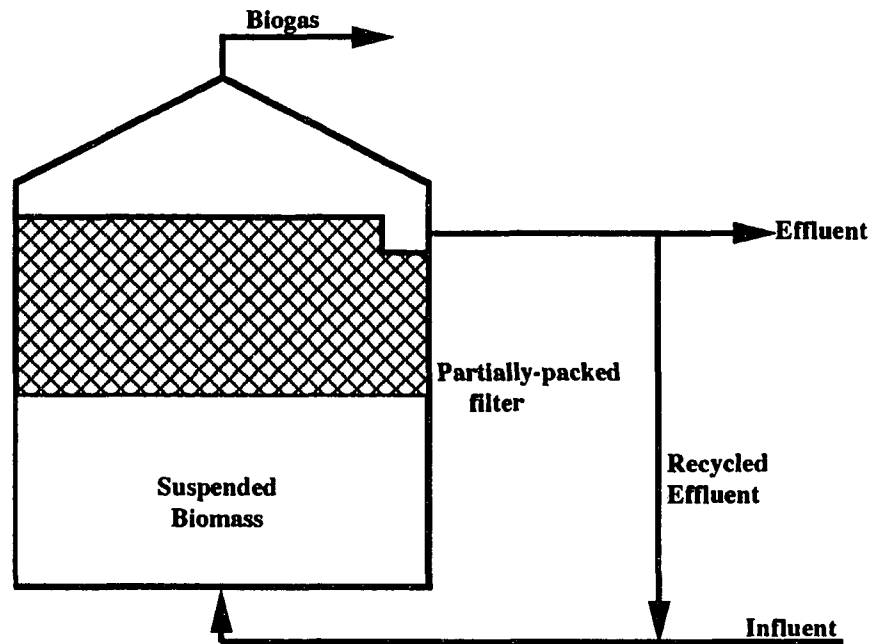


Figure 8. The hybrid anaerobic filter.

wastewater (300-1,000 mg COD/L) at 27°C. Results indicate that 95% soluble COD removal efficiency at HRT's down to 3 hours were possible.

The Expanded-Bed Anaerobic Reactor

The expanded-bed reactor (Figure 9) was developed in order to overcome the problem of clogging that sometimes occurs in the upflow anaerobic filter. The expanded-bed reactor is operated similarly to the anaerobic filter, except that the fixed attachment media of the filter is replaced by a granular matrix which does not occupy the entire reactor volume. The matrix may occupy one-third to one-half of the reactor volume when

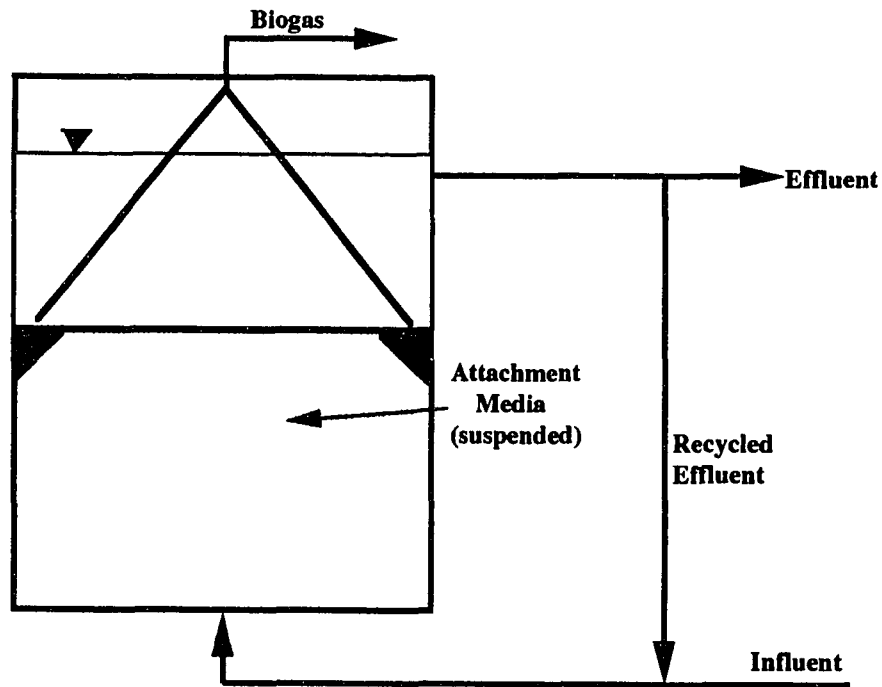


Figure 9. The anaerobic expanded-bed (fluidized-bed) reactor.

allowed to settle to the bottom of the reactor. However, during operation of the expanded-bed reactor, the upflow velocity of the influent wastewater causes the matrix to expand and become fluidized. Bacteria attach to the matrix, which may consist of sand, granular activated carbon, glass beads, or a number of other materials. It is normally necessary to recycle effluent to the reactor in order to obtain the upward liquid velocities necessary to fluidize the bed. The granular matrix provides a large surface area for biomass attachment

and also precludes clogging of the reactor due to the high porosity inherent in the fluidized bed. A basic disadvantage of the process is the high effluent recirculation required to expand the media bed. Another problem which has been encountered is one of changing specific gravity of the matrix. For example, initially, the sand used for the matrix may have a specific gravity of 2.5. However, after bacterial attachment and growth, the overall specific gravity of the sand/bacterial matrix may be considerably less. If the upflow velocity is kept constant, particles may be washed out of the reactor over time due to their decreased specific gravity (decreased settling velocity).

Wang et al. [159] studied the treatment of an acetic acid wastewater using the EBR with granular activated carbon as the media. The reactor was operated at 35°C, and a bed expansion of approximately 25% was maintained by recirculating effluent at about 1,000 times the influent feed flow rate. The HRT was maintained constant (value not given), and the acetate concentration in the feed ranged from 800 mg/L to 6,400 mg/L. The results showed that removal of acetic acid and COD exceeded 98 and 97%, respectively, for all concentrations studied (steady-state). The authors also note that the EBR responded positively to sudden increases in the organic load. A doubling of the organic load caused an almost immediate doubling in the gas production rate.

Fox et al. [38] compared the performance of EBR's with respect to media types. The media types used were low-density anthracite (0.7 mm average diameter), granular activated carbon (0.7 mm average diameter), and two sizes of sand (0.35 and 0.7 mm average diameters). Temperature was 35°C, bed expansion was 50%, and acetate was used

as the sole organic source. The HRT and organic loading rate were maintained at 12 hours and 10.6 g COD/L/day, respectively. Results from this study show that removal efficiencies for all media were consistently greater than 90%. The granular activated carbon (GAC) accumulated biomass at a faster rate during start-up than the other media studied, and, therefore, required less time to reach maximum efficiency based on COD removal.

The Upflow Anaerobic Sludge Blanket Reactor

One of the most widely-used of the so-called second generation anaerobic reactors is the upflow anaerobic sludge blanket reactor (UASB), which was introduced in 1980 by Lettinga et al. [85]. The UASB had been studied in Lettinga's laboratory in The Netherlands since 1971. The UASB is a continuous-flow, suspended growth system that is similar to the anaerobic filter, except that the UASB contains no attachment media (Figure 10). Wastewater enters the UASB at the bottom and exits at the top. The UASB relies on the formation of a "sludge blanket" which forms when the upflow velocity of the wastewater is equal to or less than the settling velocity of the biomass. The blanket is, in effect, suspended in the bottom portion of the reactor. Wastewater flows upward through the blanket, where the organic constituents of the wastewater are metabolized.

The authors studied many different substrate types and loading combinations, and found that the UASB could handle organic loading rates in excess of 25 g COD/L/day at HRTs as low as 3 hours. An important operational characteristic of the UASB is the

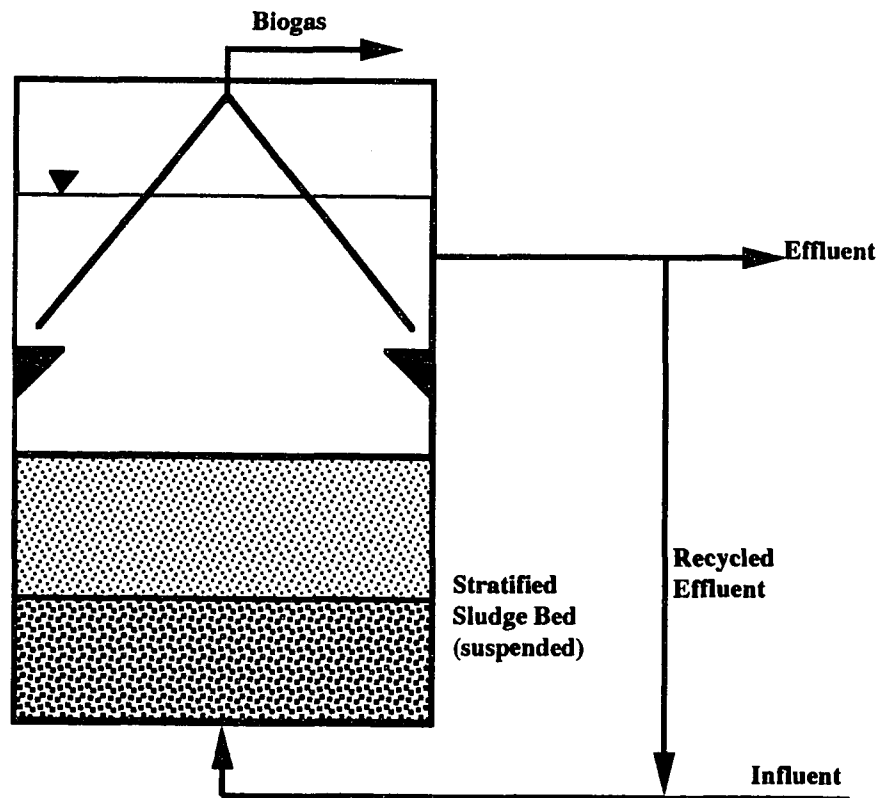


Figure 10. The upflow anaerobic sludge blanket reactor.

formation of a sludge of superior quality with respect to settling and specific gravity. The formation of this sludge, known as granular sludge, was thought to be the result of a combination of factors: (1) the sludge was exposed to varying forces of gravity compression; (2) the creation and maintenance of favorable conditions within the reactor, especially the presence of calcium ions and other nutrients, gentle mixing from gas releases, and the absence of a high concentration of poorly flocculating suspended matter

in the wastewater; and (3) the finely dispersed fraction of the sludge will naturally be washed out with the effluent, leaving the high quality sludge behind.

In a later paper, Lettinga et al. [84] studied the effect of temperature on the UASB reactor performance. The UASB was shown to be efficient in the treatment of several wastes (volatile fatty acids, alcohol, potato processing) at temperatures ranging from 19 to 35°C. The COD loads ranged from 3 to 62 g/L/day, and COD removals (filtered) were consistently greater than 90%. Numerous other studies by these and other authors report on the UASB as applied to various wastes under varied conditions [13, 37, 69, 78, 83, 132, 133, 139, 157, 160, 166].

It is generally accepted that the performance of the UASB depends largely on the formation of a granular sludge. The mechanisms responsible for granular sludge formation are not well understood, however. The phenomenon of granulation is discussed in detail in a later section.

The Anaerobic Sequencing Batch Reactor

Background and Fundamentals. A relatively new high-rate anaerobic process, termed the anaerobic sequencing batch reactor (ASBR, Figure 11), was developed in the late 1980s in the environmental engineering laboratories at Iowa State University under the direction of Dr. Richard Dague. Initial research on the ASBR dates back to the 1960s at which time Dague conducted research on "anaerobic activated sludge" as part of his doctoral research [23a]. At that time, it was recognized that the process could achieve

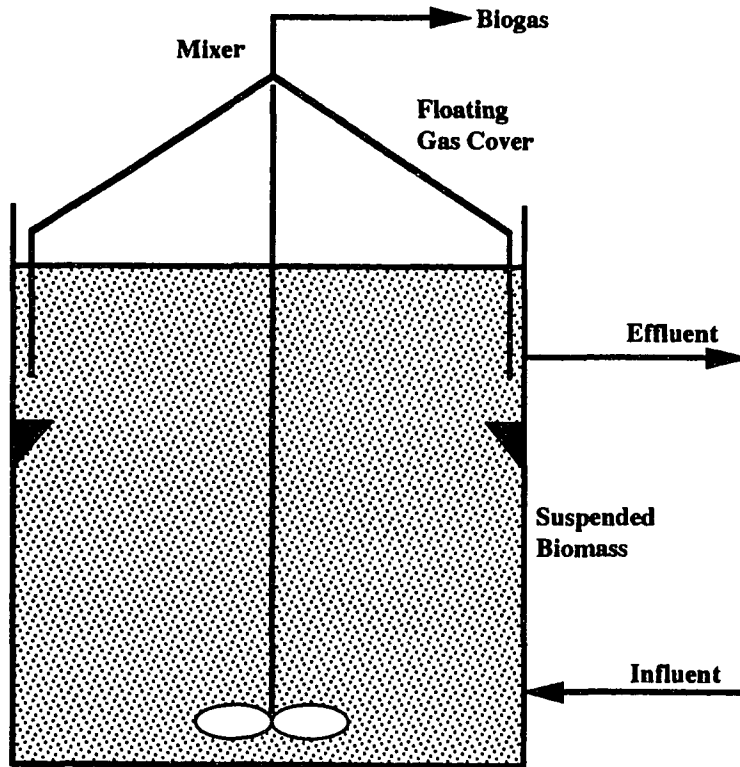


Figure 11. The anaerobic sequencing batch reactor.

long SRTs while maintaining a low HRT due to internal clarification of the biomass prior to decanting. Some twenty years later, the concept of the anaerobic batch reactor was revisited, resulting in several preliminary studies on the ASBR [24, 25, 48, 73, 116].

Since the ASBR is the topic of this document, a detailed description of the ASBR process and applications of the process to waste treatment follows.

The ASBR (Figure 11) is a suspended-growth system which operates in a cyclical batch mode with four distinct phases per cycle. The four phases are (1) the substrate feed phase, (2) the react phase, (3) the quiescent settle phase, and (4) the effluent decant phase. These four phases are outlined below and shown schematically in Figure 12.

- Substrate Feed:** The substrate is introduced into the partially-empty reactor to the design liquid volume (while mixing).
- React:** The ASBR contents are mixed continuously or intermittently and stabilization of the organic substrate is proceeds.
- Quiescent Settle:** All mixing is turned off and the biomass is allowed to settle, forming a clear supernatant.
- Effluent Decant:** The supernatant is pumped out of the ASBR to the design minimum liquid level.

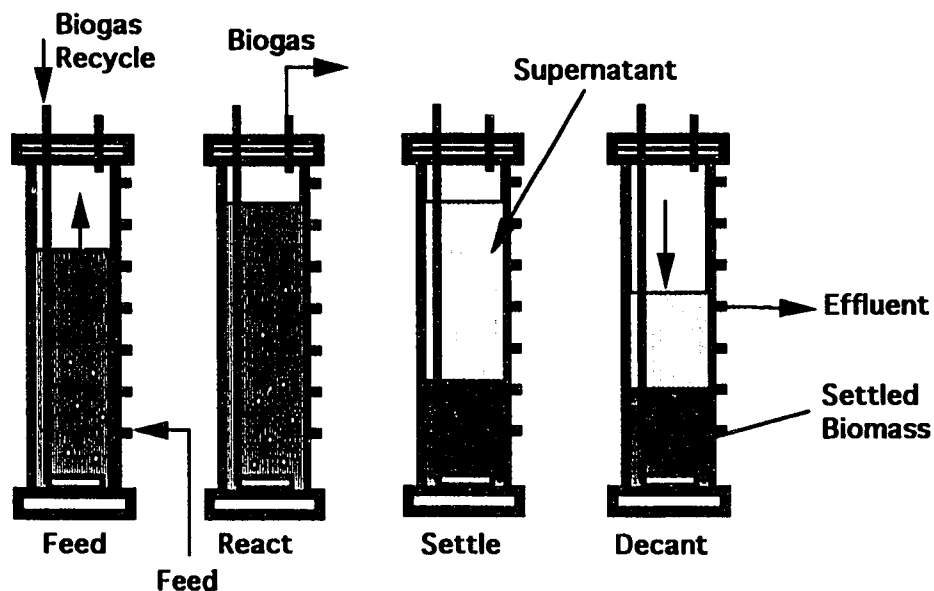


Figure 12. The phases of the anaerobic sequencing batch reactor.

The batch mode of operation inherently selects for optimum reaction kinetics during the four phases of operation. During the feed and the initial part of the react phases, the substrate concentration is at its maximum level. During the settle and decant phases, the substrate concentration is at its minimum level. The Monod function [81] can be used to describe the substrate removal rate as a function of the substrate concentration (Equation 23 and Figure 13). Examination of the Monod function reveals that at low substrate concentrations (settle and decant phases of the ASBR cycle) the substrate removal rate is low. Therefore, the biogas production rate is also low, creating optimal conditions for biomass sedimentation. Conversely, at high substrate concentrations, the removal rate (and biogas production rate) is high, providing fast metabolism of the substrate and internal gas mixing for better biomass-substrate contact. Within the context of the ASBR, the substrate concentration decreases over a cycle period, resulting in a decreasing substrate removal rate and biogas production rate over a cycle period.

$$\frac{ds}{dt} = \frac{k_m M s}{K_s + s} \quad (23)$$

- where, s = substrate concentration in the reactor, mass/volume
 k_m = maximum specific substrate removal rate (mass of substrate removed per unit biomass per time), time⁻¹
 K_s = half velocity constant equal to the substrate concentration at which ds/dt is equal to $\frac{1}{2}$ the maximum substrate removal rate (k_m), mass/volume
 M = amount of biomass in the reactor, mass/volume
 t = time

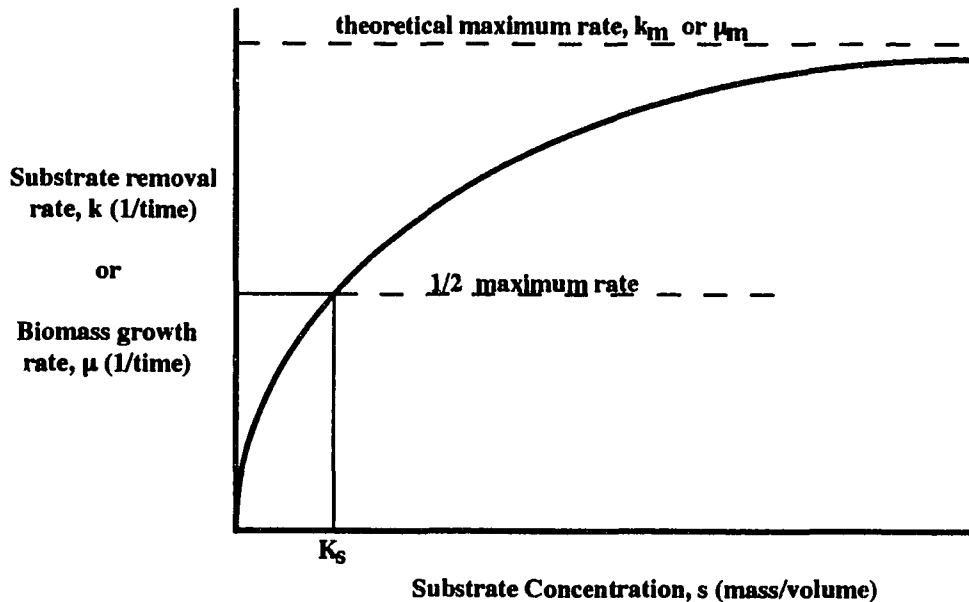


Figure 13. Graphical representation of the Monod function.

Figure 14 represents a theoretical substrate concentration curve over four cycles of ASBR operation. Note that at the end of each cycle, the substrate concentration is a minimum, resulting in a well-settling biomass just prior to the decant phase of each cycle.

Another advantage to the ASBR is that substrate conversion and biomass sedimentation occur in one reactor, eliminating the need for a separate clarifier (as in the anaerobic contact process), and saving capital costs. As previously stated, mixing may be performed continuously or intermittently. Dague et al. [26], and Sung and Dague [145] reported on the use of intermittent mixing rather than continuous mixing. Both of them

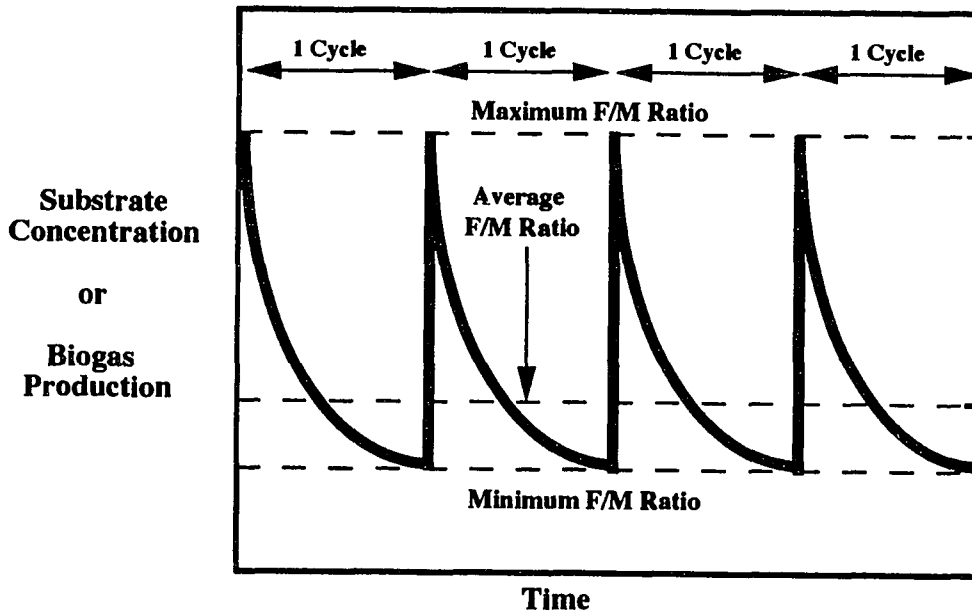


Figure 14. Theoretical substrate concentration and F/M ratio over time in the ASBR.

observed equal or greater COD removal efficiencies with intermittent mixing as compared to continuous mixing. The researchers also observed better clarification of the supernatant with intermittent mixing, most likely due to less shearing of the biomass flocs.

Research on the ASBR. The first study devoted to the ASBR process was conducted by Habben and Dague in the latter 1980s and the 1990s [24, 25, 48]. The ASBRs of this study had liquid volumes of 13 liters and were fed a synthetic substrate consisting of non-fat dry milk plus appropriate nutrients and trace elements. HRTs of

0.54, 1.08, and 2.17 days and COD loadings ranging from 0.5 to 5 g/L/day were investigated at 35°C. This initial system was capable of 80% COD removal (at the two longer HRTs) when the COD load was 3 g/L/day or less. Higher COD loads resulted in decreased efficiency and failure of the system at 5 g COD/L/day.

Pidaparti [116] and Schmit [136], in 1991 and 1992, respectively, reported on the ASBR treatment of swine waste at 35, 25, and 20°C. It was found that at 35°C (HRT = 6 days), volatile solids (VS) loading rates of 1.09 to 5.38 g/L/day were investigated, with the volatile solids destruction ranging from 87 to 74%, respectively. At 25°C (HRT = 6 days), VS loading rates of 1.04 to 6.82 g/L/day were treated to VS destruction efficiencies of 92 to 77%, respectively. At 20°C (HRT = 6, 9, and 12 days) the VS destruction decreased to an extent. At VS loadings of 0.9 to 5.4 g/L/day, VS destruction ranged from 40 to 70%, but was generally about 50% at VS loading rates greater than 2 g/L/day.

Kaiser [73] studied the ASBR treatment of non-fat dry milk at thermophilic temperatures (55°C). The writer demonstrated the capability of the ASBR to achieve stable treatment at COD loadings as high as 9 g/L/day at HRTs of 1, 2, and 5 days. This compared to only 3 or 4 g COD/L/day for the mesophilic ASBRs of Habben [48], indicating that much higher organic loading rates may be possible at higher temperatures. It was also noted, however, that the mixed liquor concentration in the thermophilic ASBRs could not be increased to high levels as is the case for mesophilic ASBRs. This phenomenon was mainly attributed to the increased endogenous decay rates at the higher temperature. Although the biomass growth rate also increases at the higher temperature, it

is probable that the increased COD loads possible in the thermophilic ASBRs was not sufficient to sustain enough growth of the biomass to overcome the increased endogenous decay rates.

Herum [56] studied the effect of applying a vacuum (six inches of water head) to the headspace of mesophilic ASBRs during the final mixing cycle, just prior to the settle phase. It was hypothesized that removal of attached biogas from the biomass would enhance settling, thereby resulting in higher MLSS levels and COD removal efficiencies. The previously-described anaerobic contact process utilized a similar process for these same reasons. The vacuum applied to the ASBR was found to significantly improve sludge settleability, with a resulting decrease in biomass lost in the effluent from the reactor (longer SRT). The increased biomass concentrations allowed for better COD removal efficiencies at all COD loading rates, but especially improved the performance of the ASBR at the higher COD loading rates (up to 10 g/L/day). The higher MLSS also provided for better recovery from shock loads, in which the COD loading rate was quickly increased.

Ndon and Dague [106a] reported on the treatment of dilute wastewater over a range of temperatures. Non-fat dry milk with BOD₅ concentrations of 200 to 500 mg/L (COD = 400 to 1,000 mg/L, respectively) was treated at temperatures of 35, 25, and 15°C. Four ASBRs were operated independently at HRTs of 12, 16, 24, and 48 hrs. Soluble COD removal efficiencies were generally in excess of 80% under all conditions and generally greater than 90% at the longer HRTs and higher temperatures. It was noted that the ASBR

is able to select for organisms that have relatively high affinities for a given substrate (low K_m values). During the latter portion of the react phase, the organisms compete for the limited remaining substrate. Those organisms that have a high affinity for the substrate (mainly acetate) are able to survive and out-compete those organisms with a lower affinity for the substrate. As a result, the ASBR selects for those organisms that can survive under limiting substrate levels, with the result being very low effluent substrate concentrations [106a].

The ASBR has also been applied to several industrial wastewaters with promising results. Tormanen [153] experimented with mesophilic ASBRs treating a high-sodium starch wastewater. Sodium levels averaged 4,000 mg/L and were not shown to be inhibitory to the process. Tormanen's system employed three ASBRs, two of which were seeded with anaerobic digester sludge and one that was seeded with granular sludge (granular sludge will be discussed in detail later). HRTs ranged from 18 hrs to 3 days, which corresponded to COD loadings of approximately 6 to 1.7 g/L/day, respectively. Efficient treatment (80 to 90% total COD removal) was reported for all three ASBRs at the majority of loading rates.

Another "real-world" waste to which the ASBR has been applied is a landfill leachate from the Iowa City, Iowa, municipal landfill [60]. Two mesophilic ASBRs were used in this study, one seeded with non-granular anaerobic digester sludge and the other with granular sludge. The granular ASBR consistently outperformed the non-granular ASBR in terms of COD removal efficiency. COD loading rates of 1.6 to 3.4 g/L/day and

HRTs of 12 to 48 hrs were tested. The granular ASBR consistently removed 90% of the influent COD, whereas the non-granular ASBR showed unstable operation, with COD removals ranging from 30 to 90%.

Perhaps the most significant study to date on the ASBR was that of Sung and Dague [145]. The researchers studied the effect of mixing and reactor configuration on the performance of the ASBR operated at 35°C and treating a non-fat dry milk substrate. Their 1992 paper presented the fundamental principles of the ASBR and included a design model based on Monod kinetics. It was observed that intermittent mixing of the ASBR was as efficient as continuous mixing in terms of methane production and COD removal efficiency. An obvious implication of this finding is that significant energy savings can be obtained by mixing the ASBR only two or three minutes out of each hour of operation.

Reactor configuration was also seen to have an influence on the maximum MLSS values that could be obtained in Sung and Dague's study [145]. Shorter, squatter reactors were able to accumulate more biomass than could be accumulated in the taller, thinner reactors. The squat ASBR (depth:diameter ratio = 0.61) was able to achieve an MLSS level near 30,000 mg/L, whereas the tall ASBR (depth:diameter ratio = 5.60) could only achieve an MLSS level of about 20,000 mg/L under most loading conditions. An interesting observation was made after approximately 10 months of operation: the biomass in all of the ASBRs began to granulate. The tall reactors achieved a higher degree of granulation than the squat reactors, which was attributed to the greater depth to which the biomass had to settle in the tall ASBRs in order to remain within the reactor. That is, a

greater depth of liquid (but equal volume) was decanted out of the tall ASBRs each cycle. Therefore, the poorer settling particles were decanted out of the ASBR, thus selecting for the fastest settling biomass, which is a characteristic of granular biomass. The granulated biomass allowed for higher COD loads to be achieved than was possible previous to these experiments. COD loads up to 12 g/L/day at an HRT of 12 hrs was treated to 90% soluble COD removal efficiency [145]. The achievement of granulation, although taking almost 300 days, was the driving force behind the experiments conducted for the research presented later in the results and discussion section of this document.

On-going ASBR research continues at Iowa State University. Two additional industrial wastes are being treated with ASBRs in the laboratories at ISU. One of these wastes is a high-strength starch wastewater, and the other is a wastewater derived from the production of a product designed to raise the freezing point of water. The latter wastewater contains large quantities of lysed bacteria, which are utilized in the production process. Efficient treatment of both wastes has been demonstrated. A modification of the ASBR process is also under study at this time. The system consists of two ASBRs in series, with the first ASBR operating at thermophilic (55°C) and the second at mesophilic (35°C) temperatures. The substrate is non-fat dry milk and system COD loading rates up to 14 g/L/day (19 g/L/day on the first stage) have been treated efficiently.

The Phenomenon of Granulation

Theory of Bacterial Adhesion and Aggregation

It has been known for some time that many bacterial species tend to adhere to solid surfaces and to other bacteria. It is generally believed that attachment to a solid particle is advantageous to bacteria for several reasons: (1) the solid particle, if organic, may serve as a source of food and nutrients to the attached bacteria; also, surfaces tend to adsorb dissolved molecules, including nutrients, which then provides an ample source of these nutrients to attached bacteria, (2) the competition between bacteria for a limited supply of food is restricted to only the attached bacteria, and (3) the extracellular enzymatic activity of a few bacteria may supply the food and nutrient requirement of the attached population as a whole [6, 36, 61, 75]. The kinetic growth rates and substrate utilization rates of bacteria have also been shown to increase after adhesion to a support or aggregation with other bacteria [11, 35, 36, 131]. In any event, the process of natural aggregation or attachment must be beneficial to the microbes which are able to perform these function; otherwise, they would not have evolved attachment mechanisms [17, 97, 123, 147].

Aggregation of bacteria can be classified in several different ways [7]. Aggregation may be natural or artificial. Natural aggregation occurs if the act of aggregating is part of the natural history of the microbe, whether in nature or in the laboratory. Aggregation is artificial if it is provoked by man-made substances or if it occurs under nonphysiological conditions. For instance, in the activated sludge process for wastewater treatment, natural aggregation occurs due to flocculation of the bacteria through their own mechanisms [39].

Under low energy (mixing) conditions and low F/M ratios (low substrate concentrations), the bacteria in an activated sludge system tend to flocculate and form aggregates of biomass. This flocculation may be enhanced by the addition of man-made chemicals. Aggregation may also be active or passive. Active aggregation occurs when naturally dispersed populations of bacteria come together and adhere to each other. Passive aggregation arises from the failure of progeny to separate from each other after cell division [7].

Microbial adhesion and aggregation (hereafter referred to simply as aggregation, unless noted otherwise) is generally believed to be the result of a number of interactions between the microbe and the surface to which it attaches, whether that surface be an inert solid, an organic particle, or another microbe. Ionic, dipolar, hydrogen bonds, and hydrophilic interactions, as well as other chemical interactions, have all been demonstrated to have an effect on microbial aggregation [57, 128, 161]. Additionally, bacterial appendages, such as flagella, fimbriae, and pili, have been shown through electron microscopy to enhance contact between microbes by physically holding on to other microbes [7, 20, 72, 75, 140]. Extracellular polymers (e.g., capsules) also tend to enhance aggregation due to physical encapsulation of nearby bacteria and one or more of the interactions listed above [57, 75, 146].

Specific interactions that enhance aggregation have been studied in pure culture with many strains of bacteria and unicellular eukaryotes. Calcium ions (Ca^{2+}) have been implicated in several instances. It is hypothesized that Ca^{2+} may act as a salt bridge

between negatively charged surfaces. For example, two carboxyl groups may be attached to each other through a Ca^{2+} bridge [123, 127]. Extracellular polysaccharides, lipids, and proteins have also been observed to affect aggregation without the help of other ions in solution. These molecules contain a wide variety of negatively and positively charged groups, polar groups, and hydrophobic or hydrophilic groups. Ionic bonds, hydrogen bonds, and hydrophobic interaction between extracellular macromolecules may bring about aggregation of nearby bacteria [15, 20, 75, 122, 130].

The previous paragraphs give a brief description of the overall process of bacterial aggregation and adhesion. It is not intended to fully describe the phenomenon, but rather to present the current theories and knowledge regarding aggregation and adhesion. The following sections discuss the more specific phenomenon of aggregation, or granulation, in anaerobic treatment systems.

General Characteristics of Granules in Anaerobic Systems

The phenomenon of granulation has been mentioned previously. A more detailed discussion of the topic is presented here. In general terms, granulation is the process by which bacteria and extracellular biopolymers and inorganic materials are incorporated into a dense, pelletized particle. Granular biomass is visually and physically different from the usual flocculent biomass, such as would be obtained from a typical anaerobic digester at a municipal wastewater treatment plant.

The definitions of flocculent and granular biomass that will be followed in this discussion are as follows [33]:

Flocculent biomass is a conglomeration of bacteria and other particles which exhibit a loose structure. After settling, a layer of flocculent biomass forms in which the detection of individual flocs is difficult, if not altogether impossible. During mixing of a flocculent biomass, there are few, if any, discrete particles, and the biomass appears to be evenly distributed throughout the liquid and is indistinguishable from the background liquid.

Granular biomass is a conglomeration of biomass and other materials which have a well-defined structure and boundary to the unaided eye. After settling, granules are still visible as separate entities, and during mixing, the MLSS appears as many discrete pellets which are distinguishable from the background liquid.

The granules are generally spherical in shape and may grow to several millimeters in diameter. Some granules are black, some are gray, and others are white, depending on the species present within the granule, the substrate, the environmental conditions, and the age of the system. Granules also settle much more rapidly than flocculent biomass. Granules settle as discrete particles, similar to the settling characteristics of sand or pebbles.

Flocculent biomass separates in the hindered settling class of settling, with a zone of clarification moving downward as the biomass settles [3, 100].

A significant amount of research has been devoted to the formation of granules in anaerobic systems. These research efforts are discussed in the following pages. The vast majority of the anaerobic work has been devoted to the granulation process in the UASB and fluidized-bed reactors. Modifications of the UASB have also been studied in relation to their granule-development capacities. The following review is intended to discuss the current theories of granule development, including hypothesized mechanisms of granulation and appropriate environmental and operational conditions necessary for efficient granulation in the various anaerobic processes. A section is included on granulation in the ASBR, however, most of the review is devoted to granulation in the UASB since a significant amount of research has been conducted on this system.

Granulation in the ASBR

First Report of Granulation

As previously stated, to date there has been only one reported incidence of granulation in the ASBR [145]. Sung and Dague [145] reported the formation of granules in four separate ASBR reactors, each with a different depth to diameter ratio. The depth to diameter ratio for the ASBRs were reported as 5.60, 1.83, 0.93, and 0.61. The basis for selecting different depth to diameter ratios was to determine the optimum ratio for the ASBR system from an operational standpoint.

What was not anticipated, however, was that each ASBR would select for a granular biomass in varying degrees. The ASBRs were operated at identical HRTs and OLRs. Therefore, the volume of liquid decanted from the ASBRs were identical, but the depth decanted per cycle varied between the four ASBRs. That is, it was required to decant a greater depth of liquid from the tall, thin ASBR than from the short, stout reactor. This, in effect, washed out the poorer-settling biomass in the tall ASBRs more rapidly than in the short ASBRs. Through this process, the tall, thin reactors tended to develop a more rapidly settling biomass than did the short, stout reactors. Granulation was observed after more than six months of operation treating a non-fat dry milk substrate at 35°C. After more than 10 months of operation, the average granule size in the four ASBRs were 1.3, 0.8, 0.6, and 0.6 mm, reported in order of decreasing depth to diameter ratios, respectively.

It was also noted, however, that the maximum MLSS concentration that could be achieved in the tall, thin ASBRs was not as high as the MLSS that could be achieved in the shorter ASBRs. The highest MLSS values were reported as (in order of decreasing depth to diameter ratio) 24,600, 26,500, 33,600, and 29,400, respectively. Additionally, the ASBRs with depth to diameter ratios of 5.60 and 1.83 were not able to achieve OLRs greater than 8 g COD/L/day. The other two ASBRs, however, were able to treat OLRs up to 12 g COD/L/day (HRT = 12 hrs). The soluble COD removal efficiency of the two short ASBRs were 81 and 72%, and the total COD removal efficiency was 92 and 90%, respectively, for the depth to diameter ratios of 0.93 and 0.61.

The reason for the failure of the two tall ASBRs at lower OLRs was reported as biomass washout due to excessive foaming. The non-fat dry milk substrate contained approximately 36% protein by weight. Protein degradation has been attributed to foaming in anaerobic digesters. The biomass tends to get trapped in the foam, and is then carried out of the reactor. In Sung and Dague's study, it was noted that excessive foaming in the tall ASBRs occurred, leading to decreased MLSS concentrations and poorer removal efficiencies [145]. Although the short ASBRs received the same protein load as the tall ASBRs, foaming was not as significant due to the larger surface area over which the foam developed. With a larger surface area, the biogas produced has a shorter distance to travel before exit from the ASBR. Therefore, less biomass will be carried up to the surface and trapped in the foam layer. It therefore appears that there is some optimum ASBR depth to diameter ratio that will rapidly select for granulation but will also not be subject to severe foaming problems.

Further studies with Granular Biomass in the ASBR

The previous paragraphs summarize the literature to date on granule-development in the ASBR. There have been, however, ASBR studies (at ISU) on the treatment of various wastewaters using granules developed in Sung and Dague's study [145], as well as using granules developed in a UASB reactor [60, 153]. These experiments were designed to study the difference between granular and flocculent biomass treating various wastes.

Hollopeter [60] studied the ASBR treatment of landfill leachate with two ASBRs, one seeded with flocculent municipal digester biomass and the other seeded with granules developed in Sung and Dague's study. Both ASBRs were acclimated to the leachate by mixing the leachate with non-fat dry milk. The proportion of leachate was gradually increased over time until full strength leachate (COD varied between 600 and 4,000 mg/L) was being fed to the systems. The non-granular ASBR was not able to operate at an HRT less than 24 hrs, and the COD removal efficiency was unstable, varying between 30% and 90% at OLRs of 1.7 and 0.7 g COD/L/day, respectively. The granular ASBR, on the other hand, achieve stable and efficient COD removals at HRTs of 48, 36, 24, and 12 hrs, and at OLRs up to 3.5 g COD/L/day (this was the highest load possible for the leachate wastewater due to the low COD concentration of the leachate). COD removals averaged over 90% at all operational conditions for the granular ASBR [60].

Tormanen [153] studied the treatment of a high-sodium starch wastewater using one ASBR seeded with granules obtained from a full-scale UASB treating a brewery wastewater, and two ASBRs seeded with municipal digester biomass. The COD of the starch wastewater was approximately 5,000 mg/L, and the sodium concentration was normally between 3,000 and 5,000 mg/L. The ASBRs were initially started using the full-strength wastewater at an HRT of 3 days, which correlated to an approximate OLR of 1.7 g COD/L/day. The HRT was then gradually reduced to 18 hrs over a period of several months, resulting in a final COD load of 6 to 7 g/L/day. The COD removal efficiency of the granular ASBR was stable from the beginning of the experiments. The non-granular

ASBRs, however, took three to four months to achieve stable operation at the initial COD loading rate.

After acclimation to the wastewater, however, all of the ASBRs in Tormanen's study were able to remove in excess of 90% of the soluble COD, with slightly lower total COD removals reported. There was not a significant difference between the granular and non-granular ASBRs, as was reported in Hollopeter's study [60]. It was observed, however, that the non-granular biomass in the ASBRs matured over time and exhibited some granular characteristics such as efficient settling. Analysis of the biomass particles from the non-granular ASBRs revealed a slight increase in size over time, but significant granulation had not occurred. The biomass from the granular ASBR, on the other hand, showed a slightly different morphology over the course of the experiments. At the start of the study, the granules were well-defined, roughly-spherical pellets. By the end of the study, the granules had approximately the same overall size, but were more filamentous in nature. This latter observation may have been effected by changing from a brewery wastewater to a starch wastewater, with the subsequent development of a different consortia of bacteria [153].

Granulation in the UASB and Expanded-Bed Processes

The majority of the literature concerning granulation in anaerobic systems to date has been focused on the UASB reactor and the fluidized-bed reactor, each of which have been described earlier. Granular biomass has been studied with respect to its morphology,

microbiology, chemistry, and activity. Numerous studies have also been conducted regarding the significance of various parameters on the formation of granules. The following paragraphs discuss these issues.

Granule Microbiology and Morphology

Several studies have been conducted to elucidate the microbiological make-up of granular biomass. From the discussion of the interaction of the various anaerobic bacterial groups presented earlier, it is apparent that the formation of a densely-populated "micro-colony," which contains members from all three groups of bacteria, would be beneficial to each group in that efficient transfer of intermediate products could result. In effect, the thermodynamics of the entire anaerobic degradation process are improved by granule formation. Although this transfer also occurs in flocculent biomass systems, the distance that each intermediate product must travel is minimized in a system in which the bacteria are fixed in a position close to other bacteria [111, 134].

Bacterial populations within granules have been studied by various techniques, including the most probable number (MPN) analysis. Table 7 shows the results of several tests designed to determine the number of specific bacterial groups in granules [31, 33].

It has been noted that the MPN technique is only accurate to within one or two orders of magnitude [33]. Therefore, the two studies referenced in Table 7 appear to be relatively consistent with each other.

More specific studies have been conducted to identify bacterial species present in granular biomass. Traditionally, scanning electron microscopy (SEM) has been used to qualitatively determine the types of bacteria present (rods, cocci, etc.). The bacteria observed with the SEM could then be compared to the morphologies of known methanogens and other anaerobes, and a qualitative analysis could be made with the identification of some of the species present within the granule [10, 31, 37, 64, 80, 89, 102, 119]. More recently, immunological probes and fluorescence techniques have become popular methods of identifying specific species of bacteria, especially methanogenic species [34, 76, 88, 101, 118, 158]. The immunological probes utilize polyclonal antibodies specific for a given bacterial species to determine the presence of that

Table 7. Bacterial counts in granules from UASB reactors [31, 33].

Bacterial Group	Substrate	Number of Bacteria/mL ^a	
		Starch ^b	Sugar ^c
Acidogens	glucose	10 ⁹	nd ^d
	sucrose	nd	10 ¹⁰
	lactate	10 ⁹	nd
Acetogens	propionate	10 ⁸	10 ⁷
	butyrate	10 ⁸	10 ⁷
	valerate	nd	10 ⁷
	ethanol	10 ⁹	nd
Methanogens	H ₂ /CO ₂	10 ⁹	10 ⁹
	acetate	10 ⁹	10 ⁸

^a Determined by most probable number analysis.

^b Granules from a UASB treating a starch wastewater.

^c Granules from a UASB treating a sugar wastewater.

^d Denotes that this number was not determined.

species within a matrix of bacteria. Fluorescence techniques rely on the fact that some methanogenic coenzymes fluoresce after absorption of light at specific wavelengths (previously presented). Fluorescence may be used to distinguish methanogens from non-methanogens [76, 101].

Species of *Methanothrix* and *Methanosarcina* have been implicated by many researchers as being the most abundant methanogens present in granules treating a wide variety of wastewaters, including sugar, starch, paper mill, and brewery wastewaters. *Methanothrix* has especially been singled out as a common bacterium in most granular sludges [31, 37, 64, 102]. It has been postulated that in anaerobic systems with low acetate concentrations, *Methanothrix* will out-compete *Methanosarcina* due to the former's lower K_m value (higher affinity) for acetate, although the two species are almost always present within the same granule in varying degrees. At high acetate concentrations, however, *Methanosarcina* is often the dominant methanogen due to its shorter regeneration time as compared to *Methanothrix* [37, 64, 102, 152]. Other significant methanogenic species in granules include *Methanobrevibacter*, *Methanospirillum*, and *Methnobacterium*. Species of these methanogenic genera are often present when the wastewater contains high concentrations of formate and methanol [76, 88, 101].

Another microbiological observation regarding granules include the predation of bacteria present within the granule by viruses and other bacterial predators [119]. Two strains of virus were observed in transmission electron microscopy images of granular cross sections. Several regions of "ghost" bacteria were observed, in which only the cell

walls remained after cell lysis by the viruses. *Methanotherix* spp. were especially prone to virus attack, although *Methanosarcina* and *Methanobrevibacter* were also subject to virus infection [33, 119]. A free-living, helical bacteria was also detected inside ghost cells of *Methanosarcina*, however, it was unclear whether the invasion caused cell lysis or the invasion came after cell lysis due to specific nutrients becoming available for the predator [119].

The morphology and overall structure of granules has been examined in several studies, and has been shown to vary according to the substrate and other factors. There are two common granule structures: the granule may be a layered structure in which the inner granule is distinctly populated with different bacteria than in the outer granule, often with a zone of transition [2, 10, 34, 89, 102, 158]; alternatively, the granule may be a non-layered structure in which the various bacteria are heterogeneously spread throughout the granule with no zones of homogeneity of one bacterium [31, 34]. Most granules contain a layer of extracellular polysaccharide, which may aid in bacterial adhesion to each other and help to hold the granule together [2, 34, 34, 102].

The layered granule structure is more commonly reported in the literature for most types of wastewater. Granular biomass treating sugar wastewaters have been shown to have layered structures [34, 89, 102]. Methanogenic bacteria have been shown to be dispersed throughout the granule; however, the inner portion of the granule normally consists mainly of *Methanotherix* spp., whereas the outer portions normally contain several species of methanogens as well as acetogens and fermentative bacteria. The middle layer

between the two extremes exhibits a syntrophic mixture of H₂-producing acetogens and H₂-utilizing methanogens [34, 89, 102]. Granules treating paper mill and brewery wastewaters exhibited similar layered structures [34, 102]. Acetate has also been shown to develop layered granules [10]. The structure reportedly consisted of an outer layer of densely-packed cells resembling *Methanosarcina*, whereas the inner layers consisted of loosely-packed ovoid cells, with cavities containing clusters of rods.

A non-layered granule structure has been reported for sugar-refining and glutamate wastewaters. The various bacteria were dispersed throughout the granules, with no obvious layers present. It was hypothesized that the degradation of these substrates is limited by the rate of acidogenesis. If this is the case, the substrate (and, consequently, its degradation products) would be fairly uniformly distributed throughout the granule. As a consequence, the bacteria would also be randomly distributed [10, 34].

Another characteristic of granules is their inherent porosity, which is necessary for substrate diffusion to the inner granule and gas release from the granule [10, 33, 77, 89]. Direct observation of gas bubble formation was reported by Bochem et al. [10]. Bubble formation was always observed to begin in the interior of the granule. The bubble then traversed the pores of the granule and was expelled at its surface. High gas production rates were observed to cause erosion of the granule pores, effectively creating larger pore volumes [10, 33].

It is also conceivable that diffusion of the substrate into the interior of the granule may become limiting over time, especially if the substrate concentration is decreased to a

low level. This may result in cell starvation and death in the granule interior, leaving a hollow granule [77]. SEM images of this phenomenon have reinforced this theory.

Hollow granules tend to accumulate gas within their core if the pores of the granule are not large enough to expel the gas at the rate at which it is produced. This phenomenon results in floating granules and loss of biomass. Shearing of the hollow granules to release the entrapped gas was shown to relieve this condition [77].

Granule Chemical Composition

Besides the organic biological composition of granules, inert material often comprise a significant portion of the granule. Inert materials include sulfides, carbonates, potassium, sodium, heavy metals, and several other compounds [2, 4, 31, 32, 33, 37, 77]. In many applications, FeS constitutes up to 30% of the ash fraction, and has been observed sticking to the sheath *Methanothrix soehngeni*. Calcium carbonate has also been observed at high concentrations within the granular matrix. It has been suggested that precipitated inert particles may act as nuclei to which bacteria attach and begin to grow as a granule. The chemical composition of various granular systems has been shown to vary significantly (Tables 8 and 9). These variations are normally attributed to the substrate, including the inorganic compounds contained in the substrate, as well as the bacteria present within the granule. Table 8 presents the general composition of typical granules, and Table 9 summarizes the literature on the elemental composition of various granules.

Table 8. General composition of granules [31].

Component	% of dry weight
Ash	10-23
Protein	35-60
Carbohydrate	
Total	6-7
Extra cellular	1-2
Total organic carbon	41-47
Kjeldahl nitrogen	10-15

Table 9. Granule chemical composition [32, 33].

Element ^a	Laboratory sample ^b	Digester sample ^c
Calcium	9.3	25.0
Magnesium	3.9	7.4
Potassium	13.5	12.0
Sodium	2.9	7.5
Phosphorous	7.6	13.0
Sulfur	18.3	22.0
Iron	9.9	43.0
Nickel	0.5	0.8
Cobalt	---	0.6
Ash	13.0	40.0

^a Units are reported as grams per 1,000 grams dry matter.

^b Granules from UASB treating a mixture of glucose, lactate, acetate, propionate, butyrate, and valerate.

^c Granules from UASB treating a starch wastewater from an industrial source.

Activity of Granular Biomass

The activity of a bacteria or bacterial system can be defined as the rate at which substrate is removed from the system per unit of biomass. In methanogenic systems, the substrate is only removed, or stabilized, through the production of methane. For this reason, the overall activity of an anaerobic system producing methane can be defined as the rate of methane production per unit of biomass (volume CH_4 /unit biomass/time or mass CH_4 /unit biomass/time), often termed the specific methanogenic activity (SMA). Alternatively, the rate of COD removal may also be measured, although this procedure is somewhat more complicated and probably not as accurate as the SMA test. Since the actual concentration of active biomass is not usually known, the volatile suspended solids (VSS) concentration is often used as a surrogate representing the active mass [99].

In the majority of studies, granular biomass displays a higher SMA than that of non-granular biomass [30, 33, 34, 87, 113, 114, 135]. However, when comparing intact granule activity to disintegrated granule activity (whole granules broken apart by high shear or other procedure), it was found that the intact and disintegrated granules displayed similar SMAs. The exception to this was the SMA resulting from sugar, protein, or other fairly complex substrates, in which the granular biomass exhibited higher SMA than the disintegrated granules [30, 32, 135].

Discussion of this latter observation leads to several observations that correlate with the observed SMA of various substrates [30, 32, 135]:

- The anaerobic degradation of sucrose, protein, or other complex starting material to methane requires the function of all three groups of bacteria (acidogens, acetogens, and methanogens). Intact granules are often layered, with the acidogenic bacteria mainly existing on the outer surface of the granule, and the other groups existing within the granule. In this manner, efficient transfer of the end-products of acidogenesis can be maintained, with a subsequently lower diffusional distance and higher overall SMA.
- The anaerobic degradation of intermediate volatile acids (propionate, butyrate, valerate) generally requires the syntrophic association of proton-reducing acetogens and proton-utilizing (H_2/CO_2) methanogens. Disintegration of the granules seldom is effective at completely dispersing the bacteria into individually cells. Therefore, this syntrophic association still remains in disintegrated granules, resulting in similar SMAs of intact and disintegrated granules when supplied with intermediate volatile acids as the starting material for methanogenesis.
- The anaerobic degradation of acetic acid generally requires only the acetoclastic methanogens (e.g., *Methanotherix*, *Methanosarcina*) for conversion to methane. Therefore, disintegrated granules should display similar SMAs for acetate as do

intact granules. In fact, the SMA of disintegrated granules may be higher due to the diffusional limitation of acetate into intact granules.

Table 10 presents a literature summary of the SMA of various systems with respect to the biomass type (granular, disintegrated granules, non-granular). The higher SMA displayed by the granular over the non-granular biomass can be explained on the basis of maturity of the system. It is generally accepted that granule formation occurs after significant populations of *Methanothrix* and *Methanosarcina*, in addition to the other methanogens and non-methanogens, have developed. In non-granular systems, the populations of these slow-growing methanogens are often limiting, resulting in a slower rate of methane production as compared to granular systems in which the granule contains a high population of the important methanogens [30, 87, 135].

Table 10. Specific methanogenic activity of various biomass [32, 87].

Test Substrate	Specific Methanogenic Activity ($\mu\text{mol CH}_4/\text{g VSS}/\text{min}$)		
	Granules	Disintegrated Granules	Non-granular
Acetate	18.4	16.3	3.6
Propionate	8.3	6.4	1.5
Butyrate	12.4	9.8	
Valerate	8.4	8.0	
Lactate	6.7	6.4	
Glucose	81.1	80.4	

Modeling the Granulation Process

Several models of granule development have been presented in the literature. Some of the models are operation-oriented, while others are strictly microbiological in nature. Still others are a combination of these principles [68, 74, 129, 162]. The more popular granulation models are presented below.

Selection Pressure. The selection pressure on an anaerobic system is a combination of hydraulic, gas, and biomass loading rates (gas and biomass loading rates are related to each other) [5, 21, 66, 67, 68]. In a UASB system, the hydraulic load (volume of liquid per volume of reactor per time) is applied by pumping the influent wastewater, together with recycled effluent, up through the UASB. The maintenance of high hydraulic loading rates will cause the light floc particles to be carried out of the UASB with the effluent waste stream, thus selecting for the more rapidly settling floc particles. Gas loading rates (volume of biogas produced per volume of reactor per time) are dependent on the biomass loading rates (mass of substrate per mass of VSS per time). As the biomass loading rate is increased, the gas production rate also increases, provided that the organic removal efficiency of the system does not decrease. The increased gas production provides for better mixing and turbulence, which further helps to remove the light floc particles from the UASB. Besides the benefit of increased gas production, the biomass loading rate also provides the energy and starting materials for biosynthetic

processes. Therefore, as the biomass loading rate is increased, there is more capacity for cell growth and, thus, for granule formation.

By combining the three forces of hydraulic, gas, and biomass loading rates, it is hypothesized that granulation can be stimulated at an early stage of UASB operation. Reports of granulation in as few as 30 days have been reported in UASB reactors by controlling these parameters [21, 66, 67, 68]. The minimum biomass loading rates required for rapid granulation have been reported as 0.6 g COD/g VSS/day [67], although more recent studies have observed granulation at lower biomass loading rates [5, 66, 68]. The upflow velocity in the UASB should be maximized in order to wash out the light floc particles, although excessive upflow rates will cause washout of all floc particles, leading to system failure [67].

Methanobacterium strain AZ. Sam-Soon et al. [129] presented a hypothesis for granule formation in UASB reactors treating carbohydrate and proteinaceous wastes. The researchers claimed that *Methanobacterium* strain AZ (*M. strain AZ*) was responsible for granule formation. Apple juice was used as the substrate in their experiments (temperature = 35°C), and the following aspects were observed [129]:

- The net biomass production was exceptionally high in most of the experiments, with a maximum of 0.36 g biomass/g COD removed.

- The majority of biomass growth was confined to regions of high H₂ partial pressure.
- The system produced soluble organic nitrogen in the regions of high H₂ partial pressure.

Upon review of pertinent literature, the researchers discovered that these observations could be explained by the activity of *M.* strain AZ, which had been studied by Zehnder and Wuhrmann in 1977 and had the following characteristics [129]:

- The organism is a pH neutrophile.
- Hydrogen serves as the sole electron donating substrate, and CO₂ serves as the sole external electron acceptor.
- The organisms is capable of synthesizing all of its amino acid requirement with the exception of cysteine.
- The organism has a high specific growth rate when all essential nutrients are available.
- During the growth of the organism, high concentrations of amino acids are secreted to the external environment.
- The organism grows in rosette-type clusters.

Sam-Soon et al. stated that the hydrogen partial pressure was the single-most important variable in the granulation process, and that high H₂ partial pressures stimulate the activity of *M. strain AZ*. The researchers provided the following explanation for their hypothesis [129, page 76]:

"When the *M. strain AZ* is surrounded by excess substrate, i.e., high H₂ partial pressure, the ATP/ADP ratio will be high. Simultaneously the high ATP level will stimulate amino acid production and cell growth. However, because *M. strain AZ* cannot manufacture the essential amino acid cysteine, cell synthesis will be limited by the rate of cysteine supply. If free and saline ammonia is present in excess there will be an over-production of the other amino acids; the organisms react to this situation by either releasing these excess amino acids to the surrounding medium and/or by linking these in polypeptide chains which it stores extracellularly by extrusion from active sites. These polypeptide chains bind species and other organisms into clusters forming a separate microbiological environment - the so-called biopellets."

The authors further state that granulation is unlikely in completely mixed systems due to the usual low H₂ partial pressure requirement for efficient methanogenesis. Granulation is also unlikely in systems treating the following substrates:

- *Acetate as sole substrate:* methanogenesis from acetate as the sole substrate does not produce H₂, and therefore will not stimulate *M. strain AZ* activity.
- *Propionate as sole substrate:* methanogenesis from propionate requires very low H₂ partial pressures.
- *Fats and oils as substrate:* Fats are broken down to volatile acids and hydrogen only under low H₂ partial pressures.

The best substrate for granulation was reported to be carbohydrates. These substrates release hydrogen during breakdown to volatile acids under a wide range of H₂ partial pressures. Rapid acidogenesis of carbohydrates result in high H₂ partial pressures and stimulate *M. strain AZ* activity.

The Spaghetti Theory. The "Spaghetti Theory" of granulation is based on the presence of *Methanothrix* bacteria as the predominant acetoclastic methanogen [162]. Granulation develops when sufficient concentrations of *Methanothrix* are present in the biomass. If present in low concentrations, conditions must be imposed on the system that will select for *Methanothrix*, such as low acetate concentration. Upon selection for *Methanothrix* bacteria, long filaments (up to 1,000 units long) will develop due to the inherent nature of *Methanothrix* to form filamentous structures. After formation of the initial *Methanothrix* clusters, full granulation of the biomass is stated to be inevitable. Other bacteria are entrapped in the *Methanothrix* clusters, and the bacterial consortia continue to grow and divide. Eventually, the aggregate will grow to sufficient sizes that they are detectable as granules, consisting of a network of *Methanothrix* bacteria interspersed with a variety of other bacteria [162].

Effect of Substrate and Temperature

Early investigations on granulation reported that the phenomenon was only achievable when treating certain types of wastewaters, most notable soluble carbohydrate

wastewaters. Reports on temperature effects were also limited to mesophilic studies. Since those early reports, granulation has been achieved in systems treating almost all types of wastewaters at a range of temperatures (Table 11). Although granules have been developed with a number of substrates, as Table 11 shows, granule stability may be affected if the substrate is changed after granule development. For example, a granular biomass developed on a sucrose wastewater may break apart upon changing to an acetic acid wastewater. The granular biomass may also be inhibited by the new substrate and

Table 11. Substrates suitable for granule formation.

Substrate	Reactor Type	Temperature (°C)	References
Volatile acid mixture	EBR ^a , UASB ^b	30, 37, 39	16, 40, 167
Propionate	UASB	35	41, 42, 74
Acetate	EBR, UASB	30, 35	29, 38, 159
Methanol/NO ₃ ⁻	UASB	30	156
Sucrose	UASB	30	139
Glucose	EBR, UASB	30	8, 167, 171
Apple juice	UASB	30	129, 160
Beet sugar	EBR	33	71
Citrate	UASB	35	165
Molasses	UASB	35	165
Potato starch	UASB	35	49, 109, 163
Maize processing	UASB	35	124
Brewery	UASB	34	51
Domestic sewage	EBR	10, 20	71

^a Expanded-bed or fluidized-bed reactor.

^b Upflow anaerobic sludge blanket reactor.

simply not perform efficiently, with no obvious break-up of the granule [79, 104, 150, 166]. This phenomenon is explained by noting that various substrates inherently select for specific bacterial species that are able to degrade the substrate. Therefore, a granule grown on sucrose will contain a diverse consortia of acidogens, acetogens, and methanogens. If this granular biomass is now used to treat acetic acid, the acidogens and acetogens will not be able to survive, and may cause the granule to break apart due to cell death and lysis.

However, some substrates appear to have no adverse effects on granule stability, even though the granules were formed with a completely different wastewater. Granules grown on non-fat dry milk have successfully been used to treat landfill leachate [60] and starch wastewater [153]. Granules grown on propionate and then switched to pyruvate and fumarate were also reported to be stable (no granule disintegration) [62]. Numerous examples exist of granules developed on a volatile acid mixture (acetic, propionic, and butyric) successfully being used to treat a wide variety of industrial wastewaters, including, potato starch, citric acid, sugar refinery, and meat processing [29, 78, 83, 133].

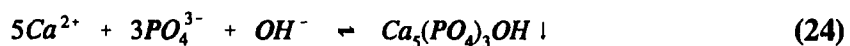
Effect of Chemical Enhancement

There are generally two mechanisms by which chemical enhancement may stimulate the granulation process: chemical addition may form precipitates to which bacteria may attach to form granules, or chemical addition may stimulate bacterial aggregation by bringing the bacteria close together and linking the bacteria via salt bridges or by other

mechanisms. Although the precise mechanisms of enhancement is not always known, several studies have investigated the effects of various metals, nutrients, and other elements on the process of granulation [1, 33, 43, 44, 46, 67, 92, 103, 106, 160].

It has been hypothesized that some granules are formed via the attachment of bacteria to inorganic precipitates present in the environment. These granules have an inherent heavier specific gravity due to the inorganic precipitate, and, therefore, have a higher settling velocity. These granules also have a high mechanical strength due to the presence of the precipitate. Inorganic compounds that have been implicated in the granulation process include precipitates of calcium (calcium carbonate, hydroxyapatite) and sulfide precipitates (metal sulfides). Obviously, in an anaerobic wastewater treatment system, other compounds and precipitates would also have an effect on granulation, but these compounds have received special attention in the literature [1, 33, 43, 44, 46, 92].

Calcium and Phosphorous. In addition to calcium carbonate (CaCO_3), which is a common precipitate in alkaline waters containing calcium, hydroxyapatite may also precipitate under various conditions. The formation of hydroxyapatite from calcium, phosphorous, and the hydroxyl ion is shown in Equation 24 [98].



An excess of calcium and phosphate is generally required for the precipitation of hydroxyapatite to occur significant amounts. A high pH (> 8) is also necessary, although

hydroxyapatite will precipitate at lower pH levels provided the calcium and phosphates concentrations are high [98]. Calcium has also been implicated in granulation through its stabilizing effect on the generally negatively-charged bacterial surface. Calcium has been shown to stabilize carboxyl groups and other negatively charged groups on extracellular biopolymers, and actually allow separated bacteria to come closer together. It has been suggested that the Ca^{2+} may act as a bridge between different biopolymers, thus, effectively joining two bacteria. Subsequent aggregation of more bacteria could lead to granulation [1, 43, 46, 92].

The effect of calcium and phosphorous concentration has been the focus of several investigations concerning granulation. Alibhai and Forster [1] reported that calcium and phosphorous stimulated the granulation process in UASB reactors at concentrations of 80 and 190 mg/L, respectively. Other multivalent cations, such as aluminum and silicon, were also observed in relatively high concentrations within the granule, suggesting that these elements may be important in granulation as well. Hulshoff Pol et al. [67] reported that moderate Ca^{2+} concentrations may enhance granulation, but that very low or very high Ca^{2+} concentrations appear to inhibit granule formation. UASB reactors treating a volatile acid wastewater were supplemented with Ca^{2+} at 6, 150, and 450 mg/L. The Ca^{2+} concentration of 150 mg/L was observed to enhance granule development the most rapidly.

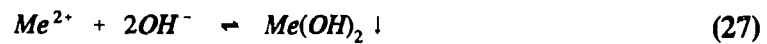
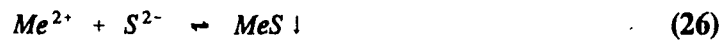
Mahoney et al. [92] reported that 100 mg/L of Ca^{2+} enhanced the formation and settleability of granules. The researchers studied the effect of calcium using two UASB reactors treating a mixture of volatile acids. One of the UASBs received 100 mg/L of

Ca^{2+} in addition to the substrate feed (calcium positive reactor), and the other UASB received no additional Ca^{2+} (control). Although granulation was observed in both of the UASB reactors, the calcium positive UASB granulated more rapidly than the control UASB. In addition, the granules that developed in the calcium-positive UASB had settling velocities that were 3 to 4 times faster than the granules that developed in the control reactor. Guiot et al. [44] reported that Ca^{2+} did not enhance the formation of granules. However, exposure of the granules to Ca^{2+} did improve their settleability, presumably due to incorporation of calcium precipitates which subsequently increased the granules' specific gravity [46].

One study designed to define the requirement for calcium and phosphorous utilized ethylene glycol-bis(β -aminoethyl ether)-N,N-tetraacetic acid (EGTA) as a calcium-specific chelant [43]. Upon treatment of granules with EGTA, the calcium and phosphorous concentrations of the granules subsequently decreased, and disintegration of the granules also occurred to varying extents. Additionally, the molar ratio of phosphorous to calcium (P/Ca) lost from the granules was approximately 0.59, which is very close to the P/Ca ratio of hydroxyapatite (P/Ca = 0.625). These observations suggested the importance of calcium and phosphorous precipitation (as hydroxyapatite) to the granulation process [43].

Iron, Nickel, Cobalt, and Other Heavy Metals. Although the beneficial effects of heavy metals on the biochemical aspects of methanogenesis have been well documented [106, 142], heavy metal precipitates may also play an important in the granulation process

of flocculent anaerobic biomass. The heavy metals precipitate in the presence of alkalinity and sulfide to form metal carbonates and metal sulfides, respectively (Equations 25 and 26). Hydroxide precipitates may also be formed, but these are normally only significant at high pH levels (Equation 27).



In Equations 25 through 27, "Me" represents any divalent heavy metal. In many anaerobic applications, sulfate is present in the influent wastewater. The sulfate is quickly reduced to sulfide by the sulfate-reducing bacteria, and these sulfides are then available to precipitate heavy metals. The solubility products of metal sulfides and other metal precipitates are extremely low (Table 12). Therefore, precipitation of the metal is very slowly reversible, and the majority of a metal will be present as metal sulfide, with smaller amounts of metal carbonates and hydroxides. The metal precipitates may act as granulation nuclei, similarly to the proposed mechanisms for hydroxyapatite [33].

Iron is normally the most abundant heavy metal in anaerobic treatment systems. Early reports [126, 138] on the effect of ferric chloride on sewage digestion indicated that

FeCl₃ concentrations in excess of 5 to 10 mg/L retarded methanogenesis and may be toxic to anaerobic bacteria. Later reports on the effect of iron reported that high iron concentrations may be inhibitory, but that the inhibition was mainly due to precipitation of iron with phosphate, resulting in limiting soluble phosphorous levels in the digester [115]. Another inhibitory effect of Fe³⁺ on anaerobic digestion results from the competing

Table 12. Solubility products of metal salts [98].

Metal Precipitate	Solubility product, K _s	pK _s
Ag ₂ CO ₃	3.0 x (10) ⁻¹²	11.5
CdCO ₃	5.0 x (10) ⁻¹²	11.3
ZnCO ₃	6.0 x (10) ⁻¹¹	10.2
FeCO ₃	3.0 x (10) ⁻¹¹	10.5
PbCO ₃	1.5 x (10) ⁻¹³	12.8
Cu ₂ CO ₃ (OH) ₂	1.6 x (10) ⁻³⁴	33.8
Cu ₃ (CO ₃) ₂ (OH) ₂	1.0 x (10) ⁻⁴⁶	46.0
Ag ₂ S	1.0 x (10) ⁻⁴⁹	49.0
CuS	4.0 x (10) ⁻³⁶	35.4
Cu ₂ S	1.0 x (10) ⁻⁴⁸	48.0
PbS	1.0 x (10) ⁻²⁸	28.0
CdS	1.0 x (10) ⁻²⁶	26.0
ZnS	1.0 x (10) ⁻²⁴	24.0
NiS	1.0 x (10) ⁻²⁴	24.0
FeS	1.0 x (10) ⁻¹⁸	18.0

reactions of the iron reducing bacteria. Under appropriate conditions, the iron reducing bacteria may out-compete the methanogens, resulting in reduced methane production [117]. Still later reports [58] indicate that moderate levels of iron (10 to 120 mg/L) stimulate methanogenesis. These investigations reported significant iron precipitation during digestion, but did not indicate that the precipitates affected the digestion process either positively or negatively.

X-ray analysis of granular biomass normally results in significant quantities of ferrous sulfide and ferrous carbonate. Ferrous sulfide is often present in sufficient quantities in granules that gives the entire granule a characteristic black color, and can constitute over 30% of the ash fraction of a granule [33]. This and other more recent studies indicate that iron precipitates may stimulate the adhesion of bacteria and the start of granulation [32, 33].

Biopolymers. Extracellular biopolymers have been briefly discussed in relation to their role in granulation. Most reports indicate that granular biomass normally contains a significant amount of extracellular polysaccharides, proteins, and lipids. This extracellular material may only comprise from 1 to 10% of the dry weight of the granule, but it has been suggested that it plays a role in stabilizing and strengthening the granule structure. The stabilization results from the numerous functional groups on the biopolymers which are capable of interacting with other biopolymers and ions. The

network formed by the polymers and ions could provide additional mechanical strength [33, 103, 130].

Morgan et al. [103] investigated the effect adding biopolymers to a UASB reactor. It was believed that the addition of biopolymers, which were extracted from granular biomass, would enhance the granulation process of a non-granular biomass. The results from this experiment indicated that initiation of granulation could be enhanced with biopolymers. However, inhibition of the UASB with respect to COD removal was also apparent with the addition of biopolymers. This latter effect was not understood by the researchers [103]

Effect of Physical Enhancement

The enhancement of granulation through physical methods, such as the addition of an attachment matrix, is the fundamental basis behind the expanded-bed reactor system. The basic principle is that bacteria will attach to and grow on a support matrix (e.g., sand or GAC) and form granules over time. Alternatively, granular biomass may be used as a portion of the seed sludge in almost any anaerobic treatment system to enhance reactor start-up.

Morgan et al. [103] reported that the addition of GAC and granular biomass (in separate experiments) to UASB reactors significantly enhanced the formation of a fully-granular biomass. Wang et al. [159] and Fox et al. [38] reported on the formation of granules in expanded-bed reactors using GAC as the support media. The formation of

granules of up to 5 mm in diameter was reported. An additional benefit to using GAC was cited as the adsorption capacity of the GAC. GAC is able to adsorb soluble substrates, thus providing an advantageous location for bacterial attachment and subsequent growth.

Other attachment media have also been used to promote granulation. Fox et al. [38], Gorris and van Deursen [40], and Ashikago et al. [5] used silica sand (average diameter = 0.3 to 0.7 mm) in expanded-bed reactors. Bacterial attachment and granulation was induced in these systems within 50 to 60 days, with granule diameters reported in the range of 0.7 to 5 mm. The small crevices of the sand particles were the first areas to be colonized, with subsequent growth of the granule developing outward from the crevices. Sand was reported to be less efficient than GAC for granule formation. Powdered zeolite with a diameter of 50 to 100 μm has also been shown to enhance granulation in expanded-bed reactors [167]. Most of the biomass in these experiments existed as a thin film on the carrier with diameters less than 0.25 mm. However, other particles were also present with diameters of over 1 mm, indicating significant growth of the biomass attached to the carrier. Other attachment media that have been successfully used include anthracite and polyvinyl chloride (PVC) particles [38, 71].

EXPERIMENTAL SETUP

Four identical reactor systems, each consisting of one ASBR, a substrate feed system, an effluent decant system, a gas mixing system, and a gas measuring system, were used for the experiments in this research. The ASBRs were constructed at the Engineering Research Institute Machine Shop at Iowa State University. Excessory materials, such as tubing, clamps, fittings, and connections, were purchased at the Chemistry Stores and Central stores, also located at Iowa State University. Additional equipment and materials were purchased as noted below. The reactor systems were housed in a constant temperature room which was kept at $35^{\circ}\text{C} \pm 0.5^{\circ}\text{C}$ for the duration of the experiments. The entire system for one of the identical units is shown in Figure 15.

Anaerobic Sequencing Batch Reactor Design

The body of the four identical ASBRs (Figure 15) were constructed of ¼-in thick Plexiglas. The reactors were cylindrical, with an inside diameter of 5.5 in, an outside diameter of 6 in, and a total depth of 37 in. The total volume of each ASBR was approximately 14 liters. The top and bottom of the cylindrical tube were flanged with an outside flange diameter of 9 in. Nine-inch diameter round plates (½-in thick) were fastened to the top and bottom flanges with 12 equally-spaced 1/2-in bolts (1½-in long). A rubber gasket was placed between the plates and the flanges to provide an air-tight seal (Figure 16). Nine side ports were equally-spaced down the side of the ASBR. These 1¼-in Plexiglas ports (3/8-in diameter) extended through to the inside of the ASBR and

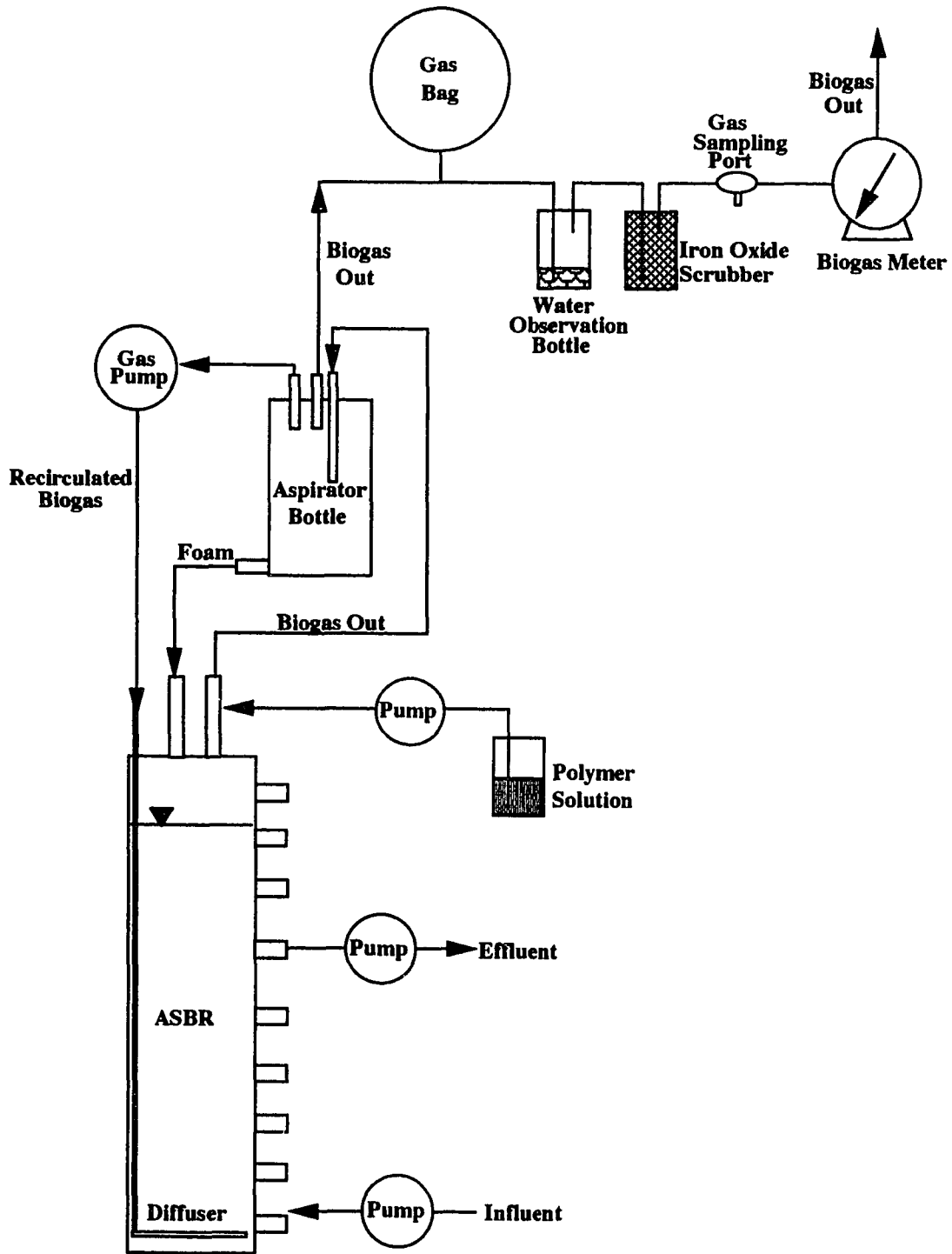


Figure 15. Anaerobic sequencing batch reactor setup.

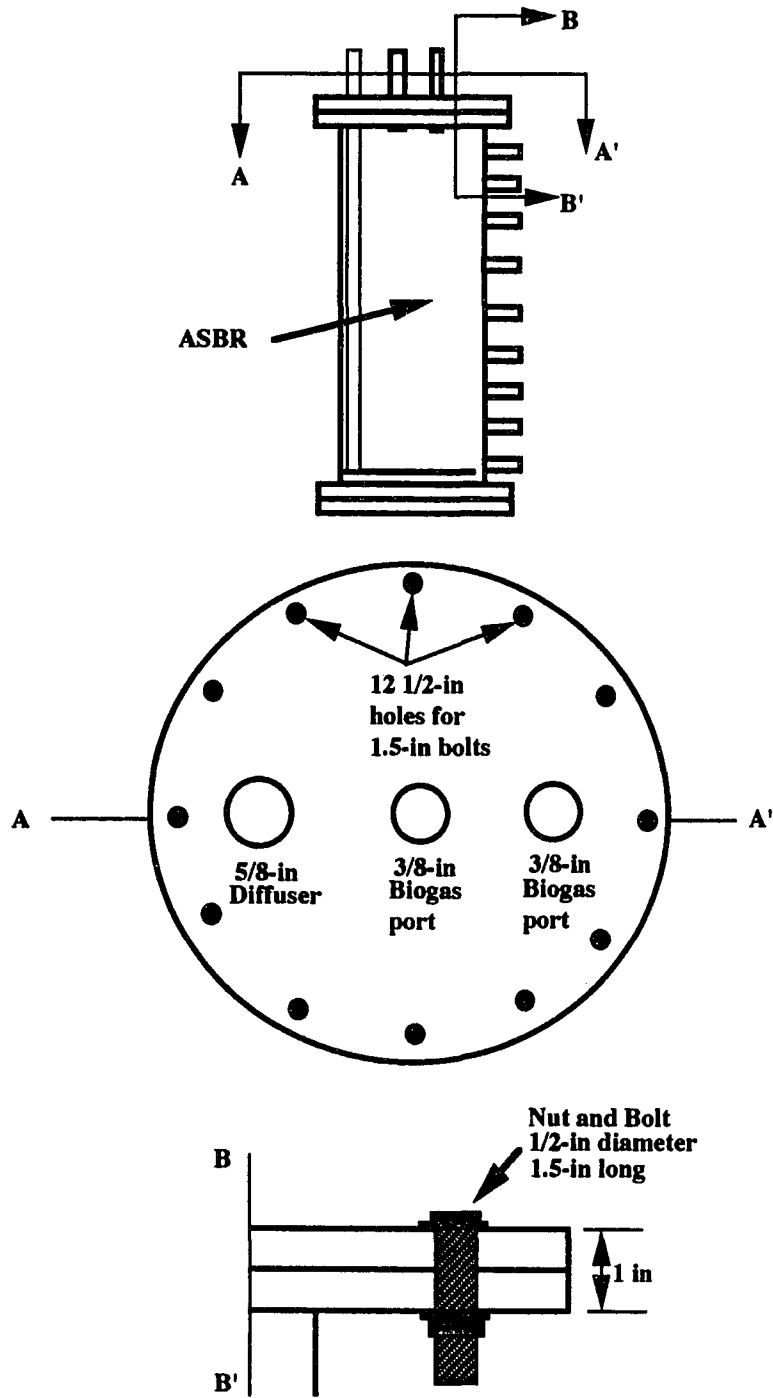


Figure 16. Schematic of the top cover of the ASBR.

extended 1.0 in on the outside (Figure 15). Each of the ports was connected to a 6-in long piece of 3/8-in diameter Nalgene tubing (Sybron Corporation, Rochester, NY), which was clamped to provide an air tight seal. The bottom port was connected to the substrate feed pump, and one of the upper ports was connected to the effluent decant pump. The decant port was selected based on the HRT of the system. As the HRT was increased, a lower port was used for decanting due to the larger volume of liquid that was required to be decanted each cycle.

The top plate on the ASBR contained two additional ports identical to those described above. One port served as the biogas outlet from the ASBR, and the other served as a liquid and foam return inlet to the ASBR. These ports are described later in the section on gas/foam separation. A third port was located in the top plate for biogas recirculation and is described in the biogas mixing section (Figures 15 and 16).

Gas/Foam Separation System

Biogas exiting the ASBR through the middle top port (Figure 16) was directed to the gas/foam separation bottle, which had a volume of approximately 3 liters (Figure 15). Under normal conditions, the separation bottle served no function. However, under conditions of excessive foaming, some foam left the ASBR in the biogas outlet port and was collected in the gas/foam separation bottle. This bottle contained three ports in the top rubber stopper and an additional port at the bottom. The ports in the stopper consisted of 1/4-in glass tubes, which extended from 1.5 in above the stopper to several

inches below the stopper. One of the ports was used as the biogas inlet (from the ASBR), one served as the biogas outlet (to the gas measuring system), and one served as a biogas outlet during biogas recirculation. Foam entering the bottle fell to the bottom and was returned via the bottom port to the ASBR. Tubing that connected the gas/foam separation bottle with other parts of the system was 3/8-in in diameter.

Biogas Recirculation System

Mixing was accomplished by recirculating the biogas in a closed loop to the bottom of the ASBR through a stainless steel ring diffuser system. The diffuser system consisted of a 5/8-in diameter pipe which extended from the bottom of the ASBR through the top plate to 2-in above the top of the ASBR. The pipe was positioned along the edge of the ASBR so that at the bottom of the pipe a 1/4-in ring diffuser could be attached (Figure 15). The diffuser consisted of two concentric rings connected by three stainless steel tubes. The inner and outer rings were 4½-in and 2½-in in diameter, respectively (Figure 17). The inner ring had six 1/32-in equally-spaced holes and the outer ring had eight 1/32-in equally spaced hole drilled in the bottom to provide the outlet of the diffusers for mixing. All parts of the diffuser system were hollow to allow the recirculated biogas to flow through them.

The recirculation system worked as follows: Biogas produced from methanogenic activity exited the ASBR through a port described earlier and was discharged to the gas/foam separation bottle. When the ASBR was mixed, a peristaltic pump turned on and

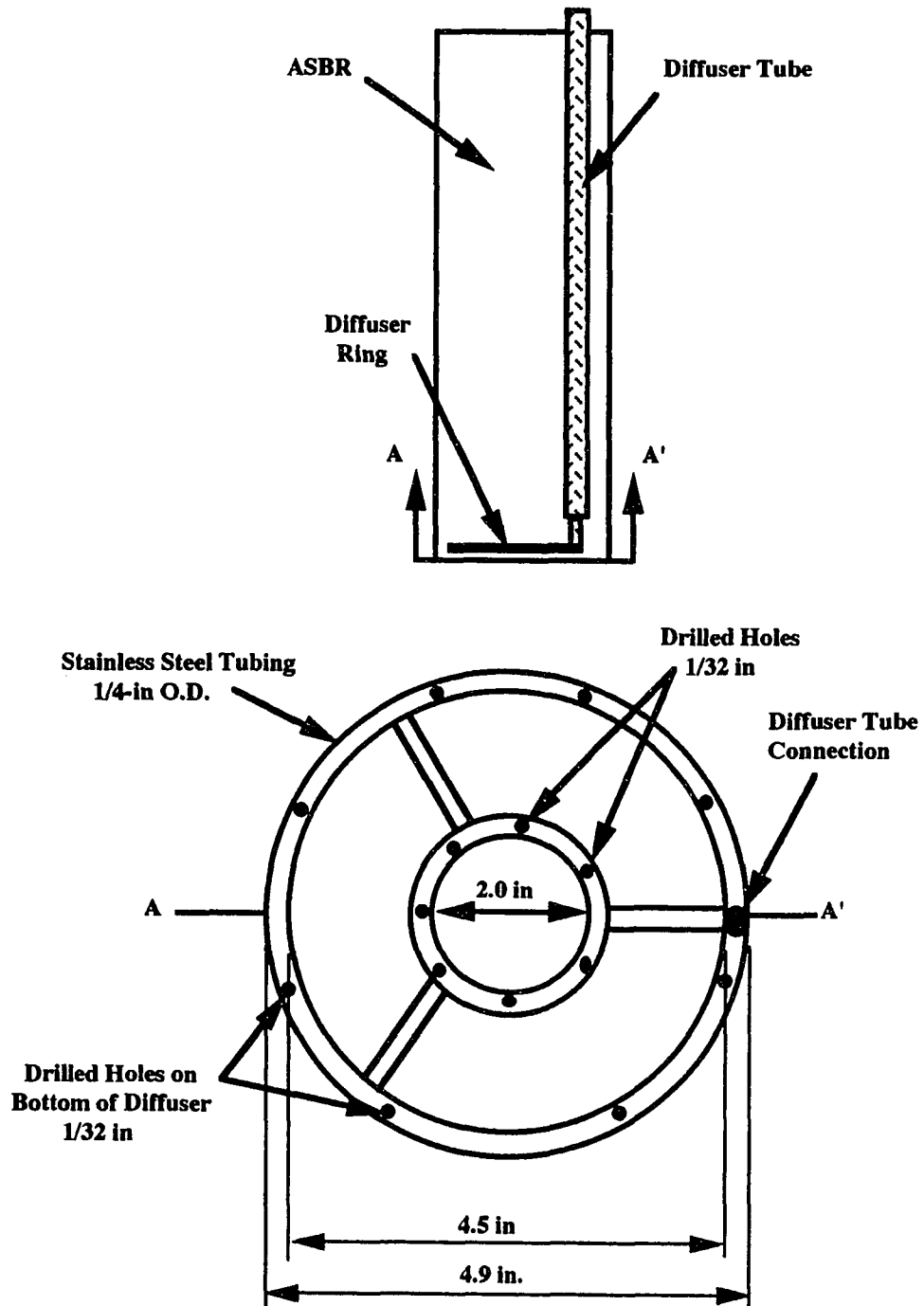


Figure 17. ASBR biogas recirculation diffuser system.

pulled biogas out of the gas/foam separation bottle via one of the top ports. The discharge end of the pump was connected with 5/8-in Nalgene tubing to the stainless steel diffuser pipe. The biogas discharged through the ring diffusers and rose to the surface of the ASBR, thereby mixing the system and completing the biogas loop.

The pump used for biogas recirculation was a 50-600 rpm variable speed peristaltic pump with a size 18 pump head (both from Cole-Parmer Instrument Company, Chicago, IL). The recirculation pumps were connected to a model XT Chronrol timer (Chronrol Corporation, San Diego, CA) which turned the gas pumps on and off at programmed times. The pump head tubing was Masterflex size 18 Norprene tubing (Cole-Parmer Instrument Company, Niles, IL). The connections between the pump tubing and the inlet and outlet tubing were 2-way, 1/4 to 5/8-in polyethylene connectors (Chemistry Stores, Iowa State University, Ames, IA).

Biogas Collection and Measurement System

The biogas that was produced ultimately left the gas/foam separation bottle via the gas exit port to the gas measurement system (Figure 15). The gas exit port was connected to a water observation bottle (one-liter volume) with 3/8-in Nalgene tubing. The observation bottle had a rubber stopper with inlet and outlet glass tubes extending out the top and bottom of the stopper. The inlet glass tube extended 1/2-in below the water level in the bottle so that bubbles of gas could be visually observed. There were two valves between the gas/foam separation bottle and the observation bottle. The first valve was a

three-way T-connection that was connected with the tubing to the gas/foam separation bottle, the observation bottle, and also to a gas bag which had a volume of four liters. The bag served as a reservoir of gas and provided gas to the ASBR (by deflating) during decanting to avoid drawing a vacuum on the system. Just before the observation bottle was a one-way check valve, the purpose of which was to prevent gas being drawn back through the observation bottle (and downstream equipment) during decanting.

A hydrogen sulfide scrubber (one-liter volume) containing sponges soaked in a solution of ferric oxide was placed after the observation bottle. The inlet and outlet from the scrubber were identical to the observation bottle, with the exception that there was no water in the scrubber. Hydrogen sulfide produced in the ASBR was removed from the gas stream by reaction with the ferric oxide to form ferrous sulfide, which formed a black precipitate in the scrubber bottle.

After the scrubber bottle, the gas passed through a cylindrical blown-glass gas sampling compartment (4-in long and 1-in diameter) which had a $\frac{1}{4}$ -in port with a rubber septum placed snugly into it (Figure 15). This compartment was used to sample the biogas with a syringe for gas composition analyses using chromatography.

The final stage of the biogas collection system was the gas meter. After exiting the gas sampling compartment, the biogas entered a wet-test gas meter (Precision Scientific, Inc., Chicago, IL), which measured the volume of biogas produced over time. The gas was vented to the buildings air ventilation system. All tubing used in the gas collection and measurement system was Nalgene brand tubing with an inside diameter of $\frac{3}{8}$ in and

a wall thickness of 1/16 in. Appropriate connectors were placed between all parts of the system so that any one component could be taken out and repaired without disrupting the flow of biogas.

Substrate Feed and Effluent Decant Systems

The substrate used in the experiments was prepared daily (described in the Experimental Procedures section) in 20-liter polyethylene carboys. Each carboy was placed on a magnetic stirring plate (Model PC-310 Laboratory Stirrer, Corning Inc., Corning, NY), and a 2-in magnetic stir bar was placed in the carboy. The magnetic stir plates were connected to a Chronrol timer which turned the magnetic stir plates on and off during the feed cycle. A 6-in section of 3/8-in glass tubing was connected with 3/8-in Nalgene tubing to the substrate feed pump. The glass end was inserted into the carboy while the other end of the tubing was connected to the pump head tubing in an identical fashion, as earlier described. The pumps were 60-rpm constant speed peristaltic pumps (Cole-Parmer Instrument Company, Chicago, IL) and were connected to a Chronrol timer which turned them on and off at the appropriate time. The discharge end of the pump was connected with 3/8-in Nalgene tubing to the bottom side port of the ASBR.

The decanting pumps, timer, and tubing were identical to those used for the substrate feed system. The selected side port for decanting was connected to the decant pump, which discharged the effluent to a sanitary sewer drain.

Coagulant Feed System

In experiments where coagulant was added to the ASBR for granulation enhancement, additional equipment was necessary. The coagulant feed system consisted of a 2-liter polyethylene bottle, which contained the respective coagulant for that experiment. A 1/8-in polyethylene Nalgene tube was inserted into the container and connected to a variable speed peristaltic pump with a size 16 pump head (Cole-Parmer). The pump head tubing was also 1/8-in Nalgene tubing. The pump outlet was connected with 1/4-in Nalgene tubing to a three-way T-connection in the ASBR foam return line. The pump was controlled by a Chronotrol timer which turned the pump on for one minute during the last mixing cycle just prior to the settle phase of the ASBR cycle (Figure 15).

EXPERIMENTAL PROCEDURES

Substrate Feed Preparation

The substrates used in this study were prepared daily to minimize biological degradation of the feed while it sat in the feed carboys. Sucrose (Chemistry Stores, ISU) was the main substrate (carbon and energy source) used. As stated in the Literature Review section, soluble carbohydrates have been cited as the best substrate to achieve granulation in UASB reactors. For this reason, sucrose was chosen as the primary substrate in most of the experiments. Since pure sucrose does not contain nitrogen or other essential nutrients and trace metals, addition of these other elements were necessary. Nitrogen was added as ammonium hydroxide, potassium and phosphorous as potassium phosphate (dibasic), and other trace metals as chloride salts. Additionally, alkalinity was added to the feed solutions in the form of sodium bicarbonate. Table 13 lists the recipe used for the sucrose experiments. COD, nitrogen, and phosphorous were added in a 100:5:1 ratio for all experiments. A review of the literature for similar experiments indicated that this ratio was common and provided a suitable environment for anaerobic biological degradation. Although the nitrogen added was in excess of that required for biomass synthesis, the additional nitrogen provided a source of alkalinity and buffering capacity in the ASBRs.

A second substrate was used in later experiments to determine if previous results could be attributed to the substrate employed. This latter substrate was a mixture of a food-grade beef extract soup base (Kraft, Inc., Glenview, IL) and glucose (Chemistry

Stores, ISU). The two substrates were blended in tap water with a warring blender in a mixture that contained a 1:1 ratio of COD from each substrate. Table 14 outlines the recipe used for the beef/glucose experiments. Table 15 lists the composition of the beef extract obtained from the Kraft Company.

One obvious difference between the two substrates was the fact that the beef/glucose feed solution contained a relatively large amount of fat, whereas the sucrose solution contained essentially zero fat. This difference became the source of some operational difficulties due to the hydrophobic nature and density of fat. The fat tended to

Table 13. Sucrose feed mixture.

Component	Amount Added (per gram of feed COD)
Sucrose, mg	960.00
Nitrogen, mg	50.00
Phosphorous, mg	10.00
Iron, mg	1.25
Manganese, mg	0.31
Cobalt, mg	0.08
Nickel, mg	0.06
Zinc, mg	0.05
Molybdenum, mg	0.06
Copper, mg	0.02
Boron, mg	0.02
Bicarbonate, g/L as CaCO ₃ ^a	2.40

^a Alkalinity was directly added at the rate of 4 grams of NaHCO₃ per liter of feed.

form a layer on the top of the feed carboys, as well as in the reactors. This observation is dealt with in more detail later. A second difference between the two substrates was that the beef also contained protein, which became an additional source of nitrogen and sulfur.

Since the feed solutions were prepared daily, stock solutions of the nutrients (termed the NPK solution) and trace metals were prepared and stored as aqueous solutions. Tables 16 and 17 list the composition of the nutrient solution and trace metal solution, respectively.

Table 14. Beef extract and glucose feed mixture.

Component	Amount Added (per gram of feed COD)
Beef extract, mg	860.00
Glucose, mg	480.00
Nitrogen, mg	50.00
Phosphorous, mg	10.00
Iron, mg	1.25
Manganese, mg	0.31
Cobalt, mg	0.08
Nickel, mg	0.06
Zinc, mg	0.05
Molybdenum, mg	0.06
Copper, mg	0.02
Boron, mg	0.02
Bicarbonate, g/L as CaCO ₃ ^a	2.00

^a Alkalinity was directly added at the rate of 3.3 grams of NaHCO₃ per liter of feed.

Table 15. Composition of the beef extract soup base.

Component	Amount (% by weight)
Hydrolyzed vegetable protein	12.9
Fat	13.5
Carbohydrates	24.0
Sodium	18.1
Potassium	8.8

Table 16. Nutrient (NPK) solution.^a

Component	Concentration (g/L)
Potassium phosphate, dibasic	68.8
Potassium	30.9
Phosphorous	12.2
Ammonium hydroxide	148.1
Ammonia	74.1
Nitrogen	61.0

^a Added 0.886 mL of this solution per gram of COD.

The sucrose solution was prepared as follows. A measured amount of sucrose (based on the COD loading) was added to approximately 1 liter of warm tap water. This mixture was placed on a magnetic stir plate until all of the sucrose had dissolved. This mixture was then poured into the 20-liter feed carboy. Sodium bicarbonate was weighed and poured into the carboy. An appropriate amount of the NPK solution was then measured with a volumetric cylinder and an appropriate volume of the trace metal solution

Table 17. Trace metal solution.^a

Element	Compound	Concentration of Element (g/L)
Iron	FeCl ₂ · 4H ₂ O	14.00
Manganese	MnCl ₂ · H ₂ O	3.50
Cobalt	CoCl ₂ · 4H ₂ O	0.93
Nickel	NiCl ₂ · 4H ₂ O	0.62
Zinc	ZnCl ₂	0.60
Molybdenum	(NH ₄) ₆ Mo ₇ O ₂₄ · 4H ₂ O	0.68
Copper	CuCl ₂ · 4H ₂ O	0.28
Boron	HBO ₃	0.22

^a Added 0.089 mL of this solution per gram of COD.

was added with a syringe. Warm tap water was then added and the volume of the feed solution was adjusted to the appropriate level, depending on the HRT of the system.

The beef/glucose feed mixture was prepared similarly. The beef extract and glucose were weighed on a balance and then placed in a warring blender along with two liters of hot tap water. Hot water was used since it tended to keep the fat in solution better than cold water. The warring blender was turned on for one or two minutes, and then the contents were poured into the feed carboy. The other ingredients were added as before. The feed carboys were then taken to the controlled-temperature room in which the reactor systems were housed, placed on the magnetic stir plates, and a magnetic stir bar was placed in each carboy. The feed lines to the ASBRs were inserted into their respective carboys and the feed preparation was then completed. The volume of feed substrate

prepared was 2 liters in excess of the amount fed to the ASBRs on a daily basis. This was done to ensure that air would not be pumped in to the reactors, which would occur if the carboys were completely empty. The remaining two liters were poured down the drain prior to making the new feeds, and the carboys were cleaned and rinsed to avoid bacteria growth.

Tap water was used in place of distilled or deionized water for two reasons. First, the logistics of the distilled water system in the environmental engineering laboratory were such that a relatively long period of time would be required to obtain sufficient distilled water to make all of the substrate feeds. Second, the tap water provided other essential nutrients for the biological systems, most notably, calcium, magnesium, and sulfur (sulfate). The average composition of the Ames' tap water is shown in Table 18.

Biological Seeding of the ASBR

Because of the nature of the experiments in this study, it was necessary to re-start the ASBRs with new biological seed every 2 to 5 months. Each time the ASBRs were re-started, the existing biomass in the reactors were emptied into carboys, and the reactors, diffusers, ports, and tubing were thoroughly cleaned. New anaerobic biological seed was obtained from the primary anaerobic digesters at the City of Ames Water Pollution Control Plant. The seed was brought back to the environmental engineering laboratory and sieved with a 1 mm screen to remove large particles, hair, gum, and other objects which inevitably become part of the anaerobic digester contents. The large particles removed

Table 18. Ames municipal water analysis.

Component	Average Concentration (mg/L)
Calcium, as Ca	130 - 140
Magnesium, as Mg	20 - 30
Sulfate, as SO ₄ ²⁻	70 - 90
Iron, as Fe	0.09 - 0.11
Carbonate hardness, as CaCO ₃	40 - 60
Noncarbonate hardness, as CaCO ₃	120 - 130
Alkalinity, as CaCO ₃	40 - 60
pH ^a	9.4 - 9.7

^a pH is reported as pH units.

were discarded and the sieved seed was then placed into carboys and purged with methane gas to remove any entrained oxygen. The ASBRs were also purged with methane, after which the seed was pumped into the sealed ASBRs. Approximately 8 to 10 liters of the seed (depending on the solids content of the seed) were pumped into each reactor, and then the liquid volume of the ASBR was adjusted to 11 liters with tap water. The liquid volume was subsequently adjusted to 12 liters with the addition of 1 liter of a substrate solution (described below). Each ASBR had a total volume of 14 liters with a 2-liter headspace. As stated, the amount of seed added to the ASBRs was dependent on the solids concentration of the seed material. The suspended solids concentration of the seed material was generally about 30,000 mg/L, although this varied each time new seed was obtained from the treatment plant. The target MLSS concentration in the reactor (liquid volume of 12 liters) was between 20,000-25,000 mg/L.

During and after seeding, the ASBRs were purged with methane to remove all of the oxygen from the system. Gas chromatography was used to determine the approximate oxygen composition of the gas in the reactor, and methane purging was continued until the oxygen peak was diminished to below detectable levels ($O_2 < 1\%$ of gas). Methane purging was then stopped. The ASBRs were then fed with 1 liter of the respective substrate solutions and the gas meter readings were recorded. At this point, the experiment was considered started.

ASBR Start-up and Operation

Each of the ASBRs was operated independently of the other ASBRs during the experiments. The operational characteristics of the ASBR were presented earlier in the Literature Review section. The ASBRs were always operated with a cycle length of six hours, corresponding to four cycles per day. The only exception to this was during the first one or two days of operation in which the ASBRs were operated with only two cycles per day to avoid loss of too much biomass. Generally, two HRTs were used throughout the study, 48 and 24 hours. After initial start-up, the ASBRs were operated at a 48-hr HRT and a COD load of 2 g/L/day until the system began to settle well. When settling was stable and clear supernatant was apparent, the HRT of the system was decreased to 24 hrs by doubling the amount fed and decanted each cycle while maintaining the COD load at 2 g/L/day. The COD load was kept constant by diluting the feed substrate. The decision of when to decrease the HRT was not always clear-cut, and factors such as COD removal

efficiency were also taken into consideration. For the majority of the tests, the ASBRs were operated at a 48-hr HRT for at least 20 to 25 days, although this varied considerably among the individual experiments.

The pumps used for feeding and decanting were constant-speed peristaltic pumps (previously described). Therefore, in order to achieve the desired feeding and decanting volumes, the feed, decant, settle, and react phases of the ASBR cycle were changed accordingly (Table 19). It was desired to decrease the HRT of the system as quickly as

Table 19. ASBR cycle time for 48 and 24-hr HRTs.

Phase	Time per cycle, hrs (min)	
	48-hr HRT	24-hr HRT
Feed	0.13 (8)	0.26 (16)
React	4.96 (297)	4.83 (289)
Settle	0.78 (47)	0.65 (39)
Decant	0.13 (8)	0.26 (16)
Total	6.00 (360)	6.00 (360)

possible. It was hypothesized that increasing the hydraulic pressure would increase the rate at which the biomass formed granules. Similarly, increasing the COD load as quickly as possible was also thought to be beneficial for granulation. Increasing the COD load provided more substrate, which, if biologically degraded, would produce more viable biomass. Increasing the COD load also resulted in more internal mixing due to higher

biogas production rates, which tended to carry lighter biomass particle upward while the heavier particles were still able to settle sufficiently.

The ASBRs were operated according to the times in Table 19 for all experiments. Termination of an experiment occurred after granulation of the biomass occurred or when it was determined (by objective and subjective analyses) that granulation would not occur within a reasonable period of time. In the experiments in which the biomass did granulate, it was normally apparent that granulation would occur within approximately one or two months of operation. Although physical granulation may not have been apparent within this time frame, the biomass generally appeared slightly different than in the ASBRs that did not granulate at all, and reactor performance based on COD removal was generally better at an early stage as compared to the granule-negative experiments.

It is noted here that the ASBRs in these experiments were seldom operating under equilibrium conditions. That is, in most of the studies under Dr. Dague's supervision, the systems are operated under specified conditions for a period of time so as to establish equilibrium, or at least pseudo-equilibrium based on a relatively constant daily methane production and COD removal at a given COD loading rate over a period of several HRTs. The experiments in this study, however, were very time-dependent. It was deemed beneficial to the granulation process to increase COD and hydraulic pressure as quickly as possible without deterioration of the system. Therefore, the systems were seldom operating under equilibrium conditions for any significant period of time. Rather, after an increase in the COD was affected, the systems were given time to adjust to the new

conditions, and, if the overall efficiency of the system remained approximately the same or increased, the COD loading rate was again increased. Of course, data were collected at each COD loading rate so that removal efficiencies, MLSS, and other pertinent operational parameters could be monitored over the entire course of an experiment.

The overall effect that this had on the data was to underestimate the COD removal efficiency and MLSS values at any given conditions. For instance, if the COD loading rate on a given ASBR was increased from 3 to 4 g/L/day, and the system immediately adjusted to this increase through increased gas production, the COD loading rate was subsequently increased to a higher value in a short time period. The alternative to this would have been to maintain the ASBR at 4 g COD/L/day for a period of 3 or 4 weeks, during which time the COD removal efficiency would have increased to a higher level and the MLSS concentration also would have increased to near equilibrium values for that loading rate. As previously stated, the basis for the rapid increase in loading rate was to put pressure on the system to select for the most active, best-settling biomass, thereby enhancing conditions for granulation.

ASBR Mixing

Mixing of the ASBR was conducted on an intermittent basis throughout the study. During the feeding phase of the cycle, the gas recirculation mixers were turned on to achieve intimate mixing between the substrate and the biomass. The mixers were turned on for three minutes every 30 minutes during the react phase to release any entrapped gas

bubbles within the ASBR and to provide contact between the substrate and biomass.

Mixing was not performed during the last 30-minute period of a cycle. That is, if the decant phase was to begin at 2:45, the last mixing cycle would occur at 2:00. The mixers would be shut off from 2:03 to 2:45, which defined the settle phase. Of course, the mixers were also off during the decant phase, which immediately follows the settle phase.

The mixing intensity was maintained at a maximum velocity gradient, G , of 100/sec and a minimum of 50/sec. This was accomplished by adjusting the speed control on the variable speed gas recirculation pump.

Granulation Enhancement

Attachment Matrices

Various attachment matrices were used to enhance granulation throughout this study (Table 20). The attachment matrices were added only once at the beginning of each experiment. Although it was physically impossible to determine whether the biomass actually attached to the matrices, performance and the on-set of granulation were compared to control reactors in which no attachment matrices were added. Preliminary experiments with only tap water and each attachment matrix were performed to indicate the degree to which the attachment matrices could be suspended during mixing of the ASBR. If the matrix settled to the bottom of the ASBR and did not mix thoroughly with the reactor contents, it was of little use for granulation enhancement. As expected, all of the matrices employed in this study were easily suspended from the bottom of the ASBR during mixing.

The matrices used in these experiments included powdered activated carbon (PAC), granular activated carbon (GAC), garnet sand, and silica sand. It was expected that the two activated carbons would enhance overall performance of the ASBR by supplying a form of buffer capacity to the ASBR. The adsorption capacity of the carbon would, in effect, store COD in the reactor, which could then be utilized by the biomass as needed. The adsorption capacity of the activated carbons was also expected to provide suitable attachment sites for the bacteria. The two types of sand were used to compare the effect of adsorption on reactor performance and granulation enhancement. Sand is also generally less expensive than activated carbon. Therefore, if the two types of matrices performed equally well, sand would be a better economic selection.

Preliminary experiments with PAC were conducted to determine the optimum concentration of attachment matrix to add at the start of the granulation experiments. The four ASBRs were seeded with municipal digester biosolids and four different concentrations of PAC were added: 500 mg/L, 1,000 mg/L, 2,000 mg/L, and 5,000 mg/L. Based on overall ASBR performance (COD removal, settling characteristics, etc.) over the first 40 days of operation, the value of 2,000 mg/L of PAC was selected for additional experimentation. This concentration was also used in later experiments with GAC, silica sand, and garnet. The attachment matrices were weighed on a digital scale and then injected into one of the top ports of the ASBR during mixing on day zero. After this day, additional matrix material was not added to any of the ASBRs.

Table 20. Attachment matrices utilized for granulation enhancement.

Attachment Matrix	Substrate	Diameter (mm)	Amount of Matrix Added (g/L)
PAC	sucrose	0.05	2.0
GAC	sucrose	0.50	2.0
Garnet sand	sucrose	0.50	2.0
Silica sand	sucrose	0.50	2.0
Control (none)	sucrose		0.0

Coagulant Addition

Additional experiments were conducted with three different coagulants, ferric chloride, a cationic polymer (MAGNIFLOC® 496C, Cytec Industries, Stamford, CT), and a polyquaternary amine (MAGNIFLOC® 591C, Cytec Industries, Stamford, CT), hereafter termed polyDADM. Table 21 lists the characteristics of these polymers as obtained from Cytec Industries. It was expected that the coagulants would function to retain the biomass in the reactor better than was observed with no coagulant addition. In so doing, the start-up period for stable operation of the ASBR should be shortened and granulation of the biomass should be enhanced due to the intimate contact between biomass particles that resulted from coagulation of the biomass. Table 22 lists the coagulants used in these experiments. Preliminary coagulation tests were conducted with the above-mentioned compounds, as well as with ferrous chloride and two additional polymers obtained from Cytec, Inc., to determine which compounds performed the best and to determine the optimum dosage required for each of the compounds. The tests were conducted in ASBRs

Table 21. Polymer characteristics.

Parameter	MAGNIFLOC® 496C	MAGNIFLOC® 591C
Type	dry powder	liquid
Charge	strongly cationic	moderately cationic
Polymer type	co-polymer	homopolymer
Chemical make-up	acrylimide acryloyloxyethyltrimethyl- ammonium chloride	diallyldimethylammonium chloride
Polymer solids	85 %	55 %
BOD ₅ ^a	400 mg/L	310 mg/L
COD ^a	4,500 mg/L	2,250 mg/L

^a Based on a 1% solution.

Table 22. Coagulants utilized for granulation enhancement.

Coagulant Added	Substrate	Dosage (mg/L/cycle)
Ferric Chloride	sucrose	5 to 10 ^a
Cationic (496C)	sucrose	1
Cationic (496C)	beef/glucose	1
PolyDADM (591C)	sucrose	2 to 5
Control	sucrose	0
Control	beef/glucose	0

^a The dosage of ferric chloride is reported as mg/L as Fe.

that had been operating in previous experiments that had been discontinued. Ferrous chloride and the additional two polymers did not achieve acceptable coagulation at any of the dosages examined, and were, therefore, not used in subsequent experiments. Ferric chloride performed well at dosages of 5 to 10 mg/L (as Fe), the cationic polymer performed well at dosages as low as 1 mg/L, and the polyDADM coagulant performed well at dosage of 5 to 10 mg/L.

Addition of coagulants began on day zero of the experiments. The coagulant was added once per cycle during the last mixing period of the cycle, just before the settling phase. The coagulants were added with a peristaltic pump (described earlier) for a period of one minute. The coagulants were prepared in one-liter solutions, which lasted approximately four days. Each cycle, 60 mL of the respective coagulant solution was fed to the appropriate ASBR as described earlier. Coagulant addition was continued until granulation occurred to a significant extent.

EXPERIMENTAL TESTING

Parameters indicating the health and performance of the ASBR systems were routinely monitored. The decision of whether to increase or decrease the COD loading rate, the HRT, or coagulant dosage (when applicable) was based on these operational parameters (Table 23). Each test is explained in detail in this section.

Table 23. Operational parameters routinely tested.

Test	Approximate Frequency
COD removal %, total and soluble	1/week
Effluent volatile acids	1/week
Alkalinity	1/week
pH	1/day
Ammonia	as needed
Effluent SS and VSS	1/week
MLSS and MLVSS	1/week
Biogas production	1/day
Biogas composition	3/week
Automate Image Analysis	2/month
Activity tests	variable ^a
SEM/TEM	1/study ^b
Biomass elemental analysis	1/study ^b

^a Activity tests were conducted on selected granular and non-granular biomass.

^b These tests were conducted on selected granules, and not on the biomass from all experiments.

Chemical Oxygen Demand

The chemical oxygen demand (COD) of a wastewater is defined as the amount of a strong oxidizing agent required to chemically oxidize the organic matter present in a given sample, expressed as oxygen. The oxidizing agent used in these experiments was potassium dichromate. A modified procedure of Standard Method #508 [144] was used as outlined below.

The sample to be tested was collected by inserting the decant tubing from the ASBR into a four-liter collection flask. The entire decanted volume from a single ASBR cycle was collected, and individual samples were taken from this decanted effluent for the individual tests. The flasks were placed on a magnetic stir plate and a magnetic stir bar was inserted into the flask. The decanted effluent was well mixed and samples for analysis were withdrawn with appropriate pipettes.

The influent and effluent from the ASBRs were tested for their respective COD values, from which the COD removal percentage could be calculated as shown in Equation 28. Additionally, both soluble and total COD in the effluent were determined. Soluble COD is defined here as the COD passing a 0.45 μm filter. Both soluble and total COD removal percentages, however, were based on the total influent COD concentration.

$$\text{COD Removal \%} = \frac{\text{COD}_i - \text{COD}_e}{\text{COD}_i} * 100 \quad (28)$$

where: COD_i = influent COD concentration, mg/L
 COD_e = effluent COD concentration, mg/L

The difference between soluble COD and total COD removal percentages is generally a measure of the COD of the solids in the effluent.

The COD test was conducted as follows. Effluent and influent samples were collected from the ASBRs. The samples were mixed well on a magnetic stir plate, and the appropriate volume of each sample was withdrawn and placed into separate 100-mL volumetric flasks. These flasks were filled to the 100-mL mark with deionized and distilled water. Approximately 30 mL of the diluted effluent samples were then vacuum filtered through 0.45 μm glass fiber filters (Fisherbrand G4, Fisher Scientific, Pittsburgh, PA). The filtrate was used in determination of the soluble COD concentration of the effluent. Five mL of each sample was then withdrawn and placed in a 30-mL screw-top test tube. Three mL of 0.1 M $\text{K}_2\text{Cr}_2\text{O}_7$ were then dispensed into the test tubes, followed by 7 mL of concentrated sulfuric acid. Table 24 lists the chemical composition of the various reagents used in the COD test. The test tubes were then capped with phenolic caps (Corning, Inc., Corning, NY) and placed in a 150°C oven for two hours. At a minimum, all samples were tested in duplicate. Additionally, four 5-mL samples consisting of distilled and deionized water were also tested in the manner previously outlined. Two of these were placed in the oven with the other samples (these were the blanks), and two were set aside and not placed in the oven (these were the standards).

After heating in the oven, the COD samples were removed and allowed to cool to room temperature. After cooling, two drops of a ferroin indicator (Table 24) were put into each sample. The samples were then titrated with 0.1 N ferrous ammonium sulfate

Table 24. Reagents used in the COD test.

Reagent Solution	Component Name	Concentration
COD Acid	H ₂ SO ₄ (conc.)	36.0 N
	Ag ₂ SO ₄	10.0 g/L
Oxidizing Solution	K ₂ Cr ₂ O ₇	4.913 g/L
	HgSO ₄	33.33 g/L
	H ₂ SO ₄ (conc.)	167.0 mL/L
	H ₂ O	833.0 mL/L
Ferrous Ammonium Sulfate	Fe(NH ₄) ₂ (SO ₄) ₂ · 6H ₂ O	39.2 g/L
	H ₂ SO ₄ (conc.)	20.0 mL/L
	H ₂ O	980.0 mL/L
Ferriin indicator	1,10-phenanthroline	14.85 g/L
	FeSO ₄ · 7H ₂ O	6.95 g/L
	H ₂ O	1.0 L/L

(FAS) to the ferriin endpoint. The standards were used to determine the precise normality of the FAS solution. The blanks provided a measure of the COD of the dilution water.

The COD of a given sample was then calculated as shown in Equation 29.

$$COD = \frac{(a - b) \cdot (N) \cdot (DF) \cdot (8,000)}{c} \quad (29)$$

- where, COD = chemical oxygen demand of the sample, mg/L
a = volume FAS used for blank, mL
b = volume FAS used for sample, mL
c = volume of sample, mL
N = normality of FAS solution, equivalents/L
DF = dilution factor of the sample
8,000 = equivalent weight of oxygen, mg/equivalent

The variable "c" in Equation 29 was in all cases 5 mL. Since the maximum COD measurable by this method is 480 mg COD/L for 5-mL samples, the samples normally required dilution so that the diluted sample had a COD less than 480 mg/L. "DF" in Equation 29 is the diluted sample volume divided by the undiluted sample volume. For example, if a sample was diluted by pipetting 20 mL of the sample into a 100-mL volumetric flask and filling the flask to the 100-mL mark, the dilution factor is 100 mL divided by 20 mL, or $DF = 5$. The normality of the FAS solution (N) is calculated using the standards. The dichromate solution is 0.1 normal. The FAS solution is also made to be 0.1 N, but this solution photo-degrades over time so that the active normality of the FAS solution is somewhat less than 0.1, as given in Equation 30.

$$N = \frac{3.0}{d} * 0.1 \quad (30)$$

- where, N = actual normality of FAS, equivalents/L (< 0.1)
 d = volume of FAS used for standards, mL (> 3.0)
 3.0 = theoretical volume of FAS required for standards if FAS was exactly 0.1 N, mL
 0.1 = theoretical normality of FAS solution, equivalents/L

Volatile Fatty Acids

Volatile fatty acids (VFAs) are classified as water-soluble fatty acids (up to six carbon atoms) that can be distilled at atmospheric pressure. They are removed from aqueous solution by distillation despite their high boiling points due to their high vapor tensions.

The VFA concentration of an anaerobic wastewater is a measure of the balance that exists among the acidogenic, acetogenic, and methanogenic bacterial populations. VFAs arise from the oxidation of sugars, alcohols, lipids, and long-chain fatty acids by the acidogenic and acetogenic bacteria. Under proper anaerobic digestion, the acetogenic bacteria convert the VFAs to acetic acid, and the methanogens convert acetic acid to methane and carbon dioxide. As such, high VFA concentrations signal an upset system in which the methanogenic bacteria are not keeping pace with the acidogenic and acetogenic bacteria.

The VFA test was conducted simultaneously with the COD test. Samples for VFA and COD determinations were taken from the same container. The method employed was Standard Method #504C [144]. One-hundred mL of the effluent sample was placed in a 500-mL distillation flask, together with 100-mL of distilled water, 5-mL of concentrated H_2SO_4 , and several glass beads. The flask was placed on a hot plate and connected with an adapter tube to a condenser. The samples were then distilled at a rate of approximately 5 mL/minute, and 150 mL of the distillate were collected. The distillate was titrated to the phenolphthalein endpoint with 0.1 N NaOH, and the VFA concentration in the original sample was calculated as shown in Equation 31.

$$VFA = \frac{(a)*(N)*(60,000)}{(b)*(0.7)} \quad (31)$$

where, VFA = concentration of volatile acids, mg/L as acetic acid
 a = volume of NaOH used, mL
 b = volume of sample, 100 mL
 N = normality of NaOH solution, equivalents/L
 60,000 = equivalent weight of acetic acid, mg/equivalent
 0.7 = empirical constant

The factor 0.7 is an empirical constant which comes from the assumption that 70% of the volatile acids will be found in the distillate. The actual value of this constant has been found to vary between 68 and 85%, depending on the nature of the acids and the rate of distillation. Care was taken to be consistent when distilling the VFA samples. The value of 70% was used in all VFA calculations.

Effluent Suspended Solids

The effluent samples taken for COD and VFA determination were also analyzed for total suspended solids (TSS) and volatile suspended solids (VSS) using a procedure similar to 208 D and E of *Standard Methods* [144]. Since the ASBR system has internal clarification, the level of TSS is a measure of how well the solids in the ASBR are settling.

A day before the test, the required number of filter papers (Fisherbrand G6, Fisher Scientific, Pittsburgh, PA) were folded in fourths and placed in aluminum weighing dishes. These were ignited at $550 \pm 10^\circ\text{C}$ for 20 minutes and then cooled to room temperature in a desiccator for not less than two hours. The filters and dishes were then weighed to the nearest 0.1 mg on a Mettler model AM 50 digital scale (Mettler Instrumentation Corporation, Hightstown, NJ) and returned to the desiccator until needed. Just before the

solids test was conducted, the filter paper and dishes were removed from the desiccator. The filter apparatus, consisting of a vacuum pump, a 500-mL suction flask, a 4-in porcelain Buchner funnel, and the necessary connecting hoses, was set up. The filter paper was removed from the aluminum weighing dish and placed in the Buchner funnel.

The samples to be tested were placed on a magnetic mixer and a specific volume was withdrawn from the sample with an appropriate pipet. The volume of the sample was dependent on the approximate solids content of the sample, but was always between 10 and 30 mL. The withdrawn (and a duplicate) sample was pipetted through the filter, and were then vacuum-filtered until no free water was left on the filter paper. The filter paper was returned to the weighing dish and these were then transferred to an oven and dried at $103 \pm 1^\circ\text{C}$ for not less than one hour. After drying, the samples were placed in a desiccator until cooled to room temperature and then weighed. The effluent TSS concentration could then be determined with Equation 32.

$$\text{Effluent TSS} = \frac{(A - B)}{V} * (10^6) \quad (32)$$

where, TSS = concentration of suspended solids, mg/L
 A = mass of dish + filter after drying at 103°C , grams
 B = initial mass of dish + filter (before filtering), grams
 V = volume of sample filtered, mL
 10^6 = conversion from g/mL to mg/L

The effluent VSS were determined by igniting the dried samples from above at $550 \pm 10^\circ\text{C}$ for 20 minutes. These samples were then cooled to room temperature and weighed again.

The residue remaining on the filter after ignition represents the fixed, or nonvolatile fraction, since the volatile portion has been destroyed. Equation 33 was used to determine the effluent VSS.

$$\text{Effluent VSS} = \frac{(A - C)}{V} * (10^6) \quad (33)$$

where, VSS = concentration of suspended solids, mg/L
 A = mass of dish + filter after drying at 103°C, grams
 C = mass of dish + filter after igniting at 550°C, grams
 V = volume of sample filtered, mL
 10⁶ = conversion from g/mL to mg/L

Mixed Liquor Suspended Solids

The mixed liquor suspended solids (MLSS) and mixed liquor volatile suspended solids (MLVSS) are a measure of the suspended solids in an operating ASBR. The MLSS is the concentration of all solids with an effective diameter greater than 0.45 μm , whereas the MLVSS measures only the volatile fraction greater than 0.45 μm . The MLVSS is a better measure of viable biomass, although neither MLSS nor MLVSS is a true measure of the amount of active microbes present. MLVSS is typically used to approximate the organic solids present in a reactor. The difference between volatile and organic matter is generally due to the volatilization of some inorganic compounds, most notably inorganic carbonates. That is, some inorganic carbonates are volatilized in the test and do not show up as fixed solids but rather as volatile solids. Therefore, equating organic residue with

volatile residue would be in error. Despite the differences in the two parameters, volatile solids were used to approximate the viable fraction because of the relative ease of the MLVSS test as compared to the total organic carbon test.

The samples used in the MLSS test were taken directly from the ASBRs during mixing. A side port was used to release approximately 20 mL of the ASBR contents into a beaker, and this volume was discarded. This was done to empty the side port of its contents, since the solids present in these ports are not representative of those present in the ASBR active volume. Another sample (30 to 40 mL) was then withdrawn from the same port and used for the MLSS test.

Filter papers were prepared exactly as in the effluent suspended solids test. Five mL of the MLSS samples were then filtered (in duplicate) and the excess water was removed with the vacuum pump. The samples were then dried in a $103 \pm 1^\circ\text{C}$ for not less than one hour. After drying, the samples were placed in a desiccator until cooled to room temperature and weighed. The MLSS concentration could then be determined with Equation 32, except that the effluent TSS term was replaced with MLSS.

MLVSS concentrations were determined by igniting the MLSS samples at 550°C for 20 minutes. After ignition of the samples, the filter papers were cooled and weighed. The MLVSS concentration was then calculated with Equation 33, except that the effluent VSS term was replaced with MLVSS.

Hydrogen Ion Concentration

One of the most important operating parameters of an anaerobic system is pH. Although acidogens and acetogens are able to survive over a fairly wide range of pH, methanogens can generally grow only within a pH range of approximately 6.5 to 7.8. The optimum pH is near 7. It was, therefore, necessary to monitor the pH daily for any significant deviation from near-neutral pH conditions.

Samples of the effluent from the ASBRs were collected in beakers for pH determination. The pH was measured using a Cole-Parmer model 05669-20 pH meter (Cole-Parmer Company, Chicago, IL) which was calibrated before each use using standard pH solutions of 4.00 and 7.00, or 7.00 and 10.00, depending on the pH of the ASBR effluent.

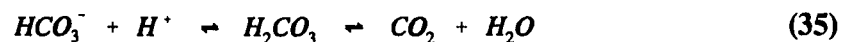
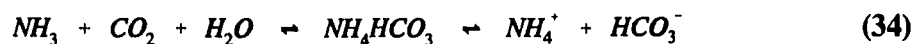
Alkalinity

The alkalinity of a water or wastewater is its quantitative capacity to neutralize strong acid to a designated pH. Alkalinity in anaerobic systems is an important parameter in that volatile acids produced by acidogenic and acetogenic bacteria tend to lower reactor pH. Sufficient alkalinity is necessary to maintain the pH of the system at or near 7.

In many wastewaters, alkalinity is a function of the carbonate, bicarbonate, and hydroxide content. In waters containing significant phosphates, silicates, and borates, the total alkalinity is also a function of these species. At typical pH values found in anaerobic systems (pH = 6.7 to 7.5), the hydroxide and carbonate concentrations are negligible as

compared to the bicarbonate concentration. Therefore, total alkalinity is essentially equal to bicarbonate alkalinity (plus borate, phosphate, and silicate alkalinity, if applicable).

For the two substrates used in these experiments (sucrose and beef extract+glucose), alkalinity was added to the feed solutions in the form of NaHCO_3 . Additionally, alkalinity was produced in the reactors in the form of ammonium bicarbonate (NH_4HCO_3). The sucrose substrate contained no nitrogen, and, therefore, all of the ammonia for these experiments was derived from addition of NH_3 to the feed solutions. The beef extract substrate, however, contained a significant amount of protein, the degradation of which resulted in additional ammonia generation within the ASBRs. The bicarbonate species were derived from two separate sources. First, bicarbonate was added directly to the reactor feed solutions, as mentioned earlier. Second, degradation of the substrates resulted in CO_2 production. CO_2 is in equilibrium with bicarbonate at the pH levels present in these systems. Therefore, CO_2 production leads to bicarbonate production. Equations 34 and 35 illustrate the production of alkalinity from ammonia, carbon dioxide, and water.



Additionally, HCO_3^- and NH_4^+ are in equilibrium with CO_3^{2-} and NH_3 , respectively. However, at the pH levels in these experiments, the latter two species represent an insignificant contribution to the buffering capacity of the system.

Standard method 403 [144] was used to determine the total alkalinity of the ASBR effluents. Potentiometric titration to pH 4.5 was performed with 0.1 N sulfuric acid throughout all experiments. The procedure was as follows. A 25-mL sample was collected in a beaker from an ASBR during the decant phase of a given cycle. The sample was quickly placed on a magnetic stir plate and a magnet stir bar was placed in the sample beaker. A calibrated pH electrode was inserted into the sample and the sample was mixed thoroughly. The sample was then titrated with 0.1 N sulfuric acid to pH 4.5. The total alkalinity of the sample was then calculated using Equation 36.

$$\text{Alk} = \frac{(A)(N)(50,000)}{V} \quad (36)$$

where, Alk = total alkalinity, mg/L as CaCO_3
 A = volume of standard acid used, mL
 N = normality of standard acid, equivalents/L
 V = volume of effluent sample titrated, mL
 50,000 = equivalent weight of CaCO_3 , mg/equivalent

Ammonia Concentration

The ammonia concentration in the ASBR is important for two reasons. A very low ammonia concentration may be indicative of a nitrogen-limited system, which would result in poor substrate removal efficiencies due to lack of bacterial growth. Conversely, a high

ammonia concentration could lead to inhibition of the microorganisms due to ammonia toxicity. Since ammonia was added to the substrate feed solutions in sufficient concentration to ensure the nitrogen was not limiting, the main reason for determining ammonia concentrations was to test for possible ammonia toxicity.

The literature generally implicates an inhibitory effect on methanogenesis at total ammonia ($\text{NH}_3 + \text{NH}_4^+$) concentrations of approximately 1,500 mg/L, as N. A more detailed description of ammonia toxicity is presented in the Literature Review section. Since the sucrose substrate did not contain nitrogen, almost all of the ammonia present in the system was due to the addition of NH_4OH to the feed solutions. Additional ammonia may be produced through cell death (followed by proteolysis), however, cell uptake of ammonia during biosynthesis is greater than the amount of ammonia produced by cell death in a system operating efficiently (cell growth $>$ cell death unless the system is inhibited or failing). Therefore, the concentration of ammonia in the ASBR systems is generally not greater than the amount of ammonia added to the feed solutions. In other words, the maximum ammonia concentration in the ASBRs fed the sucrose substrate could be calculated without actually testing for ammonia.

In the systems fed the beef extract + glucose solutions, however, degradation of the protein fraction of the beef extract led to additional ammonia production, the extent of which was dependent on the efficiency of protein breakdown. It was, therefore, necessary to measure the ammonia concentration of the ASBR effluent to ensure that ammonia inhibition did not occur.

An Orion ammonia probe (model 95-12, Orion Research Inc., Boston, MA) was used with an Altex model 4500 combination pH meter and millivolt potentiometer (Beckman Scientific Instruments, Irvine, CA) to determine total ammonia concentrations. The ammonia probe was calibrated with ammonium chloride solutions of 10, 100, 1,000, and 5,000 mg/L, as NH_3 . A standard curve was calculated for these standard solutions. Twenty mL samples were obtained from the ASBR effluents. The ammonia probe was then inserted into the sample (while mixing) and 2 mL of 6 N NaOH was added to the sample to increase the pH to above 11, which ensured that all of the ammonia would be in the unionized form (the ammonia probe measures NH_3 , not NH_4^+). The millivolt reading could then be compared to the standard curve to calculate the total ammonia concentration of the ASBR effluent.

Biogas Production and Composition

Methane and carbon dioxide (collectively termed here as biogas) are produced by the anaerobic consortia in the ASBR and other anaerobic reactors. The acidogens and acetogens oxidize higher organic molecules in a waste to long and short chain fatty acids, such as acetate, propionate, butyrate, and others. Little overall reduction in COD of the materials occurs in these steps since the degradation products are not liberated from the system. Stated differently, the COD of the degradation products in a given waste is approximately equivalent to the COD of the starting materials in the waste. During methanogenesis, however, stabilization of the waste occurs due to the liberation of

methane. Therefore, measurement of methane production is a useful tool for determining the degree of COD stabilization of a waste.

The COD-equivalent of the methane produced from anaerobic degradation of an organic substrate can be calculated by Equation 37.



The COD-equivalent of methane is, therefore, 2 moles of COD (oxygen) per mole of methane produced. Equivalently, the COD-equivalent is 0.35 L CH₄/g COD removed, or 5.61 ft³ CH₄/lb COD removed (all values are at standard temperature and pressure, 0°C and 1 atm.). Analysis of the composition of biogas produced from a reactor can then be used to determine the volume of methane produced, which enables a calculation of COD stabilized in the reactor. An example of this procedure is given below.

Given:	COD feed rate	=	1 g COD/L of reactor/day
	reactor volume	=	5 L
	biogas production	=	2.5 L/day (STP)
	CH ₄ % of biogas	=	65%

Solution:

CH₄ production = (0.65)(2.5 L/day) = 1.625 L/day (STP)

COD stabilized = 1.625 (L/day)/(0.35 L/g COD) = 4.64 g/day

COD in feed = (5 L)(1 g COD/L/day) = 5 g/day

$$\% \text{ COD reduction} = (4.64 \text{ g/day})(100)/(5 \text{ g/day}) = \underline{92.86\%}$$

As outlined in the Setup section of this document, the daily biogas production was measured with wet-test gas meters. The meter reading was taken at ambient atmospheric pressure and $35 \pm 0.5^\circ\text{C}$, both of which were recorded daily. The daily biogas volumes were then expressed as standard biogas production at 1 atm and 0°C . The biogas composition was analyzed using gas chromatography (GC). The GC system included a Model 69-350 Thermal Conductivity Gas Chromatograph (GOW-MAC Instrument Company, Bridgewater, NJ), equipped with a 6-ft. long by 1/8-in. in diameter GC column with Porapak-Q 80/100 mesh column packing. The operating conditions and parameters for the GC analysis are listed in Table 25.

Samples were collected using a 1-mL syringe (Hamilton Company, Reno, NV) equipped with 2-in-long Metal Hub Needles (Alltech Associates, Inc., Deerfield, IL). Nine-tenths of a mL of biogas was withdrawn from the gas sampling ports (earlier described) and the gas was then injected into the injection port of the gas chromatograph.

The data from the gas analyses were collected and analyzed using the Baseline 810 Chromatography Workstation software package (Waters Dynamic Solutions, Division of Millipore, Ventura, CA). The output from the analyses listed the percentages of methane, carbon dioxide, and nitrogen in the biogas. The nitrogen percentage in the biogas was actually a measure of the amount of air in the system. Theoretically, there should be no air in the system, since oxygen is toxic to anaerobic organisms. However, a small amount of air will enter the reactor due to the solubility of these gases in the feed substrate. In a well-operated system, oxygen entering the reactor through the influent will rapidly be

scavenged by facultative organisms and other oxygen-demanding substances. Therefore, the amount of nitrogen in the biogas was reflective of the air-tightness of the system. Zero, or very low, nitrogen indicated that the system was air tight, and significant nitrogen in the biogas suggested that there was a gas leak in the ASBR or gas handling equipment.

Table 25. Gas chromatography analysis setup.

Parameter	Value
Column temperature, °C	ambient
Injector port temperature, °C	100.0
Detector temperature, °C	150.0
Outlet temperature, °C	70.0
Biogas sample volume, mL	0.9
Column packing	
length, ft	6.0
diameter, in	0.38
Carrier gas	helium
Carrier gas flow rate, mL/min	60.0
Standard gas	
methane, %	70.0
carbon dioxide, %	25.0
nitrogen, %	5.0

Automated Image Analysis

Automated image analysis (AIA) was utilized to monitor the changes in biomass particle morphology and size in the ASBRs. Each ASBR was initially seeded with flocculent anaerobic digester sludge. Over time, the biomass particulates (which may or may not be biological in nature) tend to mature into large pellets, or granules. Whereas the average particle size at the beginning of each study was approximately 30 μm , over time the average particle size grew to several hundred microns, depending on the degree of granulation achieved in each ASBR. By monitoring the growth of the particle size, the physical transformation of flocculent biomass to granular biomass could be correlated with the operational state of the ASBR over the same time frame.

The AIA system was located at the Materials Testing Laboratory within the Department of Civil and Construction Engineering at Iowa State University. The AIA system consisted of a light microscope (model SZH, Olympus, Japan) with a video adaptor (Series 68, Dage-MTI, Michigan City, IN) connected to a video monitor (Sony Trinitron, Japan). The monitor was connected to a computer (model CIT-101 video terminal, C. Itoh Electronic, Inc., Los Angeles, CA) which analyzed the video images as presented below. The software used for analyses was OASYS 3 (LeMont Scientific, State College, PA).

The biomass sample to be analyzed was taken from the respective ASBR in a manner identical to the procedure for MLSS analysis. The sample was mixed on a magnetic stir plate and a broken tip pipette was used to transfer approximately 2 mL of the

sample to a modified well slide. The slide was then placed on the microscope platform and was ready for analysis.

The first step of analysis was to focus the microscope on the biomass in a way such that the majority of the biomass on the slide was in focus. Because the biomass was actually contained over the entire depth of the biomass slide, it was not possible to focus the entire contents of the sample at any given time. After focusing, the software was operated as follows. The image of the biomass was captured as a graphics file. The software then "colored" the biomass red, leaving the background liquid white. The software then calculated the area of each particle of biomass and calculated an equivalent diameter assuming the particles were spherical. The output from the software included histograms of the size distributions and total mass distribution, as well as average characteristics of the entire sample. Several analyses were made for each sample, and the cumulative results were then printed out for further analysis.

Specific Methanogenic Activity

Activity tests were conducted on the biomass from selected ASBRs to determine the differences between the specific substrate removal rates of flocculent and granular biomass. In this context, specific methanogenic activity (SMA) is defined as the rate of methane production per unit of biomass, and is defined for the entire bacterial consortium (not only methanogenic organisms). Previous research [87] in the environmental engineering laboratory at ISU indicated that granular biomass has a distinctly higher SMA than that of

flocculent biomass under identical conditions. It was also noted in the first few experiments of this research that when the biomass began to granulate in any given experiment, the biogas production rate (COD removal rate) increased significantly over a short period, and that this increase was proportionately greater than the increase in biomass concentration over the same time period. It was then decided that SMA tests should be conducted to quantify this observation.

The SMA tests were originally designed to be conducted in an anaerobic respirometer, but because of difficulties with the unit, it was decided to do the SMA tests in situ (using the entire ASBR). This change led to several difficulties. The environmental conditions were more difficult to maintain and monitor in the ASBR as compared to a small respirometer bottle. Also, it was more difficult to maintain uniform mixing conditions in the ASBR than it would have been in a small bottle. The ASBRs had to be continuously mixed at a high rate to maintain complete mix conditions. Also, the substrate concentrations added to the ASBRs were very high compared to the concentration that the microbes had been accustomed to seeing. It was observed that some of the granules in the SMA tests were damaged by shear or high rate of gas production. Therefore, because of the nature of the SMA test in the ASBR, it was not conducted during all of the experiments. Nevertheless, the ASBR units provided a comparative measure of the SMA characteristics of the various biomasses tested.

The SMA test was conducted as follows: The ASBRs to be tested were not fed for a period of 12 to 24 hrs before the SMA test in order to decrease the background substrate

concentration to its minimum level. The MLSS and MLVSS concentrations of the ASBRs were determined the day before the SMA test, since the amount of substrate added per unit mass of MLVSS was kept at a constant value for these tests. Just before the substrate was added to the reactors, a concentrated solution of sodium bicarbonate and appropriate nutrients and trace minerals were injected into the ASBR with a syringe. The amount of these compounds added was in proportion to the amount of COD added. These proportions were identical to those used to prepare the substrate feed solutions (described earlier). The substrate was then injected into the ASBR with a syringe, and the gas meter reading was recorded. Over the next 4 to 10 hours, the gas meter readings were recorded over time. Every 15 to 30 minutes, GC analyses of the biogas were conducted to determine the methane percentage of the total biogas. The pH in the ASBRs was maintained between 6.9 and 7.1 by syringe injection of HCl or NaOH, whichever was appropriate.

The cumulative methane production per unit mass of MLVSS over time was then plotted, yielding a linearly increasing portion over the first time period, which then level off to a maximum cumulative methane production for the amount of substrate added. The linear portion of the curve was indicative of the maximum SMA of the biomass.

Two different substrates were used in the SMA tests to determine whether granule morphology and consortia arrangement was the cause of the higher SMA for granules as compared to flocculent biomass. Sucrose, which requires the interaction of the entire bacterial consortia for conversion to methane, and acetate, which only requires the

methanogenic bacteria for conversion to methane, were utilized. It was predicted that the granular biomass would yield a higher SMA for sucrose, as compared to the flocculent biomass, but that the SMA for acetate would be similar. Discussion of this phenomenon can be found in the results and discussion portion of this document.

Scanning and Transmission Electron Microscopy

Scanning and transmission electron microscopy (SEM and TEM, respectively) analyses were also performed on the biomass from the ASBRs to observe the morphology and general nature of the granules developed in the experiments. Direct observation of the bacterial consortium within each granule allowed a qualitative estimation of similarities and differences among the granules developed in each of the experiments. In other words, if one experiment yielded a granule mainly consisting of cocci, while the granules from another experiment were composed of mainly rods, one plausible explanation for this is that the experimental enhancement method utilized in those experiments physically selected for those types of bacteria.

It was also desired to observe the homogeneous or heterogeneous distribution of the bacterial consortium of the granules. That is, the use of electron microscopy could elucidate whether the granule consisted of layers, with each layer consisting of a different bacterial group, or if the granules were homogenous throughout, with all groups of bacteria present in each part of the granule.

The SEM and TEM analyses were conducted at the Bessey Microscopy Facility, located at Iowa State University. Selected samples were taken to this facility, and all preparatory work and analyses were performed by the Bessey staff. The SEM used was a JEOL model JSM-35 operated at 15 kV. The samples were prepared with a Polaron sputter coater, using a palladium/platinum mixture.

Elemental Analysis of Biomass

Several reports in the literature have cited significant amounts of specific inorganic compounds or elements in granules. Others have noted that the elemental distribution of granules is very similar to that of flocculent biomass. It was decided to have the granules developed in these experiments examined for the constitutive composition of a range of elements (Table 26). An understanding of the elemental nature of granules, although not a significant contribution of this research, could lead to future research centered on the chemical enhancement of granulation.

The elemental and chemical analyses of the granules was conducted at the Analytical Services Laboratory (ASL) located within the Department of Civil and Construction Engineering at Iowa State University. All analyses were conducted by ASL staff. The samples to be analyzed were taken from the ASBRs after the respective experiments had been shut down. The samples were prepared for analysis using the methods shown in Table 26.

Table 26. Elemental analysis of granules.

Element/Compound	Method of Analysis
Carbon, organic	Total organic carbon ^a
Nitrogen, total kjeldahl	Auto-analyzer ^b
Phosphorous	Auto-analyzer ^c
Potassium	Atomic absorption ^d
Sodium	Atomic absorption ^d
Calcium	Atomic absorption ^d
Magnesium	Atomic absorption ^d
Iron	Atomic absorption ^d
Zinc	Atomic absorption ^d
Nickel	Atomic absorption ^d
Cobalt	Atomic absorption ^d
Manganese	Atomic absorption ^d

^a Dohrman Total Organic Carbon Analyzer (Rosemount Analytical Division, Santa Clara, CA).

^b Technicon Autoanalyzer II (Technicon Instruments Corporation, Tarrytown, NY).

^c Technicon Autoanalyzer II (Technicon Instruments Corporation, Tarrytown, NY).

^d Smith Hieftje 12, Model 857 (Instrumentation Laboratory, Inc., Lexington, MA).

RESULTS AND DISCUSSION

The following pages present a summary of the data collected over the course of this research. The data are presented individually for each of the different granulation-enhancement experiments. That is, all of the data for the PAC-enhancement is presented in one section, all of the data for the cationic polymer-enhancement is presented in another section, and so on. After the enhancement data has been presented, other data will be presented regarding the SMA tests, elemental analyses, and SEM analyses of the various biomasses produced during the experiments. Data tables, if not presented within the text of this section, are located in the appendices located at the end of this document. The Table of Contents and List of Tables details the organization of the document.

It is important to realize that these were not equilibrium studies. The goal of each study was to achieve granulation and system start-up in a short period of time. Therefore, the systems were pushed to their limits during their start-up period, and the line between a slightly-stressed and a heavily-stressed reactor was sometimes crossed. The goal was to slightly stress the systems in order to achieve high OLRs and short HRTs. In theory, these conditions should present the best physical conditions for granulation. The short HRT washes out the poor-settling biomass, and the high OLR creates conditions for high biomass production rates and high MLSS levels.

As previously stated, the data presented in this section reflect the stressed, non-equilibrium conditions in the reactors. Few of the curves consist of tightly grouped or smooth data points. Several of the graphs show sudden changes in the respective

parameters that are presented. The data presented here have not been "smoothed" by eliminating wild points, since the wild points were normally the result of an actual condition rather than a poorly-executed analysis. Instead, these wild points will be explained as to their cause and significance. The recovery of the systems from the highly-stressed conditions is also discussed, including the overall effect on granulation and start-up.

Sucrose Experiments

The majority of the granulation/start-up experiments were conducted using sucrose as the sole carbon source. Sucrose was selected for several reasons: (1) Sucrose is relatively easy to work with and is highly soluble in water. COD concentrations could be maintained at any desired level, resulting in a flexible COD loading rate. (2) The solutions of sucrose in water did not separate or precipitate over time. Additionally, the sucrose solutions could be kept in the constant temperature room at 35°C for two days before noticeable degradation occurred. (3) Sucrose conversion to methane requires anaerobic bacteria from all of the previously-discussed groups. And (4) sucrose and related sugars are typical constituents of several industrial wastewaters.

Control Study

It was necessary to establish a baseline control for granulation and start-up using the sucrose substrate. As previously stated, the only other granule-producing study

conducted with the ASBR used a non-fat dry milk substrate and required over 200 days for significant granulation to occur. The control study in these experiments was conducted exactly as the other experiments, with the exception that no granulation enhancement was practiced.

Operational Performance

The control ASBR was seeded with an MLSS concentration of approximately 20,000 mg/L (MLVSS approximately 12,000 mg/L). The HRT and COD loading rate were initially 2 days and 1 g/L/day, respectively. After approximately one week, the COD load was increased to 2 g/L/day at an HRT of 2 days. These conditions were maintained in the ASBR for a period of approximately 1 month due to the poor COD removal efficiency and methane production (Figures 18 and 19). It is noted here that in Figure 19 and subsequent standard methane production curves, the relative height of the methane curve to the COD load curve is approximately the COD removal efficiency of the system based on methane production. This results from the graphical method chosen to present these data. The scale of the primary Y-axis (methane production) has been set at one-third of the scale of the secondary Y-axis (COD-load). The theoretical methane yield from 1 gram of COD removed is 0.35 L, which is very close to one-third. In fact, taking into consideration biosynthesis, the value of one-third is a more realistic methane yield constant than 0.35.

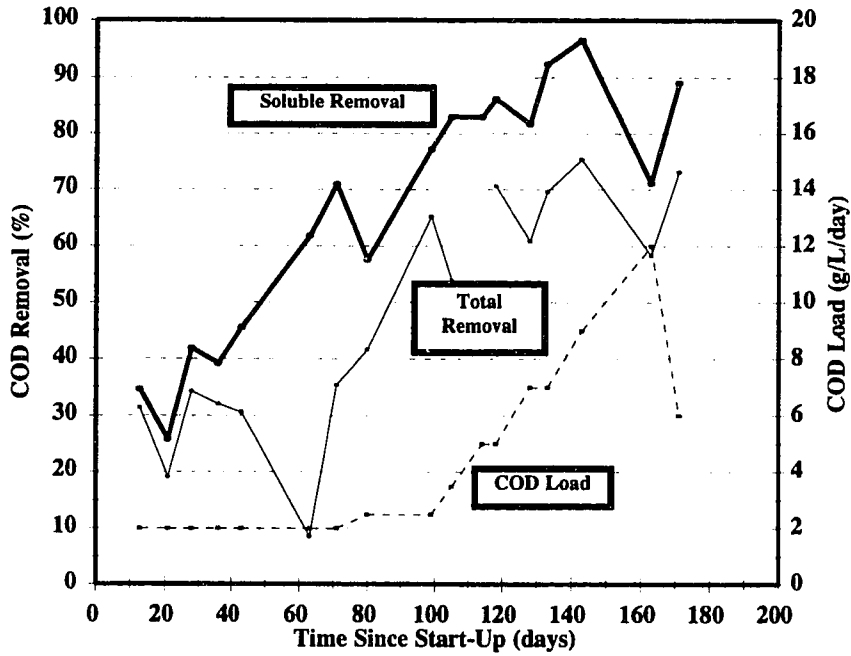


Figure 18. COD removal for the sucrose control study.

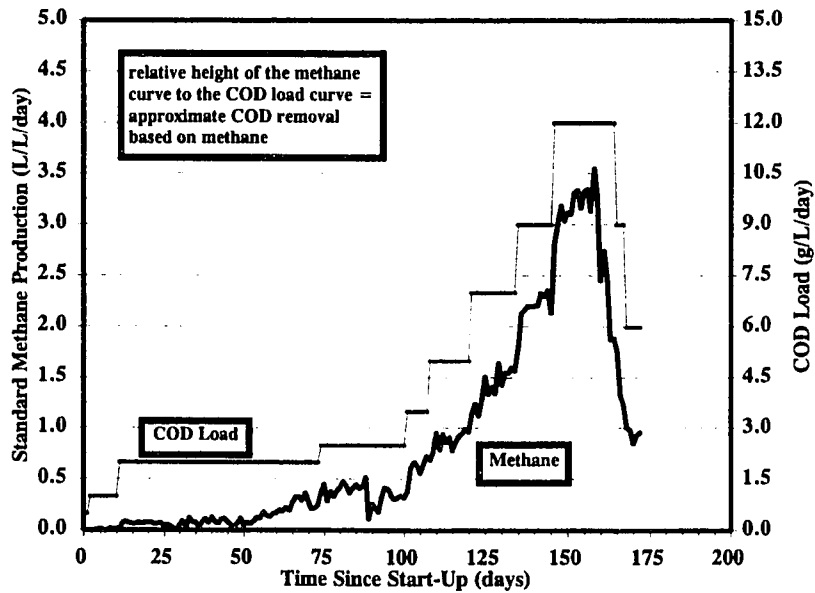


Figure 19. Methane production for the sucrose control study.

After 35 days of operation, the HRT was decreased to 36 hrs and 12 days later to 24 hrs, where it remained for the remainder of the experiment. After more than 70 days of operation, the soluble COD (SCOD) removal efficiency increased to over 70%, at which time the COD load was increased to 2.5 g/L/day. On day 100, the COD load was further increased to 3.5 g/L/day, and shortly thereafter to 5 g/L/day (day 122). After this time, the COD load was increased step-wise to a high of 12 g/L/day on day 145, with greater than 85% SCOD removal at most loading rates.

After a period of 2 weeks at 12 g COD/L/day, the reactor began to fail. The COD removal decreased (Figures 18 and 19) and the volatile acids concentration increased (Figure 20). The pH dropped slightly, but remained within acceptable limits (Figure 21). On day 162, the COD loading rate was decreased to 6 g/L/day and shortly thereafter the reactor was shut down.

Solids and Granulation

The MLSS levels in the control ASBR continued to decrease until reaching a minimum of 4,000 mg/L on day 84. After this time, the MLSS concentration continually increased to a maximum of almost 18,000 mg/L on day 159, at which time the COD load was 12 g/L/day. Simultaneous with the decreased COD removal observed at 12 g COD/L/day, the MLSS level abruptly decreased to below 14,000 mg/L. It was observed that the excessive biogas production resulted in very turbulent conditions during the settle

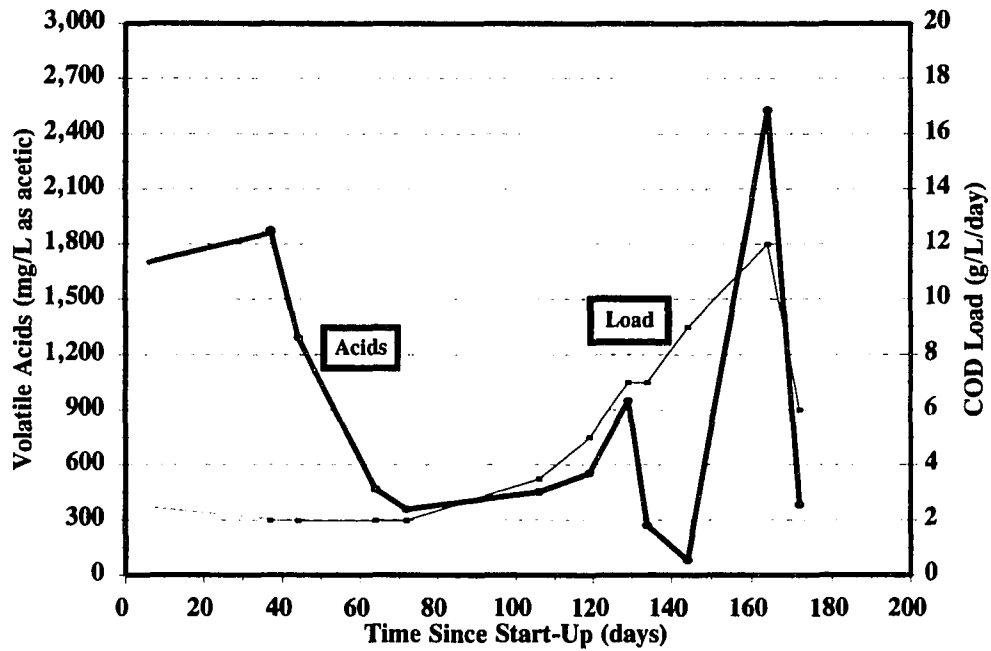


Figure 20. Volatile acids data for the sucrose control study.

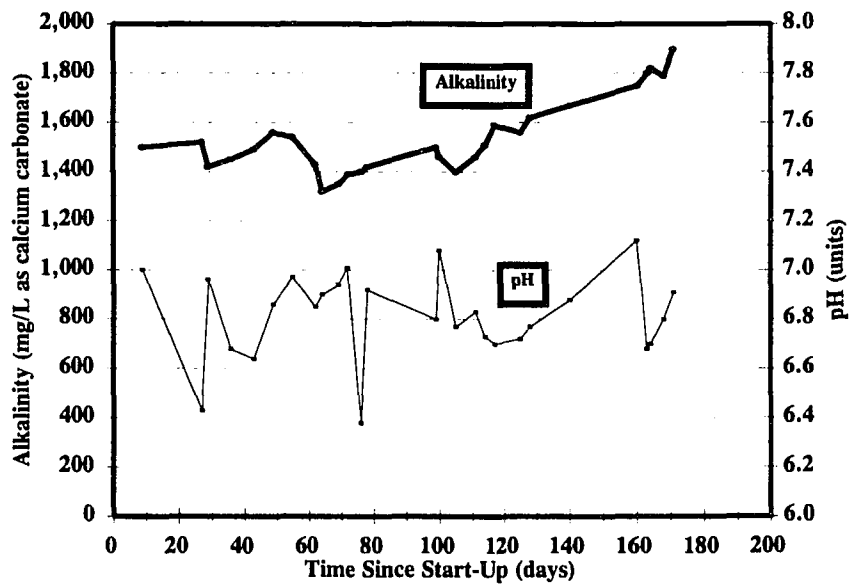


Figure 21. Alkalinity and pH data for the sucrose control study.

and decant phases. Therefore, the solids did not settle as well and were carried out in the effluent (Figure 22).

The sludge age of the system was generally in excess of 10 days for the first 100 days of operation. However, over the same period in which the COD removal efficiency improved drastically and the MLSS levels increased, the sludge age was consistently below 10 days with an average of approximately 7.5 days. This low SRT did not appear to be detrimental to the overall process. In fact, the ASBR performed significantly better over the time period during which the SRT was below 10 days (Figure 22).

Figure 23 presents the granulation data for the control reactor. Again, approximately at day 100 changes begin to occur. The biomass was decidedly flocculent over the first 4 months of operation. However, the AIA on day 120 revealed a slight increase in the average biomass particle size over previous tests, although visually the biomass still appeared to be almost completely non-granular. Approximately two weeks later, significant granulation was observed. The granulation of the biomass correlates well with the observed COD removal performance over the same time period. That is, as the biomass granulated, the COD removal efficiencies increased significantly, even as the COD load approached 12 g/L/day.

Two notes are relevant here. The first is that the SRT of the system (and of systems presented in the following paragraphs) was below the theoretical minimum for anaerobic systems. As stated earlier, the minimum SRT of an anaerobic system is normally around 10 days. Below this SRT, methanogens are washed out of the reactor at a

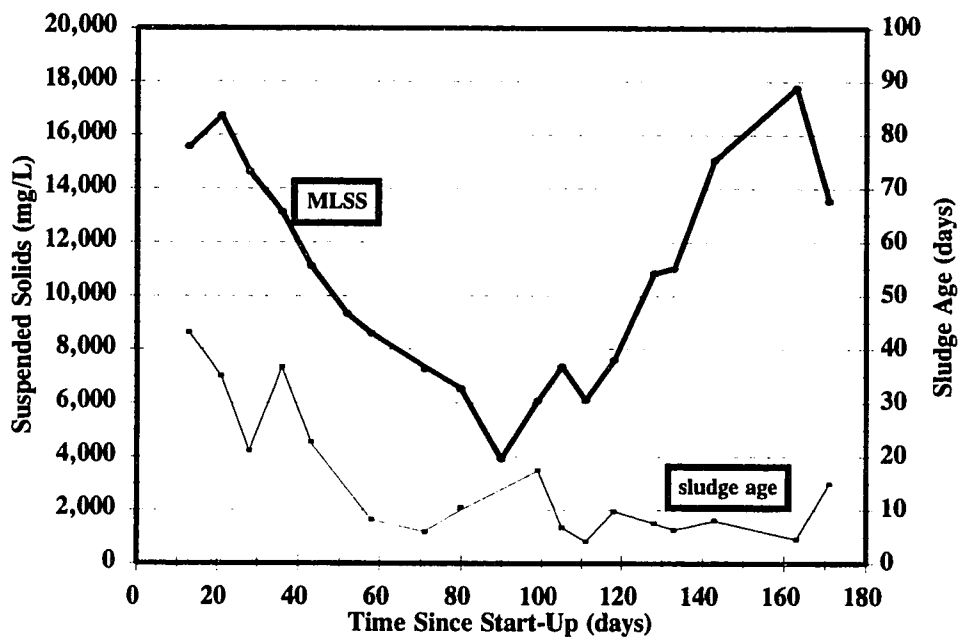


Figure 22. MLSS and SRT for the sucrose control study.

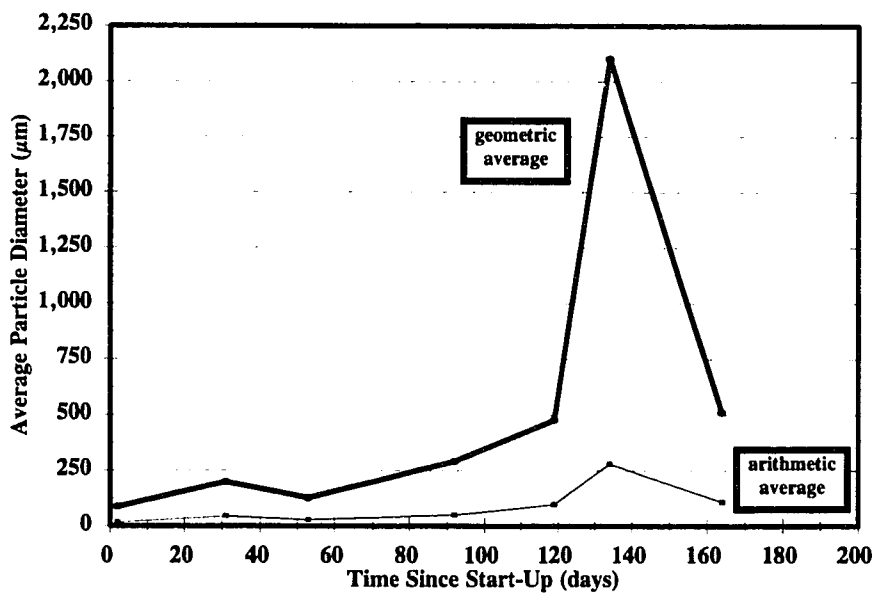


Figure 23. Average particle size data for the sucrose control study.

rate faster than they can reproduce. One explanation is that as granulation progresses, the biomass becomes segregated in the reactor, resulting in non-complete mix conditions and an underestimation of the MLSS (and SRT). A second explanation is that the methanogenic growth rates of granular biomass is higher than that of non-granular biomass. Under optimum growth conditions in pure culture, the doubling times of most methanogens is approximately 3 to 7 days. It, therefore, appears that the micro-environment that exists in a granule may approximate optimum growth conditions, allowing for faster growth rates than is possible for non-granular biomass (better thermodynamics).

The second note is a distinction between the average particle size based on the number of particles (arithmetic) and based on the weight distribution of the particles (geometric). Based strictly on the diameter of each particle in a given biomass sample, the average particle diameter of the sample may be quite small. However, in that same sample the majority of the mass of the sample may be incorporated in granules. The geometric average particle diameter is a measure of the distribution of the biomass in each range of particle size, and, therefore, better reflects the average state of granulation.

It is further noted that although the two parameters normally trend together, the absolute values of the two are quite different. Both the arithmetic and geometric average particle size are presented throughout this document. However, the geometric average particle size is considered to be more significant in terms of defining granulation.

Powdered Activated Carbon Enhancement Study

Powdered activated carbon (PAC) was used to enhance granulation. It was theorized that the PAC would act as a site of attachment for bacteria. The PAC adsorbs substrate molecules and thus should provide an ideal site for bacterial growth and granulation. This experiment was the longest of all of the experiments in this study. It was decided to try to achieve the highest possible COD load on the ASBR after granulation had been observed.

Operational Performance

The PAC-enhanced ASBR was seeded with an MLSS concentration of approximately 20,000 mg/L (MLVSS approximately 12,000 mg/L) and a PAC concentration of 2,000 mg/L. After the initial addition of PAC to the ASBR, no further additions were made. The HRT and COD loading rate were initially 2 days and 1 g/L/day, respectively. After 3 weeks of operation, the COD removal improved enough to increase the OLR to 2 g COD/L/day (HRT = 2 days). After 45 days of operation, the COD removal and settling improved and the HRT was reduced to 1 day. The COD load was further increased to 3 and 4 g/L/day on days 65 and 90, respectively. At approximately day 105, the COD removal increased significantly, and the COD load was step-wise increased to 5, 7, 9, 11, and 14 g/L/day over the next 45 days. Over this period of time, the SCOD removal efficiency of the ASBR was in excess of 95% at all loads, and the total COD (TCOD) removal efficiency was approximately 70 to 80% (Figures 24 and

25). The volatile acids concentration over this same time period was low (Figure 26), and even at the COD load of 14 g/L/day was below 100 mg/L (as acetic acid). The pH remained relatively constant between 6.8 and 7.0 (Figure 27).

After approximately 20 days operating at 14 g COD/L/day, a sudden pH drop (pH = 5.3) caused the failure of the system (Figures 24-27). COD removal was negligible and the volatile acids increased to 2,600 mg/L. It was not explicitly known what caused the severe pH drop, but it seems likely that the buffering compounds (sodium bicarbonate and ammonium hydroxide) may have been left out of the feed solution.

Although complete failure of the methanogens was apparent (zero gas production), conversion of the sucrose to acids was observed, and, therefore, the entire system was not dead. The COD load was decreased to 3.5 g/L/day to try to recover the methanogenic activity. After approximately 3 weeks, the SCOD removal increased to 90%, and the COD load was step-increased to 12 g/L/day over 50 days. Although the COD removals were generally in excess of 90% at loads of 9 g COD/L/day and less, the system began to fail again at 12 g/L/day. Again, the pH of the reactor decreased at this time (pH = 6.5). The reactor was shut-down shortly after this second pH decrease.

The recovery of the ASBR observed after complete methanogenic shut-down is significant. It is probable that the granule environment protects the methanogens to some degree from inhibitory conditions, such as the low pH observed in this study. One theory is that ion diffusion is limited into the granule. Under normal conditions the granule matrix provides an efficient route for transfer of metabolic intermediates. Under stressed

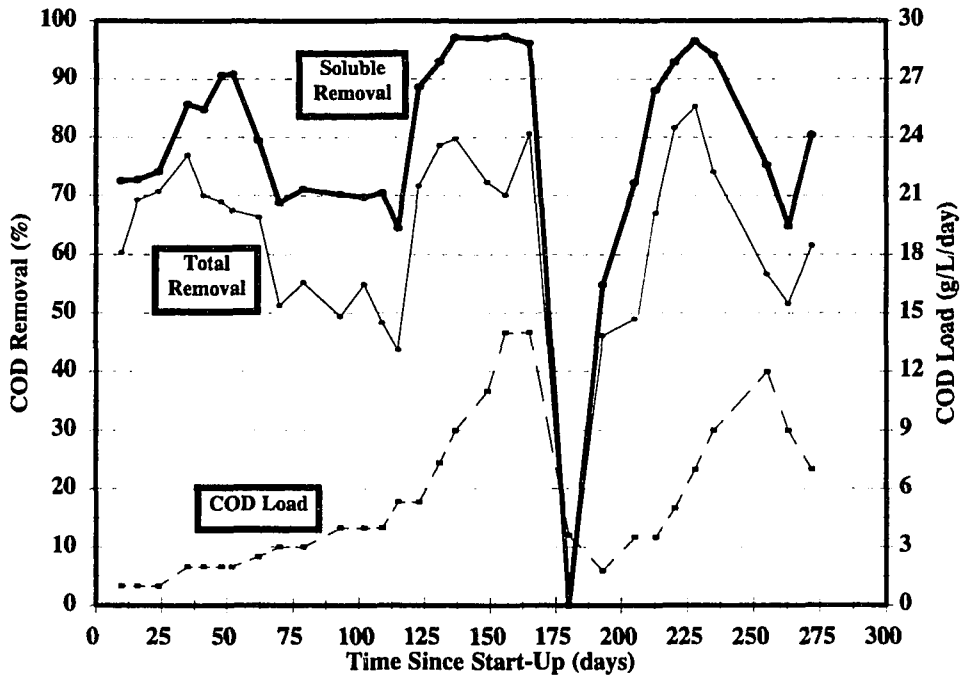


Figure 24. COD removal for the PAC-enhanced sucrose study.

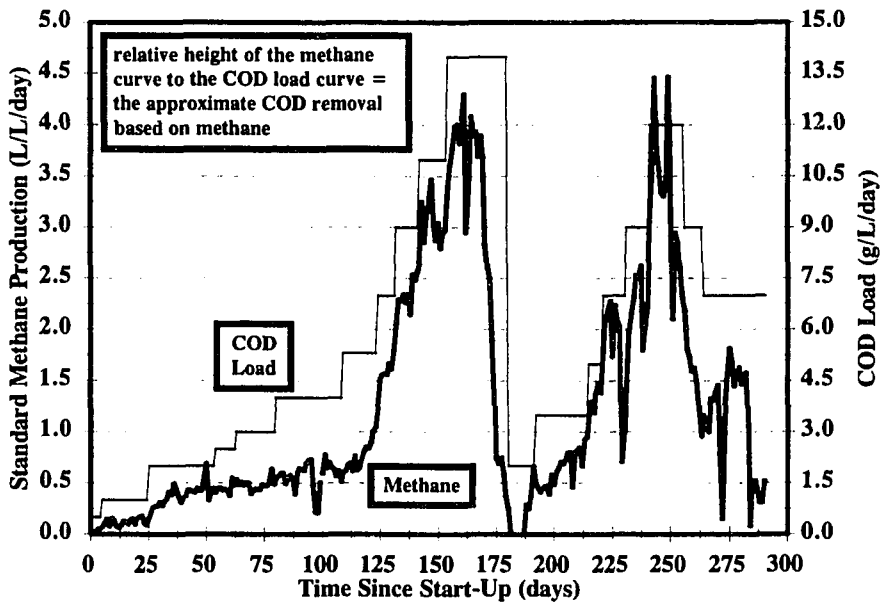


Figure 25. Methane production for the PAC-enhanced sucrose study.

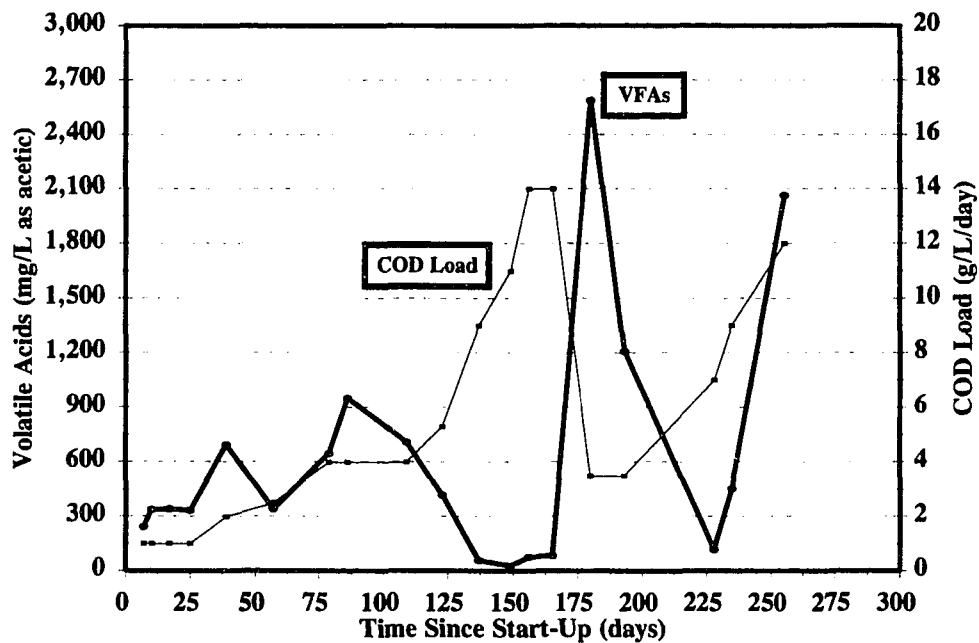


Figure 26. Volatile acids data for the PAC-enhanced sucrose study.

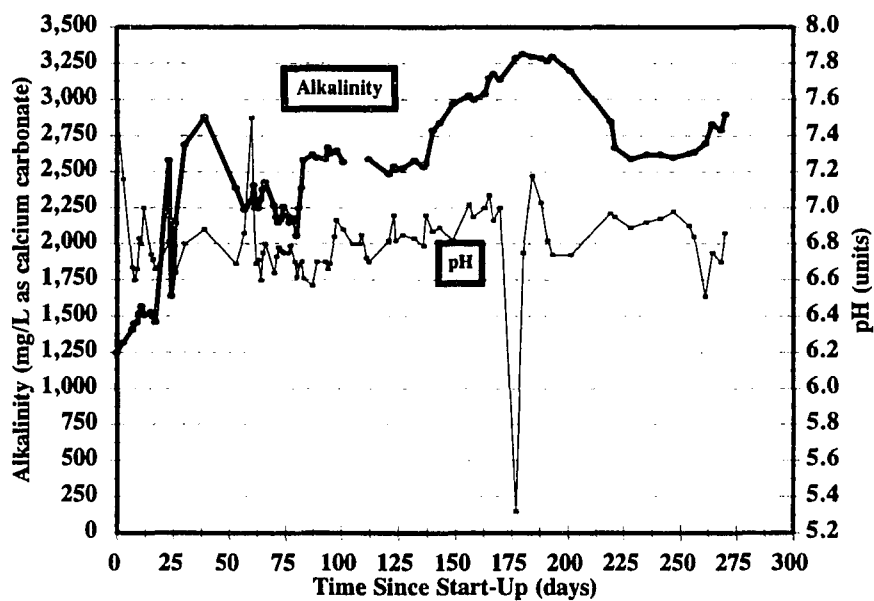


Figure 27. Alkalinity and pH data for the PAC-enhanced sucrose study.

conditions, this same property may limit the amount of inhibitory substance entering the granule, thereby reducing the adverse effect on the bacterial consortia.

Solids and Granulation

The MLSS levels in the PAC-enhanced ASBR quickly decreased to their minimum level shortly after start-up (Figure 28). The MLSS concentration decreased from approximately 21,000 mg/L at day zero to 5,000 mg/L at day 20. The solids stayed at this level until approximately day 60, at which time they began to increase slowly. At day 90, the MLSS concentration was approximately 9,000 mg/L, and stayed at this level until about day 125. Over the next 50 days, the MLSS level increased to more than 26,000 mg/L. Over this same time period, the COD loading rate was increased from 5 to 14 g/L/day. Upon reactor failure at day 165 (presented earlier), the MLSS concentration decreased to less than 15,000 mg/L over 40 days. Later, the recovery of the system resulted in an increase in the MLSS level to 27,000 mg/L. The SRT of the system fluctuated around the 10-day mark for the majority of this study (Figure 28). As the MLSS continued to increase, the effluent solids concentration also increased, resulting in a relatively constant SRT. Figure 29 presents the granulation data for the PAC-enhanced ASBR. The first granules were observed at approximately day 90, although at this time the majority of the biomass was still flocculent. From day 90 to day 120, significant granulation was observed. By day 130, the geometric average particle diameter was in excess of 1.5 mm, and just prior to reactor failure the average size was over 2.2 mm. The

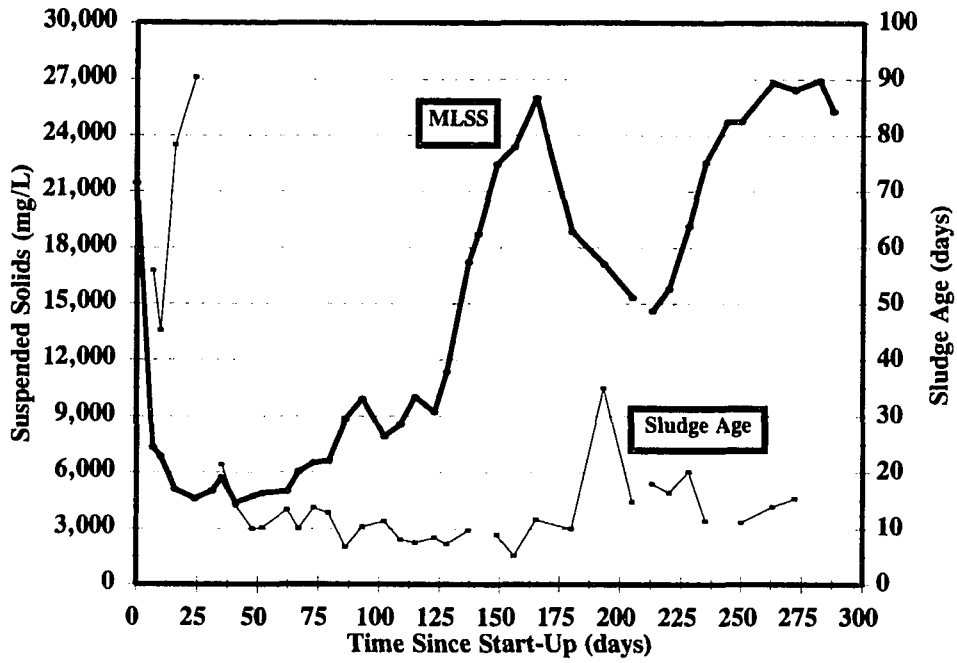


Figure 28. MLSS and SRT for the PAC-enhanced sucrose study.

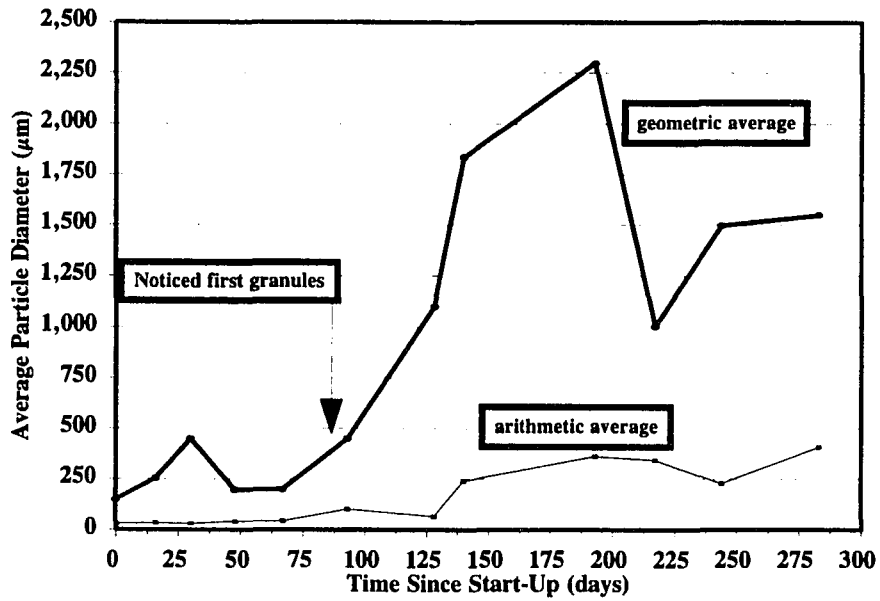


Figure 29. Average particle size for the PAC-enhanced sucrose study.

failure of the ASBR due to low pH also affected the particle size of the granules. Significant breakup of the granules was observed, and the average size decreased to approximately 1 mm. During reactor recovery, the average size again increased to over 1.5 mm.

PAC Effect

Compared to the control reactor, the PAC-enhanced ASBR was observed to granulate more rapidly. The PAC-enhanced ASBR was approximately one month ahead of the control ASBR in terms of first detection of granules and overall granulation of the biomass. The PAC-enhanced ASBR was also able to achieve higher OLRs more quickly than the control reactor. After 90 days of operation, the control reactor was operating at 2.5 g COD/L/day and removing 60% of the SCOD. After 90 days in the PAC-enhanced ASBR, however, it was treating 4 g COD/L/day at over 70% SCOD removal. Shortly thereafter the SCOD removals increased to over 95%. It seems apparent that the effect of the PAC addition was beneficial to the overall function of the ASBR.

Granular Activated Carbon Enhancement Study

Granular activated carbon (GAC) was also used as an enhancement for granulation and ASBR start-up. Several studies with the expanded-bed anaerobic reactor (presented earlier) indicated significant growth attached to GAC. GAC also offers the advantage of

better settling properties as compared to PAC. Therefore, biomass attached to GAC has a better chance of remaining in the reactor as compared to biomass attached to PAC.

Operational Performance

The GAC-enhanced ASBR was initially seeded with 19,000 mg/L of suspended solids (MLVSS = 11,400 mg/L) and 2,000 mg/L of GAC. The initial HRT and OLR were set at 2 days and 1 g COD/L/day, respectively. After 2 weeks the COD load was increased to 2 g/L/day (1-day HRT), and by day 40 the reactor was treating 4 g/L/day at approximately 70% SCOD removal efficiency (Figures 30 and 31). At approximately day 60 the COD load was increased to 5.5 g/L/day. By day 90, the load was at 9 g/L/day with over 90% SCOD removal. The volatile acids concentration decreased from approximately 1,050 mg/L to less than 70 mg/L between days 55 and 90 (Figure 32). The pH fluctuated but remained within 6.8 and 7.2 over the majority of this time period (Figure 33).

At approximately day 105, the COD load was increased to 11 g/L/day. Significant loss of biomass was observed at this point and the load was decreased to 9 g/L/day. Further increases in the COD load were not performed because it was decided to use this ASBR for specific methanogenic activity (SMA) experiments. The SMA tests disrupted the natural course of operation of the ASBR. Therefore, data beyond this point of operation were not considered with respect to comparison with the other granulation experiments.

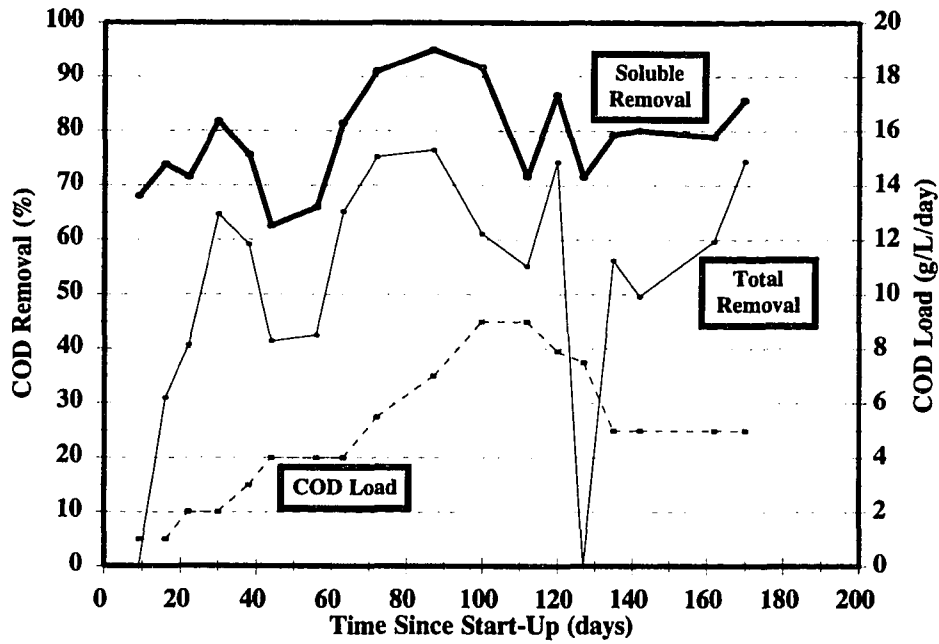


Figure 30. COD removal for the GAC-enhanced sucrose study.

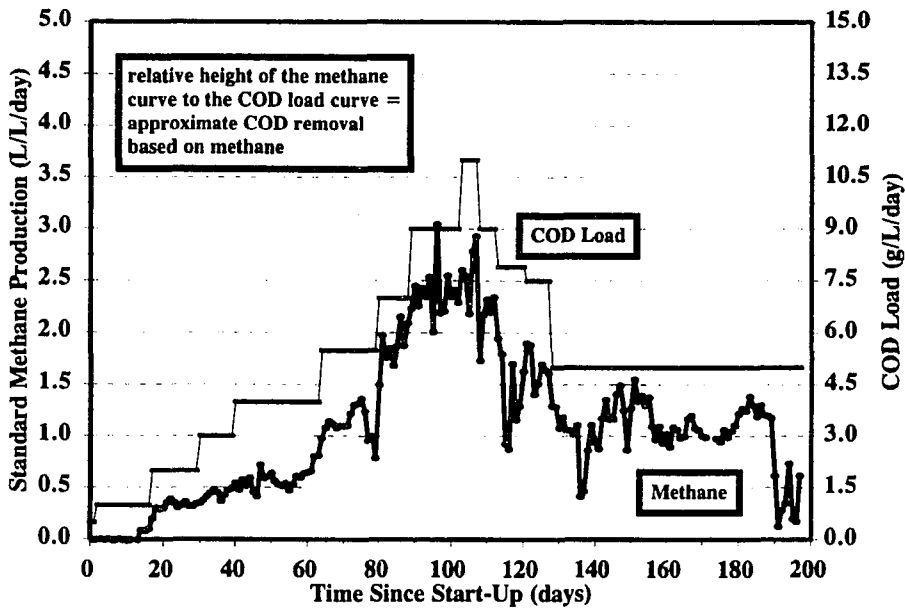


Figure 31. Methane production for the GAC-enhanced sucrose study.

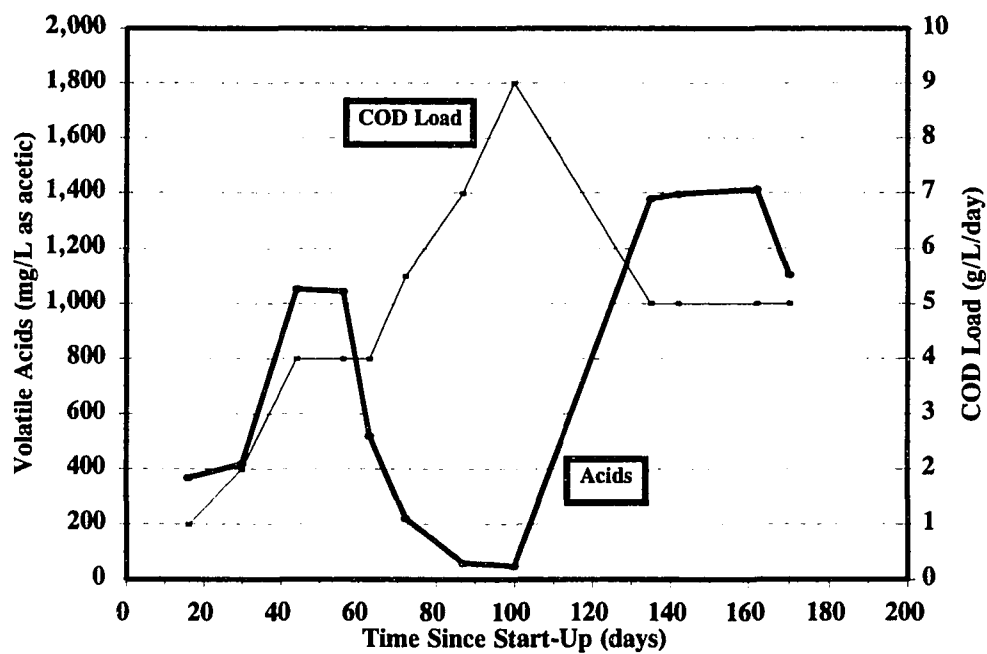


Figure 32. Volatile acids data for the GAC-enhanced sucrose study.

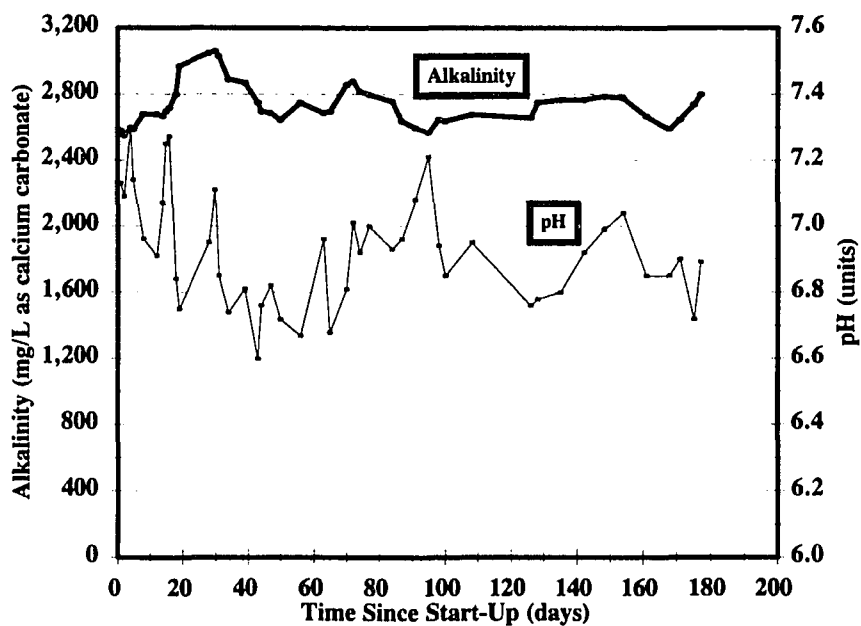


Figure 33. Alkalinity and pH data for the GAC-enhanced sucrose study.

Solids and Granulation

The MLSS level decreased from 19,000 mg/L to a minimum of 5,500 mg/L over the first 40 days of operation (Figure 34). By day 55, the MLSS level had increased to 7,000 mg/L, and by day 90 the MLSS level was approximately 18,000 mg/L. As stated earlier, significant loss of biomass occurred at about day 105, and the MLSS levels decreased to approximately 8,000 mg/L and remained there for a period of about 50 days.

At about day 40, when the MLSS level was a minimum but began to increase, the SRT of the system was approximately 6 to 7 days (Figure 34). During the most rapid increase in MLSS levels, the SRT was approximately 12 to 14 days (day 60 to 90). This latter period was also when the first granules appeared (day 70). The geometric average particle size at this time was approximately 0.5 mm, although the overall nature of the biomass appeared flocculent to the unaided eye (Figure 35). By day 80, the biomass had a significant granular nature, although the AIA test indicated that the average particle size was still 0.5 mm. Subsequent analyses showed that the average particle size increased to a maximum of 1.9 mm.

GAC Effect

The GAC had a significant beneficial effect on the overall performance and start-up of the ASBR. A COD load of 4 g/L/day was achieved in only 40 days, which is under half the time required in the previous two experiments. A COD load of 9 g/L/day was achieved in the GAC-enhanced ASBR in approximately 100 days, which is about 25

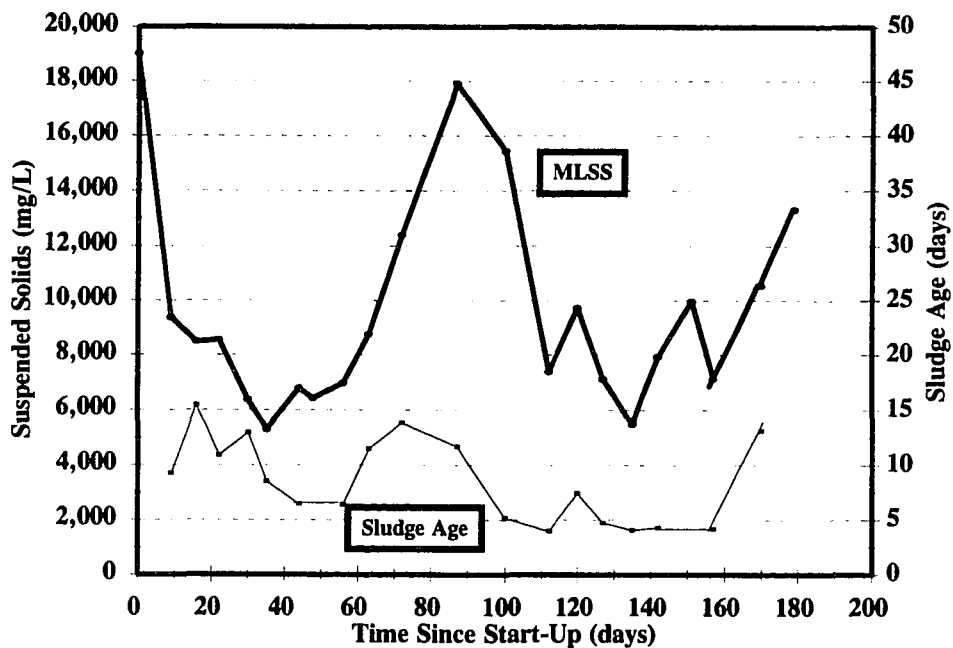


Figure 34. MLSS and SRT for the GAC-enhanced sucrose study.

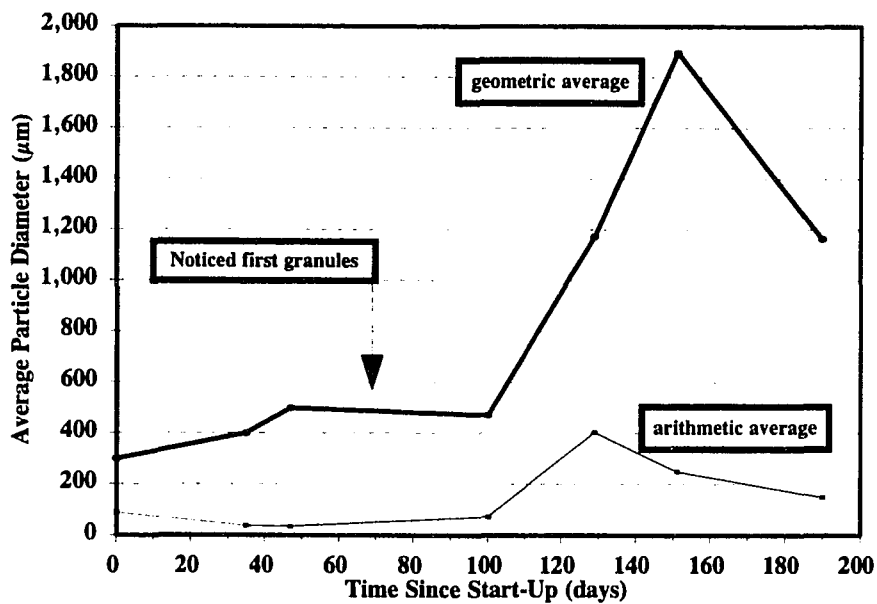


Figure 35. Average particle size for the GAC-enhanced sucrose study.

days less than in the PAC-enhanced ASBR and 45 days less than in the control ASBR. Initial granulation was also observed in a significantly shorter period of time with the GAC-enhanced ASBR. The first granules were observed at approximately day 70 in the GAC-enhanced ASBR, compared to day 90 for the PAC-enhanced ASBR and day 120 for the control ASBR. Although the GAC-enhanced experiments were not continued to determine the maximum COD load, the GAC definitely decreased the required start-up time and may have increased the rate of granulation.

Garnet Enhancement Study

Operational Performance

It was decided to use attachment matrices that did not possess significant adsorptive capacity to determine whether this property of the PAC and GAC had an effect on the overall granulation and start-up process. Two matrices, garnet and silica sand, were chosen. The garnet enhancement study was somewhat more successful than the sand enhancement study, although neither matrix appeared to have a beneficial effect. This section presents the data for the garnet study, and the following section presents the data for the sand enhancement study.

The ASBR was initially seeded with an MLSS concentration of 18,000 mg/L (MLVSS = 11,000 mg/L) and 2,000 mg/L of garnet sand, which had a specific gravity of approximately 4.2. Preliminary mixing studies indicated that the garnet sand could be easily mixed in the ASBR through normal gas recirculation. However, these tests were

conducted in pure water. It was impossible to determine whether the garnet was completely mixed with the biomass after start-up due to the black nature of the biomass.

The ASBR initially received 1 g COD/L/day at a 2-day HRT. After 10 days the load was increased to 2 g/L/day. The HRT was decreased to 36 hrs after 31 days of operation, and on day 50 it was decreased to 24 hrs. The COD load at these times were 2.7 and 3.5 g/L/day, respectively (Figures 36 and 37). Below 3.5 g COD/L/day, the SCOD removal efficiency was in excess of 75%. However, upon decreasing the HRT to 24 hrs (COD load = 3.5 g/L/day), the SCOD removal efficiency dropped to below 40%, after which it slowly increased to 78% from day 50 to day 110 (Figures 36 and 37).

The volatile acids concentration remained relatively high over the course of this study. Just prior to increasing the COD load to 2.7 g/L/day, the VFA concentration was approximately 500 mg/L. After the load was increased to 2.7 g/L/day and later to 3.5 g/L/day, the VFAs increased to over 1,400 mg/L, and were never less than 1,200 mg/L, indicating that the methanogenic population was not sufficient to degrade the acids produced by the other bacterial consortia (Figure 38). The reactor pH (Figure 39) was marginally low over the majority of the study. Although the average pH of the reactor was approximately 6.8, it fluctuated between 6.6 and 7.0. The COD load was never increased beyond 3.5 g/L/day due to the relatively poor COD removals (Figure 36), low methane production (Figure 37), and high VFAs (Figure 38).

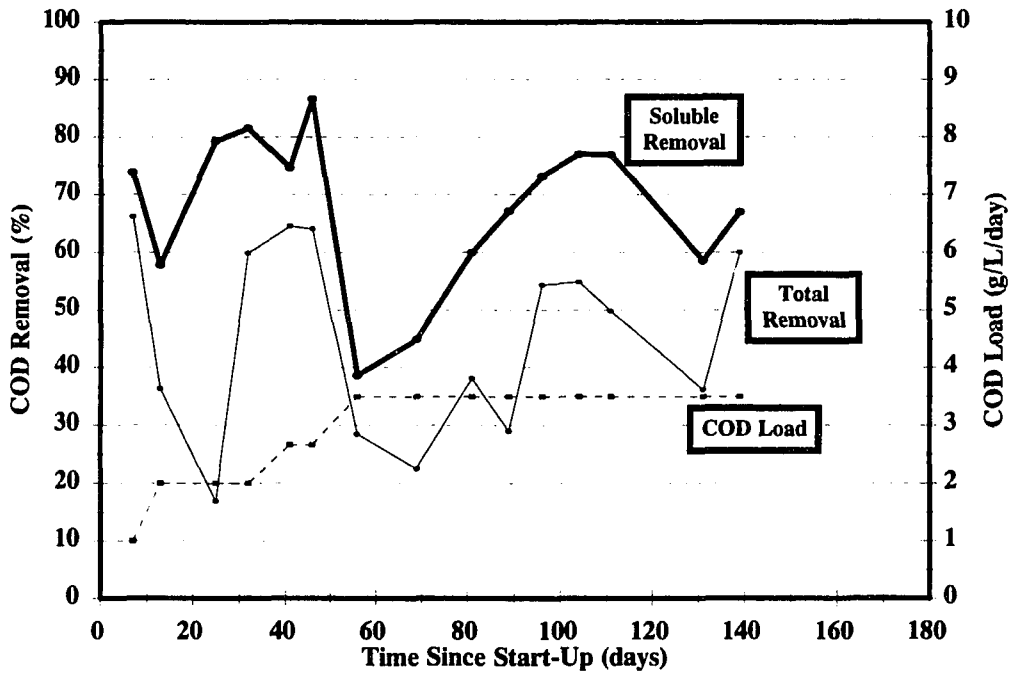


Figure 36. COD removal for the garnet-enhanced sucrose study.

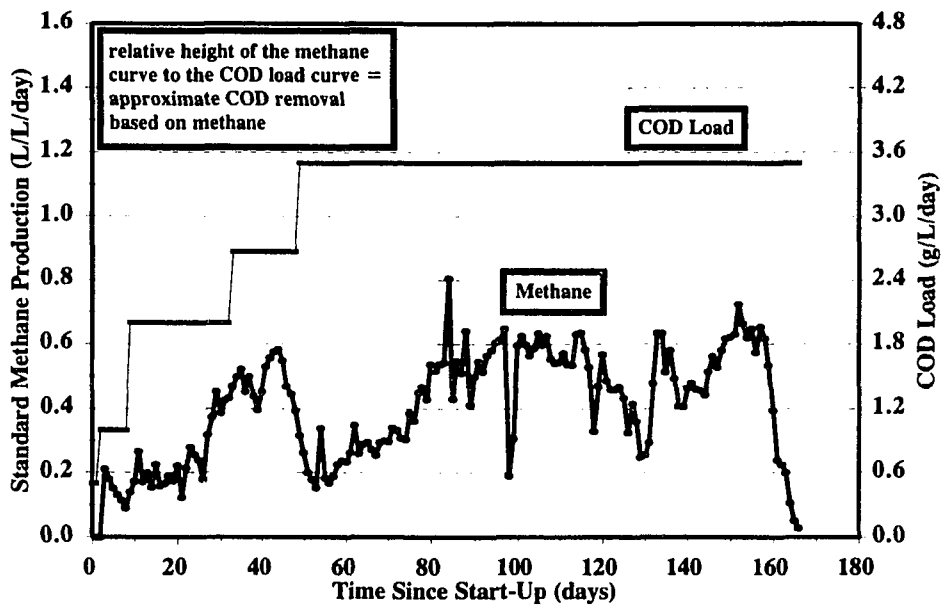


Figure 37. Methane production for the garnet-enhanced sucrose study.

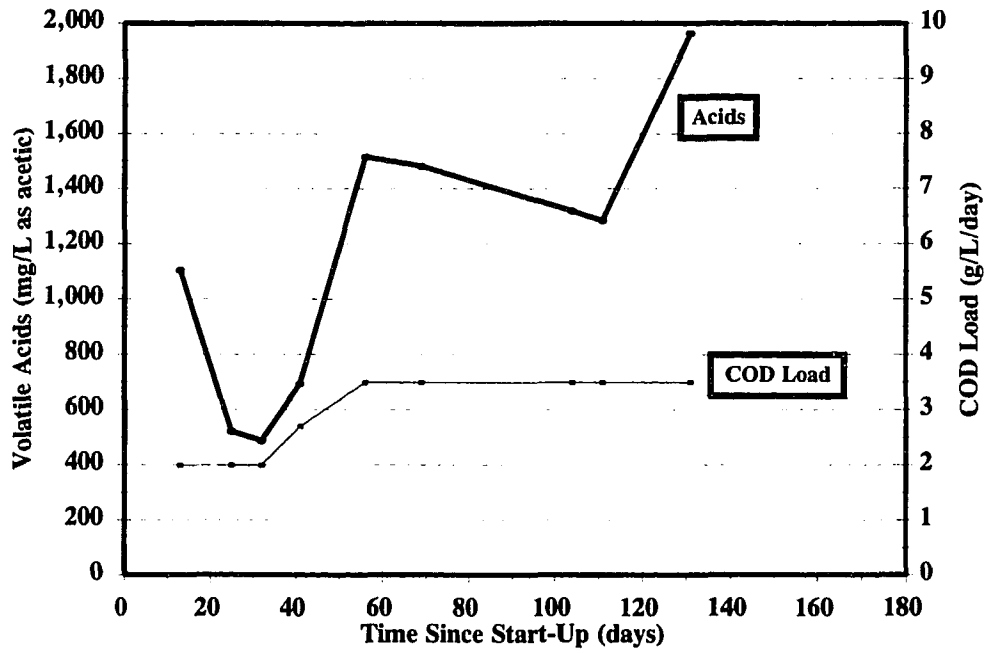


Figure 38. Volatile acids data for the garnet-enhanced sucrose study.

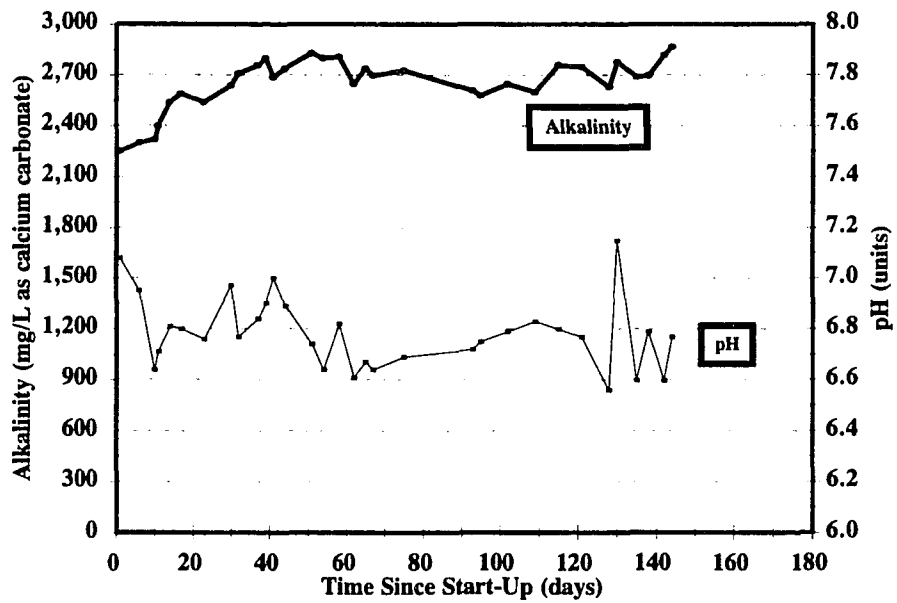


Figure 39. Alkalinity and pH data for the garnet-enhanced sucrose study.

Solids and Granulation

The MLSS concentration decreased over the first 40 days of operation to 6,100 mg/L (Figure 40). After the COD load was increased to 2.7 and 3.5 g/L/day, a marginal increase in the MLSS level was observed. After 70 days of operation the MLSS concentration was approximately 10,000 mg/L. The SRT over this same time decreased from 16 days (day 40) to approximately 9 days (day 70).

After day 70, the MLSS began to settle less efficiently with a subsequent decrease in MLSS to 5,000 mg/L and an SRT of only 3 days by day 90. At this point, the HRT of the system was increased to 2 days to try to increase the solids inventory. After approximately 2 months of operation at the 2-day HRT, the MLSS increased to over 12,000 mg/L and the SRT increased to approximately 12 days (Figure 40). However, the COD removal at this point was low (60-65%) and the ASBR was shut down.

Full granulation of the biomass did not occur over the course of the garnet-enhanced study (Figure 41). Although a few granules were detected as early as day 80, these made up a very small percentage of the total biomass. Over the first 100 days of operation, the geometric average particle diameter increased slowly to approximately 0.4 mm, although at this point the biomass was visually non-granular. By day 120, the average size had increase to 0.6 mm. At this point, the biomass was slightly granular to the unaided eye, but further granulation did not occur.

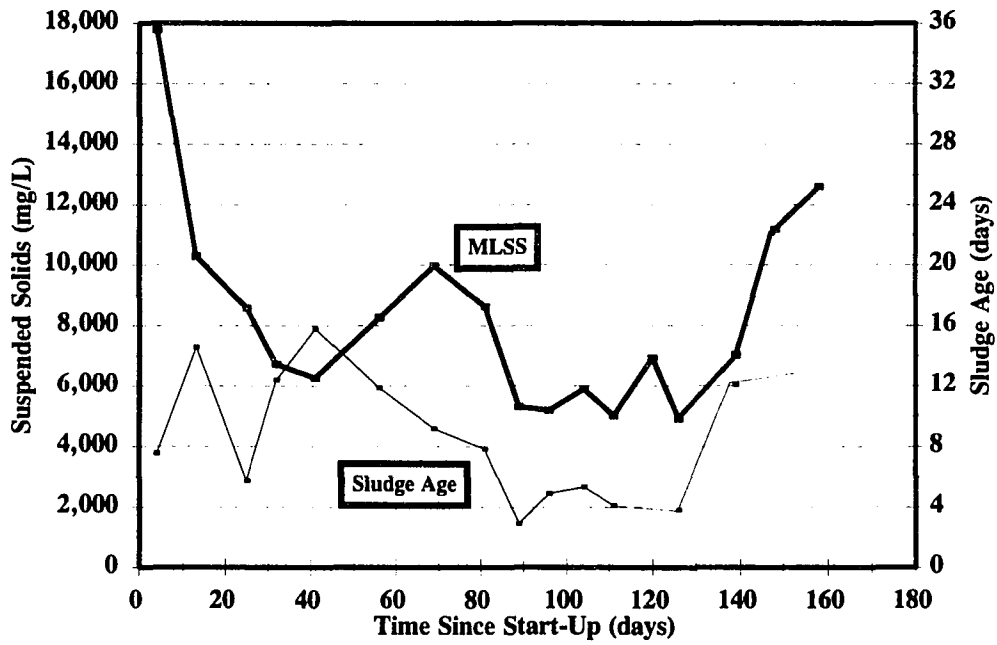


Figure 40. MLSS and SRT for the garnet-enhanced sucrose study.

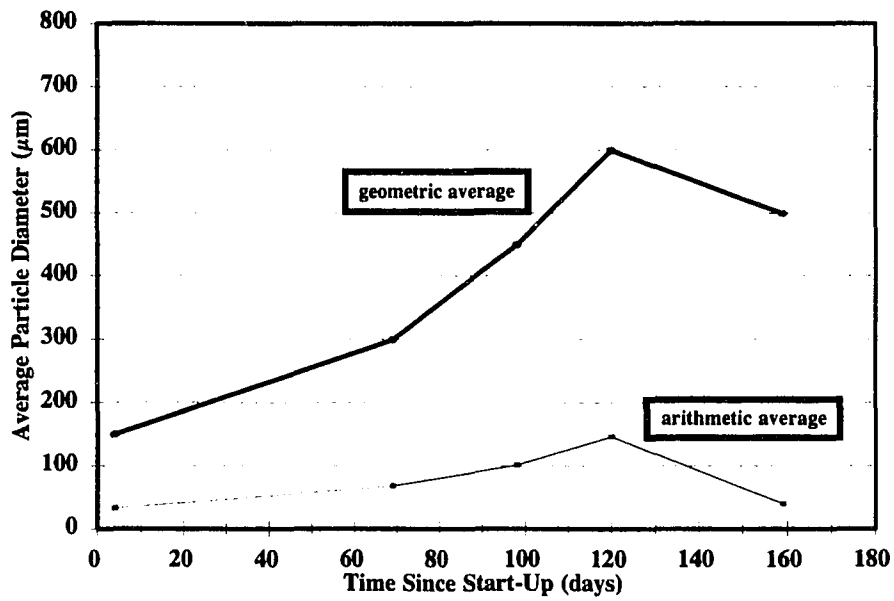


Figure 41. Average particle size for the garnet-enhanced sucrose study.

Garnet Effect

The garnet addition to the ASBR did not appear to have any beneficial effects in terms of granulation or start-up. The high VFA concentration throughout this study indicates that the methanogenic population never reached sufficient levels. This point is further substantiated by observation of the poor COD removal and methane production (Figures 36 and 37, respectively). The non-adsorptive nature of garnet may be responsible for this effect. In the PAC and GAC studies, the VFAs were fairly moderate (500 - 1,000 mg/L) during start-up, possibly because of adsorption onto the activated carbon. Adsorption of VFAs onto the carbon, in turn, would enhance methanogenic attachment to the carbon and maintain high methanogenic populations in the ASBR.

The course of granulation for the garnet study paralleled that of the control reactor over the first 4 months of operation. There were a few granules present after approximately 3 months, and over the following month the biomass began to take on a slightly granular nature. However, the biomass of the PAC and GAC-enhanced ASBRs were much more granular at an earlier time than that of the garnet-enhanced ASBR. Full granulation was not observed over the course of this study. However, if given more time, the biomass may have granulated to a more significant extent.

Silica Sand Enhancement Study

As previously stated, silica sand was also used to enhance granulation and start-up. The conditions used were identical to those in the garnet study, with the exception that

2,000 mg/L of silica sand was used as the attachment matrix. This study was only conducted for approximately 50 days. Over this period, the COD, VFA, methane, pH, alkalinity, and solids data closely paralleled that of the garnet study (Figures 42 through 46). After 48 days, the COD removal at a COD load of 2.7 g/L/day was less than 60% (Figure 42), the VFA concentration had increased to 1,400 mg/L (Figure 44), and the MLSS concentration had decreased to approximately 6,300 mg/L. At this point, owing to the poor performance of the system and similarity to the garnet-enhanced ASBR, it was decided to terminate the study in favor of another enhancement method.

Cationic Polymer Enhancement Study

After the experiments were conducted with the various attachment matrices, it was decided to try an alternative method of granulation enhancement: coagulant addition. It was hypothesized that by using coagulants, a higher MLSS level could be maintained, which would be able to degrade higher organic loads at an early stage of start-up. These high OLRs would result in high biomass production rates, possibly leading to granulation soon after start-up.

Several coagulants were tested in preliminary experiments to determine which performed the best in terms of solids separation in the ASBR. These tests were conducted on operating ASBRs at the end of previous experiments so as not to disturb the natural progression of those studies. Initially, five different coagulants were tested for use in the ASBR: a cationic polymer, an anionic polymer, a polyquaternary amine coagulant,

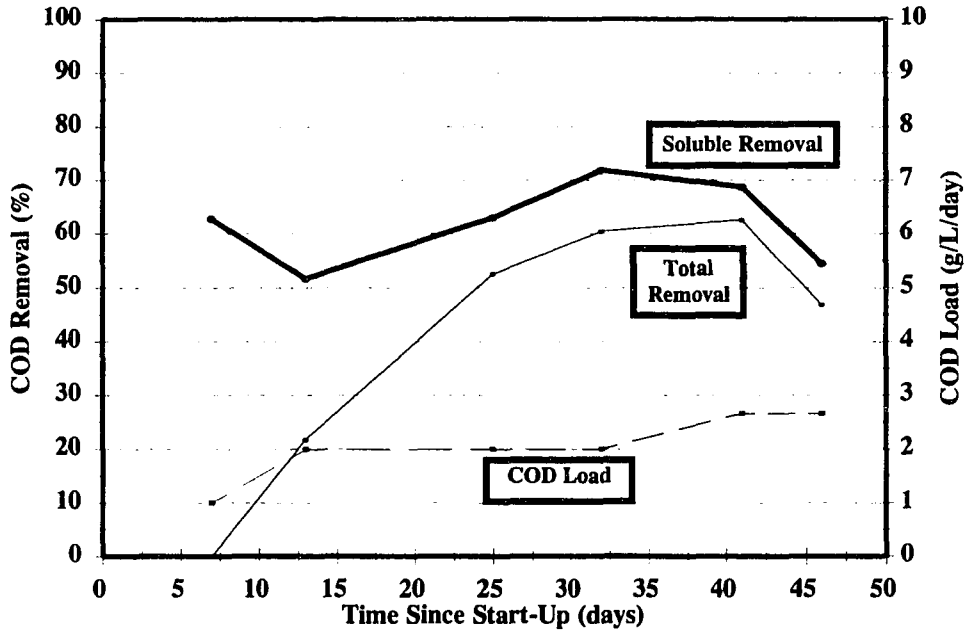


Figure 42. COD removal for the silica sand-enhanced sucrose study.

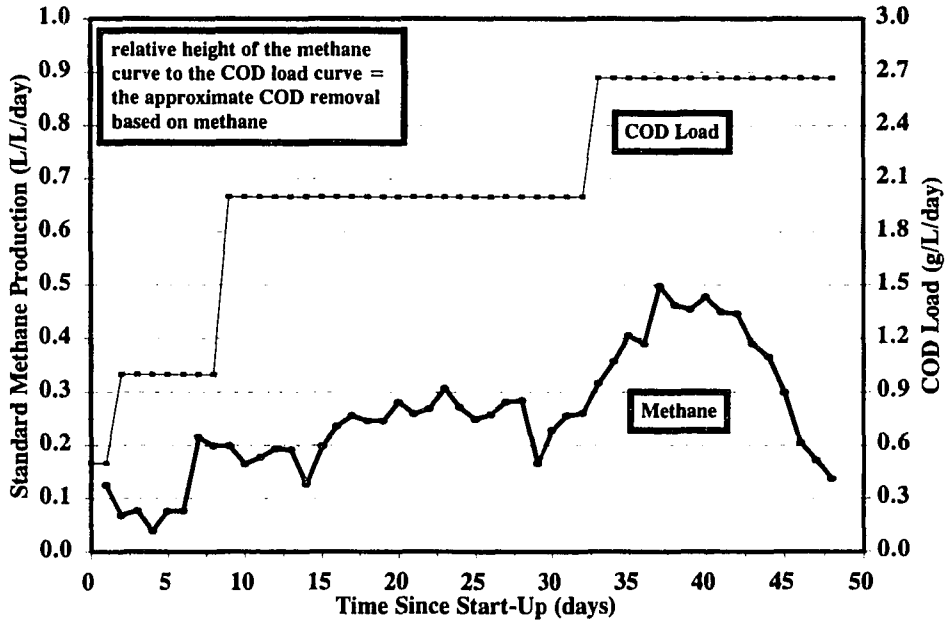


Figure 43. Methane production for the silica sand-enhanced sucrose study.

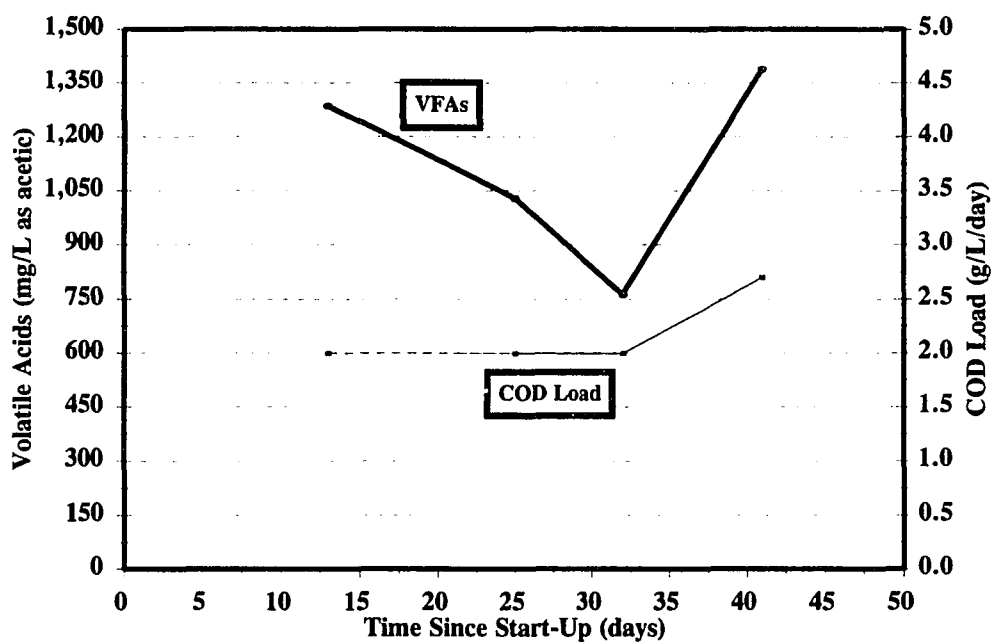


Figure 44. Volatile acids data for the silica sand-enhanced sucrose study.

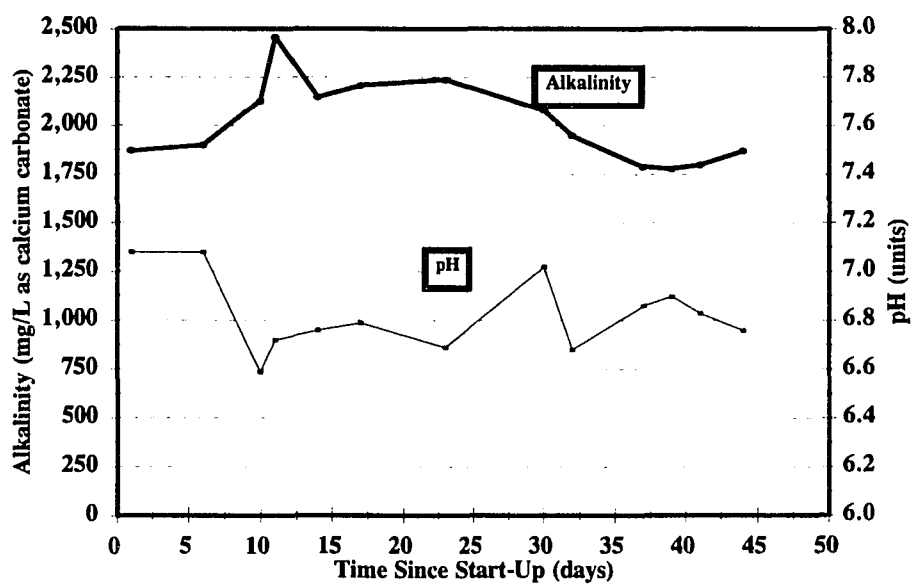


Figure 45. Alkalinity and pH data for the silica sand-enhanced sucrose study.

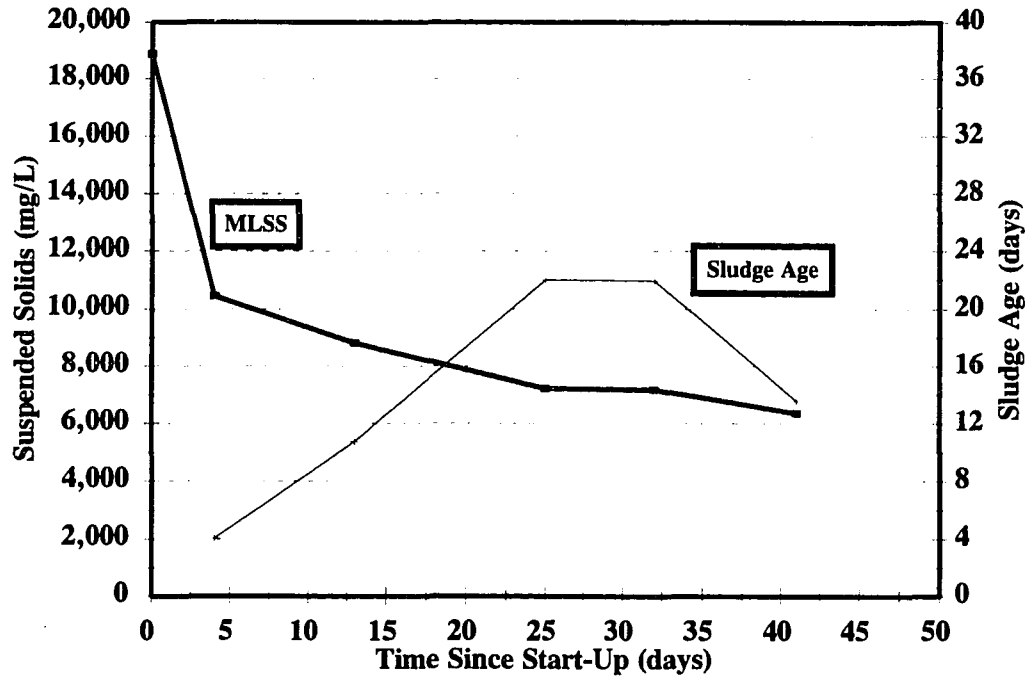


Figure 46. MLSS and SRT for the silica sand-enhanced sucrose study.

ferrous chloride, and ferric chloride. Three of these were chosen to be used in actual granulation enhancement studies. The three, which are discussed in the Experimental Procedures section of this document, were the cationic polymer (MAGNIFLOC® 496C, Cytec Industries), the polyquaternary amine (MAGNIFLOC® 591C, Cytec Industries), and ferric chloride. The two polymers had different degrees of cationic charge, and are differentiated hereafter as the cationic polymer (496C) and the polyDADM coagulant (591C). The ferric chloride ($\text{FeCl}_3 \cdot 6\text{H}_2\text{O}$) was purchased in powder form from Chemistry Stores at ISU.

The following section presents the data from the cationic polymer (496C) experiments.

Operational Performance

The most promising results of this research were obtained using the cationic polymer (MAGNIFLOC® 496C). The ASBR was seeded with approximately 18,000 mg/L of suspended solids, and initial start-up was conducted at an HRT of 2 days and an OLR of 1 g COD/L/day. The cationic polymer was initially added in liquid form at the rate of 5 mg of polymer per liter of reactor per cycle during the last mixing cycle of the ASBR (just prior to the settle phase). This dosage was decreased to 1 mg/L/cycle on day 5 after it was determined that the initial dosage was not necessary for efficient solids separation. After only 6 days of operation, the HRT was decreased to 1 day and the OLR was increased to 2 g COD/L/day (Figures 47 and 48). Two weeks later the COD load was increased to 3 g/L/day, at which time the SCOD removal efficiency was over 85%. The volatile acids concentration decreased from 500 mg/L at the 2 g/L/day load to 200 mg/L at the 3 g/L/day load (Figure 49). The pH fluctuated somewhat but averaged between 6.9 and 7.0 over this same time period (Figure 50).

On day 39, the COD load was increased to 4 g/L/day, and by day 61 the ASBR was treating 6 g COD/L/day at 95% SCOD removal efficiency. At this point the cationic polymer addition was discontinued to determine whether the reactor would function well without the benefit of the polymer. After discontinuing the polymer addition, the COD

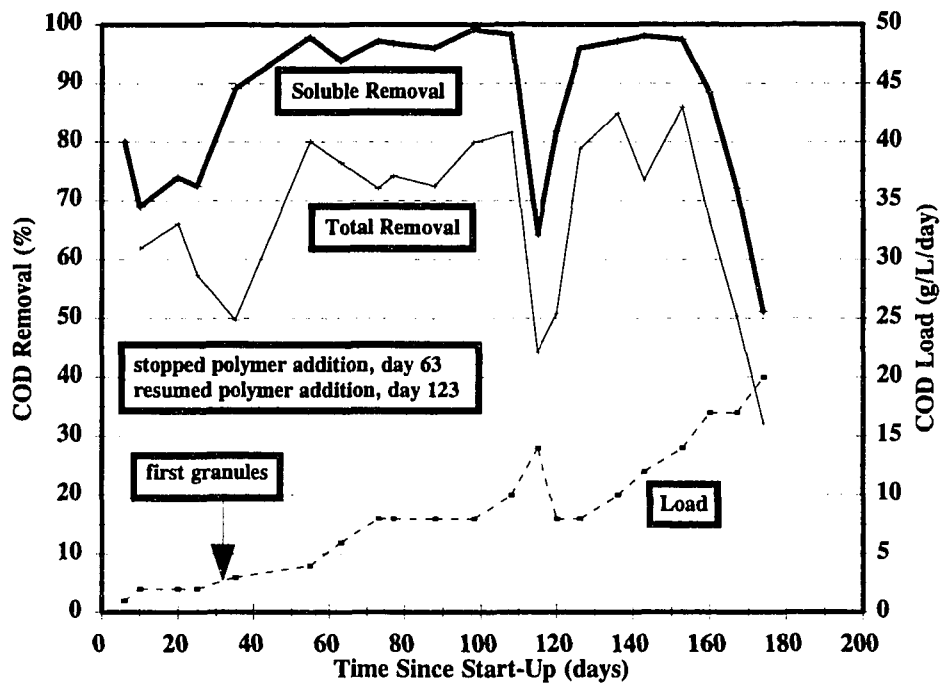


Figure 47. COD removal for the cationic polymer-enhanced sucrose study.

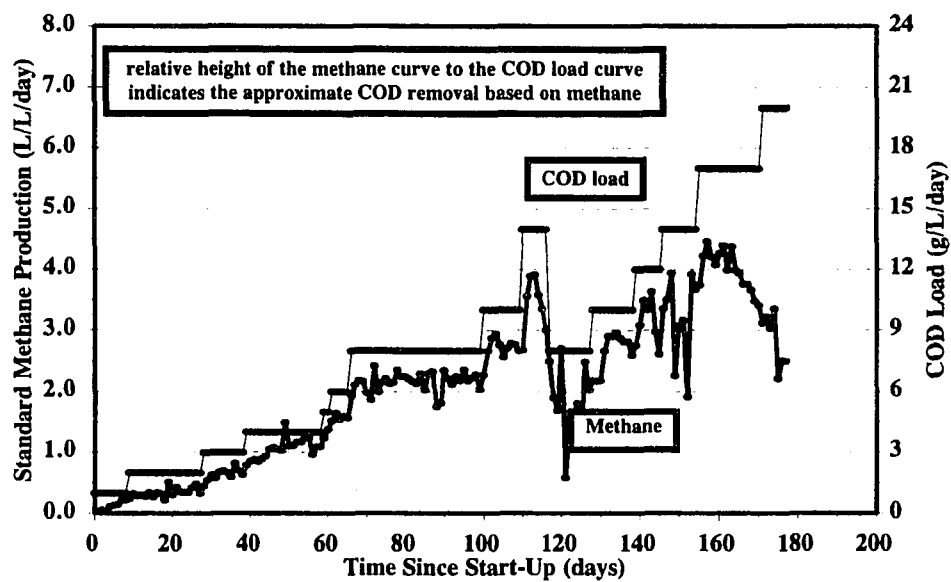


Figure 48. Methane production for the cationic polymer-enhanced sucrose study.

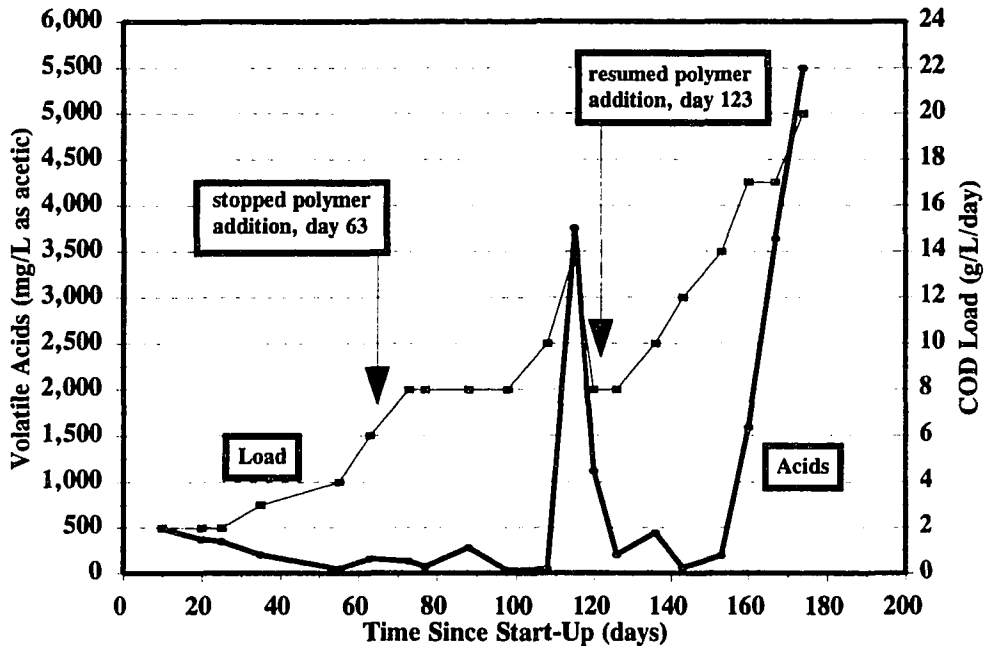


Figure 49. Volatile acids data for the cationic polymer-enhanced sucrose study.

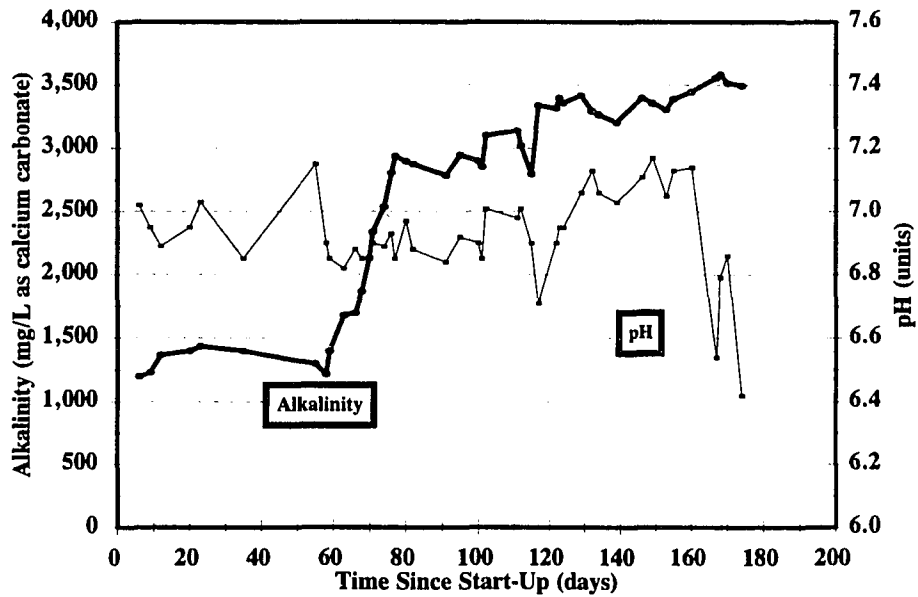


Figure 50. Alkalinity and pH data for the cationic polymer-enhanced sucrose study.

load was increased to 8 g/L/day and maintained there for 20 days to observe any detrimental effects. None were apparent and the COD load was increased to 10 g/L/day on day 100. At this point, the ASBR was achieving 98% SCOD removal (Figure 47), 80% TCOD removal, and had a VFA concentration in the effluent of less than 50 mg/L (Figure 49). The pH of the ASBR was approximately 6.95 and the alkalinity was more than 3,000 mg/L, as CaCO₃ (Figure 50). It thus appeared that the ASBR was operating under very stable conditions and would be able to handle even higher OLRs.

On day 112 the OLR was increased to 14 g COD/L/day. Over the next two days it appeared that the system was able to handle the load increase, as was evidenced by the methane production (Figure 48). However, on day 116 the methane production dropped significantly. The SCOD removal efficiency decreased to 65% (Figure 47), the volatile acids concentration increased from less than 50 mg/L to over 3,500 mg/L (Figure 49), and the pH dropped to 6.7 (Figure 50). The COD load was reduced to 8 g/L/day on day 119 to avoid complete failure of the system.

On day 123, cationic polymer addition was resumed at the rate of 1 mg/L/cycle. The SCOD removals quickly increased to over 95% and the VFAs decreased to approximately 200 mg/L. The COD load was subsequently increased to 10, 12, and 14 g/L/day on days 128, 138, and 146, respectively. The COD removal efficiencies over these OLRs were in excess of 95%. On day 155, the COD load was increased to 17 g/L/day, which was the highest OLR ever achieved in an ASBR to date. During the first week at the 17 g/L/day load, methane production was fairly stable and the SCOD removal

efficiency was approximately 85% (Figures 47 and 48). After 15 days at this load, however, the SCOD removal efficiency decreased to approximately 70%. The VFAs increased to over 3,000 mg/L over this same time (Figure 49), and the pH of the reactor began to fluctuate significantly and finally decreased to 6.55 on day 164 (Figure 50). At this point, potassium hydroxide was added to the ASBR to increase the pH to approximately 6.9, after which the ASBR appeared to achieve a stable, although highly-stressed, condition. On day 171 the COD load was increased to 20 g/L/day. This load increase appeared to break the system. COD removals decreased to below 50%, VFAs increased to 5,500 mg/L, and the pH of the system was unstable and decreased to below 6.4.

Solids and Granulation

The MLSS levels paralleled the operational performance of the ASBR rather closely. After initial start-up at 18,000 mg/L of suspended solids, the MLSS levels quickly decreased to 6,000 mg/L after only one week. This was due mainly to the inefficiency of the cationic polymer to achieve clarification at such a high solids concentration. The solids tended to form dense mats that were carried up to the liquid surface due to biogas production during the settle phase. Many of these solids were washed out in the decanted effluent. This continued for about the first week of operation, after which the solids settled very well and were not concentrated enough to float due to gasification. After reaching their minimum concentration of 6,000 mg/L on day 7, the

MLSS level increased to over 9,000 mg/L by day 25 and then slowly increased to approximately 14,000 mg/L by day 70 (Figure 51). Over the first 25 days of operation, the SRT was generally in excess of 20 days. At about day 34, however, the SRT decreased to approximately 6 days and fluctuated between 6 and 16 days for the remainder of the experiment (Figure 51).

Granulation was achieved in an extremely short time in the cationic polymer-enhanced study (Figure 52). The first granules were observed at approximately day 30, at which time the geometric average particle diameter was approximately 0.75 mm. By day 60 the average size was more than 1 mm, and by day 72 the average size had increased to more than 2.25 mm. The average size remained relatively constant over the next month, during which the OLR was increased from 6 to 14 g COD/L/day. Granule breakup was observed after the partial failure of the system at 14 g COD/L/day, and the average size quickly decreased to 1 mm by day 120. The resumed addition of cationic polymer at this time did not increase the granule size over the remainder of the study. By the end of the experiment, the average size was approximately 0.9 mm (Figure 52).

Cationic Polymer Effect

The cationic polymer enhancement had the most beneficial effects on reactor start-up and granulation out of all of the enhancement methods studied. COD removals were in excess of 95% at a COD load of 6 g/L/day after only 60 days of operation. Granulation was also enhanced significantly, with the first granules appearing after only 30 days.

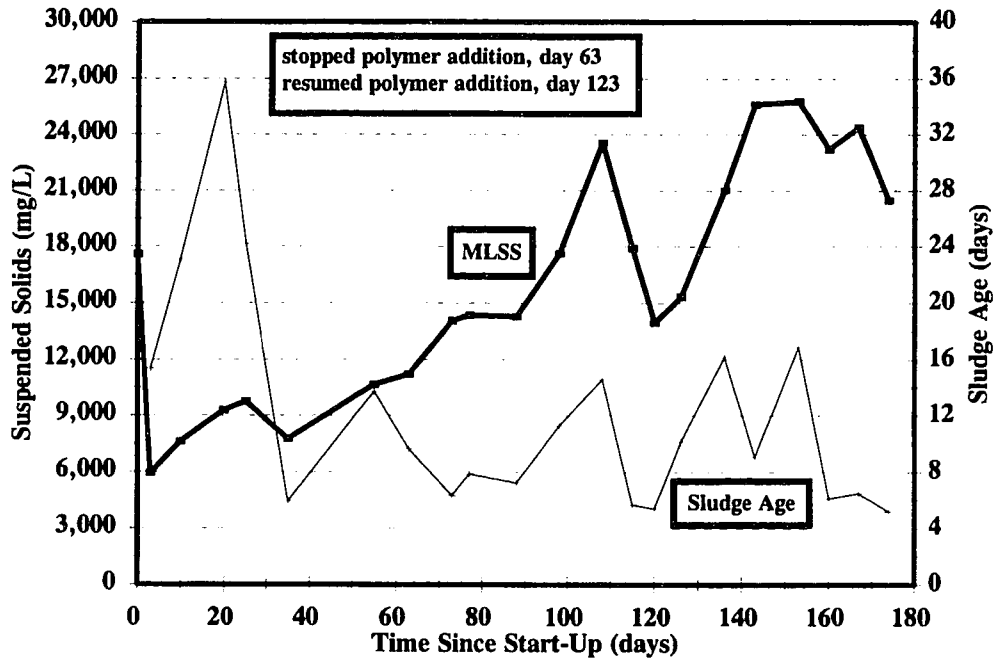


Figure 51. MLSS and SRT for the cationic polymer-enhanced sucrose study.

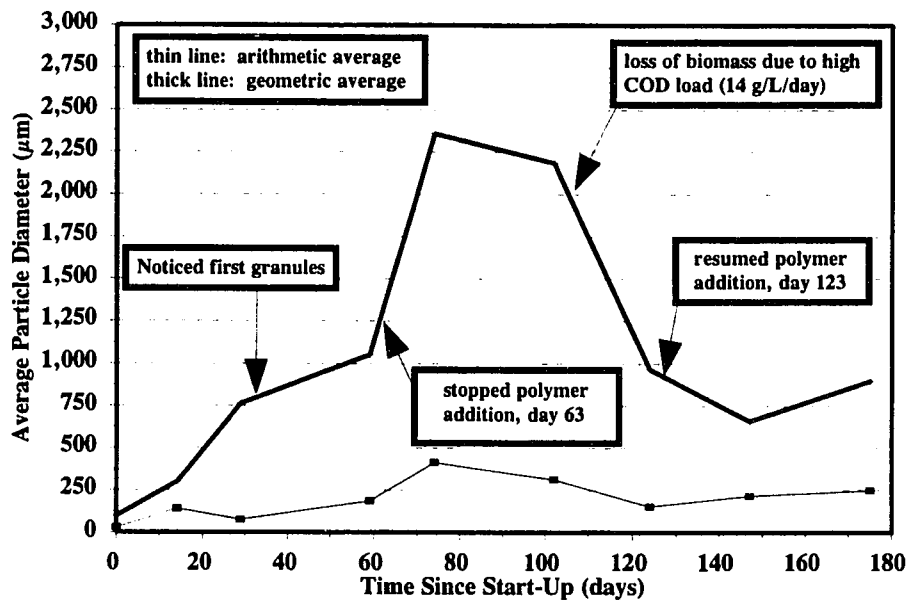


Figure 52. Average particle size for the cationic polymer-enhanced sucrose study.

Almost complete granulation was achieved after 60 days. In addition, it was not necessary to continue polymer addition after 2 months of operation. COD loads up to 10 g/L/day were treated to 95% SCOD removal efficiency without polymer addition, although the system began to fail when the load was increased to 14 g/L/day. Upon resumed addition of the polymer, COD loads up to 14 g/L/day were treated to 95% SCOD removal efficiency. A COD load of 17 g/L/day resulted in reduced efficiency (70%), and at 20 g/L/day the system began to fail.

Examination of the data reveals that the cationic polymer had significant beneficial effects during the initial start-up period. The polymer maintained the solids in the system more efficiently than in the other studies resulting in efficient treatment at relatively high OLRs after only a few weeks of operation. High removal rates results in high biomass production rates, which is a necessary factor for granulation.

The cationic polymer also had beneficial effects after the system had already matured. With no polymer addition, the highest COD load attained was 10 g/L/day. With polymer addition, more than 14 g/L/day could be treated. The most plausible explanation for this difference is the ability of the polymer to retain solids. At the high COD loads, biogas production at the end of the cycle was normally still significant, resulting in turbulent conditions during the settling phase. The cationic polymer helped to settle the solids in these turbulent conditions. In the reactor with no polymer addition, however, many of these solids were washed out.

PolyDADM Enhancement Study

The other polymer used in these experiments was a polyquaternary amine (591C), termed polyDADM for brevity. The polyDADM was slightly less cationic in nature than the cationic polymer and had a different chemical make-up (Experimental Procedures section).

Operational Performance

The ASBR in the polyDADM enhancement study was initially seeded with 18,000 mg/L of suspended solids and operated at an HRT and OLR of 2 days and 1 g COD/L/day, respectively. The polyDADM coagulant was added during the last mixing cycle just prior to the settle phase at a rate of 5 mg/L/cycle. After 5 days of operation, the coagulant dosage was decreased to 2.5 mg/L/cycle, but was increased back to 5 mg/L/cycle 2 days later due to poor clarification at the lower dosage. The coagulant dosage was maintained at 5 mg/L/cycle until day 60, when it was again reduced to 2.5 mg/L/cycle. On day 70, the dosage was reduced further to 1 mg/L/cycle.

After 6 days of operation at 1 g COD/L/day (2-day HRT), the COD load was increased to 2 g/L/day by decreasing the HRT to 1 day and maintaining a constant influent COD concentration of 2 g/L. On day 39, the COD load was increased to 3 g/L/day, although the SCOD removal efficiency was only 67% (Figures 53 and 54). The volatile acids concentration over the first 39 days was relatively constant at 500 mg/L, and the pH was between 6.9 and 7.0 (Figures 55 and 56).

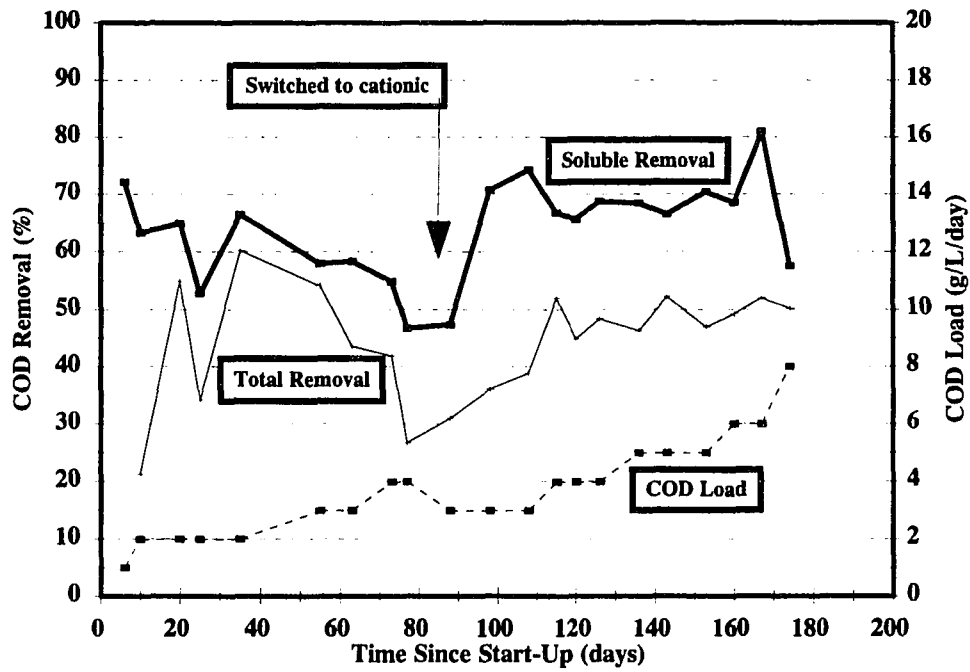


Figure 53. COD removal for the polyDADM-enhanced sucrose study.

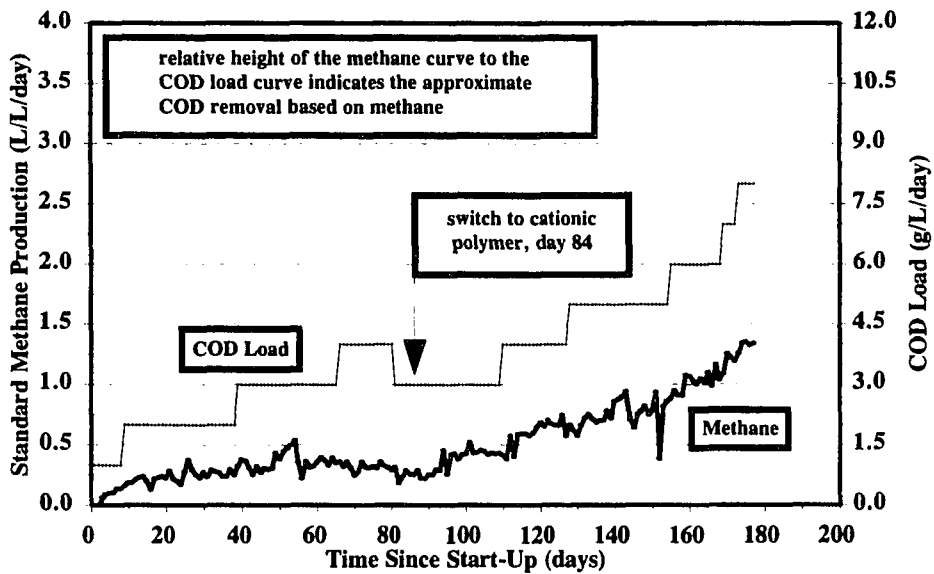


Figure 54. Methane production for the polyDADM-enhanced sucrose study.

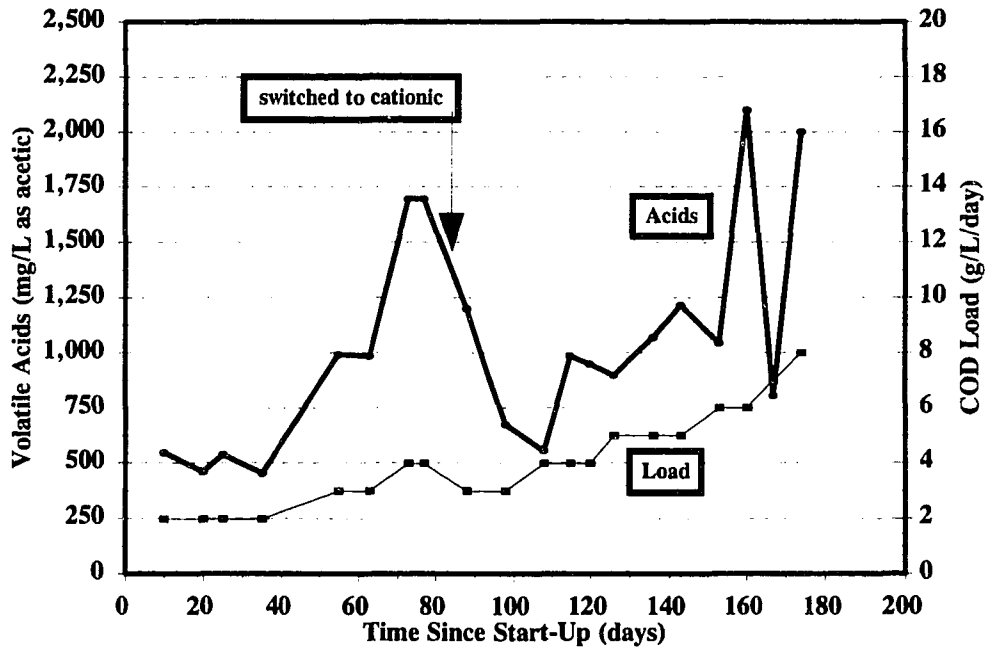


Figure 55. Volatile acids data for the polyDADM-enhanced sucrose study.

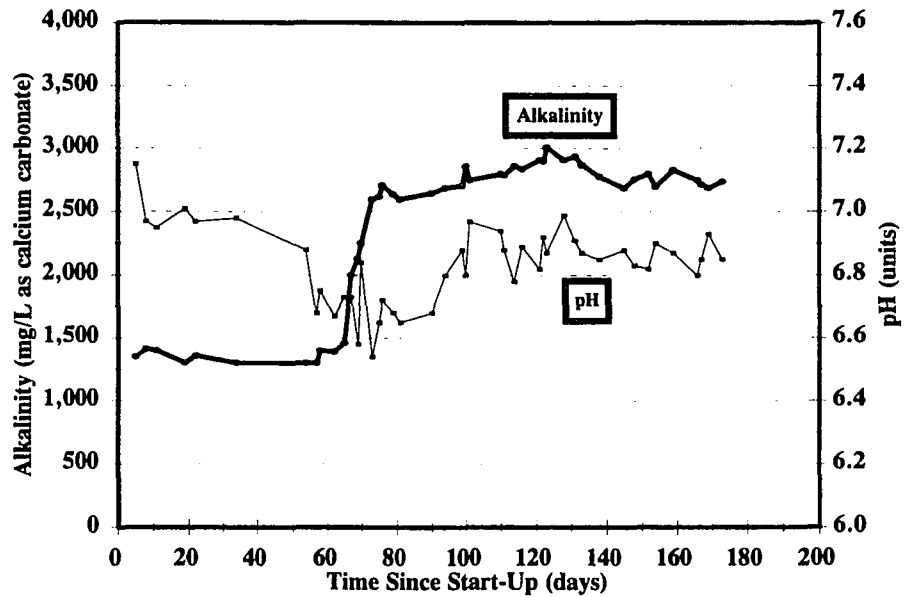


Figure 56. Alkalinity and pH data for the polyDADM-enhanced sucrose study.

After the increase to 3 g COD/L/day on day 39, the VFA concentration increased to 1,000 mg/L at day 55, while the SCOD removal efficiency decreased to 58% (Figures 55 and 53, respectively). The pH of the system dropped over this time to an average of 6.7 (Figure 56). On day 72, the COD load was increased to 4 g/L/day to try to push the system somewhat, but the COD removal efficiency dropped to below 50% and the VFAs increased to over 1,700 mg/L. The COD load was decreased to 3 g/L/day to avoid system failure.

Since the polyDADM-enhanced ASBR was performing much worse than the cationic polymer-enhanced ASBR, it was decided on day 84 to switch the coagulant from polyDADM to cationic polymer to determine whether the stressed conditions could be alleviated. Improvement of the system would also lend support to the beneficial effects observed for the cationic polymer-enhanced test that was being conducted in parallel. Almost immediately the methane production increased to a limited extent after switching coagulants (Figure 54). The SCOD removal increased to over 70% by day 95 (Figure 53), and the VFAs decreased to 600 mg/L (Figure 55). The pH of the system also increased to between 6.8 and 7.0 and remained within this range throughout the remainder of the experiment (Figure 56).

On day 110 the COD load was increased to 4 g/L/day and on day 130 it was further increased to 5 g/L/day. The SCOD removal efficiency during this time remained at approximately 70% and the VFAs fluctuated between 1,000 and 1,200 mg/L. On day 155 the COD load was increased to 6 g/L/day and the SCOD removal efficiency increased to

over 80%. Upon further increase of the COD load to 8 g/L/day (day 170), the COD removal efficiency decreased to below 60% (Figure 53).

Solids and Granulation

The MLSS levels decreased from 18,000 mg/L to a minimum of 5,200 mg/L during the first 25 days of operation (Figure 57). Over the next 50 days the solids level slowly increased to approximately 10,000 mg/L on day 75. During the remainder of the experiment the solids level fluctuated marginally but was normally around 9,000 mg/L. The SRT changed drastically over the first 70 days of operation, with a high of 57 days (day 58) and a low of 6 days (day 12). After the switch to cationic polymer on day 84, the SRT remained fairly constant with an average of 10 days. After the COD load was increased to 6 g/L/day, however, the SRT fell below 5 days (Figure 57).

The biomass never fully-granulated in the polyDADM study (Figure 58). The geometric average particle diameter increased gradually from 0.1 mm to 0.35 mm during the first 100 days of operation. At the end of the study, the average diameter again began to increase, and the biomass visually appeared to be granulating to a limited extent. However, the individual particles were still quite small and obvious granulation was not apparent (Figure 58).

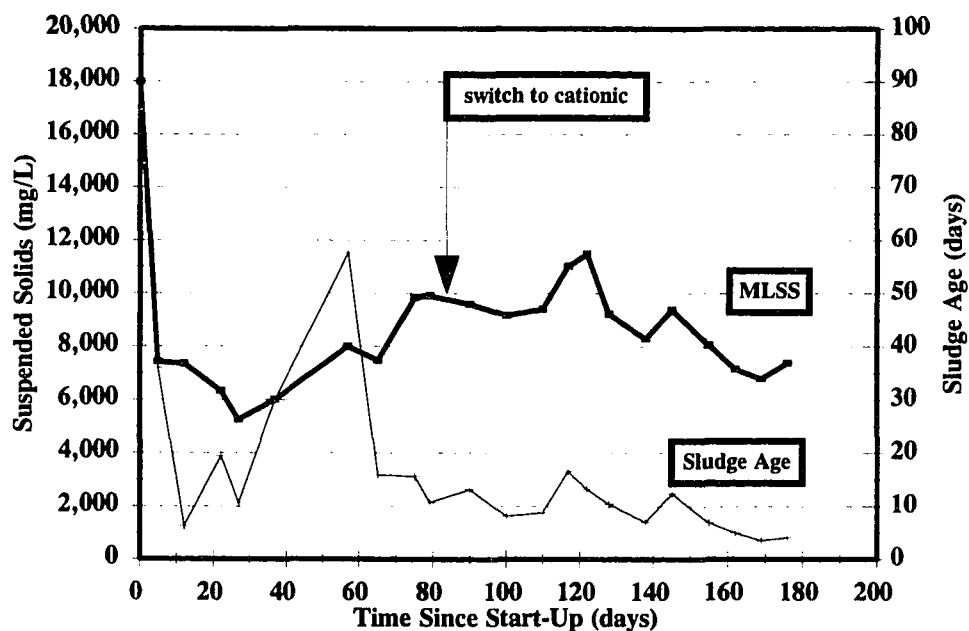


Figure 57. MLSS and SRT for the polyDADM-enhanced sucrose study.

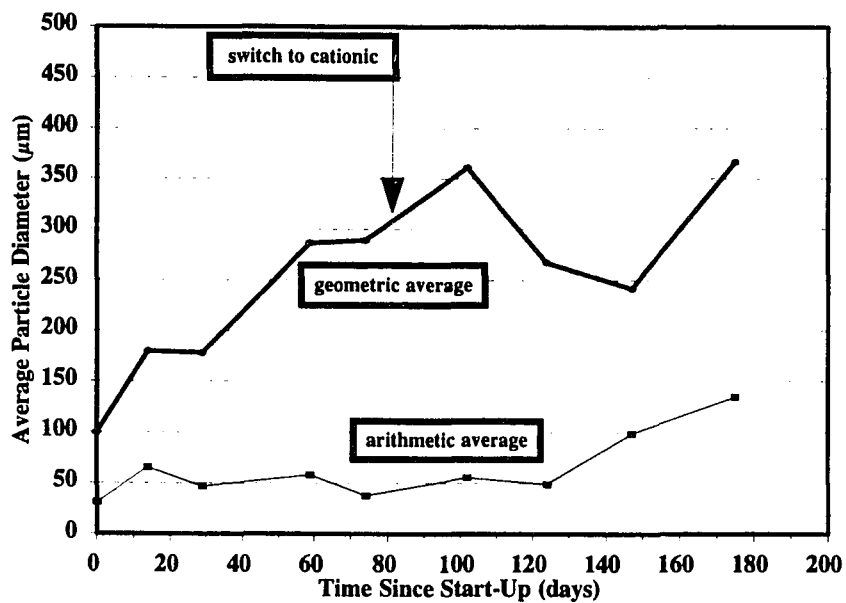


Figure 58. Average particle size for the polyDADM-enhanced sucrose study.

PolyDADM Effect

The polyDADM coagulant appeared to have a non-stimulatory (if not inhibitory) effect on ASBR start-up and granulation. Although COD removal and methane production occurred, it did not reach the levels achieved in most of the other experiments.

Additionally, the average particle size actually lagged behind that of the control study, indicating that the polyDADM coagulant may have inhibited granule formation. The switch to cationic polymer was able to increase COD removals, but granulation of the biomass did not occur to a significant extent.

It seems likely that the chemical nature of the polyDADM coagulant may have inhibited the methanogens, since sucrose conversion to acids was observed but methane production was low. An alternative explanation is that the chemical nature of the polyDADM selected for different species of methanogens than those selected for by the cationic polymer. This latter possibility would account for only a marginal increase in performance after the switch to the cationic polymer. There may have been insufficient numbers of the desired methanogens present prior to the switch, so that even when the polyDADM was removed from the system the desired methanogens were simply not present.

A third possibility is that the polyDADM suppressed the pH enough to effect the methanogens. Prior to the switch to cationic polymer, the pH of the system was consistently between 6.6 and 6.7, even when additional buffering capacity was provided

(Figure 56). After switching to the cationic polymer, however, the pH increased to a constant value between 6.8 and 7.0, which is more suitable for most methanogenic species.

Ferric Chloride Enhancement Study

Ferric chloride ($\text{FeCl}_3 \cdot 6\text{H}_2\text{O}$) was also used for enhancement of start-up and granulation. Ferric chloride was selected because of its common use in drinking water treatment as a coagulant. Iron is also a necessary trace metal and has been implicated by some authors to be limiting in some anaerobic treatment applications [58, 115, 126, 138].

Operational Performance

The ferric chloride (FeCl_3)-enhanced ASBR was seeded with 18,000 mg/L of suspended solids and initially operated at an HRT an OLR of 2 days and 1 g/L/day, respectively. The FeCl_3 dosage applied to the ASBR was 5 mg/L/cycle (as Fe) throughout the experiment. After 6 days of operation the COD load was increased to 2 g/L/day and the HRT was decreased to 1 day. The SCOD removal efficiency was approximately 60% at this time and the TCOD removal was slightly less at 55% (Figure 59). Methane production indicated a lower COD removal efficiency, although methane production was inconsistent over the course of the experiment (Figure 60).

The COD load was never increased beyond 2 g/L/day during the entire course of the experiment due to the extremely low COD removals observed. At day 35, the SCOD removal efficiency was 40% and by day 55 it had decreased to 34% (Figure 59). The

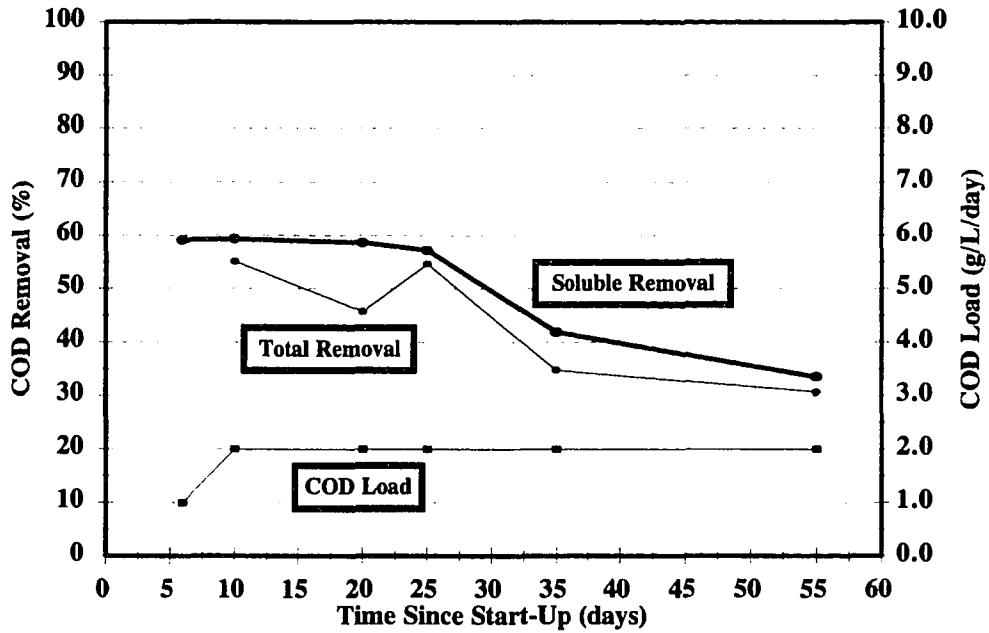


Figure 59. COD removal for the ferric chloride-enhanced sucrose study.

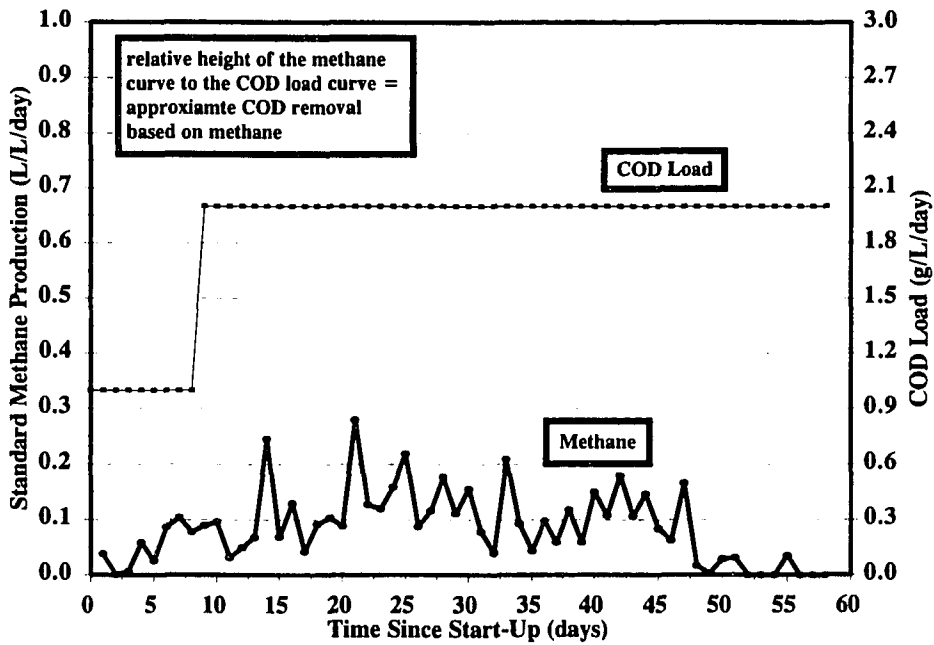


Figure 60. Methane production for the ferric chloride-enhanced sucrose study.

VFAs reached a low of 650 mg/L on day 23, but increased steadily thereafter to 1,000 mg/L on day 55 (Figure 61). The pH of the system was always between 6.8 and 7.0, and the alkalinity averaged 1,300 mg/L as CaCO₃ (Figure 62). This experiment was terminated after 55 days of operation due to the obvious poor performance of the reactor.

Solids and Granulation

The solids level decreased from its initial value of 18,000 mg/L to 6,200 mg/L at day 10. A marginal increase in the MLSS level occurred over the remainder of the experiment, but it never exceeded 7,800 mg/L (Figure 63). The SRT of the system was always in excess of 15 days and normally was greater than 30 days. This latter observation is a point of confusion and is in direct contrast to normal anaerobic treatment theory. It is generally thought that longer SRTs create stable conditions for anaerobic treatment. In fact, the basis of the anaerobic filter is the efficient retention of biomass and long SRT attainable. However, in these experiments shorter SRTs appear to be beneficial to start-up and granulation in the ASBR.

Granulation did not occur over this short experiment (Figure 64). The majority of the biomass was in the form of small, pin-point flocs that settled unusually well. The efficient clarification during this experiment was also evidenced by the similar SCOD and TCOD removal efficiencies (Figure 59). That is, few solids were lost in the effluent. This fact, together with the small increase in MLSS, suggests that the biomass production rates were very low.

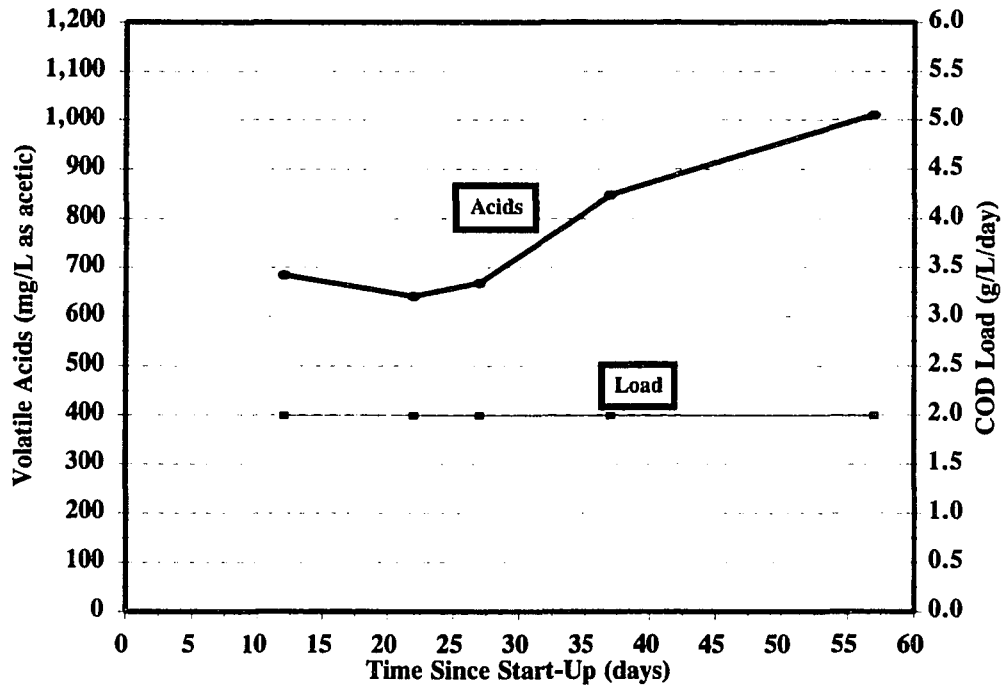


Figure 61. Volatile acids data for the ferric chloride-enhanced sucrose study.

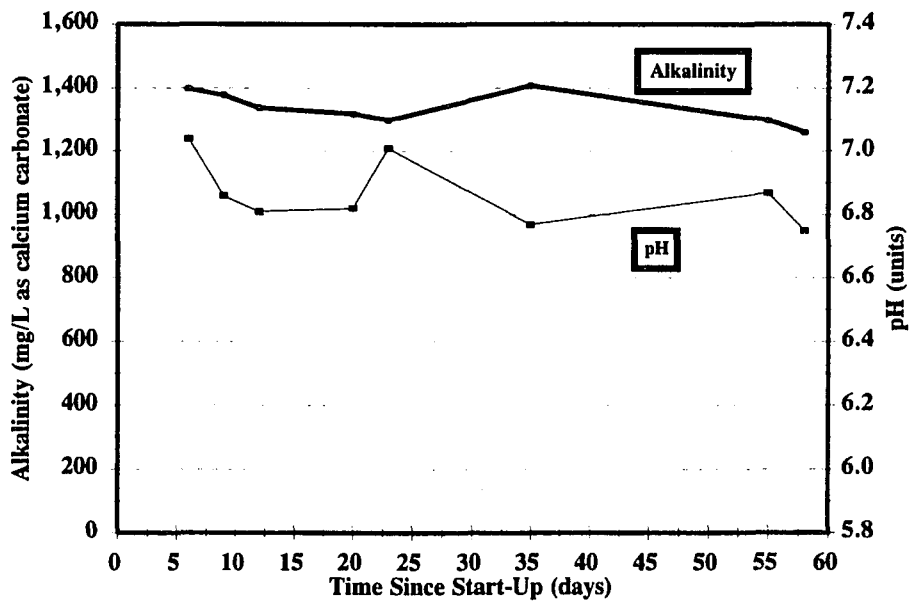


Figure 62. Alkalinity and pH data for the ferric chloride-enhanced sucrose study.

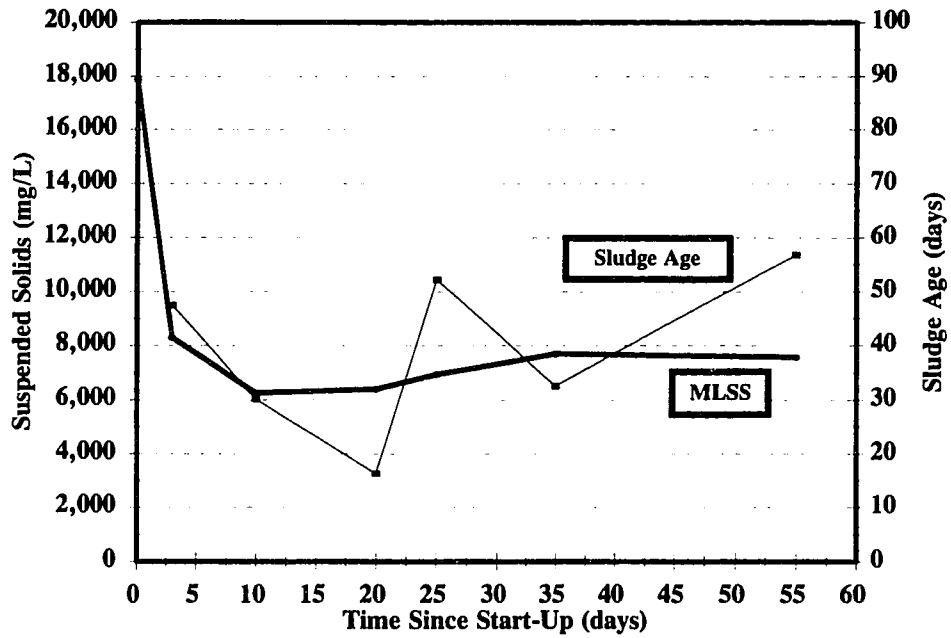


Figure 63. MLSS and SRT for the ferric chloride-enhanced sucrose study.

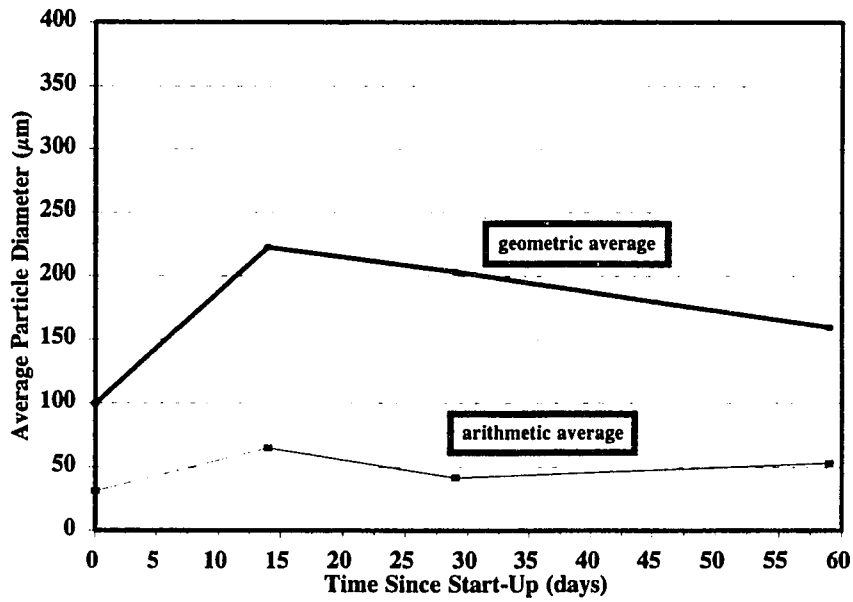


Figure 64. Average particle size for the ferric chloride-enhanced sucrose study.

Ferric Chloride Effect

It is obvious after examining the data from this experiment that the ferric chloride had an inhibitory effect on the start-up and granulation of the ASBR. Perhaps the most plausible explanation is that the ferric ions contributed by the ferric chloride were reduced to ferrous ions in the anaerobic environment, and subsequently precipitated with sulfide to form ferrous sulfide (FeS). Ferrous sulfide is relatively insoluble in water and is generally present in pin-point flocs. Also, if the iron is present at high concentrations, the FeS formed may scavenge the system of the majority of the available sulfur. This would result in inhibition of the system due to a limiting supply of sulfur, which is a necessary nutrient for life. These two points correlate well with the observed ASBR performance.

Beef Extract/Glucose Experiments

Completion of the previously presented experiments yielded several enhancement methods capable of improving the start-up and granulation in ASBRs treating a sucrose wastewater. However, since sucrose was used as the sole carbon source in all of the experiments to this point, it was decided to use a different substrate in similar experiments to determine what effect (if any) the type of substrate had on start-up and granulation parameters. The substrate chosen for study was a combination of beef extract and glucose, combined in a 50/50 ratio based on COD contribution. The characteristics of the beef extract are given in the Experimental Procedures section of this document. Glucose was purchased in powder form from Chemistry Stores at ISU.

Due to the long nature of these experiments, the best enhancement method from the sucrose experiments was chosen for study in the beef extract/glucose experiments, namely, cationic polymer enhancement. A control ASBR was also operated in parallel to the cationic polymer-enhanced ASBR. The beef extract contained a high amount of protein (12.9% by weight) and fat (13.5% by weight) in addition to a significant amount of carbohydrates (24.0% by weight). It was anticipated that the protein content of the beef extract would eliminate some of the requirement for alkalinity addition. This point was apparent throughout the study and is evidenced by the lower sodium bicarbonate addition required to maintain optimum pH conditions (compared to the sucrose experiments, see Tables 13 and 14 in the Experimental Procedures section). It was further anticipated that the high fat content may cause problems due to floating biomass. This latter point is addressed in the following paragraphs.

Control Study

Operational Performance

The control ASBR was initially seeded with 25,000 mg/L of suspended solids (MLVSS = 15,000 mg/L). The HRT and OLR were set at 2 days and 1 g COD/L/day, respectively. Polymer was not added to the control reactor. After 7 days of operation, the HRT was decreased to 1 day and the OLR was increased to 2 g COD/L/day. On day 30 the HRT was increased to 2 days due to poor performance and maintained at 2 days until day 47 (Figures 65 and 66). At day 60 the COD load was increased from 2 to 3 g/L/day,

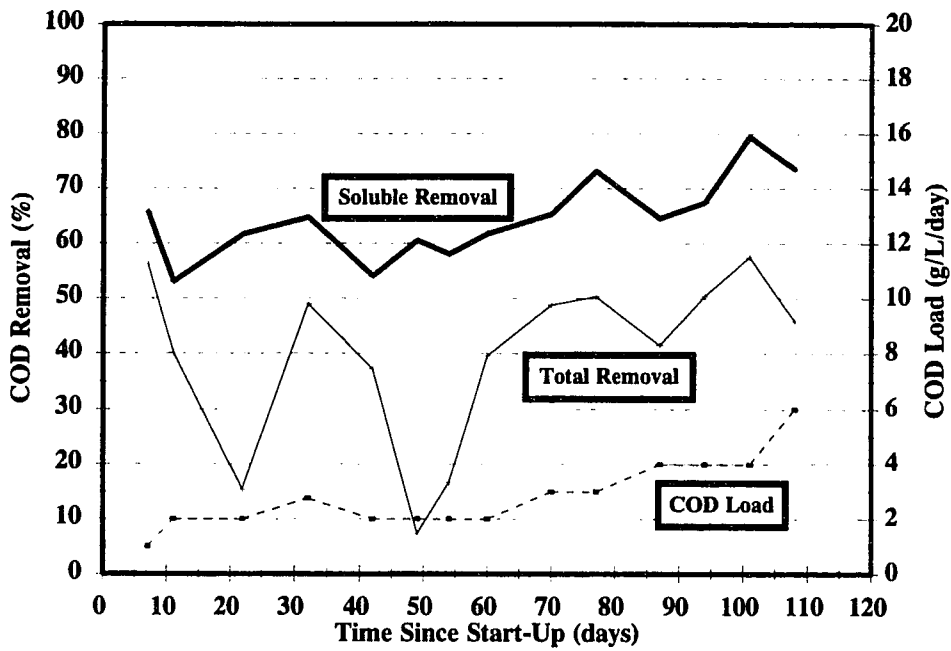


Figure 65. COD removal for the beef/glucose control study.

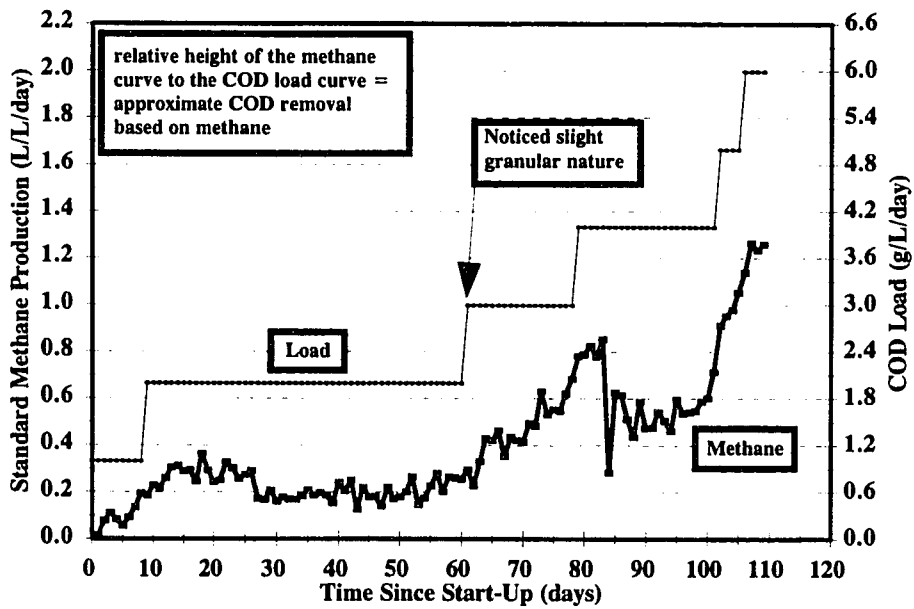


Figure 66. Methane production for the beef/glucose control study.

even though the COD removal efficiency was only 60%. The VFA concentration reached a maximum of 1,600 mg/L on day 30 but subsequently decreased to 500 mg/L by day 60 (Figure 67). The alkalinity and pH remained relatively constant at 2,750 mg/L and 6.90 to 7.1, respectively, throughout the study (Figure 68).

After 18 days at a COD load of 3 g/L/day the COD removal efficiency and methane production began to improve. On day 78 the COD load was increased to 4 g/L/day and maintained at that level until day 100. The SCOD removal efficiency was approximately 70% at the 4 g/L/day COD load (Figure 65). On day 101 the COD load was increased to 6 g/L/day, resulting in decreased COD removals and increased VFA concentrations (Figure 65 and 67).

Solids and Granulation

Figures 69 and 70 present the solids and granulation data from the control experiment. The MLSS level decreased from 25,000 mg/L at day zero to 7,500 mg/L at day 7. The MLSS level remained relatively constant at 7,000 mg/L until day 80 at which time it briefly decreased to 4,000 mg/L before increasing again to 7,000 mg/L (Figure 69). The SRT likewise decreased from 69 days to 7 days during the first 21 days of operation. After this point the SRT fluctuated, reaching 26 days on day 40 and then decreasing to 8 days by the end of the experiment (day 109).

The geometric average particle size gradually increased over the course of the experiment to approximately 0.5 mm by day 109 (Figure 70). At this point the biomass

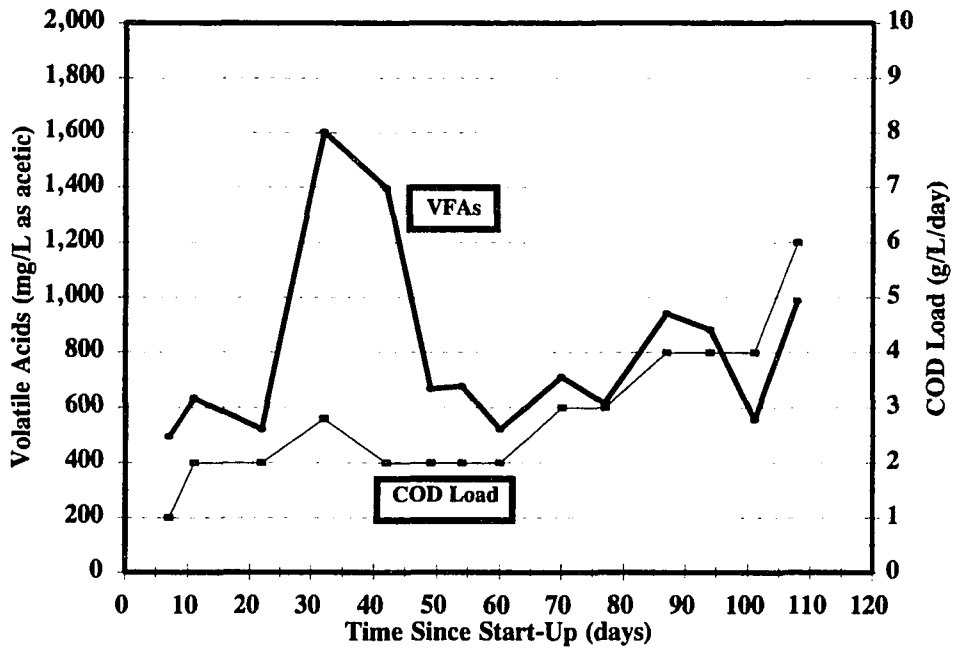


Figure 67. Volatile acids data for the beef/glucose control study.

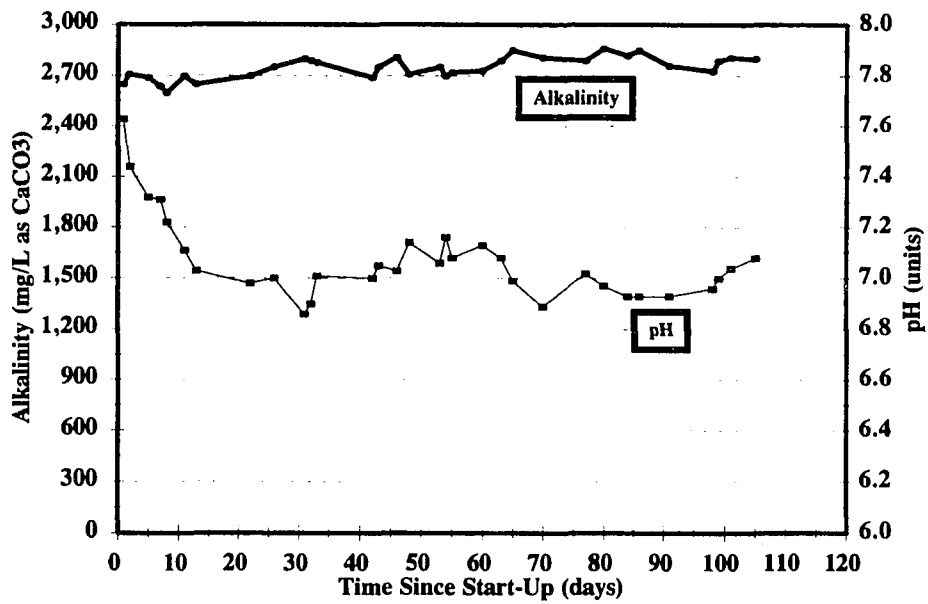


Figure 68. Alkalinity and pH data for the beef/glucose control study.

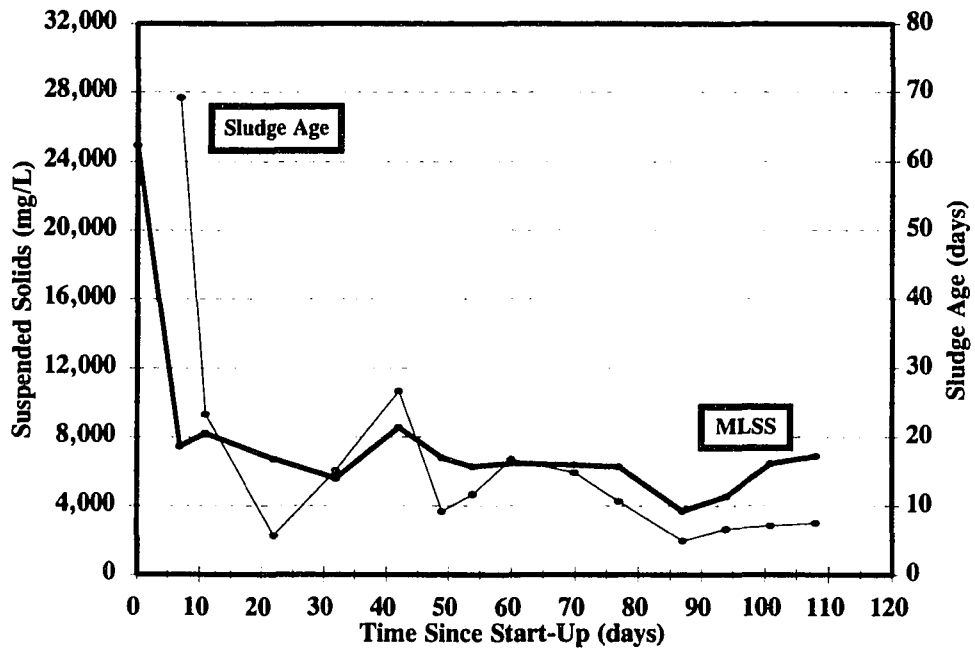


Figure 69. MLSS and SRT for the beef/glucose control study.

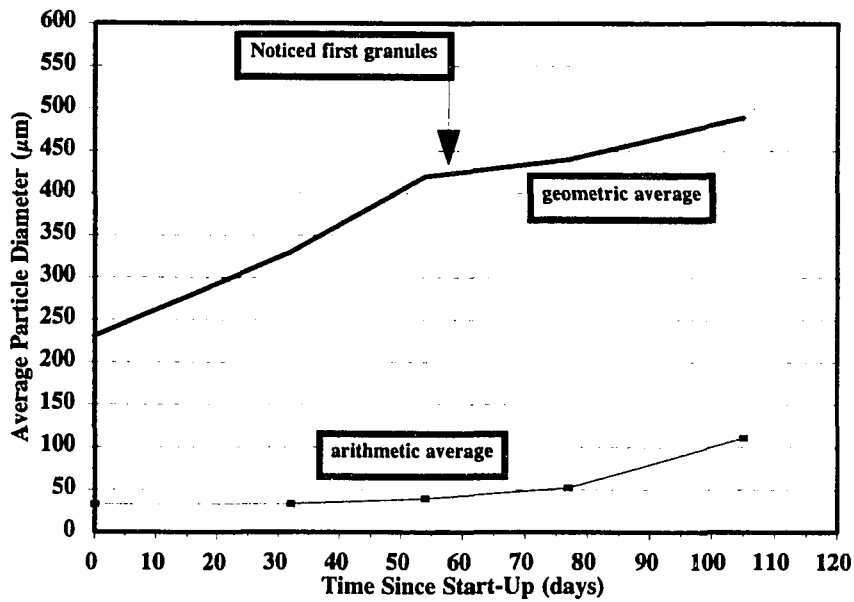


Figure 70. Average particle size for the beef/glucose control study.

had a slight granular nature but did not approach the granular character observed in the sucrose experiments. The first granules were observed at approximately day 60.

After approximately day 30 the biomass settling characteristics changed significantly. Prior to this the biomass settled normally, comparable to the biomass observed in the sucrose experiments. However, as the experiment progressed the biomass began to float to the top of the ASBR during the settle phase, most likely due to high fat concentrations in the reactor. (Alternatively, it is also possible that the high protein content of the beef substrate caused the floating biomass. Protein has hydrophobic and hydrophilic regions and may act similarly to soap or fat molecules under certain conditions. The fat, however, is a more likely suspect due to the fact that other proteinaceous wastes have been treated in the ASBR without causing the biomass to float.) For this reason, the decant port was relocated to one of the bottom ports on the ASBR. This phenomenon reached an extreme by day 50 at which time the entire biomass population floated to the top of the ASBR during the settle phase. This condition continued for the remainder of the experiment. This would not have caused a serious problem except that as the biomass began to granulate, the heavier biomass particles tended to sink during the decant phase and were washed out of the reactor. This observation may have lead to inhibition of granulation since the heavier (and better settling) particles were washed out of the ASBR rather than being retained, as is normally the case.

The phenomenon of biomass flotation due to fat accumulation must be studied further. This obviously presents serious difficulties in developing a granular biomass. In

addition, the biomass caught in the floating layer is essentially unavailable for substrate degradation since it seldom contacts the liquid portion of the reactor. This latter point was most probably the cause of the relatively poor COD removals observed throughout this study.

Cationic Polymer Enhancement Study

Operational Performance

An ASBR enhanced with cationic polymer was operated in parallel with the control reactor. The cationic polymer-enhanced ASBR was seeded with 25,000 mg/L of suspended solids (MLVSS = 15,000 mg/L) and operated at an HRT and OLR of 2 days and 1 g COD/L/day, respectively. The cationic polymer dosage was initially 2 mg/L/cycle. After 1 week of operation the HRT was decreased to 1 day, the COD load was increased to 2 g/L/day, and the polymer dosage was reduced to 1 mg/L/cycle. The ASBR was operated under these conditions for two weeks, during which the SCOD removal efficiency was in excess of 80% (Figures 71 and 72) and the volatile acids concentration averaged 250 mg/L (Figure 73). The alkalinity and pH were consistent throughout the study. The alkalinity increased gradually over the course of the study from 2,400 mg/L to 3,200 mg/L, as CaCO₃. The pH fluctuated marginally but remained within 6.8 and 7.2 throughout the experiment (Figure 74).

On day 22 the COD load was increased to 3 g/L/day and the SCOD removal efficiency increased to over 85% while the VFA concentration remained at 250 mg/L, as

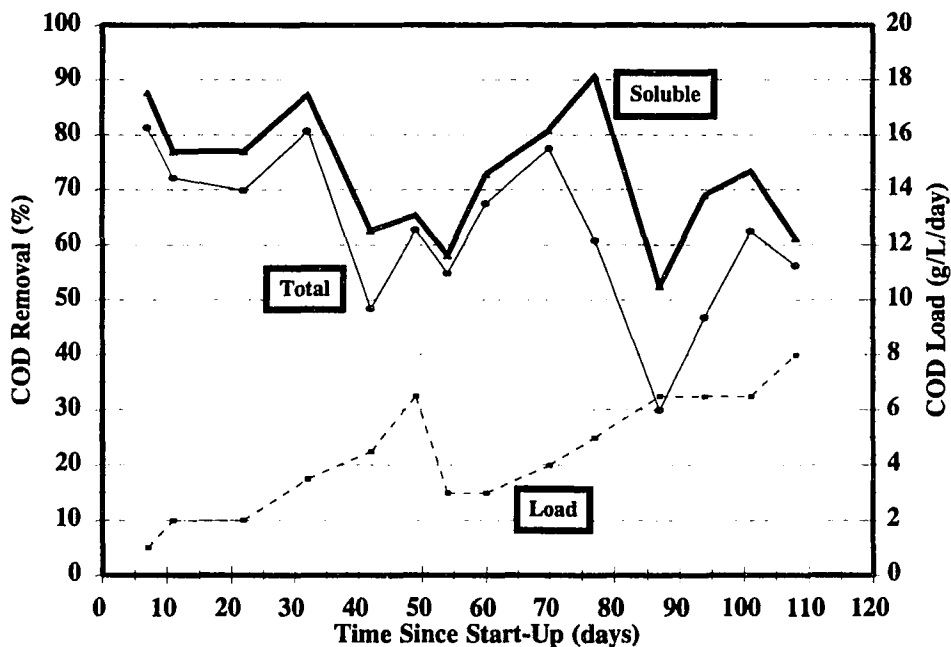


Figure 71. COD removal for the cationic polymer-enhanced beef/glucose study.

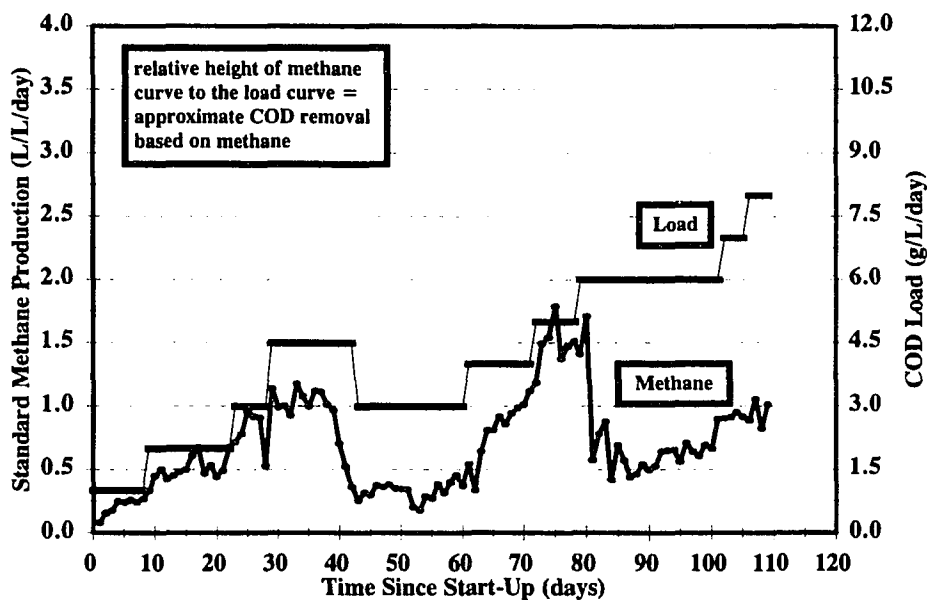


Figure 72. Methane production for the cationic polymer-enhanced beef/glucose study.

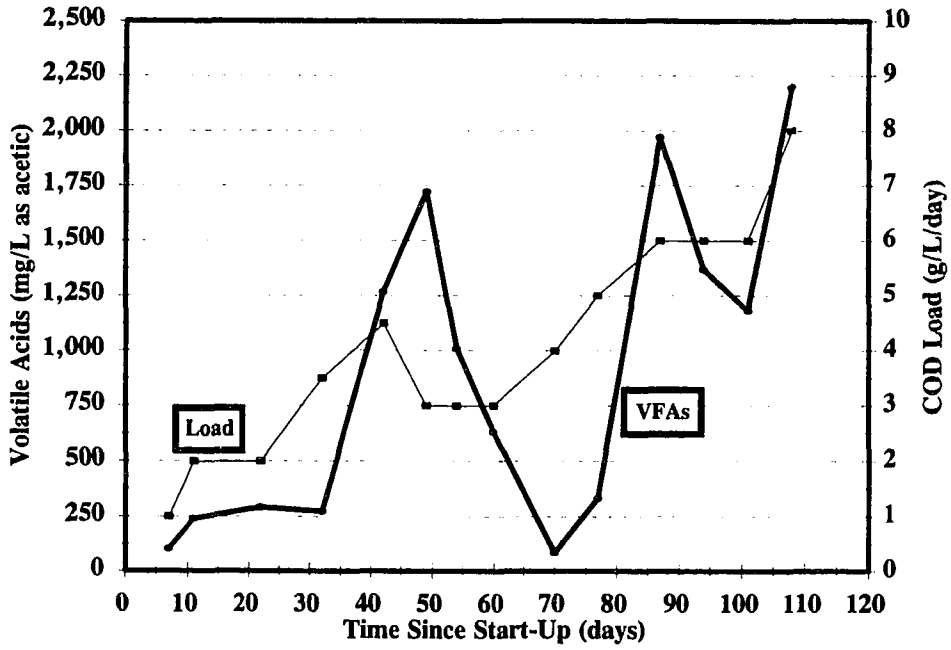


Figure 73. Volatile acids data for the cationic polymer-enhanced beef/glucose study.

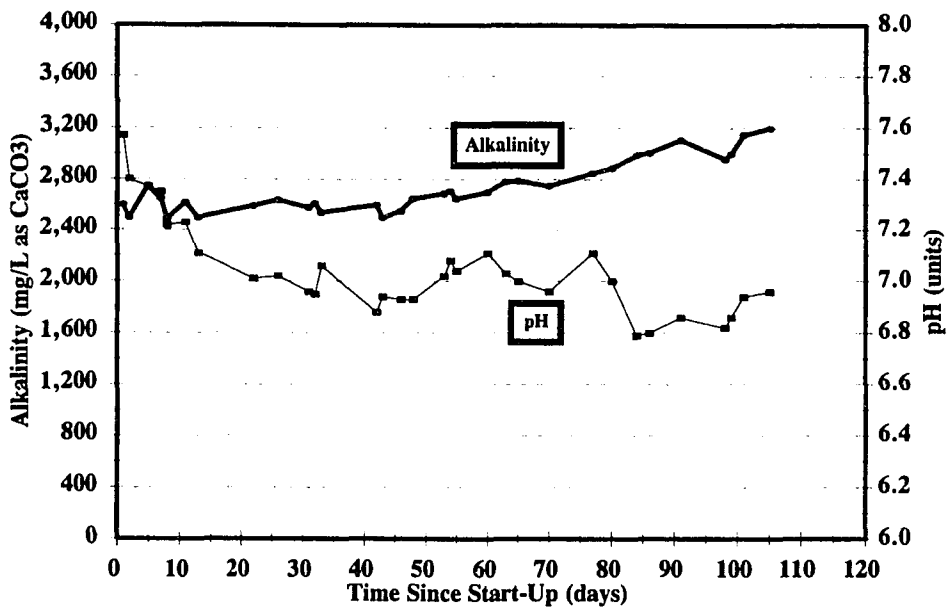


Figure 74. Alkalinity and pH data for the cat. polymer-enhanced beef/glucose study.

acetic. On day 39 the COD load was increased to 4.5 g/L/day. At this point the biomass began to float as in the control experiment. This observation is discussed further below. After the COD load was increased to 4.5 g/L/day, the SCOD removal efficiency decreased to 62% and the VFA concentration increased to 1,700 mg/L due to loss of biomass (Figures 71 and 73). At this point the COD load was decreased to 3 g/L/day to avoid failure of the system. On day 60 the COD load was increased again to 4 g/L/day. The SCOD removal efficiency increased to 80% and the VFA concentration decreased to below 100 mg/L. On day 71 the COD load was increased to 5 g/L/day and the SCOD removal efficiency increased further to 90% (Figure 71).

On day 79 the COD load was increased to 6 g/L/day resulting in a decreased SCOD removal efficiency which leveled off at approximately 70%. The VFA concentration increased from 250 mg/L to almost 2,000 mg/l before leveling off at 1,300 mg/L on day 95. On day 98 the COD load was increased to its final value of 8 g/L/day, resulting in decreased COD removals and increased VFA concentrations (Figure 71 and 73, respectively).

Solids and Granulation

Figures 75 and 76 present the MLSS and particle size analyses, respectively, for the cationic polymer-enhanced ASBR study. The MLSS level decreased from 25,000 mg/L to a relatively constant value of 11,000 mg/L after 20 days of operation. As the COD load was increased from 2 to 3 g/L/day, the biomass began to granulate, with the first granules

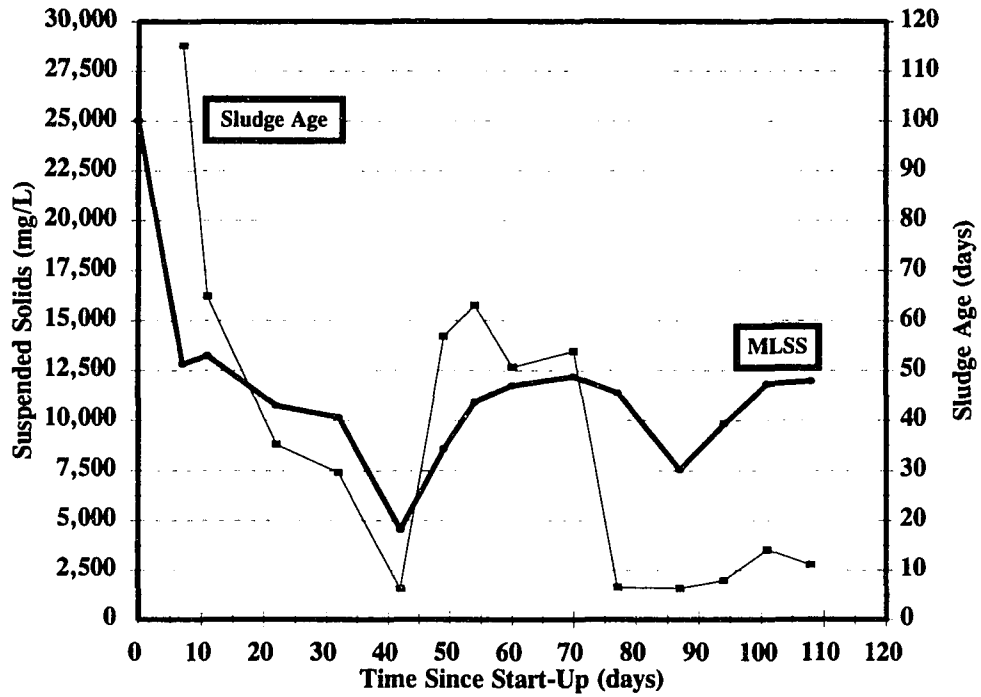


Figure 75. MLSS and SRT for the cationic polymer-enhanced beef/glucose study.

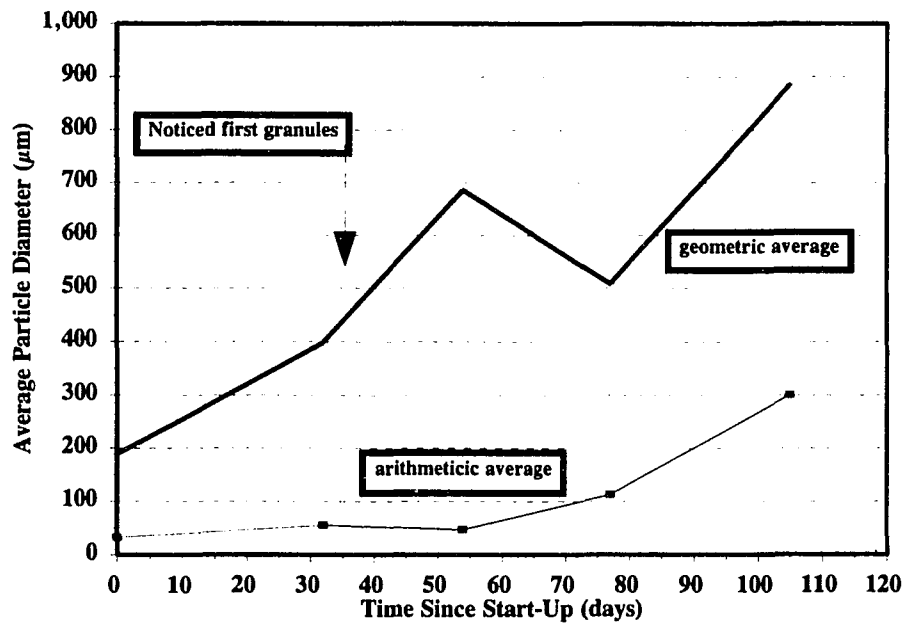


Figure 76. Average particle size for the cationic polymer-enhanced beef/glucose study.

noticed on day 39 (Figure 76). Also, at this point, the biomass began to float. A significant amount of biomass washed out of the ASBR and the MLSS level decreased to 5,000 mg/L by day 42. After relocating the effluent port to a lower level on the ASBR, the MLSS level increased to 12,500 mg/L over the next 25 days (Figure 75). During this same time the SRT of the system increased from 7 days to over 60 days. This increase was due to the compact nature of the floating biomass. The combined action of the fat and polymer created a fairly dense floating layer at the top of the ASBR. Very few solids were lost during the decant operations, resulting in an increasing MLSS concentration and SRT.

At day 80 another loss of biomass occurred. This loss was due to the increasing granular nature of the biomass. The action of flotation was counteracted by the settling characteristics of the granules, which resulted in a dispersed, or suspended biomass throughout the ASBR. Many of the granules were washed out during this time, leaving behind the floating biomass layer at the top of the reactor.

Granulation was observed in the cationic polymer study. As previously stated, the first granules were observed after only 39 days of operation. At this point the geometric average particle size was approximately 0.45 mm. By day 50 the average size had increased to 0.7 mm. During the second period of biomass washout (day 80), however, many of the larger granules were lost and the average size decreased to 0.5 mm. By the end of the experiment the average size was again increasing and was nearly 0.9 mm.

Cationic Polymer Effect

As was observed in the sucrose experiment, the cationic polymer has significant beneficial effects on the start-up and granulation of the ASBR. The COD load and COD removal efficiency were significantly higher at any given time in the cationic polymer experiment as compared to the control. The progress of granulation was also enhanced by polymer addition.

As stated earlier, the subject of anaerobic degradation of fat must be further addressed. The fat content of the beef extract caused serious difficulties in the operation of the ASBR. In practice it appears that removal of fat from the wastewater stream would be advantageous. Alternatively, the biological degradation of fat in anaerobic reactors would preclude the necessity of fat removal with the added benefit of increased methane production.

Summary of Enhancement Studies

The overall effects of the enhancement methods used in this research were varied, both among the specific enhancement techniques and between the two substrates used. The best method employed was the addition of the cationic polymer during the first two months of operation. GAC and PAC also had stimulatory effects on start-up and granulation, though most probably through different mechanisms. Table 27 presents a summary of these experiments in terms of the required time to attain specific COD loading rates and granulation.

Table 27. Start-up and granulation summary.

Substrate	Enhancement	Time Required for Objective to be Attained						
		3 g/L/day	4 g/L/day	5 g/L/day	8 g/L/day	14 g/L/day	first granules	full granulation
sucrose	none	90	100	107	135	---	130	140+
sucrose	PAC	63	80	110	130	150	90	100+
sucrose	GAC	30	38	62	88	---	71	80+
sucrose	garnet ^a	48	---	---	---	---	75	---
sucrose	sand	---	---	---	---	---	---	---
sucrose	cationic ^b	29	39	59	64	110	31	55+
sucrose	polyDADM ^c	39	66	130	170	---	101	---
sucrose	FeCl ₃	---	---	---	---	---	---	---
beef/glucose	none	61	80	100	---	---	61	---
beef/glucose	cationic	21	35	43	107	---	39	90+

^a The granules observed in this reactor were different than those from other experiments. It is believed that these granules were inorganic particles, since further granulation of the biomass did not occur.

^b The COD load was subsequently increased to 6 g/L/day on day 61.

^c The COD load had to be decreased back to 3 g/L/day on day 81 due to poor performance; switched to cationic on day 84.

The enhancement mechanism of the GAC and PAC were probably similar. Both materials have a high adsorption capacity and probably adsorbed a significant amount of volatile acids during the start-up phase. This would have had two stimulatory effects: (1) Volatile acids are often present at significant concentrations during start-up due to the more rapid growth rates of the acidogenic and acetogenic bacteria as compared to the methanogens. High initial VFAs may inhibit the growth of the desired methanogens that have a relatively low K_m value for acetate. Through adsorption on to activated carbon the bulk liquid concentration of VFAs is reduced, thereby creating more favorable conditions

for the desired methanogens. And (2) the activated carbon with adsorbed VFAs provides an ideal site for bacterial attachment. The adsorptive capacity of activated carbon is normally easily inhabited by bacteria. However, with an abundant supply of food the surface provides an even better site for bacterial growth.

GAC appears to have an advantage over PAC, especially during the first few weeks after start-up. Although PAC has a larger surface area per mass of carbon, its small size does not allow for efficient sedimentation in the solids-concentrated environment of the ASBR. GAC, however, settles rapidly and is retained in the reactor more efficiently. Although the lower surface area of GAC may not build up as high of a concentration of biomass per mass of carbon (compared to PAC), the biomass that does become attached will be retained in the reactor.

The enhancement mechanism of the cationic polymer is necessarily different from that of activated carbon. During the start-up with cationic polymer enhancement the effluent from the ASBRs contained few solids (after the initial washout of biomass during the first week of operation). Therefore, the bacteria that was initially present in the seed biomass were retained within the reactor more efficiently than in other studies. By artificially maintaining high MLSS concentrations during the critical start-up period, COD removals were improved and the biomass concentrations could increase more rapidly. Although not explicitly proven, the cationic polymer also may have facilitated cell contact among adjacent bacteria. Since the surface charge of most bacteria is generally negative, the positive charge of the cationic polymer should act to bridge bacteria together. As more

bacteria began to come in contact with each other, granulation naturally progressed until further addition of the polymer was unnecessary.

Specific Methanogenic Activity Experiments

Background and Theory

Several specific methanogenic activity tests were conducted during this research. As previously stated, the GAC-enhanced ASBR was used extensively for this purpose. The PAC-enhanced and garnet-enhanced ASBRs were also used to a lesser extent to determine typical SMAs of the biomass. Both flocculent and granular biomass were used in the SMA tests. Sucrose and acetate were used individually as the substrate, and nutrients, trace metals, and buffering compounds were added as required (Experimental Procedures section). Sucrose and acetate were used in separate SMA tests to try to determine bacterial arrangement within the granule structure. Granule structure was discussed in the Literature Review section of this document and is briefly reviewed here.

There are generally two different bacterial arrangements normally found in granules: layered and non-layered (Figures 77 and 78, respectively). Layered granules generally have three fairly distinct zones of bacteria. The outer zone often consists of a heterogeneous consortia of many bacterial species and morphologies. The inner zone is usually a fairly homogenous core of rod-shaped bacteria, often cited as *Methanotrix*-type cells. The middle layer is a transition zone between the two extremes, and consists mainly of acetogenic and methanogenic bacteria which exist in a symbiotic relationship (Figure

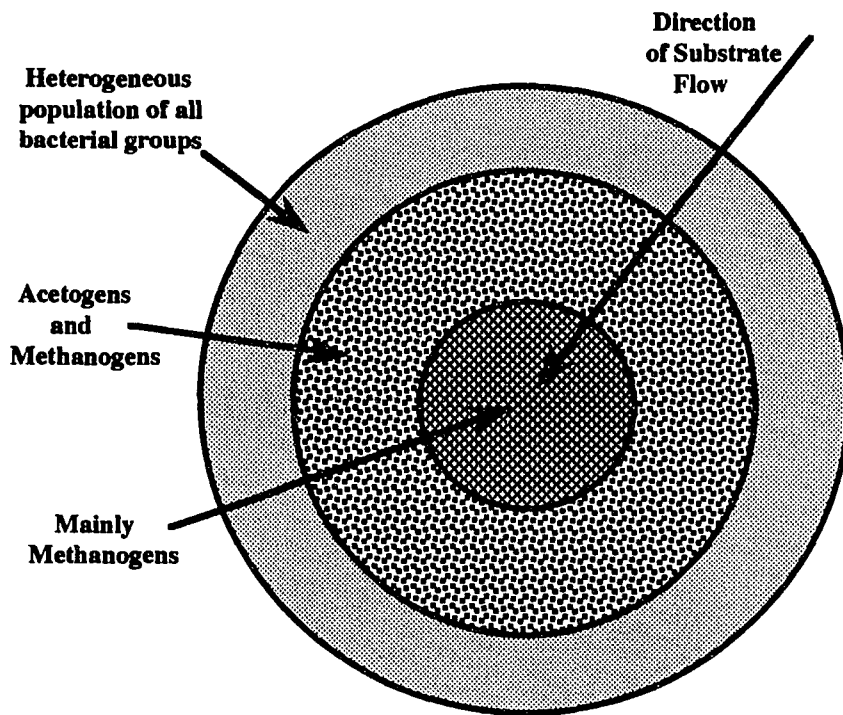


Figure 77. Idealized granule exhibiting a layered structure.

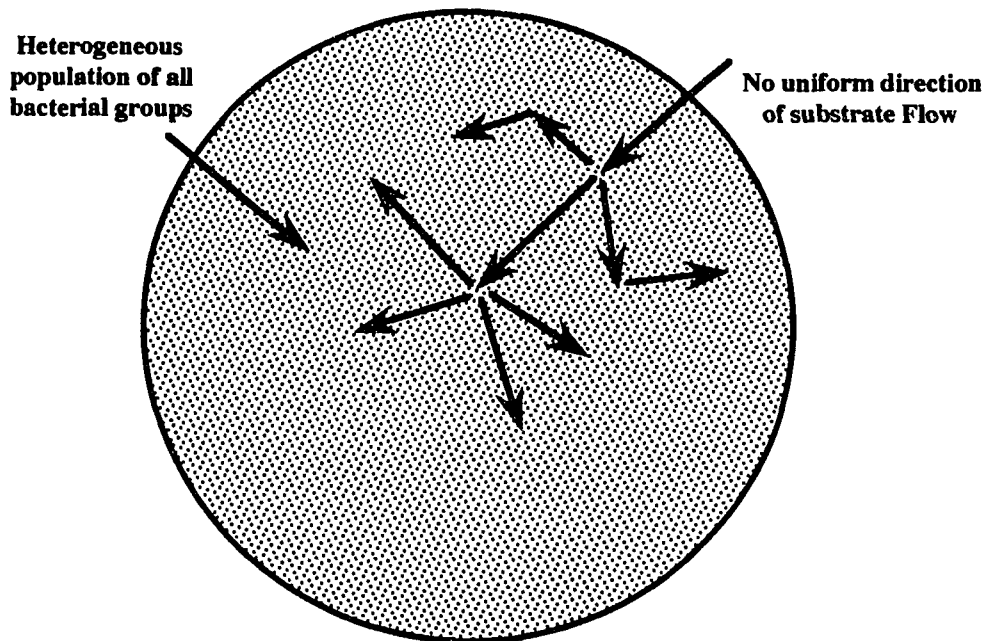


Figure 78. Idealized granule exhibiting a non-layered structure.

77). One theory is that complex substrates (sucrose) are converted to volatile acids by the outer-zone bacteria. The volatile acids are then immediately used by the nearby acetogenic bacteria in the middle zone. Hydrogen and carbon dioxide produced by the acetogens are rapidly converted to methane by the methanogens present in the middle layer. Acetate produced by the acetogens diffuses into the core of the granule where the acetoclastic methanogens convert it to methane and carbon dioxide.

Non-layered granules generally consist of a heterogeneous consortia of bacteria throughout the entire structure with no obvious zones of homogeneity (Figure 78). Alternatively, non-layered granules may also consist of a homogeneous population of only one or two bacterial species, as may be the case for granules developed on simple substrates such as acetate. In heterogeneous non-layered granules there is no obvious direction of intermediate flow as was discussed for layered granules. Rather, intermediate degradation products may diffuse in any direction and methane production may theoretically occur throughout the granule.

The layered or non-layered structure of a granule may be tentatively elucidated by conducting SMA tests with different substrates. For example, consider a granule with a layered structure which is fed sucrose as its sole carbon source. The sucrose is degraded to acids in the outer layer, followed by acetogenesis and methanogenesis in the middle and inner layers, respectively. The progression of sucrose degradation to acids and finally to methane can occur rapidly because of the thermodynamic advantage of granule biomass over flocculent biomass. However, now suppose the same layered granule is fed a simple

substrate such as acetate. The majority of the acetoclastic methanogens are located in the center of the granule, and, therefore, the acetate must diffuse into the granule before methanogenesis can occur. Stated differently, methane production (SMA) may actually occur more rapidly from sucrose than from acetate in a layered granule.

Now consider a granule with a non-layered structure. Since the methanogenic organisms are located throughout the granule, methanogenesis from acetate should theoretically occur more rapidly than methanogenesis from sucrose due to the fewer intermediate steps. Therefore, the SMA of the biomass fed acetate should be greater than (or at least equal to) the SMA from sucrose degradation.

Specific Methanogenic Activity Results

Sucrose Tests

The results of the various SMA experiments are presented in Table 28. Eight tests were conducted with sucrose as the substrate: 2 tests with flocculent biomass (GAC and garnet studies) and 6 with granular biomass (GAC and PAC tests). The granular tests were conducted with biomass at various stages of granulation. The GAC series of experiments especially provided a time-dependent progression of SMA from flocculent biomass (day 65) to slightly granular (day 93) to fully granular (days 133, 135, and 190).

Examination of the GAC SMA data from day 65 to 93, an obvious increase (doubling) in activity is observed, coinciding with granulation of the biomass in the GAC-enhanced ASBR. After the biomass had fully granulated the SMA increased still further

Table 28. Summary of specific methanogenic activity experiments.

Experiment	Time Since Start-Up (days)	Biomass Type	SMA ^a (ml/g/min) ^b	SMA (μmoles/g/min) ^c
Sucrose				
Garnet	83	flocculent	0.12	6.70
GAC	65	flocculent	0.07	3.13
GAC	93	granular	0.16	7.14
GAC	113	granular	0.22	9.82
GAC	135	granular	0.19	8.48
GAC	190	granular	0.17	7.59
PAC	158	granular	0.13	5.80
PAC	228	granular	0.14	6.25
Acetate				
GAC	76	flocculent	0.09	4.02
GAC	195	granular	0.19	6.70
PAC	169	granular	0.02	0.89

^a Specific methanogenic activity.

^b Units are milliliters of methane per gram of volatile suspended solids per minute (@ STP).

^c Units are micromoles of methane per gram of volatile suspended solids per minute (@STP).

from 0.16 mL CH₄/g MLVSS/min at day 93 to 0.22 mL CH₄/g MLVSS/min at day 113. Beyond this point the SMA of the GAC-enhanced biomass decreased slightly to 0.19 mL CH₄/g MLVSS/min on day 135 and 0.17 mL CH₄/g MLVSS/min by the end of the GAC study (day 190). Figure 79 presents the data for the GAC SMA tests (sucrose) in graphical form.

Figure 80 shows a comparison of the SMA curves for biomass developed in two separate studies. The granular data are from the GAC-enhanced ASBR on day 113 of that experiment. The flocculent data are from the garnet-enhanced ASBR on day 83. Both of the biomass samples were mature, but the activity of the granular biomass was considerably higher than that of the flocculent biomass. The granular biomass from the PAC study had a slightly lower SMA than that of the GAC study. This observation may have been due to the extremely high MLSS levels of the PAC-enhanced ASBR (up to 27,000 mg/L). The biogas-recirculation mixing may not have been sufficient to completely-mix the ASBR during the SMA test, which would have resulted in underestimating the SMA of the biomass.

Acetate Tests

Results of the SMA tests using acetate as a substrate are inconclusive concerning their relationship to granule structure. The SMA on acetate of the GAC-enhanced biomass increased significantly after granulation had occurred in the ASBR. This can be explained due to the increase in numbers of methanogenic organisms compared to the other groups of

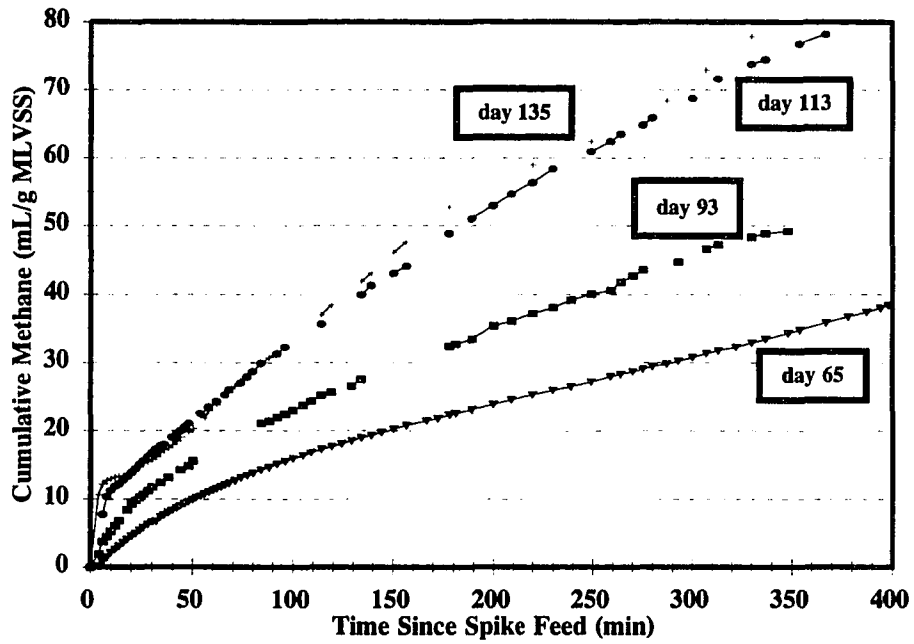


Figure 79. SMA over the course of the GAC-enhanced study.

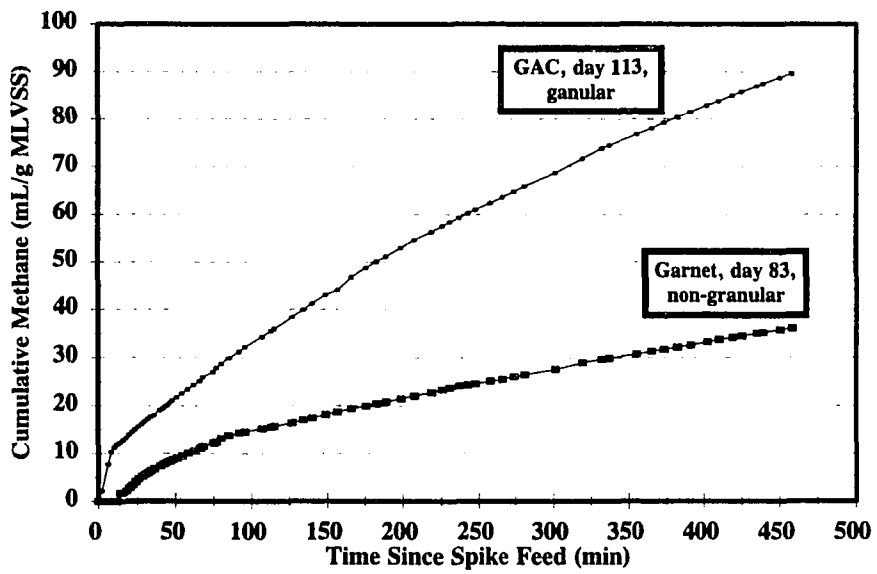


Figure 80. SMA comparison of granular and non-granular biomass.

bacteria (higher percentage of methanogens in the granular biomass compared to the non-granular biomass). After granulation had occurred, the SMA using acetate and sucrose were similar (0.19 and 0.17 mL CH₄/g MLVSS/min, respectively). These two tests were conducted on days 190 and 195 of the study (Table 28 and Figure 81). Therefore, the biomass did not have time to change significantly between the tests. This observation (similar SMA on acetate and sucrose) tends to favor the non-layered structure theory for the GAC-enhanced biomass. That this is the case should not be surprising given the large size of GAC particles. If the GAC particles did act as attachment surfaces, then it is likely that bacteria from all groups attached to the GAC. The GAC particles are many magnitudes of order larger than individual bacteria, so the chance that only one type of

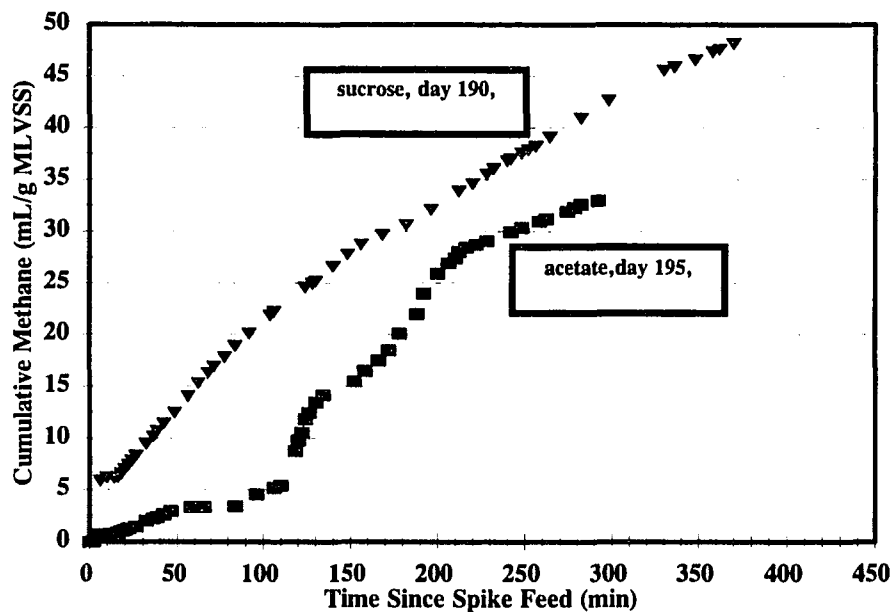


Figure 81. SMA comparison of GAC granules fed acetate and sucrose.

bacteria attached to the surface is remote. GAC adsorbs most organic compounds, including sucrose, propionate, butyrate, and acetate. Therefore, the GAC surface may have stimulated all groups of bacteria to attach randomly.

The acetate SMA test with the PAC-enhanced granules yielded significantly different results from those of the GAC granules. The SMA value from this test was the lowest out of all of the SMA test conducted (0.02 mL CH₄/g MLVSS/min). The same biomass degrading sucrose had an SMA of 0.13 mL CH₄/g MLVSS/min. This observation tends to favor the layered granule theory, with acetate diffusion into the granule being a major limiting factor.

Electron Microscopy

The granule morphology and microbiology were characterized using scanning and transmission electron microscopy. The samples to be analyzed were taken from the appropriate ASBR and taken to the Bessey Microscopy Facility at ISU. It was desired to view the outer surface as well as the interior of the granules to determine whether the granule structure had a layered or non-layered arrangement.

Scanning electron microscopy (SEM) was used to view the surface of the granules at 2 different magnifications, normally 100x and 4,000x. Additionally, it was also attempted to cut a granule in half and view its cross section. This presented problems in that the granule diameter was too large to view the entire cross section and still define any details of the granule structure. Therefore, images were taken in the center of the granule

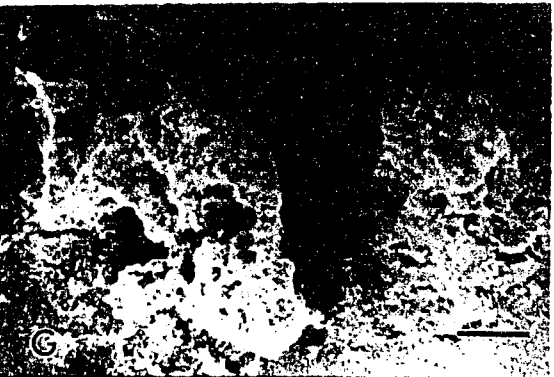
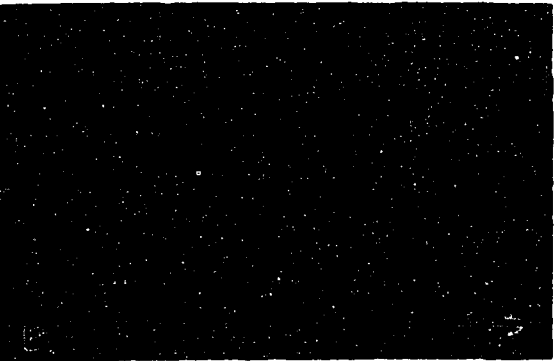
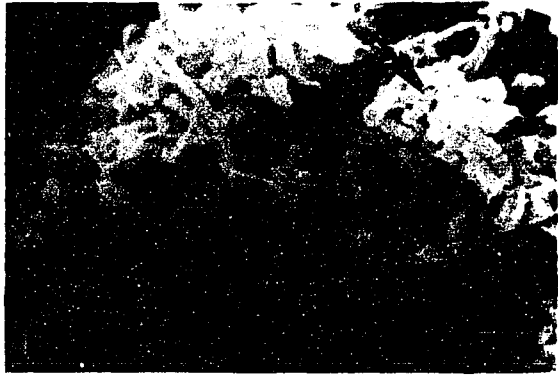
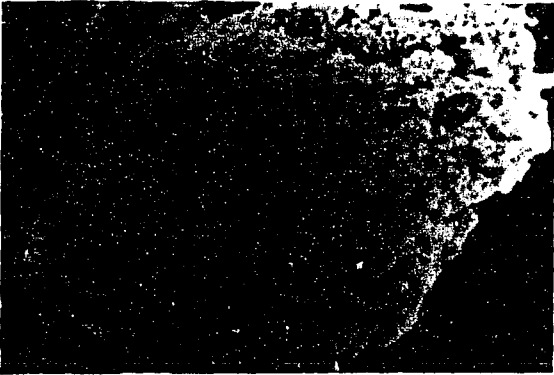
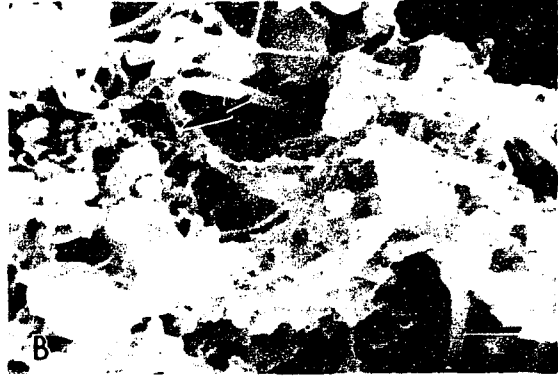
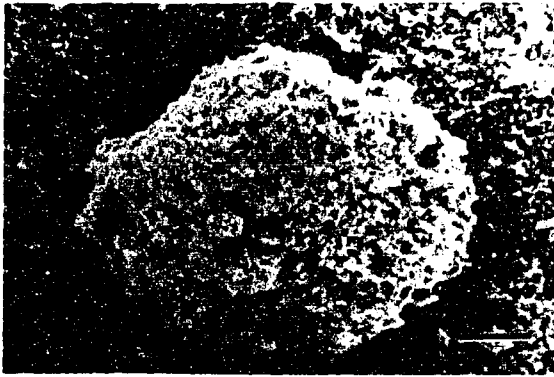
and at the edge of the granule, noting any significant differences in bacterial morphologies present. Transmission electron microscopy was also attempted to elucidate the granule cross-section arrangement, although similar problems arose.

Granule Surface

Figure 82 shows SEM images of the outer surface of 4 different granules developed in 4 different experiments: sucrose control, sucrose + cationic polymer, sucrose + PAC, and sucrose + GAC. At 100x magnification (Figure 82 a, c, e, g) the surfaces of all the granules appear to be rather rough and porous. Upon closer examination at 4000x magnification (Figure 82 b, d, f, h) it is observed that the surface of the granule is literally covered with bacteria of all morphologies. The most populous bacterial shapes appear to be short rods in chains, large irregular cocci in clumps, small cocci, and bent rods. Several other shapes are present as well. The rods in chains appear similar to literature SEM images of *Methanothrix soehngenii*, and the large irregular cocci are similar to *Methanosarcina barkeri*. However, it is not possible to positively identify bacterial species only from photographs.

The bacterial populations present in all of the granules in Figure 82 appear to be similar, which is not surprising considering the fact that all of the granules were developed on a sucrose substrate. It is also apparent that most of the granule structure is bacterial. That is, there is little material present in the images that could not be recognized as bacteria. However, there does appear to be extracellular material present that is acting to

Figure 82. SEM images of granule surfaces: (a) sucrose control granule at 100x, bar = 100 μm ; (b) sucrose control granule at 4000x, bar = 2 μm ; (c) sucrose + cationic polymer granule at 100x, bar = 100 μm ; (d) sucrose + cationic polymer granule at 4000x, bar = 2 μm ; (e) sucrose + GAC granule at 100x, bar = 100 μm ; (f) sucrose + GAC granule at 4000x, bar = 2 μm ; sucrose + PAC at 100x, bar = 100 μm ; (g) sucrose + PAC granule at 4000x, bar = 2 μm .

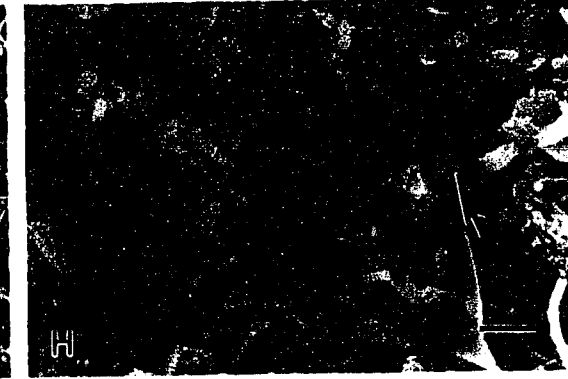
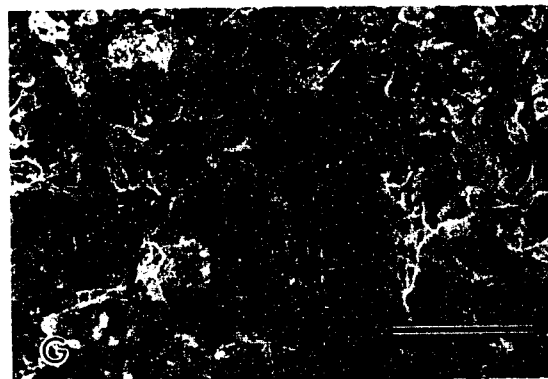
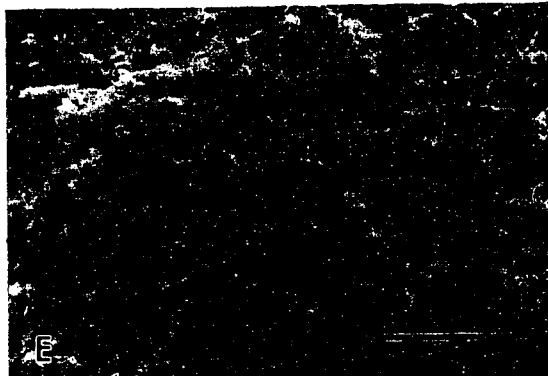
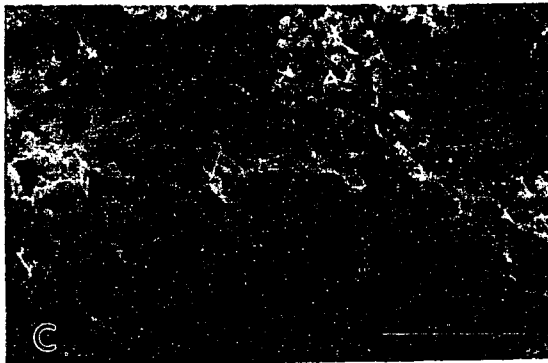
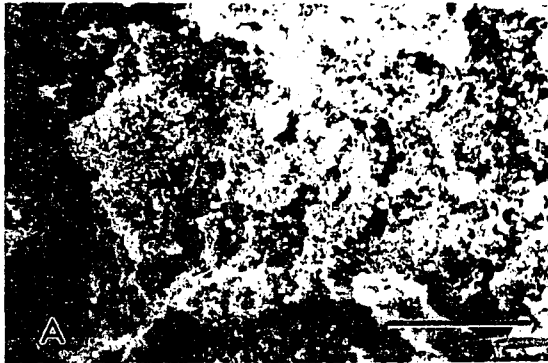


bind clumps of bacteria together. This observation is especially prevalent in Figure 82d, which is a granule formed with cationic polymer enhancement. It is possible that the extracellular material in this photo is at least partially cationic polymer. The areas of extracellular material are denoted by the arrows in Figure 82. It is also instructive to note the highly-porous structure of the granules. The granule pores allow substrate to enter into the granule and methane and carbon dioxide to exit without breaking the granule apart.

Figure 83 presents for additional granules developed from the following experiments: sucrose + cationic polymer (at a later time during the experiment), sucrose + polyDADM, beef/glucose control, and beef/glucose + cationic polymer. The images on the left are at a magnification of 400x (compared to 100x in Figure 82), while those on the right are at a magnification of 4000x. At the lower magnification the granule surfaces in Figure 83 appear to be similar with the exception that the granule developed with cationic polymer treating sucrose (Figure 83a) lacks the filamentous nature of the other 3 granules. These filamentous strands apparent on the granule surface are similar to those described by Hulshoff Pol [67]. These filaments probably represent a second common morphology of *Methanotrix soehngeni*, which may form short chains or very long filaments. Again it is noted that the granule surface is highly porous and is mostly bacterial in nature.

Two obvious differences are apparent between the granules developed on sucrose (Figure 83b and 83d) and those developed on beef/glucose (Figure 83f and 83h). First, there are many more large irregular cocci in the sucrose granules, as was observed in the

Figure 83. SEM images of granule surfaces: (a) sucrose + cationic polymer granule at 400x, bar = 20 μm ; (b) sucrose + cationic polymer granule at 4000x, bar = 2 μm ; (c) sucrose + polyDADM granule at 400x, bar = 20 μm ; (d) sucrose + polyDADM granule at 4000x, bar = 2 μm ; (e) beef/glucose control granule at 400x, bar = 20 μm ; (f) beef/glucose control granule at 4000x, bar = 2 μm ; (g) beef/glucose + cationic polymer granule at 400x, bar = 20 μm ; (h) beef/glucose + cationic polymer granule at 4000x, bar = 2 μm .



previous sucrose granules (Figure 82). The second difference is that there appears to be more non-bacterial material in the beef/glucose granules, denoted by the arrows in Figure 83f and 83h. This material may be fat deposits which caused the granules to rise to the liquid surface of the ASBR during the beef/glucose experiments.

There also appears to be a difference between the sucrose granules enhanced with cationic polymer and polyDADM (Figure 83b and 83d, respectively). The granule developed with cationic polymer enhancement has a significant higher population of small cocci or short rods (Figure 83b). This difference may have been the result of the chemical nature of the two polymers, and may have resulted in the poorer performance of the polyDADM-enhanced ASBR.

The most significant difference between the two granules developed on the beef/glucose substrate is the presence of a relatively large number of small spiral bacteria and spirochetes in the granule developed with cationic polymer addition (Figure 83f and 83h). Again, this difference may have resulted in the improved performance of the ASBR enhanced with cationic polymer.

Granule Structure and Arrangement

To determine whether the granules were formed in a layered or non-layered arrangement, it was necessary to cut the granule in half (SEM) or into thin sections (TEM) in order to obtain a cross-sectional view of the granules. Unfortunately the granules were

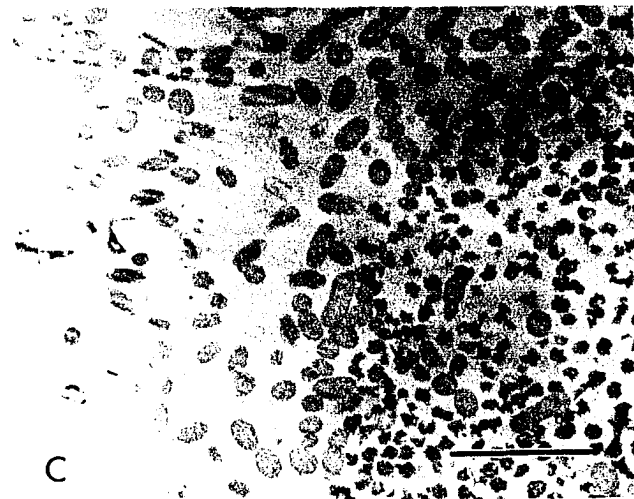
not easily cut without disturbing the natural granule structure. Therefore, only two successful analyses of this type were made.

Figure 84 shows the cross-section views of two granules (all images are at a magnification of 4000x): Figures 84a and 84b are SEM images of the inner and outer portion, respectively, of a granule developed in the sucrose + cationic polymer experiment. Figure 84c is a thin-section TEM image of a granule developed in the sucrose + PAC experiment. The blurry portion of Figure 84b is due to the fact that the image is taken directly on the edge of the granule. The image is focused on the cut surface, and, therefore, the focus falls off at the granule edge.

There appears to be a slight difference in the bacterial species present in the inner and outer zones of the granule developed in the sucrose + cationic polymer study (Figure 84a and 84b). The inner zone consists of many more irregular cocci and bent rods. The outer zone has a higher population of long filaments and appears to contain more extracellular material. Although not conclusive evidence, it does appear that this granule is arranged in at least a partially layered structure.

Figure 84c presents more conclusive evidence of a layered structure. As stated, Figure 84c is a TEM image of a thin-sectioned granule developed in the PAC-enhanced sucrose experiment. The image was taken towards the center of the granule, and clearly shows a definite layered structure. The inner zone consists of a fairly homogeneous population of small irregularly-shaped bacteria. The outer zone appears to be more heterogeneous, consisting of a wide array of cocci and rods.

Figure 84. Images of granule interior: (a) SEM of sucrose + cationic polymer granule inner layer at 4000x, bar = 2 μm ; (b) SEM of sucrose + cationic polymer granule outer layer at 4000x, bar = 2 μm ; (c) TEM of sucrose + PAC granule layered structure at 4000x, bar = 2 μm .



Although the SEM and TEM images presented on the previous pages do not provide definite proof for the structure and arrangement of the granules developed in this study, they do indicate that, at the very least, the granules are not homogeneous throughout. That is, the granules are comprised of numerous bacterial species of all morphotypes, and the various groups are not randomly spread throughout the granule. Rather, the organisms are grouped in pseudo-layers or regions. This observation is consistent with the majority of previous literature on the subject. From the discussion presented earlier (Literature Review section), it is apparent that the formation of a densely-populated "micro-colony," which contains members from all groups of bacteria, is beneficial to each group in that efficient transfer of intermediate products could result. In effect, the thermodynamics of the entire anaerobic degradation process are improved by granule formation. The precise structure of the granules (layered or non-layered) formed appears to be dependent on the substrate [111, 134].

Species of *Methanothrix* and *Methanosarcina* have been implicated by many researchers as being the most abundant methanogens present in granules treating a wide variety of wastewaters (including sucrose wastewaters, which was the substrate used for most of these experiments), and bacteria similar in shape to both of these genera were observed in these studies [37, 64, 102, 152]. Additionally, the two species are almost always present within the same granule in varying degrees [76, 88, 101]. This was also observed in these SEM and TEM images.

Granule Elemental Analysis

The granules produced in the PAC and GAC experiments were analyzed for a variety of elements and compounds and compared to the seed biomass obtained from the City of Ames anaerobic digesters. Any significant differences between the seed biomass and the final granular biomass may give some insight as to the roles that various elements play in the granulation process. Only two samples were analyzed in this manner due to the cost of the tests. The purpose for conducting this portion of the research was to identify possible chemical enhancement methods for future research.

The seed and granular biomass samples were homogenized in a blender and then sent to the Analytical Services Laboratory at ISU for analysis. Although this method of analysis did not give the actual composition of the granules, it did relate the overall environmental conditions present in the system. Table 29 presents the results from this study. Examination of the data in Table 29 reveals that the overall chemical composition of the granular systems was quite different from that of the seed biomass (municipal digester). Especially significant is the much lower calcium, zinc, iron, and magnesium concentrations in the granular biomass as compared to the seed biomass. Conversely, the concentration of potassium and sodium was much higher in the granular systems, probably the result of nutrient (K_2HPO_4) and alkalinity ($NaHCO_3$) additions to the substrate feed solutions. One final note is that the organic carbon and nitrogen content of the granular systems was much higher than that of the seed biomass. This point is easily explained by

the growth of the bacteria in the ASBR systems. That is, the volatile percentage of total biomass increased from approximately 55% in the initial seed biomass to 90% in the granular biomass. Since carbon and nitrogen are two of the most abundant element in biomass, the concentrations of these elements naturally increased.

Table 29. Chemical composition of granular and initial seed biomass.

Element/ Compound ^b	Initial Seed ^a		GAC Granules ^a		PAC Granules ^a	
	Total Concentration (mg/L) ^c	Specific Concentration (mg/g) ^d	Total Concentration (mg/L) ^c	Specific Concentration (mg/g) ^d	Total Concentration (mg/L) ^c	Specific Concentration (mg/g) ^d
TOC	1,700	118	2,100	383	4,200	229
TKN	1,820	126	1,300	237	3,260	178
P	653	45	252	46	449	25
Ca	1,430	99	168	31	354	19
Mg	106	7	15	3	24	1
Na	216	15	2,260	412	2,780	152
K	170	12	565	103	702	38
Fe	580	40	100	18	173	9
Ni	2	0.1	6	1	10	0.5
Zn	330	23	47	9	56	3

^a MLSS of initial seed, GAC biomass, and PAC biomass = 14440, 5490, and 18320 mg/L, respectively.

^b Reported as the element.

^c Units are milligram of the element per liter of solution.

^d Units are milligram of the element per gram of biomass.

CONCLUSIONS AND RECOMMENDATIONS

The research presented in this document resulted in several significant findings. Further discussion of each of these points may be found in the Results and Discussion section. After careful analysis of the data from these experiments, the following conclusions and recommendations are presented:

- (1) The previously-reported required time for granulation in an ASBR [145] of almost 300 days was greatly in excess of that required in these experiments. Although a different substrate was used in the earlier study (non-fat dry milk), the results from this study indicate that granulation can be initiated with no enhancement in approximately 4 months with complete granulation within 5 months. The key to granulation without employing an attachment matrix or coagulant is to "push" the system by operating at high OLRs and low HRTs. This finding is similar to previous research by Hulshoff Pol and Lettinga [66, 67, 68].
- (2) The time required for granulation can be significantly reduced by using an enhancement technique. Methods used in these experiments that were found to have a stimulatory effect on granulation and start-up were the addition of powdered activated carbon (PAC), granular activated carbon (GAC), and cationic polymer.

- (3) Addition of 2,000 mg/L of PAC during the initial start-up of an ASBR treating sucrose resulted in a more rapid start-up, increased COD removals, and more rapid granulation as compared to the sucrose control reactor. Essentially complete granulation of the biomass was observed after 4 months of operation. The adsorptive capacity of the GAC is a significant characteristic for granulation and start-up enhancement.
- (4) Addition of 2,000 mg/L of GAC during the initial start-up of an ASBR treating sucrose resulted in a significantly reduced start-up time and rapid granulation. The first granules were observed after 70 days of operation, and the biomass was essentially completely granulated within the first 100 days. The adsorptive capacity of the GAC is a significant characteristic for granulation and start-up enhancement.
- (5) Cationic polymer addition was the most promising method used in this study for start-up and granulation enhancement (polymer dosage of 1 mg/L/cycle). The ASBR was able to attain high COD loads (6 g/L/day) within 2 months of operation, and the biomass granulated within 50 to 60 days after start-up. Additionally, it was not necessary to continue polymer addition after two months of operation. The efficient solids clarification of the polymer, as well

as its cationic charge which permits close contact among adjacent bacteria, appears to be significant in terms of granulation and start-up enhancement.

- (6) The other enhancement techniques used in these experiments had no beneficial effects on start-up and granulation. These techniques include garnet addition, silica sand addition, ferric chloride addition, and polyquaternary amine (polyDADM coagulant) addition.
- (7) The maximum COD load attainable in these experiments without polymer addition was 12 g/L/day. A COD load of 14 g/L/day was treated for a period of 2 weeks before biomass washout lead to decreased COD removals and system inhibition (PAC-enhanced and cationic polymer-enhanced sucrose studies).
- (8) The maximum COD load attainable with cationic polymer addition was 17 g/L/day. At this load, the SCOD removal efficiency was almost 90% for one week, after which is decreased to 70%. A COD load of 20 g/L/day resulted in significant deterioration of COD removal.
- (9) The specific methanogenic activity (SMA) of the biomass increases over time and reaches a maximum shortly after granulation is complete.

- (10) The SMA of granular biomass is significantly higher than that of flocculent biomass for these experiments.
- (11) The granules developed in these experiments appear to be arranged in a layered structure (SEM and TEM analyses). The inner zone consists of a relatively homogeneous population of only a few bacterial species, while the outer zone consists of a heterogeneous population of many bacterial shapes and morphologies.
- (12) The long start-up periods often associated with anaerobic systems may be overcome by using enhancement techniques. It is felt that the results from this research can be applied directly to full-scale systems with significant reductions in the required time to attain design operating conditions.
- (13) It is recommended that further research be conducted on chemical enhancement techniques for ASBR operation. The elemental analyses of the granular biomass developed in these experiments was significantly different from that of the initial seed biomass. Chemical addition may be an alternative method for granulation enhancement.

- (14) It is recommended that further studies on fat degradation and treatability be conducted. Additionally, other substrates should be studied with respect to their effect on granulation and start-up. It appears that the specific substrate used has an effect on the rates of start-up and granulation.

APPLICATIONS

Background

In order for research to be meaningful it should have some application to "real-world" problems and situations. The purpose of this section is to relate the results of this research to a meaningful engineering application.

As industries are forced to pay higher rates to municipalities for treating their wastewaters, it is becoming more popular for industries to build their own treatment systems. However, the long start-up period of most anaerobic systems can result in poor waste treatment, and, therefore, prolonged pay-back of the investment into the treatment process. The use of enhancement techniques can shorten the start-up time and even present an economic incentive.

Economics

As with anything beneficial, there is a cost for gaining an advantage. In this case the cost is the direct expense of the cationic polymer, PAC, or GAC. The costs for these materials as quoted by their manufacturers are \$2.10/lb, \$1.50/lb, and \$1.50/lb, respectively. However, the use of these materials for enhancing start-up of anaerobic reactors provides better treatment during start-up and allows for a shorter period of time until design loading conditions are reached.

Cationic Polymer

The daily cost for using the cationic polymer (dosage of 1 mg/L/cycle), assuming a 1,000,000 gallon ASBR operating at 4 cycles per day and treating a flow rate of 10^6 gpd with a BOD_5 concentration of 6,000 mg/L, is calculated as follows:

$$\begin{aligned}
 \text{Daily usage of polymer} &= (1 \text{ mg/L/cycle})(4 \text{ cycles/day})(1 \text{ mgal})(8.34) \\
 &= \underline{33.36 \text{ lbs/day}} \\
 \text{Daily cost of polymer} &= (33.36 \text{ lbs/day})(\$2.10/\text{lb}) \\
 &= \underline{\$70 \text{ per day}}
 \end{aligned}$$

This cost may be off-set by the increased BOD removals which would decrease the sewer-use fees paid to the local municipality. Typical sewer-use fees are approximately \$0.05 per pound of BOD_5 discharged to the sewer. The amount of BOD removed during the start-up period varies over time, but simplifying assumptions can be made by reviewing the data from the cationic polymer-enhanced sucrose study. Assuming that the ASBR removes 80 and 50% of the BOD_5 with and without cationic polymer addition, respectively, during the start-up period, the savings in sewer-use fees can be calculated as follows (the constant 8.34 has units of $\text{lb}\cdot\text{L}\cdot\text{mgal}^{-1}\cdot\text{mg}^{-1}$):

$$\begin{aligned}
 \text{Without polymer: sewer-use fee} &= (1 \text{ mgd})(6,000 \text{ mg } BOD/\text{L})(8.34)(0.5)(\$0.05/\text{lb}) \\
 &= \underline{\$1,251 \text{ per day}}
 \end{aligned}$$

With polymer: sewer-use fee = (1 mgd)(6,000 mg BOD/L)(8.34)(0.2)(\$0.05/lb)

= \$500 per day

Savings = \$751 per day

From this greatly simplified analysis it is obvious that the use of cationic polymer would more than pay for itself on a daily basis. This analysis did not include the benefit of the extra methane that would be produced, which would further increase the total savings.

PAC and GAC

The cost of adding PAC or GAC to an ASBR represents a capital cost to the investor. Using the same ASBR as was presented for the cationic polymer analysis, the total amount of carbon required is as follows:

Volume of tank	=	1 mgal
Concentration of carbon	=	2,000 mg/L
Mass of carbon	=	(1 mgal)(2,000 mg/L)(8.34)
	=	16,680 lb
Cost of carbon	=	(16,680 lb)(\$1.50/lb)
	=	<u>\$25,020</u>

The justification for this cost comes from the fact that the ASBR will reach design load more quickly and have better removals during the start-up period. The assumptions are as follows: carbon-enhanced system reaches design load in 80 days (GAC results); ASBR with no carbon enhancement reaches design load in 125 days. The average BOD removal over the start-up is 75% for the carbon-enhanced system and 60% for the non-enhanced system. Both systems remove 90% of the BOD when they reach design loadings. The savings in sewer-use fees due to the carbon enhancement is calculated below:

$$\begin{aligned} \text{Non-enhanced ASBR: sewer fees} &= (1 \text{ mgd})(6,000 \text{ mg/L})(8.34)(0.4)(\$0.05)(125 \text{ days}) \\ &= \underline{\$125,100} \end{aligned}$$

$$\begin{aligned} \text{GAC-enhanced ASBR: sewer fees} &= (1 \text{ mgd})(6,000 \text{ mg/L})(8.34)(0.25)(\$0.05)(75 \text{ days}) \\ &\quad + (1 \text{ mgd})(6,000)(8.34)(0.1)(\$0.05)(50 \text{ days}) \\ &= \underline{\$59,420} \end{aligned}$$

$$\begin{aligned} \text{Savings} &= \$125,100 - \$59,420 \\ &= \underline{\$65,678} \end{aligned}$$

From these analyses it appears that the economics of enhancement are advantageous for full-scale applications. These analyses did not include the additional methane that would be produced (and available as an energy source). Perhaps most significantly, these analyses did not include the benefit of "peace-of-mind" that results from a rapid start-up.

The investor will be much more comfortable when they can see the rewards of installing anaerobic treatment soon after start-up, rather than waiting 6 months to a year for their pay-off to be realized.

REFERENCES

1. Alibhai, K. R. K., and Forster, C. F. (1986). An examination of the granulation process in UASB reactors. *Environmental Technology Letters*, **7**, 193-200.
2. Alibhai, K. R. K., and Forster, C. F. (1986). Physicochemical and biological characteristics of sludges produced in anaerobic upflow sludge blanket reactors. *Enzyme Microb. Technol.*, **8**, 601-606.
3. Andras, E., Kennedy, K. J., and Richardson, D. A. (1989). Test for characterizing settleability of anaerobic sludge. *Environmental Technology Letters*, **10**, 463-470.
4. Archer, D. B. (1988). Report on the microbiological aspects of granulation. *Granular Anaerobic Sludge; Microbiology and Technology*, G. Lettinga, A. J. B. Zehnder, J. T. C. Grotenhuis, and L. W. Hulshoff Pol, eds., 107-112, Pudoc, Wageningen, The Netherlands.
5. Ashikago, N., Shibasaki, K., Kobayashi, S., and Menju, T. (1994). Affect of the operating factors on sludge pelletization in the anaerobic fluidized-bed reactor. *Proceedings of the Seventh Annual International Symposium on Anaerobic Digestion*, 688-697, January 23-27, Cape Town, South Africa.
6. Atkinson, B. (1984). Consequences of aggregation. *Microbial Adhesion and Aggregation*, K. C. Marshall, ed., 351-372, Springer-Verlag, Berlin, Germany.
7. Atkinson, B., Garrod, D. R., Hirsch, P., Jenkins, D., Johnson, B. F., Reichenbach, H., Rose, A. H., Schink, B., Vincent, B., and Wilderer, P. A. (1984). Aggregation. *Microbial Adhesion and Aggregation*, K. C. Marshall, ed., 303-322, Springer-Verlag, Berlin, Germany.
8. Beeftink, H. H., and van den Heuvel, J. C. (1988). Physical properties of bacterial aggregates in a continuous-flow reactor with biomass retention. *Granular Anaerobic Sludge; Microbiology and Technology*, G. Lettinga, A. J. B. Zehnder, J. T. C. Grotenhuis, and L. W. Hulshoff Pol, eds., 162-169, Pudoc, Wageningen, The Netherlands.
9. Black, M. G., Brown, J. M., and Kaye, E. (1974). Operational experiences with an abattoir waste digestion plant at Leeds. *Water Pollution Control*, **73**, **5**, 532-537.

10. Bochem, H. P., Schoberth, S. M., Sprey, B., and Wengler, P. (1982). Thermophilic biomethanation of acetic acid: morphology and ultrastructure of a granular consortium. *Canadian J. of Microbiology*, **28**, 500-510.
11. Breznak, J. A., Cooksey, K. E., Eckhardt, F. E. W., Filip, Z., Fletcher, M., Gibbons, R. J., Güde, H., Hamilton, W. A., Hattori, T., Hoppe, H.-G., Matthyse, A. G., Savage, D. C., and Shilo, M. (1984). Activity on surfaces. *Microbial Adhesion and Aggregation*, K. C. Marshall, ed., 203-222, Springer-Verlag, Berlin, Germany.
12. Brock, T. D., and Madigan, M. T. (1991). *Biology of Microorganisms, 6th edition*, Prentice Hall, Englewood Cliffs, NJ.
13. Brummeler, E. T., Hulshoff Pol, L. W., Dolfing, J., Lettinga, G., and Zehnder, A. J. B. (1985). Methanogenesis in an upflow anaerobic sludge blanket reactor at pH 6 on an acetate-propionate mixture. *Applied and Environmental Microbiology*, **49**, 6, 1472-1477.
14. Bryant, M. P. (1979). Microbial methane production - theoretical aspects. *Journal of Animal Science*, **48**, 1, 193-201.
15. Busch, P. L., and Stumm, W. (1968). Chemical interactions in the aggregation of bacteria-bioflocculation in waste treatment. *Environmental Science and Technology*, **2**, 1, 49-53.
16. Caerteling, C. G. M., Gijzen, H. J., Op den Camp, H. J. M., Lubberding, H. J., and Vogels, G. D. (1988). Anaerobic degradation of papermill sludge in a rudad-digester. *Granular Anaerobic Sludge; Microbiology and Technology*, G. Lettinga, A. J. B. Zehnder, J. T. C. Grotenhuis, and L. W. Hulshoff Pol, eds., 71-77, Pudoc, Wageningen, The Netherlands.
17. Caldwell, D. E. (1984). Surface colonization parameters from cell density and distribution. *Microbial Adhesion and Aggregation*, K. C. Marshall, ed., 125-136, Springer-Verlag, Berlin, Germany.
18. Callander, I. J., and Barford, J. P. (1983). Precipitation, chelation, and the availability of metals as nutrients in anaerobic digestion. Part I: Methodology. *Biotechnology and Bioengineering*, **25**, 1947-1957.

19. Callander, I. J., and Barford, J. P. (1983). Precipitation, chelation, and the availability of metals as nutrients in anaerobic digestion. Part II: Applications. *Biotechnology and Bioengineering*, **25**, 1959-1972.
20. Characklis, W. G. (1984). Biofilm development: a process analysis. *Microbial Adhesion and Aggregation*, K. C. Marshall, ed., 137-158, Springer-Verlag, Berlin, Germany.
- 20a. Chyi, Y. T., and Dague, R. R. (1992). Effects of particle size in anaerobic acidogenesis using cellulose as a sole carbon source. Poster presentation at the 65th Water Environment Federation Annual Conference, New Orleans, LA, September 20-24, 191-202.
21. Colleran, E. (1988). Report on the technological aspects of granulation. *Granular Anaerobic Sludge; Microbiology and Technology*, G. Lettinga, A. J. B. Zehnder, J. T. C. Grotenhuis, and L. W. Hulshoff Pol, eds., 235-240, Pudoc, Wageningen, The Netherlands.
22. Coulter, J. B., Soneda, S., and Ettinger, M. B. (1957). Anaerobic contact process for sewage disposal. *Sewage and Industrial Wastes*, **29**, 4, 469-477.
23. Dague, R. R. (1981). State of the art in anaerobic waste treatment. *19th Water Resources Design Conference*. Iowa State University, Ames, Iowa, February 4-5.
- 23a. Dague, R. R. (1967). Solids retention in anaerobic waste treatment systems. Doctoral Dissertation, University of Kansas, Lawrence, Kansas.
24. Dague, R. R., and Habben, C. E. (1992). Initial studies on the anaerobic sequencing batch reactor. *Proceedings of the 16th Conference of the International Association for Water Pollution Control and Research*, Washington, D.C., May 24-30.
25. Dague, R. R., Habben, C. E., and Pidaparti, S. R. (1992). Initial studies on the anaerobic sequencing batch reactor. *Wat. Sci. Tech.*, **26**, 9-11, 2429-2432.
26. Dague, R. R., McKinney, R. E., and Pfeffer, J. T. (1970). Solids retention in anaerobic waste treatment systems. *Journal Water Pollution Control Federation*, **42**, 2, Part 2, R29-R45.
27. Daniels, L. (1984). Biological methanogenesis: physiological and practical aspects. *Trends in Biotechnology*, **2**, 4, 98-108.

28. Defour, D., Derycke, D., Liessens, J., and Pipyn, P. (1994). Field experience with different systems for biomass accumulation in anaerobic reactor technology. *Proceedings of the Seventh Annual International Symposium on Anaerobic Digestion*, 240-249, January 23-27, Cape Town, South Africa.
29. de Zeeuw, W. J. (1988). Granular sludge in UASB-reactors. *Granular Anaerobic Sludge; Microbiology and Technology*, G. Lettinga, A. J. B. Zehnder, J. T. C. Grotenhuis, and L. W. Hulshoff Pol, eds., 132-145, Pudoc, Wageningen, The Netherlands.
30. Dolfig, J. (1985). Kinetics of methane formation by granular sludge at low substrate concentrations. *Appl. Microbiol. Biotechnol.*, **22**, 77-81.
31. Dolfig, J., Griffioen, A., van Neerven, A. R. W., and Zevenhuizen, L. P. T. M. (1985). Chemical and bacteriological composition of granular methanogenic sludge. *Can. J. Microbiol.*, **31**, 744-750.
- 31a. Droste, R. L., Guiot, S. R., Gorur, S. S., and Kennedy, K. J. (1987). Treatment of domestic strength wastewater with anaerobic hybrid reactors. *Water Pollution Research Journal of Canada*, **22**, 3, 474-489.
32. Dubourguier, H. C., Buisson, M. N., Tissier, J. P., Prensier, G., and Albagnac, G. (1988). Structural characteristics and metabolic activities of granular methanogenic sludge on a mixed defined substrate. *Granular Anaerobic Sludge; Microbiology and Technology*, G. Lettinga, A. J. B. Zehnder, J. T. C. Grotenhuis, and L. W. Hulshoff Pol, eds., 78-86, Pudoc, Wageningen, The Netherlands.
33. Dubourguier, H. C., Prensier, G., and Albagnac, G. (1988). Structure and microbial activities of granular anaerobic sludge. *Granular Anaerobic Sludge; Microbiology and Technology*, G. Lettinga, A. J. B. Zehnder, J. T. C. Grotenhuis, and L. W. Hulshoff Pol, eds., 18-33, Pudoc, Wageningen, The Netherlands.
34. Fang, H. H. P., Chui, H. K., and Li, Y. Y. (1994). Microbial structure and activity of UASB granules treating different wastewaters. *Proceedings of the Seventh Annual International Symposium on Anaerobic Digestion*, 80-89, January 23-27, Cape Town, South Africa.

35. Filip, Z., and Hattori, T. (1984). Utilization of substrates and transformation of solid substrata. *Microbial Adhesion and Aggregation*, K. C. Marshall, ed., 251-282, Springer-Verlag, Berlin, Germany.
36. Fletcher, M. (1984). Comparative physiology of attached and free-living bacteria. *Microbial Adhesion and Aggregation*, K. C. Marshall, ed., 223-232, Springer-Verlag, Berlin, Germany.
37. Forster, C. F. (1991). Anaerobic upflow sludge blanket reactors: aspects of their microbiology and their chemistry. *Journal of Biotechnology*, 17, 221-232.
38. Fox, P., Suidan, M. T., and Bandy, J. T. (1990). A comparison of media types in acetate fed expanded-bed anaerobic reactors. *Water Research*, 24, 7, 827-835.
39. Gerardi, M. H., and Berger, D. (1987). Floc formation in the activated sludge process. *Public Works*, October, 78-81.
40. Gorris, L. G. M., and van Deursen, J. M. A. (1988). Biofilm development in lab-scale methanogenic fluidized bed reactors. *Granular Anaerobic Sludge; Microbiology and Technology*, G. Lettinga, A. J. B. Zehnder, J. T. C. Grotenhuis, and L. W. Hulshoff Pol, eds., 87-95, Pudoc, Wageningen, The Netherlands.
41. Grotenhuis, J. T. C., Kissel, J. C., Plugge, C. M., Stams, A. J. M., and Zehnder, A. J. B. (1991). Role of substrate concentration in particle size distribution of methanogenic granular sludge in UASB reactors. *Wat. Res.*, 25, 1, 21-27.
42. Grotenhuis, J. T. C., Koornneef, E., and Plugge, C. M. (1987). Immobilization of anaerobic bacteria in methanogenic aggregates. *Granular Anaerobic Sludge; Microbiology and Technology*, G. Lettinga, A. J. B. Zehnder, J. T. C. Grotenhuis, and L. W. Hulshoff Pol, eds., 42-47, Pudoc, Wageningen, The Netherlands.
43. Grotenhuis, J. T. C., Van Lier, J. B., Pluffe, C. M., Stams, A. J. M., Zehnder, A. J. B. (1991). Effect of ethylene glycol-bis(B-aminoethyl ether)-N,N-tetraacetic acid (EGTA) on stability and activity of methanogenic granular sludge. *Appl. Microbiol. Biotechnol.*, 36, 109-114.

44. Guiot, S. R., Gorur, S. S., Bourque, D., and Samson, R. (1988). Metal effect on microbial aggregation during upflow anaerobic sludge bed-filter (UBF) reactor start-up. *Granular Anaerobic Sludge; Microbiology and Technology*, G. Lettinga, A. J. B. Zehnder, J. T. C. Grotenhuis, and L. W. Hulshoff Pol, eds., 187-194, Pudoc, Wageningen, The Netherlands.
45. Guiot, S. R., MacLeod, F. A., and Pauss, A. (1990). Thermodynamical and microbiological evidence of trophic microniches for propionate degradation in a methanogenic sludge-bed reactor. *Microbiology and Biochemistry of Strict Anaerobes Involved in Interspecies Hydrogen Transfer*, J.-P. Bélaïch, M. Bruschi, and J.-L. Garcia, eds., 173-184, Plenum Press, New York, NY.
46. Guiot, S. R., Rocheleau, S., Hawari, J., and Samson, R. (1992). Induction of granulation by sulphonated-lignin and calcium in an upflow anaerobic sludge bed reactor. *J. Chem. Tech. Biotechnol.*, **53**, 45-56.
- 46a. Guiot, S. R., and van den Berg, L. (1985). Performance of an upflow anaerobic reactor combining a sludge blanket and a filter treating sugar waste. *Biotechnology and Bioengineering*, **27**, 800-806.
47. Gujer, W., and Zehnder, A. J. B. (1983). Conversion processes in anaerobic digestion. *Water Science and Technology*, **15**, 127-167.
48. Habben, C. E. (1991). Initial studies on the anaerobic sequencing batch reactor. Masters Thesis, Iowa State University, Ames, Iowa.
49. Hack, P. J. F. M., Vellinga, S. H. J., and Habets, L. H. A. (1988). Growth of granular sludge in the biopaq IC-reactor. *Granular Anaerobic Sludge; Microbiology and Technology*, G. Lettinga, A. J. B. Zehnder, J. T. C. Grotenhuis, and L. W. Hulshoff Pol, eds., 211-215, Pudoc, Wageningen, The Netherlands.
50. Hammond, S. M., Lambert, P. A., and Rycroft, A. N. (1984). *The Bacterial Cell Surface*, Croom Helm Limited, London, England.
51. Hanaoka, T., Nakahata, S., Shouji, T., Sasaki, M., Maaskant, W., and Wildschut, L. (1994). Granular sludge formation from digested sewage sludge in a UASB reactor treating low strength brewery wastewater. *Proceedings of the Seventh Annual International Symposium on Anaerobic Digestion*, 518-527, January 23-27, Cape Town, South Africa.

52. Harper, S. R., and Pohland, F. G. (1990). Effects of elevated hydrogen partial pressures on anaerobic treatment of carbohydrate. *Microbiology and Biochemistry of Strict Anaerobes Involved in Interspecies Hydrogen Transfer*, J.-P. Bélaich, M. Bruschi, and J.-L. Garcia, eds., 387-390, Plenum Press, New York, NY.
53. Heinrichs, D. M., Poggi-Varaldo, H. M., and Oleszkiewicz, J. A. (1990). Effects of ammonia on anaerobic digestion of simple organic substrates. *Journal of Environmental Engineering*, **116**, 4, 698-710.
54. Henry, E., Ford, T., and Mitchell, R. (1990). Hydrogen production in anaerobic biofilms. *Microbiology and Biochemistry of Strict Anaerobes Involved in Interspecies Hydrogen Transfer*, J.-P. Bélaich, M. Bruschi, and J.-L. Garcia, eds., 391-394, Plenum Press, New York, NY.
55. Hentz, M., and Harremoes, P. (1983). Anaerobic treatment of wastewater in fixed film reactors--a literature review. *Water Science and Technology*, **15**, 8/9, 1-101.
56. Herum, B. A. H. (1993). The effect of applied vacuum on the performance of the anaerobic sequencing batch reactor. Masters Thesis, Iowa State University, Ames, Iowa.
57. Hirsch, P. (1984). Microcolony formation and consortia. *Microbial Adhesion and Aggregation*, K. C. Marshall, ed., 373-394, Springer-Verlag, Berlin, Germany.
58. Hoban, D. J., and van den Berg, L. (1979). Effect of iron on conversion of acetic acid to methane during methanogenic fermentations. *Journal of Applied Bacteriology*, **47**, 153-159.
59. Holland, K. T., Knapp, J. S., and Shoesmith, J. G. (1987). *Anaerobic Bacteria*, Blackie and Son Limited, Glasgow.
60. Hollopeter, J. A. (1993). Anaerobic sequencing batch reactor treatment of municipal landfill leachate at 35°C. Masters Thesis, Iowa State University, Ames, Iowa.
61. Hoppe, H.-G. (1984). Attachment of bacteria: advantage or disadvantage for survival in the aquatic environment. *Microbial Adhesion and Aggregation*, K. C. Marshall, ed., 283-302, Springer-Verlag, Berlin, Germany.

62. Houwen, F. P., Guangsheng, C., Folkers, G. E., v.d. Heuvel, W. M. J. G., and Dijkema, C. (1988). Pyruvate and fumarate conversion by a methanogenic propionate-oxidizing coculture. *Granular Anaerobic Sludge; Microbiology and Technology*, G. Lettinga, A. J. B. Zehnder, J. T. C. Grotenhuis, and L. W. Hulshoff Pol, eds., 62-70, Pudoc, Wageningen, The Netherlands.
63. Houwen, F. P., Plokker, J., Dijkema, C., and Stams, A. J. M. (1990). Syntrophic propionate oxidation. *Microbiology and Biochemistry of Strict Anaerobes Involved in Interspecies Hydrogen Transfer*, J.-P. Bélaich, M. Bruschi, and J.-L. Garcia, eds., 281-290, Plenum Press, New York, NY.
64. Howgrave-Graham, A. R., and Wallis, F. M. (1991). A bacterial population analysis of granular sludge from an anaerobic digester treating a maize-processing waste. *Bioresource Technology*, **37**, 149-156.
65. Hughes, M. N., and Poole, R. K. (1989). *Metals and Micro-organisms*, Chapman and Hall, London, England.
66. Hulshoff Pol, L. W. (1989). The phenomenon of granulation of anaerobic sludge. Doctoral Thesis, Wageningen Agricultural University, Wageningen, The Netherlands.
67. Hulshoff Pol, L. W., de Zeeuw, W. J., Velzeboer, C. T. M., and Lettinga, G. (1983). Granulation in UASB-reactors. *Wat. Sci. Tech.*, **15**, 291-304.
68. Hulshoff Pol, L. W., Heijnekamp, K., and Lettinga, G. (1988). The selection pressure as a driving force behind the granulation of anaerobic sludge. *Granular Anaerobic Sludge; Microbiology and Technology*, G. Lettinga, A. J. B. Zehnder, J. T. C. Grotenhuis, and L. W. Hulshoff Pol, eds., 153-161, Pudoc, Wageningen, The Netherlands.
69. Hulshoff Pol, L. W., and Lettinga, G. (1986). New technologies for anaerobic wastewater treatment. *Water Science and Technology*, **18**, 12, 41-53.
70. Huser, A., Wuhrmann, K., and Zehnder, A. J. B. (1982). *Methanothrix soehngenii* gen. nov. sp. nov., a new acetotrophic non-hydrogen-oxidizing methane bacterium. *Archives of Microbiology*, **132**, 1-9.

71. Iza, J., Garcia, P. A., Sanz, I., and Fdz-Polanco, F. (1988). Granulation results in anaerobic fluidized bed reactors. *Granular Anaerobic Sludge; Microbiology and Technology*, G. Lettinga, A. J. B. Zehnder, J. T. C. Grotenhuis, and L. W. Hulshoff Pol, eds., 195-202, Pudoc, Wageningen, The Netherlands.
 72. Jones, G. W. (1984). Adhesion to animal surfaces. *Microbial Adhesion and Aggregation*, K. C. Marshall, ed., 71-84, Springer-Verlag, Berlin, Germany.
 73. Kaiser, S. K. (1991). Initial studies of the anaerobic sequencing batch reactor at a thermophilic temperature. Masters Thesis, Iowa State University, Ames, Iowa.
 74. Kissel, J. C., Grotenhuis, J. T. C., and Zehnder, A. J. B. (1988). Modeling granule growth in a propionate-fed UASBR. *Granular Anaerobic Sludge; Microbiology and Technology*, G. Lettinga, A. J. B. Zehnder, J. T. C. Grotenhuis, and L. W. Hulshoff Pol, eds., 48-54, Pudoc, Wageningen, The Netherlands.
 75. Kjelleberg, S. (1984). Adhesion to inanimate surfaces. *Microbial Adhesion and Aggregation*, K. C. Marshall, ed., 51-70, Springer-Verlag, Berlin, Germany.
 76. Kobayashi, H. A., Conway de Macario, E., Williams, R. S., and Macario, A. J. L. (1988). Direct characterization of methanogens in two high-rate anaerobic biological reactors. *Applied and Environmental Microbiology*, **54**, 3, 693-698.
 77. Kosaric, N., Blaszczyk, R., Orphan, L., and Valladares, J. (1990). The characteristics of granules from upflow anaerobic sludge blanket reactors. *Wat. Res.*, **24**, 12, 1473-1477.
 78. Koster, I. W., and Lettinga, G. (1985). Application of the upflow anaerobic sludge bed (UASB) process for treatment of complex wastewaters at low temperatures. *Biotechnology and Bioengineering*, **27**, 1411-1417.
 79. Kudo, A., Kennedy, K., and Andras, E. (1991). Anaerobic (UASB) treatment of pulp (CTMP) wastewater and the toxicity on granules. *Water Science and Technology*, **23**, 1919-1928.
 80. Lauwers, A. M., Heinen, W., Gorris, L. G. M., and Van der Drift, C. (1990). Early stages in biofilm development in methanogenic fluidized-bed reactors. *Appl. Microbiol. Biotechnol.*, **33**, 352-358.
-

81. Lawrence, A. W., and McCarty, P. L. (1969). Kinetics of methane fermentation in anaerobic treatment. *Journal Water Pollution Control Federation*, **41**, 2, Part 2, R1-R17.
82. Leentvaar, J., and Rebhun, M. (1983). Strength of ferric hydroxide flocs. *Water Res.*, **17**, 8, 895-902.
83. Lettinga, G., and Hulshoff Pol, L. W. (1991). UASB-process design for various types of wastewaters. *Wat. Sci. Tech.*, **24**, 8, 87-107.
84. Lettinga, G., Hulshoff Pol, L. W., Koster, I. W., Wiegant, W. M., de Zeeuw, W. J., Rinzema, A., Grin, P. C., Roersma, R. E., and Hobma, S. W. (1984). High-rate anaerobic waste-water treatment using the UASB reactor under a wide range of temperature conditions. *Biotechnology and Genetic Engineering Reviews*, **2**, 253-283.
85. Lettinga, G., van Velsen, A. F. M., Hobma, S. W., de Zeeuw, W., and Klapwijk, A. (1980). Use of the upflow sludge blanket (USB) reactor for biological wastewater treatment, especially for anaerobic treatment. *Biotechnology and Bioengineering*, **22**, 699-734.
86. Lindley, N. D., Gros, E., Le Bloas, P., Cocaign, M., and Loubière, P. (1990). Carbon and energy flow during acetogenic metabolism of unicarbon and multicarbon substrates. *Microbiology and Biochemistry of Strict Anaerobes Involved in Interspecies Hydrogen Transfer*, J.-P. Bélaich, M. Bruschi, and J.-L. Garcia, eds., 213-224, Plenum Press, New York, NY.
87. Lu, J. (1993). A comparison of the methanogenic biological activity of flocculent and granular sludges. Masters Thesis, Iowa State University, Ames, Iowa.
88. Macario, A. J. L., and Conway de Macario, E. (1988). Quantitative immunologic analysis of the methanogenic flora of digesters reveals a considerable diversity. *Applied and Environmental Microbiology*, **54**, 1, 79-86.
89. MacLeod, F. A., Guiot, S. R., and Costerton, J. W. (1990). Layered structure of bacterial aggregates produced in an upflow anaerobic sludge bed and filter reactor. *Applied and Environmental Microbiology*, **56**, 6, 1598-1607.
90. Mah, R. A., Smith, M. R., and Baresi, L. (1978). Studies on acetate-fermenting strain *Methanosarcina*. *Applied and Environmental Microbiology*, **35**, 1174-1184.

91. Mah, R. A., Xun, L. Y., Boone, D. R., Ahring, B., Smith, P. H., and Wilkie, A. (1990). Methanogenesis from propionate in sludge and enrichment systems. *Microbiology and Biochemistry of Strict Anaerobes Involved in Interspecies Hydrogen Transfer*, J.-P. Bélaich, M. Bruschi, and J.-L. Garcia, eds., 99-114, Plenum Press, New York, NY.
92. Mahoney, E. M., Varangu, L. K., Cairns, W. L., Kosaric, N., and Murray, G. E. (1987). The effect of calcium on microbial aggregation during UASB reactor start-up. *Water Science and Technology*, **19**, 249-260.
93. McCarty, P. L. (1964). Anaerobic waste treatment fundamentals. Part one: chemistry and microbiology. *Public Works*, **95**, 9, 107-112.
94. McCarty, P. L. (1964). Anaerobic waste treatment fundamentals. Part two: environmental requirements and control. *Public Works*, **95**, 10, 123-126.
95. McCarty, P. L. (1964). Anaerobic waste treatment fundamentals. Part three: toxic materials and their control. *Public Works*, **95**, 11, 91-94.
96. McCarty, P. L. (1964). Anaerobic waste treatment fundamentals. Part four: process design. *Public Works*, **95**, 12, 95-99.
97. McFeters, G. A., Bazin, M. J., Bryers, J. D., Caldwell, D. E., Characklis, W. G., Lund, D. B., Mirelman, D., Mitchell, R., Schubert, R. H. W., Tanaka, T., and White, D. C. (1984). Biofilm development and its consequences. *Microbial Adhesion and Aggregation*, K. C. Marshall, ed., 109-124, Springer-Verlag, Berlin, Germany.
98. Metcalf and Eddy, Inc. (1991). *Wastewater Engineering: Treatment, Disposal, and Reuse; 3rd edition*, G. Tchobanoglous and F. L. Burton, editors, McGraw-Hill Publishing Company, New York, NY.
99. Meyer, V., and Oellermann, R. A. (1994). Special methanogenic activity test (SMA). *Proceedings of the Seventh Annual International Symposium on Anaerobic Digestion*, 70-73, January 23-27, Cape Town, South Africa.
100. Moosbrugger, R. E. (1994). Settleability assessment of granular biomass from upflow anaerobic sludge bed reactors. *Proceedings of the Seventh Annual International Symposium on Anaerobic Digestion*, 215-218, January 23-27, Cape Town, South Africa.

101. Morgan, J. W., Evison, L. M., and Forster, C. F. (1991). Changes to the microbial ecology in anaerobic digesters treating ice cream wastewater during start-up. *Wat. Res.*, **25**, 6, 639-653.
102. Morgan, J. W., Evison, L. M., and Forster, C. F. (1991). The internal architecture of anaerobic sludge granules. *J. Chem. Tech. Biotechnol.*, **50**, 211-226.
103. Morgan, J. W., Evison, L. M., and Forster, C. F. (1992). Upflow sludge blanket reactors: the effect of bio-supplements on performance and granulation. *J. Chem. Tech. Biotechnol.*, **51**, 243-255.
104. Morgan, J. W., Goodwin, J. A. S., Wase, D. A. J., and Forster, C. F. (1990). The effects of using various types of carbonaceous substrates on UASB granules and on reactor performance. *Biological Wastes*, **34**, 55-71.
105. Morrison, R. T., and Boyd, R. N. (1992). *Organic Chemistry, 6th edition*, Prentice Hall, Englewood Cliffs, NJ.
106. Murray, W. D., and van den Berg, L. (1981). Effects of nickel, cobalt, and molybdenum on performance of methanogenic fixed-film reactors. *Applied and Environmental Microbiology*, **42**, 502-505.
- 106a. Ndon, U. J., and Dague, R. R. (1994). Low temperature treatment of dilute wastewaters using the anaerobic sequencing batch reactor. *Proceedings of the 49th Purdue Industrial Waste Conference*, May 9-11, West Lafayette, IN.
107. Nozhevnikova, A. N., Bodnar, I. V., Slobodkin, A. I., and Sokolova, T. G. (1990). Hydrogen content in biogas as a state indicator of methanogenesis from wastes. *Microbiology and Biochemistry of Strict Anaerobes Involved in Interspecies Hydrogen Transfer*, J.-P. Bélaich, M. Bruschi, and J.-L. Garcia, eds., 423-426, Plenum Press, New York, NY.
108. Odom, J. M., and Singleton, R., Jr. (1993). *The Sulfate-Reducing Bacteria: Contemporary Perspectives*, Springer-Verlag New York, Inc., New York, NY.
109. Paris, J. M., Vicent, T., Balaguer, M. D., Cassu, C., Cairo, J., and Canals, J. (1988). Stability and control of UASB reactors treating potato-starch wastewater: comparison of laboratory and full-scale results. *Granular Anaerobic Sludge; Microbiology and Technology*, G. Lettinga, A. J. B. Zehnder, J. T. C. Grotenhuis, and L. W. Hulshoff Pol, eds., 179-186, Pudoc, Wageningen, The Netherlands.

- 109a. Parkin, G. F., Speece, R. E., Yang, C. H. J., and Kocher, W. M. (1983). Response of methane fermentation to industrial toxicants. *Journal Water Pollution Control Federation*, **55**, 1, 44-53.
110. Patel, G. B. (1984). Characterization and nutritional properties of *Methanothrix concilii* sp. nov., a mesophilic, acetoclastic methanogen. *Can. J. Microbiol.*, **30**, 1383-1396.
111. Pauss, A., Samson, R, and Guiot, S. (1990). Thermodynamic evidence of trophic microniches in methanogenic granular sludge-bed reactors. *Applied Microbiology and Biotechnology*, **33**, 88-92.
112. Peinemann, S., and Gottschalk, G. (1990). ATP-synthesis coupled to the terminal step of methanogenesis. *Microbiology and Biochemistry of Strict Anaerobes Involved in Interspecies Hydrogen Transfer*, J.-P. Bélaich, M. Bruschi, and J.-L. Garcia, eds., 521-526, Plenum Press, New York, NY.
113. Pereboom, J. H. F. (1994). Size distribution model for methanogenic granules from full scale UASB and IC reactors. *Proceedings of the Seventh Annual International Symposium on Anaerobic Digestion*, 487-496, January 23-27, Cape Town, South Africa.
114. Pereboom, J. H. F., and Vereijken, T. L. F. M. (1994). Methanogenic granule development in full scale internal circulation reactors. *Proceedings of the Seventh Annual International Symposium on Anaerobic Digestion*, January 23-27, Cape Town, South Africa.
115. Pfeffer, J. T., and White, J. E. (1964). The role of iron in anaerobic digestion. *Proceedings of the 19th Industrial Waste Conference*, Purdue University, West Lafayette, Indiana.
116. Pidaparti, S. (1991). Sequencing batch reactor treatment of swine waste at 35°C and 25°C. Masters Thesis, Iowa State University, Ames, Iowa.
117. Potekhina, J. (1990). The role of Fe(III) reduction in anaerobic processes. *Microbiology and Biochemistry of Strict Anaerobes Involved in Interspecies Hydrogen Transfer*, J.-P. Bélaich, M. Bruschi, and J.-L. Garcia, eds., 443-446, Plenum Press, New York, NY.

118. Prensier, G., Dubourguier, H. C., Thomas, I., Albagnac, G., and Buisson, M. N. (1988). Specific immunological probes for studying the bacterial associations in granules and biofilms. *Granular Anaerobic Sludge; Microbiology and Technology*, G. Lettinga, A. J. B. Zehnder, J. T. C. Grotenhuis, and L. W. Hulshoff Pol, eds., 55-61, Pudoc, Wageningen, The Netherlands.
119. Prensier, G., Roustan, J. L., Dubourguier, H. C., and Albagnac, G. (1988). Presence of viruses and other potential bacterial predators in granular methanogenic sludges. *Granular Anaerobic Sludge; Microbiology and Technology*, G. Lettinga, A. J. B. Zehnder, J. T. C. Grotenhuis, and L. W. Hulshoff Pol, eds., 96-101, Pudoc, Wageningen, The Netherlands.
120. Reis, M. A. M., Lemos, P. C., Almeida, J., and Carrondo, M. T. J. (1990). Effect of sulfide and reactor operational parameters on sulfate reducing bacteria. *Microbiology and Biochemistry of Strict Anaerobes Involved in Interspecies Hydrogen Transfer*, J.-P. Bélaich, M. Bruschi, and J.-L. Garcia, eds., 459-462, Plenum Press, New York, NY.
121. Rinzema, A., van Lier, J., and Lettinga, G. (1988). Sodium inhibition of acetoclastic methanogens in granular sludge from a UASB reactor. *Granular Anaerobic Sludge; Microbiology and Technology*, G. Lettinga, A. J. B. Zehnder, J. T. C. Grotenhuis, and L. W. Hulshoff Pol, eds., 216-222, Pudoc, Wageningen, The Netherlands.
122. Robb, I. D. (1984). Stereo-chemistry and function of polymers. *Microbial Adhesion and Aggregation*, K. C. Marshall, ed., 39-50, Springer-Verlag, Berlin, Germany.
123. Rose, A. H. (1984). Physiology of cell aggregation: flocculation by *Saccharomyces cerevisiae* as a model system. *Microbial Adhesion and Aggregation*, K. C. Marshall, ed., 323-336, Springer-Verlag, Berlin, Germany.
124. Ross, W. R. (1984). The phenomenon of sludge pelletisation in the anaerobic treatment of a maize processing waste. *Water SA*, **10**, 4, 197-204.
125. Rouvière, P. E., Kuhner, C. H., and Wolfe, R. S. (1990). Biochemistry of the methylcoenzyme M methylreductase system. *Microbiology and Biochemistry of Strict Anaerobes Involved in Interspecies Hydrogen Transfer*, J.-P. Bélaich, M. Bruschi, and J.-L. Garcia, eds., 259-268, Plenum Press, New York, NY.

126. Rudolfs, W., and Setter, L. R. (1931). After-effect of ferric chloride on sludge digestion. *Sewage Works Journal*, **3**, 3, 352-361.
127. Rutter, P. R., and Vincent, B. (1984). Physicochemical interactions of the substratum, microorganisms, and the fluid phase. *Microbial Adhesion and Aggregation*, K. C. Marshall, ed., 21-38, Springer-Verlag, Berlin, Germany.
128. Rutter, P. R., Dazzo, F. B., Freter, R., Gingell, D., Jones, G. W., Kjelleberg, S., Marshall, K. C., Mrozek, H., Rades-Rohkohl, E., Robb, I. D., Silverman, M., and Tylewska, S. (1984). Mechanisms of adhesion. *Microbial Adhesion and Aggregation*, K. C. Marshall, ed., 5-19, Springer-Verlag, Berlin, Germany.
129. Sam-Soon, P., Loewenthal, R. E., Dold, P. L., and Marais, G. (1987). Hypothesis for pelletisation in the upflow anaerobic sludge bed reactor. *Water SA*, **13**, 2, 69-80.
130. Sandford, P. A., and Laskin, A. (1977). *Extracellular Microbial Polysaccharides*, American Chemical Society, Washington, D. C.
131. Savage, D. C. (1984). Activities of microorganisms attached to living surfaces. *Microbial Adhesion and Aggregation*, K. C. Marshall, ed., 233-250, Springer-Verlag, Berlin, Germany.
132. Sayed, S., de Zeeuw, W., and Lettinga, G. (1984). Anaerobic treatment of slaughterhouse waste using a flocculant sludge UASB reactor. *Agricultural Wastes*, **11**, 197-226.
133. Sayed, S., van Campen, L., and Lettinga, G. (1987). Anaerobic treatment of slaughterhouse waste using a granular sludge UASB reactor. *Biological Wastes*, **21**, 11-28.
134. Schink, B., and Thauer, R. K. (1988). Energetics of syntrophic methane formation and the influence of aggregation. *Granular Anaerobic Sludge; Microbiology and Technology*, G. Lettinga, A. J. B. Zehnder, J. T. C. Grotenhuis, and L. W. Hulshoff Pol, eds., 5-17, Pudoc, Wageningen, The Netherlands.
135. Schmidt, J. E., and Ahring, B. K. (1991). Acetate and hydrogen metabolism in intact and disintegrated granules from an acetate-fed, 55°C, UASB reactor. *Applied Microbiol. Biotechnol.*, **35**, 681-685.

136. Schmit, C. G. (1992). Anaerobic sequencing batch reactor treatment of swine waste at 20°C. Masters Thesis, Iowa State University, Ames, Iowa.
137. Schwitzguébel, J. P., and Péringer, P. (1990). Anaerobic digestion of proteins, peptides and amino acids. *Microbiology and Biochemistry of Strict Anaerobes Involved in Interspecies Hydrogen Transfer*, J.-P. Bélaich, M. Bruschi, and J.-L. Garcia, eds., 471-472, Plenum Press, New York, NY.
- 137a. Seagram, E. A., Levine, A. D., and Dague, R. R. (1990). High pH effects in anaerobic treatment of liquid industrial byproducts. *Proceedings of the 45th Purdue Industrial Waste Conference*, May 8-10, West Lafayette, IN.
138. Setter, L. R. (1930). Effect of iron on the anaerobic decomposition of sewage solids. *Sewage Works Journal*, 2, 4, 504-520.
139. Sierra-Alvarez, R., Hulshoff Pol, L. W., and Lettinga, G. (1988). Start-up of a UASB reactor on a carbohydrate substrate. *Granular Anaerobic Sludge; Microbiology and Technology*, G. Lettinga, A. J. B. Zehnder, J. T. C. Grotenhuis, and L. W. Hulshoff Pol, eds., 223-228, Pudoc, Wageningen, The Netherlands.
140. Silverman, M., Belas, R., and Simon, M. (1984). Genetic control of bacterial adhesion. *Microbial Adhesion and Aggregation*, K. C. Marshall, ed., 95-108, Springer-Verlag, Berlin, Germany.
141. Sparling, R., and Gottschalk, G. (1990). Molecular hydrogen and energy conservation in methanogenic and acetogenic bacteria. *Microbiology and Biochemistry of Strict Anaerobes Involved in Interspecies Hydrogen Transfer*, J.-P. Bélaich, M. Bruschi, and J.-L. Garcia, eds., 3-10, Plenum Press, New York, NY.
142. Speece, R. E., and McCarty, P. L. (1964). Nutrient requirements and biological solids accumulation in anaerobic digestion. *Advances in Water Pollution Research*, 2, 305-322.
143. Stams, A. J. M., and Zehnder, A. J. B. (1990). Ecological impact of syntrophic alcohol and fatty acid oxidation. *Microbiology and Biochemistry of Strict Anaerobes Involved in Interspecies Hydrogen Transfer*, J.-P. Bélaich, M. Bruschi, and J.-L. Garcia, eds., 87-98, Plenum Press, New York, NY.
144. *Standard Methods for the Examination of Water and Wastewater*. 14th Edition, American Public Health Association, Washington, D.C., 1975.

145. Sung, S., and Dague, R. R. (1992). Fundamental principles of the anaerobic sequencing batch reactor process. *Proceedings of the 47th Purdue Industrial Waste Conference*, May 11-13, West Lafayette, IN.
 146. Switzenbaum, M. S., Robins, J. P., and Hickey, R. F. (1988). Immobilization of anaerobic biomass. *Granular Anaerobic Sludge; Microbiology and Technology*, G. Lettinga, A. J. B. Zehnder, J. T. C. Grotenhuis, and L. W. Hulshoff Pol, eds., 115-131, Pudoc, Wageningen, The Netherlands.
 147. Szewzyk, U., and Schink, B. (1988). Colony formation and life cycles of anaerobic bacteria attached to surfaces. *Granular Anaerobic Sludge; Microbiology and Technology*, G. Lettinga, A. J. B. Zehnder, J. T. C. Grotenhuis, and L. W. Hulshoff Pol, eds., 102-104, Pudoc, Wageningen, The Netherlands.
 148. Takashima, M., and Speece, R. E. (1989). Mineral nutrient requirements for high-rate methane formation of acetate at low SRT. *Journal Water Pollution Control Federation*, **61**, 11/12, 1645-1651.
 149. Takashima, M., and Speece, R. E. (1990). Mineral requirements for methane fermentation. *Critical Reviews in Environmental Control*, **19**, 5, 465-479.
 150. Thaveesri, J., Boucneau, G., Gernaey, K., Kaonga, B., and Verstraete, W. (1994). Organic and ammonium nitrogen in relation to granular sludge growth. *Proceedings of the Seventh Annual International Symposium on Anaerobic Digestion*, 54-63, January 23-27, Cape Town, South Africa.
 151. Thiele, J. H., Chartrain, M., and Zeikus, J. G. (1988). Control of interspecies electron flow during anaerobic digestion: role of floc formation in syntrophic methanogenesis. *Applied Environmental Microbiology*, **54**, 1, 10-19.
 152. Tilche, A., and Yang, X. (1988). Light and scanning electron microscope observations on the granular biomass of experimental SBAF and HABR reactors. *Granular Anaerobic Sludge; Microbiology and Technology*, G. Lettinga, A. J. B. Zehnder, J. T. C. Grotenhuis, and L. W. Hulshoff Pol, eds., 170-178, Pudoc, Wageningen, The Netherlands.
 153. Tormanen, T. W. (1993). Anaerobic sequencing batch reactor treatment of a high-sodium starch waste at 35°C. Masters Thesis, Iowa State University, Ames, Iowa.
-

154. Ueki, K., and Ueki, A. (1990). Relationship between methanogenesis and sulfate reduction in anaerobic digestion of municipal sewage sludge. *Microbiology and Biochemistry of Strict Anaerobes Involved in Interspecies Hydrogen Transfer*, J.-P. Bélaich, M. Bruschi, and J.-L. Garcia, eds., 485-488, Plenum Press, New York, NY.
155. Vallom, J. K., and McLoughlin, A. J. (1984). Lysis as a factor in sludge flocculation. *Water Res.*, **18**, 12, 1523-1528.
156. van der Hoek, J. P. (1988). Granulation in denitrifying sludge. *Granular Anaerobic Sludge; Microbiology and Technology*, G. Lettinga, A. J. B. Zehnder, J. T. C. Grotenhuis, and L. W. Hulshoff Pol, eds., 203-210, Pudoc, Wageningen, The Netherlands.
157. Van Lier, J. B., Lettinga, G., Macario, A. J. L., and Conway de Macario, E. (1992). Permanent increase of the process temperature of mesophilic upflow anaerobic sludge bed (UASB) reactors to 46, 55, 64, and 75°C. *Proceedings of the 47th Purdue Industrial Waste Conference*, May 11-13, West Lafayette, IN.
158. Visser, F. A., Van Lier, J. B., Macario, A. J. L., Conway de Macario, E. (1991). Diversity and population dynamics of methanogenic bacteria in a granular consortium. *Applied and Environmental Microbiology*, **57**, 6, 1728-1734.
159. Wang, Y-T., Suidan, M. T., and Rittmann, B. E. (1985). Performance of expanded-bed methanogenic reactor. *Journal of Environmental Engineering, American Society of Civil Engineers*, **111**, 4, 460-471.
160. Wentzel, M. C., Moosbrugger, R. E., Sam-Soon, P. A. L. N. S., Ekama, G. A., and Marais, G. v. R. (1994). Tentative guidelines for waste selection, process design, operation and control of upflow anaerobic sludge bed reactors. *Proceedings of the Seventh Annual International Symposium on Anaerobic Digestion*, 32-41, January 23-27, Cape Town, South Africa.
161. White, D. C. (1984). Chemical characterization of films. *Microbial Adhesion and Aggregation*, K. C. Marshall, ed., 159-176, Springer-Verlag, Berlin, Germany.
162. Wiegant, W. M. (1988). The 'spaghetti theory' on anaerobic sludge formation, or the inevitability of granulation. *Granular Anaerobic Sludge; Microbiology and Technology*, G. Lettinga, A. J. B. Zehnder, J. T. C. Grotenhuis, and L. W. Hulshoff Pol, eds., 146-152, Pudoc, Wageningen, The Netherlands.

163. Wijnbenga, D. J., and Bos, H. T. P. (1988). Physical and biological factors influencing the growth of anaerobic granular sludge. *Granular Anaerobic Sludge; Microbiology and Technology*, G. Lettinga, A. J. B. Zehnder, J. T. C. Grotenhuis, and L. W. Hulshoff Pol, eds., 229-234, Pudoc, Wageningen, The Netherlands.
164. Winther-Nielsen, M., and Ahring, B. K. (1990). Thermophilic degradation of butyrate, propionate and acetate in granular sludge. *Microbiology and Biochemistry of Strict Anaerobes Involved in Interspecies Hydrogen Transfer*, J.-P. Bélaich, M. Bruschi, and J.-L. Garcia, eds., 493-496, Plenum Press, New York, NY.
165. Wu, W., Hu, J., Gu, X., Zhao, Y., Zhang, H., and Gu, H. (1987). Cultivation of an anaerobic granular sludge in UASB reactors with aerobic activated sludge as seed. *Water Res.*, **21**, 789-799.
166. Yang, G., and Anderson, G. K. (1993). Effects of wastewater composition on stability of UASB. *Journal of Environmental Engineering-ASCE*, **119**, 5, 958-975.
167. Yoda, M., Kitagawa, M., and Miyaji, Y. (1989). Granular sludge formation in the anaerobic expanded microcarrier bed process. *Wat. Sci. Tech.*, **21**, 109-120.
- 167a. Young, J. C., and McCarty, P. L. (1969). The anaerobic filter for waste treatment. *Journal Water Pollution Control Federation*, **41**, 5, part 2, R160-R173.
168. Zehnder, A. J. B. (1988). *Biology of Anaerobic Microorganisms*, John Wiley and Sons, New York, NY.
169. Zeikus, J. G., and Bowen, V. G. (1975). Comparative ultrastructure of methanogenic bacteria. *Can. J. Microbiol.*, **21**, 121-129.
170. Zeikus, J. G., Kerby, R., and Krzycki, J. A. (1985). Single-carbon chemistry of acetogenic and methanogenic bacteria. *Science*, **227**, March 8, 1167-1173.
171. Zoutberg, G. R., Mulder, R., Teixeira de Mattos, M. J., and Neijssel, O. M. (1988). Aggregate formation in anaerobic gaslift reactors. *Granular Anaerobic Sludge; Microbiology and Technology*, G. Lettinga, A. J. B. Zehnder, J. T. C. Grotenhuis, and L. W. Hulshoff Pol, eds., 34-41, Pudoc, Wageningen, The Netherlands.
172. Zubay, G. (1993). *Biochemistry, 3rd edition*, Wm. C. Brown Publisher, Dubuque, IA.

APPENDIX: EXPERIMENTAL DATA TABLES

Table 30. COD data for the sucrose control test.

Date	Time from Start-Up (days)	HRT (days)	Influent COD (mg/L)	COD Load (g/L/day)	Effluent TCOD (mg/L)	TCOD Removal (%)	Effluent SCOD (g/L/day)	SCOD Removal (%)
09-Aug-93	13	2.0	4,000	2.0	2,743	31.4	2,613	34.7
17-Aug-93	21	2.0	4,000	2.0	3,233	19.2	2,968	25.8
24-Aug-93	28	2.0	4,000	2.0	2,630	34.3	2,324	41.9
01-Sep-93	36	2.0	4,000	2.0	2,719	32.0	2,430	39.3
08-Sep-93	43	1.5	3,000	2.0	2,082	30.6	1,632	45.6
28-Sep-93	63	1.0	2,000	2.0	1,827	8.7	763	61.9
06-Oct-93	71	1.0	2,000	2.0	1,292	35.4	581	71.0
15-Oct-93	80	1.0	2,500	2.5	1,458	41.7	1,060	57.6
03-Nov-93	99	1.0	2,500	2.5	870	65.2	570	77.2
09-Nov-93	105	1.0	3,500	3.5	1,610	54.0	596	83.0
18-Nov-93	114	1.0	5,000	5.0			852	83.0
22-Nov-93	118	1.0	5,000	5.0	1,465	70.7	687	86.3
02-Dec-93	128	1.0	7,000	7.0	2,736	60.9	1,284	81.7
07-Dec-93	133	1.0	7,000	7.0	2,125	69.6	535	92.4
17-Dec-93	143	1.0	9,000	9.0	2,211	75.4	308	96.6
06-Jan-94	163	1.0	12,000	12.0	5,000	58.3	3,455	71.2
14-Jan-94	171	1.0	6,000	6.0	1,608	73.2	655	89.1

Table 31. Biogas data for the sucrose control test.

Date	Time (days)	HRT (days)	Nominal COD Load (g/L/day)	Methane (% of total)	Std. Methane Production (L/L/day)
26-Jul-93	0	2.0	0.5		
27-Jul-93	1	2.0	0.5	63.00	0.00
28-Jul-93	2	2.0	1.0	63.00	0.00
29-Jul-93	3	2.0	1.0	63.00	0.00
30-Jul-93	4	2.0	1.0	63.00	0.01
31-Jul-93	5	2.0	1.0	63.00	0.02
01-Aug-93	6	2.0	1.0	63.00	0.00
02-Aug-93	7	2.0	1.0	63.00	0.00
03-Aug-93	8	2.0	1.0	63.16	0.02
04-Aug-93	9	2.0	1.0	63.32	0.01
05-Aug-93	10	2.0	1.0	63.48	0.02
06-Aug-93	11	2.0	2.0	63.64	0.01
07-Aug-93	12	2.0	2.0	59.82	0.08
08-Aug-93	13	2.0	2.0	56.00	0.09
09-Aug-93	14	2.0	2.0	52.19	0.08
10-Aug-93	15	2.0	2.0	48.37	0.06
11-Aug-93	16	2.0	2.0	44.55	0.06
12-Aug-93	17	2.0	2.0	43.99	0.08
13-Aug-93	18	2.0	2.0	43.44	0.07
14-Aug-93	19	2.0	2.0	42.88	0.08
15-Aug-93	20	2.0	2.0	42.32	0.08
16-Aug-93	21	2.0	2.0	41.77	0.08
17-Aug-93	22	2.0	2.0	41.21	0.06
18-Aug-93	23	2.0	2.0	40.65	0.06
19-Aug-93	24	2.0	2.0	40.10	0.08
20-Aug-93	25	2.0	2.0	39.54	0.04
21-Aug-93	26	2.0	2.0	38.98	0.06
22-Aug-93	27	2.0	2.0	38.43	0.04
23-Aug-93	28	2.0	2.0	37.87	0.02
24-Aug-93	29	2.0	2.0	45.13	0.01
25-Aug-93	30	4.0	2.0	52.39	0.05
26-Aug-93	31	2.0	2.0	59.65	0.10
27-Aug-93	32	2.0	2.0	60.13	0.03
28-Aug-93	33	2.0	2.0	60.37	0.13
29-Aug-93	34	2.0	2.0	60.62	0.08
30-Aug-93	35	2.0	2.0	60.86	0.08
31-Aug-93	36	2.0	2.0	61.10	0.03
01-Sep-93	37	2.0	2.0	60.25	0.08
02-Sep-93	38	2.0	2.0	59.41	0.12
03-Sep-93	39	2.0	2.0	58.56	0.08
04-Sep-93	40	1.5	2.0	57.71	0.13
05-Sep-93	41	1.5	2.0	56.87	0.09
06-Sep-93	42	1.5	2.0	56.02	0.07
07-Sep-93	43	1.5	2.0	55.17	0.11
08-Sep-93	44	1.5	2.0	54.33	0.12

Table 31. (continued).

Date	Time (days)	HRT (days)	Nominal COD Load (g/L/day)	Methane (% of total)	Std. Methane Production (L/L/day)
09-Sep-93	45	1.5	2.0	53.48	0.08
10-Sep-93	46	1.5	2.0	52.97	0.05
11-Sep-93	47	1.5	2.0	52.47	0.03
12-Sep-93	48	1.5	2.0	51.96	0.07
13-Sep-93	49	1.5	2.0	51.45	0.12
14-Sep-93	50	1.5	2.0	50.95	0.05
15-Sep-93	51	1.0	2.0	50.44	0.08
16-Sep-93	52	1.0	2.0	51.62	0.06
17-Sep-93	53	1.0	2.0	52.80	0.09
18-Sep-93	54	1.0	2.0	53.98	0.13
19-Sep-93	55	1.0	2.0	55.16	0.12
20-Sep-93	56	1.0	2.0	56.34	0.18
21-Sep-93	57	1.0	2.0	57.52	0.15
22-Sep-93	58	1.0	2.0	58.70	0.14
23-Sep-93	59	1.0	2.0	59.88	0.16
24-Sep-93	60	1.0	2.0	61.06	0.17
25-Sep-93	61	1.0	2.0	62.24	0.20
26-Sep-93	62	1.0	2.0	63.42	0.19
27-Sep-93	63	1.0	2.0	64.60	0.23
28-Sep-93	64	1.0	2.0	65.78	0.20
29-Sep-93	65	1.0	2.0	70.85	0.28
30-Sep-93	66	1.0	2.0	75.92	0.33
01-Oct-93	67	1.0	2.0	74.50	0.33
02-Oct-93	68	1.0	2.0	73.08	0.29
03-Oct-93	69	1.0	2.0	71.66	0.37
04-Oct-93	70	1.0	2.0	70.24	0.28
05-Oct-93	71	1.0	2.0	68.82	0.21
06-Oct-93	72	1.0	2.0	69.29	0.22
07-Oct-93	73	1.0	2.0	69.76	0.25
08-Oct-93	74	1.0	2.5	70.23	0.38
09-Oct-93	75	1.0	2.5	70.70	0.45
10-Oct-93	76	1.0	2.5	71.17	0.29
11-Oct-93	77	1.0	2.5	71.64	0.38
12-Oct-93	78	1.0	2.5	72.11	0.33
13-Oct-93	79	1.0	2.5	72.58	0.39
14-Oct-93	80	1.0	2.5	71.73	0.42
15-Oct-93	81	1.0	2.5	70.88	0.48
16-Oct-93	82	1.0	2.5	70.03	0.43
17-Oct-93	83	1.0	2.5	69.18	0.37
18-Oct-93	84	1.0	2.5	68.33	0.41
19-Oct-93	85	1.0	2.5	68.51	0.45
20-Oct-93	86	1.0	2.5	68.69	0.41
21-Oct-93	87	1.0	2.5	68.87	0.43
22-Oct-93	88	1.0	2.5	69.05	0.52
23-Oct-93	89	1.0	2.5	69.23	0.11

Table 31. (continued).

Date	Time (days)	HRT (days)	Nominal COD Load (g/L/day)	Methane (% of total)	Std. Methane Production (L/L/day)
24-Oct-93	90	1.0	2.5	69.41	0.26
25-Oct-93	91	1.0	2.5	69.59	0.22
26-Oct-93	92	1.0	2.5	69.77	0.18
27-Oct-93	93	1.0	2.5	69.95	0.34
28-Oct-93	94	1.0	2.5	68.35	0.42
29-Oct-93	95	1.0	2.5	66.76	0.40
30-Oct-93	96	1.0	2.5	65.16	0.34
31-Oct-93	97	1.0	2.5	63.56	0.30
01-Nov-93	98	1.0	2.5	61.96	0.32
02-Nov-93	99	1.0	2.5	60.37	0.34
03-Nov-93	100	1.0	2.5	58.77	0.32
04-Nov-93	101	1.0	3.5	75.04	0.38
05-Nov-93	102	1.0	3.5	73.02	0.61
06-Nov-93	103	1.0	3.5	71.00	0.67
07-Nov-93	104	1.0	3.5	68.99	0.64
08-Nov-93	105	1.0	3.5	66.97	0.56
09-Nov-93	106	1.0	3.5	64.95	0.65
10-Nov-93	107	1.0	3.5	62.93	0.73
11-Nov-93	108	1.0	5.0	62.60	0.69
12-Nov-93	109	1.0	5.0	62.26	0.77
13-Nov-93	110	1.0	5.0	61.93	0.96
14-Nov-93	111	1.0	5.0	61.59	0.79
15-Nov-93	112	1.0	5.0	61.26	0.94
16-Nov-93	113	1.0	5.0	60.92	0.86
17-Nov-93	114	1.0	5.0	59.10	0.92
18-Nov-93	115	1.0	5.0	57.27	0.78
19-Nov-93	116	1.0	5.0	57.85	0.87
20-Nov-93	117	1.0	5.0	58.42	0.92
21-Nov-93	118	1.0	5.0	59.00	0.95
22-Nov-93	119	1.0	5.0	59.57	1.00
23-Nov-93	120	1.0	5.0	60.15	0.96
24-Nov-93	121	1.0	7.0	59.46	1.13
25-Nov-93	122	1.0	7.0	58.77	1.24
26-Nov-93	123	1.0	7.0	58.08	1.12
27-Nov-93	124	1.0	7.0	57.38	1.29
28-Nov-93	125	1.0	7.0	56.69	1.51
29-Nov-93	126	1.0	7.0	56.00	1.34
30-Nov-93	127	1.0	7.0	55.99	1.41
01-Dec-93	128	1.0	7.0	55.98	1.34
02-Dec-93	129	1.0	7.0	55.97	1.65
03-Dec-93	130	1.0	7.0	55.96	1.43
04-Dec-93	131	1.0	7.0	55.96	1.55
05-Dec-93	132	1.0	7.0	55.95	1.55
06-Dec-93	133	1.0	7.0	55.94	1.61
07-Dec-93	134	1.0	7.0	55.93	1.57

Table 31. (continued).

Date	Time (days)	HRT (days)	Nominal COD Load (g/L/day)	Methane (% of total)	Std. Methane Production (L/L/day)
08-Dec-93	135	1.0	9.0	55.92	1.81
09-Dec-93	136	1.0	9.0	56.11	2.13
10-Dec-93	137	1.0	9.0	56.30	2.17
11-Dec-93	138	1.0	9.0	56.49	2.20
12-Dec-93	139	1.0	9.0	56.68	2.20
13-Dec-93	140	1.0	9.0	56.87	2.21
14-Dec-93	141	1.0	9.0	57.06	2.21
15-Dec-93	142	1.0	9.0	57.25	2.33
16-Dec-93	143	1.0	9.0	57.43	2.30
17-Dec-93	144	1.0	9.0	57.62	2.36
18-Dec-93	145	1.0	9.0	57.81	2.14
19-Dec-93	146	1.0	12.0	58.00	2.81
20-Dec-93	147	1.0	12.0	58.19	3.01
21-Dec-93	148	1.0	12.0	58.38	3.19
22-Dec-93	149	1.0	12.0	58.57	3.04
23-Dec-93	150	2.0	12.0	58.76	3.12
24-Dec-93	151	2.0	12.0	58.38	3.10
25-Dec-93	152	2.0	12.0	58.00	3.31
26-Dec-93	153	2.0	12.0	57.62	3.34
27-Dec-93	154	2.0	12.0	57.25	3.17
28-Dec-93	155	2.0	12.0	56.87	3.32
29-Dec-93	156	2.0	12.0	56.49	3.35
30-Dec-93	157	2.0	12.0	56.11	3.13
31-Dec-93	158	2.0	12.0	55.73	3.55
01-Jan-94	159	2.0	12.0	55.35	3.28
02-Jan-94	160	1.0	12.0	54.97	2.45
03-Jan-94	161	1.0	12.0	54.59	2.74
04-Jan-94	162	1.0	12.0	54.22	2.46
05-Jan-94	163	1.0	12.0	53.84	1.88
06-Jan-94	164	1.0	12.0	53.46	1.89
07-Jan-94	165	1.0	9.0	53.08	1.77
08-Jan-94	166	1.0	9.0	53.08	1.33
09-Jan-94	167	1.0	9.0	53.08	1.23
10-Jan-94	168	1.0	6.0	53.08	1.01
11-Jan-94	169	1.0	6.0	53.08	0.98
12-Jan-94	170	1.0	6.0	53.08	0.85
13-Jan-94	171	1.0	6.0	53.08	0.93
14-Jan-94	172	1.0	6.0	53.08	0.96

Table 32. Volatile acids data for the sucrose control test.

Date	Time from Start (days)	COD Load (g/L/day)	Volatile Acids (mg/L as acetic)
01-Sep-93	37	2.0	1,877
08-Sep-93	44	2.0	1,294
28-Sep-93	64	2.0	471
06-Oct-93	72	2.0	360
09-Nov-93	106	3.5	454
22-Nov-93	119	5.0	557
02-Dec-93	129	7.0	951
07-Dec-93	134	7.0	274
17-Dec-93	144	9.0	86
06-Jan-94	164	12.0	2,529
14-Jan-94	172	6.0	385

Table 33. Particle size analysis for the sucrose control test.

Date	Time from Start-up (days)	COD Load (g/L/day)	Average Diameter (arithmetic, μm)	Average Diameter (geometric, μm)
28-Jul-93	2	1.0	16	89
26-Aug-93	31	2.0	46	200
17-Sep-93	53	2.0	28	128
26-Oct-93	92	2.0	51	292
22-Nov-93	119	5.0	99	480
07-Dec-93	134	7.0	281	2,104
06-Jan-94	164	12.0	110	513

Table 34. Alkalinity and pH data for the sucrose control test.

Date	Time (days)	COD Load (g/L/day)	Alkalinity (mg/L as CaCO ₃)	pH (units)
05-Aug-93	9	1.0	1,500	7.00
23-Aug-93	27	2.0	1,520	6.43
25-Aug-93	29	2.0	1,420	6.96
01-Sep-93	36	2.0	1,450	6.68
08-Sep-93	43	2.0	1,490	6.64
14-Sep-93	49	2.0	1,560	6.86
20-Sep-93	55	2.0	1,540	6.97
27-Sep-93	62	2.0	1,430	6.85
29-Sep-93	64	2.0	1,320	6.90
04-Oct-93	69	2.0	1,350	6.94
07-Oct-93	72	2.0	1,390	7.01
11-Oct-93	76	2.0	1,400	6.38
13-Oct-93	78	2.0	1,420	6.92
03-Nov-93	99	2.5	1,500	6.80
04-Nov-93	100	2.5	1,460	7.08
09-Nov-93	105	3.5	1,400	6.77
15-Nov-93	111	5.0	1,460	6.83
18-Nov-93	114	5.0	1,510	6.73
21-Nov-93	117	5.0	1,590	6.70
29-Nov-93	125	7.0	1,560	6.72
02-Dec-93	128	7.0	1,620	6.77
14-Dec-93	140	9.0	1,670	6.88
03-Jan-94	160	12.0	1,750	7.12
06-Jan-94	163	12.0	1,800	6.68
07-Jan-94	164	9.0	1,820	6.70
11-Jan-94	168	6.0	1,790	6.80
14-Jan-94	171	6.0	1,900	6.91

Table 35. Solids data for the sucrose control test.

Date	Time (days)	COD Load (g/L/day)	HRT (days)	MLSS (mg/L)	MLVSS (% of MLSS)	Effluent TSS (mg/L)	Effluent VSS (% of TSS)	SRT (days)
28-Jul-93	1	0.5	2.0	40,420	42.5			
09-Aug-93	13	2.0	2.0	15,560	50.4	485	74.9	43.2
17-Aug-93	21	2.0	2.0	16,720	57.4	780	70.3	35.0
24-Aug-93	28	2.0	2.0	14,620	61.1	1,040	81.2	21.2
01-Sep-93	36	2.0	2.0	13,130	63.6	565	80.6	36.7
08-Sep-93	43	2.0	1.5	11,110	66.1	663	72.8	22.8
17-Sep-93	52	2.0	1.0	9,330	70.8			
23-Sep-93	58	2.0	1.0	8,590	70.5	1,055	69.2	8.3
01-Oct-93	66	2.0	1.0			508	74.9	
06-Oct-93	71	2.0	1.0	7,270	72.3	1,255	70.5	5.9
11-Oct-93	76	2.5	1.0			435	73.6	
13-Oct-93	78	2.5	1.0			873	74.2	
15-Oct-93	80	2.5	1.0	6,530	75.8	613	77.1	10.5
25-Oct-93	90	2.5	1.0	3,940	82.0			
03-Nov-93	99	2.5	1.0	6,080	84.9	465	63.2	17.6
09-Nov-93	105	3.5	1.0	7,360	86.4	1,095	85.8	6.8
15-Nov-93	111	5.0	1.0	6,110	85.9	1,435	87.3	4.2
22-Nov-93	118	5.0	1.0	7,600	85.7	805	82.3	9.8
02-Dec-93	128	7.0	1.0	10,840	88.2	1,463	85.8	7.6
07-Dec-93	133	7.0	1.0	11,020	88.2	1,790	85.8	6.3
17-Dec-93	143	9.0	1.0	15,060	89.5	1,988	83.8	8.1
06-Jan-94	163	12.0	1.0	17,770	90.1	3,907	87.9	4.7
14-Jan-94	171	6.0	1.0	13,550	88.7	955	84.0	15.0

Table 36. COD data for the sucrose+PAC test.

Date	Time from		Influent	COD	Effluent	TCOD	Effluent	SCOD
	Start-Up	HRT	COD	Load	TCOD	Removal	SCOD	Removal
	(days)	(days)	(mg/L)	(g/L/day)	(mg/L)	(%)	(g/L/day)	(%)
26-Jan-93	10	2.00	2,000	1.0	794	60.3	549	72.6
01-Feb-93	16	2.00	2,000	1.0	613	69.4	545	72.8
09-Feb-93	24	2.00	2,000	1.0	585	70.8	516	74.2
20-Feb-93	35	4.00	8,000	2.0	1,844	77.0	1,145	85.7
26-Feb-93	41	2.00	4,000	2.0	1,196	70.1	606	84.9
05-Mar-93	48	1.00	2,000	2.0	618	69.1	184	90.8
09-Mar-93	52	1.00	2,000	2.0	650	67.5	182	90.9
19-Mar-93	62	1.00	2,500	2.5	839	66.4	513	79.5
27-Mar-93	70	1.00	3,000	3.0	1,462	51.3	936	68.8
05-Apr-93	79	1.00	3,000	3.0	1,343	55.2	865	71.2
19-Apr-93	93	1.00	4,000	4.0	2,022	49.5	1,187	70.3
28-Apr-93	102	1.00	4,000	4.0	1,804	54.9	1,208	69.8
05-May-93	109	0.75	3,000	4.0	1,549	48.4	885	70.5
11-May-93	115	0.75	4,000	5.3	2,250	43.8	1,418	64.6
19-May-93	123	0.75	4,000	5.3	1,130	71.8	451	88.7
27-May-93	131	0.75	5,500	7.3	1,174	78.7	380	93.1
02-Jun-93	137	0.75	6,750	9.0	1,362	79.8	184	97.3
14-Jun-93	149	0.75	8,250	11.0	2,280	72.4	240	97.1
21-Jun-93	156	0.75	10,500	14.0	3,129	70.2	263	97.5
30-Jun-93	165	0.75	10,500	14.0	2,036	80.6	401	96.2
15-Jul-93	180	1.00	3,600	3.6	4,769	0.0	3,600	0.0
28-Jul-93	193	2.00	3,538	1.8	1,905	46.2	1,595	54.9
09-Aug-93	205	1.00	3,500	3.5	1,783	49.1	968	72.3

Table 36. (continued).

Date	Time from		Influent	COD	Effluent	TCOD	Effluent	SCOD
	Start-Up	HRT	COD	Load	TCOD	Removal	SCOD	Removal
	(days)	(days)	(mg/L)	(g/L/day)	(mg/L)	(%)	(g/L/day)	(%)
17-Aug-93	213	1.00	3,500	3.5	1,151	67.1	417	88.1
24-Aug-93	220	1.00	5,000	5.0	917	81.7	352	93.0
01-Sep-93	228	1.00	7,000	7.0	1,025	85.4	236	96.6
08-Sep-93	235	1.00	9,000	9.0	2,330	74.1	528	94.1
28-Sep-93	255	1.00	12,000	12.0	5,193	56.7	2,958	75.4
06-Oct-93	263	1.00	9,000	9.0	4,349	51.7	3,165	64.8
15-Oct-93	272	1.00	7,000	7.0	2,695	61.5	1,370	80.4

Table 37. Biogas data for the sucrose+ PAC test.

Date	Day	HRT (days)	Nominal COD Load (g/L/day)	Methane (% of total)	Std. Methane Production (L/L/day)
16-Jan-93	0	2.00	0.5		
17-Jan-93	1	2.00	0.5	66.36	0.03
18-Jan-93	2	2.00	0.5	66.36	0.02
19-Jan-93	3	2.00	0.5	66.36	0.05
20-Jan-93	4	2.00	0.5	66.36	0.05
21-Jan-93	5	2.00	1.0	66.36	0.07
22-Jan-93	6	2.00	1.0	66.36	0.11
23-Jan-93	7	2.00	1.0	66.36	0.15
24-Jan-93	8	2.00	1.0	64.43	0.08
25-Jan-93	9	2.00	1.0	62.49	0.16
26-Jan-93	10	2.00	1.0	62.72	0.14
27-Jan-93	11	2.00	1.0	62.95	0.08
28-Jan-93	12	2.00	1.0	63.18	0.06
29-Jan-93	13	2.00	1.0	62.97	0.09
30-Jan-93	14	2.00	1.0	62.75	0.13
31-Jan-93	15	2.00	1.0	62.54	0.12
01-Feb-93	16	2.00	1.0	62.32	0.10
02-Feb-93	17	2.00	1.0	63.33	0.14
03-Feb-93	18	2.00	1.0	64.34	0.15
04-Feb-93	19	2.00	1.0	65.35	0.10
04-Feb-93	19	2.00	1.0	66.35	0.12
05-Feb-93	20	2.00	1.0	67.36	0.16
06-Feb-93	21	2.00	1.0	68.37	0.17
07-Feb-93	22	2.00	1.0	67.16	0.18
08-Feb-93	23	2.00	1.0	65.95	0.11
09-Feb-93	24	2.00	1.0	64.74	0.09
10-Feb-93	25	2.00	2.0	63.53	0.16
11-Feb-93	26	2.00	2.0	62.32	0.22
12-Feb-93	27	2.00	2.0	61.11	0.27
13-Feb-93	28	2.00	2.0	59.99	0.27
14-Feb-93	29	4.00	2.0	58.87	0.28
15-Feb-93	30	2.00	2.0	57.75	0.32
16-Feb-93	31	4.00	2.0	57.20	0.28
17-Feb-93	32	4.00	2.0	56.64	0.33
18-Feb-93	33	4.00	2.0	56.09	0.34
19-Feb-93	34	4.00	2.0	55.54	0.42
20-Feb-93	35	4.00	2.0	54.98	0.39
21-Feb-93	36	4.00	2.0	54.43	0.50
22-Feb-93	37	2.00	2.0	55.36	0.45
23-Feb-93	38	2.00	2.0	56.30	0.37
24-Feb-93	39	2.00	2.0	57.23	0.31
25-Feb-93	40	2.00	2.0	58.19	0.35
26-Feb-93	41	2.00	2.0	59.15	0.37
27-Feb-93	42	2.00	2.0	60.10	0.43
28-Feb-93	43	1.50	2.0	61.06	0.43

Table 37. (continued).

Date	Day	HRT (days)	Nominal		Methane (% of total)	Std. Methane Production (L/L/day)
			COD Load (g/L/day)			
01-Mar-93	44	1.50	2.0		62.02	0.41
02-Mar-93	45	1.50	2.0		62.59	0.41
03-Mar-93	46	1.00	2.0		63.16	0.45
04-Mar-93	47	1.00	2.0		63.73	0.42
05-Mar-93	48	1.00	2.0		64.30	0.43
07-Mar-93	50	1.00	2.0		64.87	0.69
08-Mar-93	51	1.00	2.0		65.44	0.33
09-Mar-93	52	1.00	2.0		66.01	0.41
10-Mar-93	53	1.00	2.0		66.54	0.45
11-Mar-93	54	1.00	2.5		67.07	0.41
12-Mar-93	55	1.00	2.5		65.75	0.45
13-Mar-93	56	1.00	2.5		64.43	0.45
14-Mar-93	57	1.00	2.5		63.11	0.43
15-Mar-93	58	1.00	2.5		63.21	0.44
16-Mar-93	59	1.00	2.5		63.31	0.42
17-Mar-93	60	1.00	2.5		62.90	0.38
18-Mar-93	61	1.00	2.5		62.48	0.55
19-Mar-93	62	1.00	2.5		62.07	0.48
20-Mar-93	63	1.00	3.0		61.65	0.53
21-Mar-93	64	1.00	3.0		60.51	0.48
22-Mar-93	65	1.00	3.0		59.38	0.51
23-Mar-93	66	1.00	3.0		58.24	0.48
24-Mar-93	67	1.00	3.0		58.61	0.50
25-Mar-93	68	1.00	3.0		58.98	0.50
26-Mar-93	69	1.00	3.0		58.67	0.39
27-Mar-93	70	1.00	3.0		58.35	0.42
28-Mar-93	71	1.00	3.0		58.04	0.45
29-Mar-93	72	1.00	3.0		57.73	0.44
30-Mar-93	73	1.00	3.0		57.41	0.44
31-Mar-93	74	1.00	3.0		57.10	0.49
01-Apr-93	75	1.00	3.0		59.25	0.47
02-Apr-93	76	1.00	3.0		61.41	0.48
03-Apr-93	77	1.00	3.0		63.56	0.50
04-Apr-93	78	1.00	3.0		61.39	0.64
05-Apr-93	79	1.00	3.0		59.22	0.49
06-Apr-93	80	1.00	4.0		57.05	0.55
07-Apr-93	81	1.00	4.0		54.88	0.57
08-Apr-93	82	1.00	4.0		54.04	0.60
09-Apr-93	83	1.00	4.0		53.20	0.60
10-Apr-93	84	1.00	4.0		52.36	0.50
11-Apr-93	85	1.00	4.0		51.33	0.54
12-Apr-93	86	1.00	4.0		50.29	0.58
13-Apr-93	87	1.00	4.0		51.37	0.55
14-Apr-93	88	1.00	4.0		52.45	0.39
15-Apr-93	89	1.00	4.0		53.53	0.60

Table 37. (continued).

Date	Day	HRT (days)	Nominal COD Load (g/L/day)	Methane (% of total)	Std. Methane Production (L/L/day)
16-Apr-93	90	1.00	4.0	54.61	0.64
17-Apr-93	91	1.00	4.0	55.19	0.63
18-Apr-93	92	1.00	4.0	55.77	0.62
19-Apr-93	93	1.00	4.0	56.35	0.69
20-Apr-93	94	1.00	4.0	56.93	0.73
21-Apr-93	95	1.00	4.0	57.51	0.73
22-Apr-93	96	1.00	4.0	58.09	0.48
23-Apr-93	97	1.00	4.0	58.67	0.22
24-Apr-93	98	1.00	4.0	59.25	0.21
25-Apr-93	99	1.00	4.0	59.83	0.51
26-Apr-93	100	1.00	4.0	60.41	0.60
27-Apr-93	101	1.00	4.0	60.99	0.78
28-Apr-93	102	1.00	4.0	61.57	0.65
29-Apr-93	103	1.00	4.0	61.28	0.70
30-Apr-93	104	1.00	4.0	60.99	0.65
01-May-93	105	1.00	4.0	60.69	0.63
02-May-93	106	1.00	4.0	60.40	0.56
03-May-93	107	1.00	4.0	60.11	0.62
04-May-93	108	1.00	4.0	59.53	0.52
05-May-93	109	0.75	5.3	58.96	0.60
06-May-93	110	0.75	5.3	58.38	0.62
07-May-93	111	0.75	5.3	57.80	0.68
08-May-93	112	0.75	5.3	57.22	0.70
09-May-93	113	0.75	5.3	56.65	0.62
10-May-93	114	0.75	5.3	56.54	0.77
11-May-93	115	0.75	5.3	56.43	0.63
12-May-93	116	0.75	5.3	56.33	0.65
13-May-93	117	0.75	5.3	56.22	0.74
14-May-93	118	0.75	5.3	56.12	0.81
15-May-93	119	0.75	5.3	56.46	0.85
16-May-93	120	0.75	5.3	56.80	0.84
17-May-93	121	0.75	5.3	57.15	0.90
18-May-93	122	0.75	5.3	57.49	1.01
19-May-93	123	0.75	5.3	57.83	1.05
20-May-93	124	0.75	7.0	58.18	1.25
21-May-93	125	0.75	7.0	58.52	1.52
22-May-93	126	0.75	7.0	58.86	1.56
23-May-93	127	0.75	7.0	59.21	1.57
24-May-93	128	0.75	7.0	59.17	1.57
25-May-93	129	0.75	7.0	59.13	1.68
26-May-93	130	0.75	7.0	59.09	1.62
27-May-93	131	0.75	7.0	59.24	1.80
28-May-93	132	0.75	9.0	59.38	2.06
29-May-93	133	0.75	9.0	59.52	2.30
30-May-93	134	0.75	9.0	59.67	2.28

Table 37. (continued).

Date	Day	HRT (days)	Nominal COD Load (g/L/day)	Methane (% of total)	Std. Methane Production (L/L/day)
31-May-93	135	0.75	9.0	59.81	2.35
01-Jun-93	136	0.75	9.0	59.95	2.27
02-Jun-93	137	0.75	9.0	60.09	2.35
03-Jun-93	138	0.75	9.0	60.24	2.15
04-Jun-93	139	0.75	9.0	60.28	2.54
05-Jun-93	140	0.75	9.0	60.32	2.49
06-Jun-93	141	0.75	9.0	60.36	2.57
07-Jun-93	142	0.75	11.0	59.89	2.65
08-Jun-93	143	0.75	11.0	59.42	3.25
09-Jun-93	144	0.75	11.0	58.95	2.86
10-Jun-93	145	0.75	11.0	58.47	3.15
11-Jun-93	146	0.75	11.0	58.00	3.24
12-Jun-93	147	0.75	11.0	57.53	3.47
13-Jun-93	148	0.75	11.0	57.06	3.03
14-Jun-93	149	0.75	11.0	56.59	2.88
15-Jun-93	150	0.75	11.0	56.11	3.04
16-Jun-93	151	0.75	11.0	55.76	2.80
17-Jun-93	152	0.75	11.0	55.41	2.95
18-Jun-93	153	0.75	11.0	55.06	2.98
19-Jun-93	154	0.75	14.0	54.71	3.39
20-Jun-93	155	0.75	14.0	55.02	3.62
21-Jun-93	156	0.75	14.0	55.33	3.79
22-Jun-93	157	0.75	14.0	55.64	3.98
23-Jun-93	158	0.75	14.0	55.95	4.01
24-Jun-93	159	0.75	14.0	56.26	3.82
25-Jun-93	160	0.75	14.0	56.57	4.00
26-Jun-93	161	0.75	14.0	56.88	4.31
27-Jun-93	162	0.75	14.0	57.19	2.95
28-Jun-93	163	0.75	14.0	57.50	3.40
29-Jun-93	164	0.75	14.0	57.80	4.09
30-Jun-93	165	0.75	14.0	56.65	3.92
01-Jul-93	166	0.75	14.0	55.50	3.94
02-Jul-93	167	0.75	14.0	54.35	3.70
03-Jul-93	168	0.75	14.0	53.57	3.89
04-Jul-93	169	0.75	14.0	52.79	3.69
05-Jul-93	170	0.75	14.0	52.01	2.83
06-Jul-93	171	0.75	14.0	51.22	2.60
07-Jul-93	172	1.00	14.0	50.44	2.50
08-Jul-93	173	1.00	14.0	49.66	1.90
09-Jul-93	174	1.00	14.0	48.88	1.31
10-Jul-93	175	1.00	14.0	48.10	0.74
11-Jul-93	176	1.00	14.0	47.32	0.69
12-Jul-93	177	1.00	14.0	46.53	0.75
13-Jul-93	178	1.00	14.0	45.75	0.58
14-Jul-93	179	1.00	14.0	59.48	0.37

Table 37. (continued).

Date	Day	HRT (days)	Nominal COD Load (g/L/day)	Methane (% of total)	Std. Methane Production (L/L/day)
15-Jul-93	180	1.00	2.0	59.31	0.26
16-Jul-93	181	1.00	2.0	59.15	0.03
17-Jul-93	182	1.00	2.0	58.98	0.00
18-Jul-93	183	1.00	2.0	58.82	0.00
19-Jul-93	184	1.00	2.0	58.65	0.00
20-Jul-93	185	1.00	2.0	58.49	0.00
21-Jul-93	186	1.00	2.0	58.32	0.00
22-Jul-93	187	1.00	2.0	58.16	0.00
23-Jul-93	188	1.00	2.0	57.99	0.29
24-Jul-93	189	1.00	2.0	57.83	0.24
25-Jul-93	190	1.00	2.0	57.66	0.38
26-Jul-93	191	1.00	2.0	57.50	0.67
27-Jul-93	192	1.00	3.5	56.95	0.50
28-Jul-93	193	1.00	3.5	56.40	0.45
29-Jul-93	194	1.00	3.5	55.86	0.41
30-Jul-93	195	1.00	3.5	55.31	0.45
31-Jul-93	196	1.00	3.5	54.76	0.47
01-Aug-93	197	1.00	3.5	54.21	0.44
02-Aug-93	198	1.00	3.5	53.66	0.39
03-Aug-93	199	1.00	3.5	54.77	0.58
04-Aug-93	200	1.00	3.5	55.87	0.49
05-Aug-93	201	1.00	3.5	56.97	0.62
06-Aug-93	202	1.00	3.5	58.08	0.64
07-Aug-93	203	1.00	3.5	58.71	0.71
08-Aug-93	204	1.00	3.5	59.34	0.69
09-Aug-93	205	1.00	3.5	59.98	0.72
10-Aug-93	206	1.00	3.5	60.61	0.80
11-Aug-93	207	1.00	3.5	61.24	0.80
12-Aug-93	208	1.00	3.5	61.18	0.46
13-Aug-93	209	1.00	3.5	61.12	0.81
14-Aug-93	210	1.00	3.5	61.06	0.83
15-Aug-93	211	1.00	3.5	61.00	0.85
16-Aug-93	212	1.00	3.5	60.94	0.67
17-Aug-93	213	1.00	3.5	60.87	0.93
18-Aug-93	214	1.00	3.5	60.81	0.95
19-Aug-93	215	1.00	5.0	60.75	1.17
20-Aug-93	216	1.00	5.0	60.69	1.30
21-Aug-93	217	1.00	5.0	60.63	1.19
22-Aug-93	218	1.00	5.0	60.57	1.38
23-Aug-93	219	1.00	5.0	60.51	1.48
24-Aug-93	220	1.00	5.0	59.38	1.39
25-Aug-93	221	1.00	7.0	58.25	1.78
26-Aug-93	222	1.00	7.0	57.12	2.10
27-Aug-93	223	1.00	7.0	58.10	2.20
28-Aug-93	224	1.00	7.0	57.71	2.29

Table 37. (continued).

Date	Day	HRT (days)	Nominal COD Load (g/L/day)	Methane (% of total)	Std. Methane Production (L/L/day)
29-Aug-93	225	1.00	7.0	57.32	1.74
30-Aug-93	226	1.00	7.0	56.93	2.24
31-Aug-93	227	1.00	7.0	56.55	2.07
01-Sep-93	228	1.00	7.0	56.44	2.03
02-Sep-93	229	1.00	7.0	56.33	0.71
03-Sep-93	230	1.00	7.0	56.22	1.03
04-Sep-93	231	1.00	9.0	56.11	1.40
05-Sep-93	232	1.00	9.0	56.00	1.99
06-Sep-93	233	1.00	9.0	55.89	2.16
07-Sep-93	234	1.00	9.0	55.78	2.32
08-Sep-93	235	1.00	9.0	55.67	2.53
09-Sep-93	236	1.00	9.0	55.57	2.52
10-Sep-93	237	1.00	9.0	55.89	2.62
11-Sep-93	238	1.00	9.0	56.21	1.80
12-Sep-93	239	1.00	9.0	56.53	2.04
13-Sep-93	240	1.00	9.0	56.85	2.24
14-Sep-93	241	1.00	12.0	57.17	3.05
15-Sep-93	242	1.00	12.0	57.49	3.53
16-Sep-93	243	1.00	12.0	56.56	4.46
17-Sep-93	244	1.00	12.0	55.62	3.73
18-Sep-93	245	1.00	12.0	54.68	3.56
19-Sep-93	246	1.00	12.0	53.74	3.34
20-Sep-93	247	1.00	12.0	52.81	3.31
21-Sep-93	248	1.00	12.0	51.87	3.39
22-Sep-93	249	1.00	12.0	50.93	4.47
23-Sep-93	250	1.00	12.0	49.99	3.11
24-Sep-93	251	1.00	12.0	49.06	2.10
25-Sep-93	252	1.00	12.0	48.12	2.95
26-Sep-93	253	1.00	12.0	47.18	2.86
27-Sep-93	254	1.00	12.0	46.24	2.60
28-Sep-93	255	1.00	12.0	45.31	2.31
29-Sep-93	256	1.00	9.0	46.39	2.18
30-Sep-93	257	1.00	9.0	47.47	1.81
01-Oct-93	258	1.00	9.0	47.53	1.75
02-Oct-93	259	1.00	9.0	47.60	1.60
03-Oct-93	260	1.00	9.0	47.67	1.63
04-Oct-93	261	1.00	9.0	47.73	1.50
05-Oct-93	262	1.00	9.0	47.80	1.21
06-Oct-93	263	1.00	9.0	48.78	0.96
07-Oct-93	264	1.00	7.0	49.77	1.16
08-Oct-93	265	1.00	7.0	50.75	1.07
09-Oct-93	266	1.00	7.0	51.73	1.00
10-Oct-93	267	1.00	7.0	52.72	1.33
11-Oct-93	268	1.00	7.0	53.70	1.30

Table 37. (continued).

Date	Day	HRT (days)	Nominal COD Load (g/L/day)	Methane (% of total)	Std. Methane Production (L/L/day)
12-Oct-93	269	1.00	7.0	54.69	1.38
13-Oct-93	270	1.00	7.0	55.67	1.46
14-Oct-93	271	1.00	7.0	55.72	0.79
15-Oct-93	272	1.00	7.0	55.78	0.15
16-Oct-93	273	1.00	7.0	55.83	1.27
17-Oct-93	274	1.00	7.0	55.89	1.52
18-Oct-93	275	1.00	7.0	55.94	1.82
19-Oct-93	276	1.00	7.0	55.83	1.67
20-Oct-93	277	1.00	7.0	55.71	1.46
21-Oct-93	278	1.00	7.0	55.59	1.55
22-Oct-93	279	1.00	7.0	55.47	1.64
23-Oct-93	280	1.00	7.0	55.36	1.47
24-Oct-93	281	1.00	7.0	55.24	1.52
25-Oct-93	282	1.00	7.0	55.12	1.59
26-Oct-93	283	1.00	7.0	58.72	1.06
27-Oct-93	284	1.00	7.0	62.32	0.09
28-Oct-93	285	1.00	7.0	62.32	0.53
29-Oct-93	286	1.00	7.0	62.32	0.52
30-Oct-93	287	1.00	7.0	62.32	0.45
31-Oct-93	288	1.00	7.0	62.32	0.31
01-Nov-93	289	1.00	7.0	62.32	0.31
02-Nov-93	290	1.00	7.0	62.32	0.52

Table 38. Volatile acids data for the sucrose+PAC test.

Date	Time from Start (days)	COD Load (g/L/day)	Volatile Acids (mg/L as acetic)
23-Jan-93	7	1.0	246
26-Jan-93	10	1.0	339
02-Feb-93	17	1.0	343
10-Feb-93	25	1.0	334
24-Feb-93	39	2.0	694
14-Mar-93	57	2.5	343
05-Apr-93	79	4.0	647
12-Apr-93	86	4.0	951
05-May-93	109	4.0	711
19-May-93	123	5.3	420
02-Jun-93	137	9.0	60
14-Jun-93	149	11.0	26
21-Jun-93	156	14.0	77
30-Jun-93	165	14.0	86
15-Jul-93	180	3.5	2,589
28-Jul-93	193	3.5	1,209
01-Sep-93	228	7.0	120
08-Sep-93	235	9.0	454
28-Sep-93	255	12.0	2,066
06-Oct-93	263	9.0	2,494

Table 39. Particle size analysis for the sucrose+PAC test.

Date	Time from Start-up (days)	COD Load (g/L/day)	Average Diameter (arithmetic, μm)	Average Diameter (geometric, μm)
16-Jan-93	0	0.5	31	150
01-Feb-93	16	1.0	34	254
15-Feb-93	30	2.0	32	450
05-Mar-93	48	2.0	43	198
24-Mar-93	67	3.0	45	201
19-Apr-93	93	4.0	104	450
24-May-93	128	7.0	67	1,100
05-Jun-93	140	9.0	242	1,837
28-Jul-93	193	3.5	362	2,300
21-Aug-93	217	5.0	345	1,003
17-Sep-93	244	12.0	229	1,500
26-Oct-93	283	7.0	407	1,550

Table 40. Alkalinity and pH data for the sucrose+PAC test.

Date	Time (days)	COD Load (g/L/day)	Alkalinity (mg/L as CaCO ₃)	pH (units)
16-Jan-93	0	0.5	1,250	7.53
19-Jan-93	3	0.5	1,320	7.16
23-Jan-93	7	1.0	1,410	6.67
24-Jan-93	8	1.0	1,450	6.60
25-Jan-93	9	1.0	1,460	6.66
26-Jan-93	10	1.0	1,520	6.83
27-Jan-93	11	1.0	1,570	6.80
28-Jan-93	12	1.0	1,510	7.00
31-Jan-93	15	1.0	1,530	6.74
01-Feb-93	16	1.0	1,500	6.71
02-Feb-93	17	1.0	1,460	6.66
08-Feb-93	23	1.0	2,580	6.81
09-Feb-93	24	1.0	1,640	6.76
10-Feb-93	25	1.0	1,800	6.93
11-Feb-93	26	2.0	2,140	6.64
15-Feb-93	30	2.0	2,690	6.80
24-Feb-93	39	2.0	2,880	6.88
10-Mar-93	53	2.5	2,390	6.69
14-Mar-93	57	2.5	2,240	6.86
17-Mar-93	60	2.5	2,300	7.50
18-Mar-93	61	2.5	2,410	7.00
19-Mar-93	62	2.5	2,290	6.69
20-Mar-93	63	3.0	2,250	6.71
21-Mar-93	64	3.0	2,310	6.60
22-Mar-93	65	3.0	2,380	6.75
23-Mar-93	66	3.0	2,430	6.80
27-Mar-93	70	3.0	2,270	6.64
28-Mar-93	71	3.0	2,190	6.73
29-Mar-93	72	3.0	2,150	6.78
30-Mar-93	73	3.0	2,170	6.76
31-Mar-93	74	3.0	2,260	6.75
02-Apr-93	76	3.0	2,200	6.75
03-Apr-93	77	3.0	2,150	6.79
05-Apr-93	79	3.0	2,180	6.70
06-Apr-93	80	4.0	2,060	6.62
07-Apr-93	81	4.0	2,250	6.68
08-Apr-93	82	4.0	2,390	6.70
09-Apr-93	83	4.0	2,580	6.61
13-Apr-93	87	4.0	2,620	6.57
15-Apr-93	89	4.0	2,600	6.70
19-Apr-93	93	4.0	2,590	6.70
20-Apr-93	94	4.0	2,670	6.66
21-Apr-93	95	4.0	2,630	6.69
23-Apr-93	97	4.0	2,640	6.84
24-Apr-93	98	4.0	2,650	6.93
27-Apr-93	101	4.0	2,570	6.88

Table 40. (continued).

Date	Time (days)	COD Load (g/L/day)	Alkalinity (mg/L as CaCO ₃)	pH (units)
01-May-93	105	4.0	2,590	6.80
03-May-93	107	4.0	2,490	6.80
04-May-93	108	4.0	2,540	6.80
05-May-93	109	4.0	2,520	6.85
07-May-93	111	5.3	2,530	6.72
08-May-93	112	5.3	2,580	6.70
17-May-93	121	5.3	2,540	6.82
19-May-93	123	5.3	2,560	6.96
20-May-93	124	7.0	2,790	6.82
23-May-93	127	7.0	2,840	6.85
28-May-93	132	9.0	2,970	6.83
01-Jun-93	136	9.0	3,030	6.79
02-Jun-93	137	9.0	3,000	6.96
05-Jun-93	140	9.0	3,040	6.87
08-Jun-93	143	11.0	3,150	6.89
14-Jun-93	149	11.0	3,180	6.82
21-Jun-93	156	14.0	3,140	7.02
23-Jun-93	158	14.0	3,290	6.95
28-Jun-93	163	14.0	3,320	7.00
30-Jun-93	165	14.0	3,300	7.07
02-Jul-93	167	14.0	3,290	6.93
05-Jul-93	170	14.0	3,270	7.00
12-Jul-93	177	14.0	3,300	5.32
15-Jul-93	180	3.5	3,200	6.75
19-Jul-93	184	3.5	2,850	7.18
23-Jul-93	188	3.5	2,670	7.03
26-Jul-93	191	3.5	2,590	6.82
28-Jul-93	193	3.5	2,620	6.74
05-Aug-93	201	3.5	2,620	6.74
23-Aug-93	219	5.0	2,600	6.97
25-Aug-93	221	5.0	2,630	6.95
01-Sep-93	228	7.0	2,640	6.89
08-Sep-93	235	9.0	2,700	6.92
14-Sep-93	241	12.0	2,830	6.94
20-Sep-93	247	12.0	2,790	6.98
27-Sep-93	254	12.0	2,900	6.90
29-Sep-93	256	12.0	2,830	6.84
04-Oct-93	261	12.0	2,870	6.51
07-Oct-93	264	12.0	2,750	6.75
11-Oct-93	268	12.0	2,680	6.70
13-Oct-93	270	12.0	2,700	6.86

Table 41. Solids data for the sucrose + PAC test.

Date	Time (days)	COD Load (g/L/day)	HRT (days)	MLSS (mg/L)	MLVSS (% of MLSS)	Effluent TSS (mg/L)	Effluent VSS (% of TSS)	SRT (days)
16-Jan-93	0	0.5	2.00	21,453	62.9			
23-Jan-93	7	1.0	2.00	7,355	63.0	214	77.5	55.9
26-Jan-93	10	1.0	2.00	6,880	63.9	342	56.8	45.3
01-Feb-93	16	1.0	2.00	5,120	67.0	188	46.6	78.3
09-Feb-93	24	1.0	2.00	4,645	72.0	136	54.4	90.4
16-Feb-93	31	2.0	4.00	5,035	74.2			
20-Feb-93	35	2.0	4.00	5,745	79.0	1,137	74.5	21.4
26-Feb-93	41	2.0	2.00	4,395	80.2	628	79.2	14.2
05-Mar-93	48	2.0	1.00	4,750	81.5	520	74.8	10.0
09-Mar-93	52	2.0	1.00	4,932	82.8	557	71.8	10.2
19-Mar-93	62	2.5	1.00	5,015	86.4	406	79.8	13.4
24-Mar-93	67	3.0	1.00	6,080	85.3	660	78.1	10.1
30-Mar-93	73	3.0	1.00	6,535	87.0	530	77.9	13.8
05-Apr-93	79	3.0	1.00	6,630	86.7	588	76.2	12.8
12-Apr-93	86	4.0	1.00	8,850	85.4	1,356	82.6	6.7
19-Apr-93	93	4.0	1.00	9,950	83.6	1,090	73.6	10.4
28-Apr-93	102	4.0	1.00	7,940	87.7	756	80.9	11.4
05-May-93	109	5.3	0.75	8,590	88.1	848	82.6	8.1
11-May-93	115	5.3	0.75	10,015	88.5	1,063	83.3	7.5
19-May-93	123	5.3	0.75	9,250	88.8	868	83.7	8.5
24-May-93	128	7.0	0.75	11,390	88.0	1,287	80.1	7.3
02-Jun-93	137	9.0	0.75	17,230	90.0	1,415	84.8	9.7
06-Jun-93	141	9.0	0.75	18,740	90.0			
14-Jun-93	149	11.0	0.75	22,480	91.2	2,045	83.9	9.0
21-Jun-93	156	14.0	0.75	23,400	91.1	3,443	89.3	5.2
30-Jun-93	165	14.0	0.75	26,020	91.8	1,768	86.9	11.7
15-Jul-93	180	2.0	1.00	18,860	90.5	1,950	87.6	10.0
28-Jul-93	193	3.5	1.00	17,140	91.2	577	77.4	35.0
09-Aug-93	205	3.5	1.00	15,340	89.4	1,070	86.7	14.8

Table 41. (continued).

Date	Time (days)	COD Load (g/L/day)	HRT (days)	MLSS (mg/L)	MLVSS (% of MLSS)	Effluent TSS (mg/L)	Effluent VSS (% of TSS)	SRT (days)
17-Aug-93	213	3.5	1.00	14,620	89.9	873	83.2	18.1
24-Aug-93	220	5.0	1.00	15,810	90.8	1,150	75.9	16.4
01-Sep-93	228	7.0	1.00	19,150	90.5	1,000	85.7	20.2
08-Sep-93	235	9.0	1.00	22,590	90.8	2,118	84.9	11.4
17-Sep-93	244	12.0	1.00	24,730	91.7			
23-Sep-93	250	12.0	1.00	24,780	91.0	2,425	83.7	11.1
06-Oct-93	263	9.0	1.00	26,850	90.1	2,050	84.4	14.0
15-Oct-93	272	7.0	1.00	26,470	89.8	1,785	86.5	15.4
25-Oct-93	282	7.0	1.00	26,975	90.1			
31-Oct-93	288	7.0	1.00	25,300	87.8			

Table 42. COD data for the sucrose+GAC test.

Date	Day	HRT (days)	Influent COD (mg/L)	COD Load (g/L/day)	Effluent TCOD (mg/L)	TCOD Removal (%)	Effluent SCOD (mg/L)	SCOD Removal (%)
28-Apr-93	9	2.0	2,000	1	2,101	0.0	638	68.1
05-May-93	16	2.0	2,000	1	1,380	31.0	522	73.9
11-May-93	22	2.0	4,000	2	2,370	40.8	1,140	71.5
19-May-93	30	1.5	3,000	2	1,058	64.7	547	81.8
27-May-93	38	1.0	3,000	3	1,223	59.2	730	75.7
02-Jun-93	44	1.0	4,000	4	2,343	41.4	1,495	62.6
14-Jun-93	56	1.0	4,000	4	2,299	42.5	1,359	66.0
21-Jun-93	63	1.0	4,000	4	1,390	65.3	741	81.5
30-Jun-93	72	1.0	5,500	6	1,360	75.3	490	91.1
15-Jul-93	87	1.0	7,000	7	1,645	76.5	347	95.0
28-Jul-93	100	1.0	9,000	9	3,492	61.2	736	91.8
09-Aug-93	112	1.0	9,000	9	4,031	55.2	2,552	71.6
17-Aug-93	120	2.0	15,800	8	4,063	74.3	2,090	86.8
24-Aug-93	127	2.0	15,000	8	15,000	0.0	4,281	71.5
01-Sep-93	135	2.0	10,000	5	4,375	56.3	2,066	79.3
08-Sep-93	142	2.0	10,000	5	5,033	49.7	1,988	80.1
28-Sep-93	162	2.0	10,000	5	4,015	59.9	2,106	78.9
06-Oct-93	170	2.0	10,000	5	2,553	74.5	1,429	85.7

Table 43. Biogas data for the sucrose + GAC test.

Date	Time (days)	HRT (days)	Nominal		Methane (% of total)	Std Methane Production (L/L/day)
			COD Load (g/L/day)			
19-Apr-93	0	2.0	0.5		65.36	0.00
20-Apr-93	1	2.0	0.5		65.36	0.00
21-Apr-93	2	2.0	1.0		65.36	0.00
22-Apr-93	3	2.0	1.0		65.36	0.01
23-Apr-93	4	2.0	1.0		65.36	0.00
24-Apr-93	5	2.0	1.0		65.36	0.01
25-Apr-93	6	2.0	1.0		65.36	0.00
26-Apr-93	7	2.0	1.0		65.36	0.00
27-Apr-93	8	2.0	1.0		65.36	0.01
28-Apr-93	9	2.0	1.0		65.36	0.00
29-Apr-93	10	2.0	1.0		62.47	0.00
30-Apr-93	11	2.0	1.0		59.59	0.00
01-May-93	12	2.0	1.0		56.70	0.00
02-May-93	13	2.0	1.0		53.82	0.00
03-May-93	14	2.0	1.0		50.94	0.09
04-May-93	15	2.0	1.0		53.21	0.09
05-May-93	16	2.0	1.0		55.49	0.11
06-May-93	17	2.0	2.0		57.76	0.20
07-May-93	18	2.0	2.0		60.04	0.31
08-May-93	19	2.0	2.0		62.31	0.30
09-May-93	20	2.0	2.0		64.59	0.31
10-May-93	21	2.0	2.0		64.13	0.36
11-May-93	22	2.0	2.0		63.67	0.39
12-May-93	23	2.0	2.0		63.22	0.35
13-May-93	24	2.0	2.0		62.76	0.32
14-May-93	25	2.0	2.0		62.30	0.34
15-May-93	26	2.0	2.0		61.81	0.37
16-May-93	27	2.0	2.0		61.32	0.32
17-May-93	28	2.0	2.0		60.83	0.32
18-May-93	29	2.0	2.0		60.34	0.35
19-May-93	30	4.0	3.0		59.85	0.35
20-May-93	31	2.0	3.0		59.36	0.38
21-May-93	32	4.0	3.0		58.87	0.42
22-May-93	33	4.0	3.0		58.37	0.45
23-May-93	34	4.0	3.0		57.88	0.48
24-May-93	35	4.0	3.0		58.57	0.46
25-May-93	36	4.0	3.0		59.26	0.37
26-May-93	37	4.0	3.0		59.94	0.43
27-May-93	38	2.0	3.0		59.13	0.48
28-May-93	39	2.0	3.0		58.32	0.50
29-May-93	40	2.0	4.0		57.51	0.55
30-May-93	41	2.0	4.0		56.70	0.49
31-May-93	42	2.0	4.0		55.88	0.58
01-Jun-93	43	2.0	4.0		55.07	0.53
02-Jun-93	44	1.5	4.0		54.26	0.60

Table 43. (continued).

Date	Time (days)	HRT (days)	Nominal COD Load (g/L/day)	Methane (% of total)	Std Methane Production (L/L/day)
03-Jun-93	45	1.5	4.0	53.45	0.46
04-Jun-93	46	1.5	4.0	52.53	0.42
05-Jun-93	47	1.0	4.0	51.61	0.72
06-Jun-93	48	1.0	4.0	50.68	0.59
07-Jun-93	49	1.0	4.0	50.92	0.61
08-Jun-93	50	1.0	4.0	51.17	0.64
09-Jun-93	51	1.0	4.0	51.41	0.57
10-Jun-93	52	1.0	4.0	51.65	0.54
11-Jun-93	53	1.0	4.0	51.89	0.52
12-Jun-93	54	1.0	4.0	52.13	0.54
13-Jun-93	55	1.0	4.0	52.37	0.48
14-Jun-93	56	1.0	4.0	52.61	0.53
15-Jun-93	57	1.0	4.0	52.85	0.61
16-Jun-93	58	1.0	4.0	54.43	0.60
17-Jun-93	59	1.0	4.0	56.01	0.64
18-Jun-93	60	1.0	4.0	57.59	0.65
19-Jun-93	61	1.0	4.0	59.17	0.66
20-Jun-93	62	1.0	4.0	59.07	0.80
21-Jun-93	63	1.0	4.0	58.97	0.81
22-Jun-93	64	1.0	5.5	58.87	0.98
23-Jun-93	65	1.0	5.5	58.78	1.08
24-Jun-93	66	1.0	5.5	58.68	1.15
25-Jun-93	67	1.0	5.5	58.58	1.12
26-Jun-93	68	1.0	5.5	58.48	1.08
27-Jun-93	69	1.0	5.5	58.38	1.10
28-Jun-93	70	1.0	5.5	58.29	1.10
29-Jun-93	71	1.0	5.5	58.19	1.11
30-Jun-93	72	1.0	5.5	58.85	1.22
01-Jul-93	73	1.0	5.5	59.51	1.30
02-Jul-93	74	1.0	5.5	60.17	1.32
03-Jul-93	75	1.0	5.5	59.81	1.36
04-Jul-93	76	1.0	5.5	59.44	1.24
05-Jul-93	77	1.0	5.5	59.08	0.96
06-Jul-93	78	1.0	5.5	58.72	1.00
07-Jul-93	79	1.0	5.5	58.36	0.79
08-Jul-93	80	1.0	7.0	58.00	1.50
09-Jul-93	81	1.0	7.0	57.64	1.98
10-Jul-93	82	1.0	7.0	57.28	1.77
11-Jul-93	83	1.0	7.0	56.92	1.85
12-Jul-93	84	1.0	7.0	56.56	1.69
13-Jul-93	85	1.0	7.0	56.20	1.88
14-Jul-93	86	1.0	7.0	59.64	2.15
15-Jul-93	87	1.0	7.0	59.27	1.88
16-Jul-93	88	1.0	7.0	58.91	2.09
17-Jul-93	89	1.0	9.0	58.54	2.23

Table 43. (continued).

Date	Time (days)	HRT (days)	Nominal COD Load (g/L/day)	Methane (% of total)	Std Methane Production (L/L/day)
18-Jul-93	90	1.0	9.0	58.17	2.45
19-Jul-93	91	1.0	9.0	57.81	2.26
20-Jul-93	92	1.0	9.0	57.44	2.43
21-Jul-93	93	1.0	9.0	57.07	2.35
22-Jul-93	94	1.0	9.0	56.70	2.54
23-Jul-93	95	1.0	9.0	56.34	2.01
24-Jul-93	96	1.0	9.0	55.97	3.05
25-Jul-93	97	1.0	9.0	55.60	2.19
26-Jul-93	98	1.0	9.0	55.24	2.21
27-Jul-93	99	1.0	9.0	54.85	2.55
28-Jul-93	100	1.0	9.0	54.46	2.35
29-Jul-93	101	1.0	9.0	54.07	2.42
30-Jul-93	102	1.0	9.0	53.68	2.29
31-Jul-93	103	1.0	11.0	53.29	2.60
01-Aug-93	104	1.0	11.0	52.90	2.55
02-Aug-93	105	1.0	11.0	52.50	2.19
03-Aug-93	106	1.0	11.0	53.32	2.78
04-Aug-93	107	1.0	11.0	54.13	2.93
05-Aug-93	108	1.0	9.0	54.94	1.73
06-Aug-93	109	1.0	9.0	55.75	2.17
07-Aug-93	110	1.0	9.0	57.40	2.32
08-Aug-93	111	1.0	9.0	59.04	2.20
09-Aug-93	112	1.0	9.0	60.69	2.34
10-Aug-93	113	2.0	7.9	62.33	1.95
11-Aug-93	114	2.0	7.9	63.98	1.80
12-Aug-93	115	2.0	7.9	62.55	0.92
13-Aug-93	116	2.0	7.9	61.13	0.88
14-Aug-93	117	2.0	7.9	59.70	1.70
15-Aug-93	118	2.0	7.9	58.28	1.16
16-Aug-93	119	2.0	7.9	56.85	1.30
17-Aug-93	120	2.0	7.9	55.43	1.63
18-Aug-93	121	2.0	7.5	54.00	1.90
19-Aug-93	122	2.0	7.5	52.57	1.89
20-Aug-93	123	2.0	7.5	51.15	1.41
21-Aug-93	124	2.0	7.5	49.72	1.51
22-Aug-93	125	2.0	7.5	48.30	1.70
23-Aug-93	126	2.0	7.5	46.87	1.65
24-Aug-93	127	2.0	7.5	50.07	1.61
25-Aug-93	128	2.0	5.0	53.28	1.30
26-Aug-93	129	2.0	5.0	56.48	1.29
27-Aug-93	130	2.0	5.0	54.05	1.08
28-Aug-93	131	2.0	5.0	53.88	1.19
29-Aug-93	132	2.0	5.0	53.70	1.07
30-Aug-93	133	2.0	5.0	53.53	1.06
31-Aug-93	134	2.0	5.0	53.35	1.02

Table 43. (continued).

Date	Time (days)	HRT (days)	Nominal COD Load (g/L/day)	Methane (% of total)	Std Methane Production (L/L/day)
01-Sep-93	135	2.0	5.0	53.49	1.11
02-Sep-93	136	2.0	5.0	53.63	0.42
03-Sep-93	137	2.0	5.0	53.77	0.47
04-Sep-93	138	2.0	5.0	53.91	0.86
05-Sep-93	139	2.0	5.0	54.05	1.11
06-Sep-93	140	2.0	5.0	54.19	0.94
07-Sep-93	141	2.0	5.0	54.33	0.88
08-Sep-93	142	2.0	5.0	54.47	1.17
09-Sep-93	143	2.0	5.0	54.61	1.35
10-Sep-93	144	2.0	5.0	55.04	1.17
11-Sep-93	145	4.0	5.0	55.47	1.17
12-Sep-93	146	4.0	5.0	55.90	1.41
13-Sep-93	147	4.0	5.0	56.33	1.49
14-Sep-93	148	4.0	5.0	56.76	1.26
15-Sep-93	149	4.0	5.0	57.19	0.86
16-Sep-93	150	4.0	5.0	56.86	1.27
17-Sep-93	151	4.0	5.0	56.53	1.55
18-Sep-93	152	4.0	5.0	56.21	1.34
19-Sep-93	153	4.0	5.0	55.88	1.40
20-Sep-93	154	4.0	5.0	55.55	1.30
21-Sep-93	155	4.0	5.0	55.23	1.38
22-Sep-93	156	2.0	5.0	54.90	1.10
23-Sep-93	157	2.0	5.0	54.57	0.97
24-Sep-93	158	2.0	5.0	54.25	1.09
25-Sep-93	159	2.0	5.0	53.92	0.93
26-Sep-93	160	2.0	5.0	53.59	1.02
27-Sep-93	161	2.0	5.0	53.27	0.90
28-Sep-93	162	2.0	5.0	52.94	1.09
29-Sep-93	163	2.0	5.0	53.54	1.06
30-Sep-93	164	2.0	5.0	54.13	0.99
01-Oct-93	165	2.0	5.0	54.49	1.00
02-Oct-93	166	2.0	5.0	54.86	1.17
03-Oct-93	167	2.0	5.0	55.22	1.20
04-Oct-93	168	2.0	5.0	55.59	1.08
05-Oct-93	169	2.0	5.0	55.95	1.06
06-Oct-93	170	2.0	5.0	55.64	1.01
07-Oct-93	171	2.0	5.0	55.33	0.99
08-Oct-93	172	2.0	5.0	55.02	0.97
09-Oct-93	173	2.0	5.0	54.71	0.98
10-Oct-93	174	2.0	5.0	54.40	0.98
11-Oct-93	175	2.0	5.0	54.09	0.95
12-Oct-93	176	2.0	5.0	53.78	1.06
13-Oct-93	177	2.0	5.0	53.47	0.99
14-Oct-93	178	2.0	5.0	54.37	1.05
15-Oct-93	179	2.0	5.0	55.27	1.11

Table 43. (continued).

Date	Time (days)	HRT (days)	Nominal COD Load (g/L/day)	Methane (% of total)	Std Methane Production (L/L/day)
16-Oct-93	180	2.0	5.0	56.17	1.22
17-Oct-93	181	2.0	5.0	57.08	1.27
18-Oct-93	182	2.0	5.0	57.98	1.25
19-Oct-93	183	2.0	5.0	57.96	1.39
20-Oct-93	184	2.0	5.0	57.95	1.30
21-Oct-93	185	2.0	5.0	57.94	1.19
22-Oct-93	186	2.0	5.0	57.92	1.30
23-Oct-93	187	2.0	5.0	57.91	1.21
24-Oct-93	188	2.0	5.0	57.89	1.20
25-Oct-93	189	2.0	5.0	57.88	1.18
26-Oct-93	190	2.0	5.0	60.68	0.62
27-Oct-93	191	2.0	5.0	63.47	0.13
28-Oct-93	192	2.0	5.0	63.47	0.29
29-Oct-93	193	2.0	5.0	63.47	0.35
30-Oct-93	194	2.0	5.0	63.47	0.74
31-Oct-93	195	2.0	5.0	63.47	0.20
01-Nov-93	196	2.0	5.0	63.47	0.18
02-Nov-93	197	2.0	5.0	63.47	0.61

Table 44. Volatile acids data for the sucrose+ GAC test.

Date	Time from Start (days)	COD Load (g/L/day)	Volatile Acids (mg/L as acetic)
05-May-93	16	1.0	369
19-May-93	30	2.0	420
02-Jun-93	44	4.0	1,054
14-Jun-93	56	4.0	1,046
21-Jun-93	63	4.0	523
30-Jun-93	72	5.5	223
15-Jul-93	87	7.0	60
28-Jul-93	100	9.0	50
01-Sep-93	135	5.0	1,380
08-Sep-93	142	5.0	1,397
28-Sep-93	162	5.0	1,414
06-Oct-93	170	5.0	1,106

Table 45. Particle size analysis for the sucrose+ GAC test.

Date	Time from Start-up (days)	COD Load (g/L/day)	Average Diameter (arithmetic, μm)	Average Diameter (geometric, μm)
19-Apr-93	0	1.0	89	300
24-May-93	35	3.0	38	400
05-Jun-93	47	4.0	35	500
28-Jul-93	100	9.0	74	472
26-Aug-93	129	5.0	405	1,174
17-Sep-93	151	5.0	250	1,899
26-Oct-93	190	5.0	150	1,166

Table 46. Alkalinity and pH data for the sucrose + GAC test.

Date	Time (days)	COD Load (g/L/day)	Alkalinity (mg/L as CaCO ₃)	pH (units)
20-Apr-93	1	0.5	2,580	7.13
21-Apr-93	2	1.0	2,550	7.09
23-Apr-93	4	1.0	2,600	7.30
24-Apr-93	5	1.0	2,590	7.14
27-Apr-93	8	1.0	2,680	6.96
01-May-93	12	1.0	2,680	6.91
03-May-93	14	1.0	2,670	7.07
04-May-93	15	1.0	2,700	7.25
05-May-93	16	1.0	2,720	7.27
07-May-93	18	2.0	2,800	6.84
08-May-93	19	2.0	2,970	6.75
17-May-93	28	2.0	3,050	6.95
19-May-93	30	2.0	3,060	7.11
20-May-93	31	3.0	3,030	6.85
23-May-93	34	3.0	2,890	6.74
28-May-93	39	3.0	2,870	6.81
01-Jun-93	43	4.0	2,750	6.60
02-Jun-93	44	4.0	2,700	6.76
05-Jun-93	47	4.0	2,690	6.82
08-Jun-93	50	4.0	2,650	6.72
14-Jun-93	56	4.0	2,750	6.67
21-Jun-93	63	4.0	2,690	6.96
23-Jun-93	65	5.5	2,700	6.68
28-Jun-93	70	5.5	2,860	6.81
30-Jun-93	72	5.5	2,880	7.01
02-Jul-93	74	5.5	2,820	6.92
05-Jul-93	77	5.5	2,800	7.00
12-Jul-93	84	5.5	2,760	6.93
15-Jul-93	87	7.0	2,640	6.96
19-Jul-93	91	9.0	2,600	7.08
23-Jul-93	95	9.0	2,570	7.21
26-Jul-93	98	9.0	2,650	6.94
28-Jul-93	100	9.0	2,640	6.85
05-Aug-93	108	9.0	2,680	6.95
23-Aug-93	126	8.0	2,660	6.76
25-Aug-93	128	5.0	2,750	6.78
01-Sep-93	135	5.0	2,770	6.80
08-Sep-93	142	5.0	2,770	6.92
14-Sep-93	148	5.0	2,790	6.99
20-Sep-93	154	5.0	2,780	7.04
27-Sep-93	161	5.0	2,670	6.85
04-Oct-93	168	5.0	2,590	6.85
07-Oct-93	171	5.0	2,650	6.90
11-Oct-93	175	5.0	2,740	6.72
13-Oct-93	177	5.0	2,800	6.89

Table 47. Solids data for the sucrose+GAC test.

Date	Day	COD Load (g/L/day)	HRT (days)	MLSS (mg/L)	MLVSS (% of MLSS)	Effluent TSS (mg/L)	Effluent VSS (% of TSS)	SRT (days)
19-Apr-93	0	0.5	2.0	19,000	63.3			
28-Apr-93	9	1.0	2.0	9,375	62.0	2,044	61.4	9.3
05-May-93	16	1.0	2.0	8,490	63.3	1,105	62.9	15.5
11-May-93	22	2.0	2.0	8,570	69.9	1,550	70.6	10.9
19-May-93	30	3.0	1.5	6,390	76.8	754	75.4	12.9
24-May-93	35	3.0	1.0	5,310	75.5	623	75.5	8.5
02-Jun-93	44	4.0	1.0	6,800	82.9	1,080	80.8	6.5
06-Jun-93	48	4.0	1.0	6,440	83.9			
14-Jun-93	56	4.0	1.0	6,980	84.5	1,155	79.2	6.4
21-Jun-93	63	4.0	1.0	8,760	86.2	790	82.9	11.5
30-Jun-93	72	5.5	1.0	12,400	88.0	913	86.1	13.9
15-Jul-93	87	7.0	1.0	17,910	88.8	1,543	88.0	11.7
28-Jul-93	100	9.0	1.0	15,440	90.7	3,037	88.9	5.2
09-Aug-93	112	9.0	1.0	7,400	89.9	1,923	86.7	4.0
17-Aug-93	120	7.9	2.0	9,720	88.7	2,612	88.4	7.5
24-Aug-93	127	7.5	2.0	7,130	89.7	3,005	89.0	4.8
01-Sep-93	135	5.0	2.0	5,510	90.5	2,708	89.1	4.1
08-Sep-93	142	5.0	2.0	7,940	87.1	3,695	86.5	4.3
17-Sep-93	151	5.0	4.0	9,970	84.8			
23-Sep-93	157	5.0	2.0	7,150	83.5	3,240	87.0	4.2
01-Oct-93	165	5.0	2.0			1,118	85.2	
06-Oct-93	170	5.0	2.0	10,550	87.5	1,665	84.1	13.2
11-Oct-93	175	5.0	2.0			425	75.3	
13-Oct-93	177	5.0	2.0			2,805	88.7	
15-Oct-93	179	5.0	2.0	13,320	83.3	445	74.2	67.2

Table 48. COD data for the sucrose+ garnet test.

Date	Time from Start-Up (days)	HRT (days)	Influent COD (mg/L)	COD Load (g/L/day)	Effluent TCOD (mg/L)	TCOD Removal (%)	Effluent SCOD (mg/L)	SCOD Removal (%)
27-May-93	7	2.0	2,000	1.0	676	66.2	524	73.8
02-Jun-93	13	2.0	4,000	2.0	2,546	36.4	1,687	57.8
14-Jun-93	25	2.0	4,000	2.0	3,324	16.9	828	79.3
21-Jun-93	32	2.0	4,000	2.0	1,603	59.9	737	81.6
30-Jun-93	41	1.5	4,000	2.7	1,419	64.5	1,013	74.7
05-Jul-93	46	1.5	4,000	2.7	1,440	64.0	533	86.7
15-Jul-93	56	1.0	3,500	3.5	2,503	28.5	2,148	38.6
28-Jul-93	69	1.0	3,500	3.5	2,710	22.6	1,928	44.9
09-Aug-93	81	1.0	3,500	3.5	2,164	38.2	1,402	59.9
17-Aug-93	89	1.0	3,500	3.5	2,483	29.1	1,151	67.1
24-Aug-93	96	2.0	7,000	3.5	3,195	54.4	1,880	73.1
01-Sep-93	104	2.0	7,000	3.5	3,159	54.9	1,610	77.0
08-Sep-93	111	2.0	7,000	3.5	3,511	49.8	1,616	76.9
28-Sep-93	131	2.0	7,000	3.5	4,468	36.2	2,898	58.6
06-Oct-93	139	2.0	7,000	3.5	2,797	60.0	2,309	67.0

Table 49. Biogas data for the sucrose + garnet test.

Date	Time (days)	HRT (days)	Nomial COD Load (g/L/day)	Std. Methane Production (L/L/day)
20-May-93	0	2.0	0.5	
21-May-93	1	2.0	0.5	0.00
22-May-93	2	2.0	1.0	0.00
23-May-93	3	2.0	1.0	0.21
24-May-93	4	2.0	1.0	0.18
25-May-93	5	2.0	1.0	0.15
26-May-93	6	2.0	1.0	0.13
27-May-93	7	2.0	1.0	0.11
28-May-93	8	2.0	1.0	0.09
29-May-93	9	2.0	2.0	0.14
30-May-93	10	2.0	2.0	0.17
31-May-93	11	2.0	2.0	0.27
01-Jun-93	12	2.0	2.0	0.17
02-Jun-93	13	2.0	2.0	0.20
03-Jun-93	14	2.0	2.0	0.15
04-Jun-93	15	2.0	2.0	0.23
05-Jun-93	16	2.0	2.0	0.16
06-Jun-93	17	2.0	2.0	0.17
07-Jun-93	18	2.0	2.0	0.19
08-Jun-93	19	2.0	2.0	0.18
09-Jun-93	20	2.0	2.0	0.22
10-Jun-93	21	2.0	2.0	0.12
11-Jun-93	22	2.0	2.0	0.21
12-Jun-93	23	2.0	2.0	0.28
13-Jun-93	24	2.0	2.0	0.26
14-Jun-93	25	2.0	2.0	0.24
15-Jun-93	26	2.0	2.0	0.18
16-Jun-93	27	2.0	2.0	0.32
17-Jun-93	28	2.0	2.0	0.37
18-Jun-93	29	2.0	2.0	0.45
19-Jun-93	30	2.0	2.0	0.39
20-Jun-93	31	2.0	2.0	0.43
21-Jun-93	32	2.0	2.0	0.43
22-Jun-93	33	1.5	2.7	0.47
23-Jun-93	34	1.5	2.7	0.50
24-Jun-93	35	1.5	2.7	0.52
25-Jun-93	36	1.5	2.7	0.45
26-Jun-93	37	1.5	2.7	0.50
27-Jun-93	38	1.5	2.7	0.44
28-Jun-93	39	1.5	2.7	0.40
29-Jun-93	40	1.5	2.7	0.45
30-Jun-93	41	1.5	2.7	0.53
01-Jul-93	42	1.5	2.7	0.56
02-Jul-93	43	1.5	2.7	0.58
03-Jul-93	44	1.5	2.7	0.58

Table 49. (continued).

Date	Time (days)	HRT (days)	Nominal COD Load (g/L/day)	Std. Methane Production (L/L/day)
04-Jul-93	45	1.5	2.7	0.55
05-Jul-93	46	1.5	2.7	0.47
06-Jul-93	47	1.5	2.7	0.45
07-Jul-93	48	1.5	2.7	0.39
08-Jul-93	49	1.0	3.5	0.32
09-Jul-93	50	1.0	3.5	0.26
10-Jul-93	51	1.0	3.5	0.20
11-Jul-93	52	1.0	3.5	0.18
12-Jul-93	53	1.0	3.5	0.15
13-Jul-93	54	1.0	3.5	0.34
14-Jul-93	55	1.0	3.5	0.19
15-Jul-93	56	1.0	3.5	0.17
16-Jul-93	57	1.0	3.5	0.19
17-Jul-93	58	1.0	3.5	0.23
18-Jul-93	59	1.0	3.5	0.24
19-Jul-93	60	1.0	3.5	0.24
20-Jul-93	61	1.0	3.5	0.26
21-Jul-93	62	1.0	3.5	0.35
22-Jul-93	63	1.0	3.5	0.26
23-Jul-93	64	1.0	3.5	0.29
24-Jul-93	65	1.0	3.5	0.30
25-Jul-93	66	1.0	3.5	0.27
26-Jul-93	67	1.0	3.5	0.26
27-Jul-93	68	1.0	3.5	0.29
28-Jul-93	69	1.0	3.5	0.30
29-Jul-93	70	1.0	3.5	0.30
30-Jul-93	71	1.0	3.5	0.34
31-Jul-93	72	1.0	3.5	0.33
01-Aug-93	73	1.0	3.5	0.31
02-Aug-93	74	1.0	3.5	0.30
03-Aug-93	75	1.0	3.5	0.38
04-Aug-93	76	1.0	3.5	0.36
05-Aug-93	77	1.0	3.5	0.45
06-Aug-93	78	1.0	3.5	0.47
07-Aug-93	79	1.0	3.5	0.43
08-Aug-93	80	1.0	3.5	0.54
09-Aug-93	81	1.0	3.5	0.52
10-Aug-93	82	1.0	3.5	0.54
11-Aug-93	83	1.0	3.5	0.54
12-Aug-93	84	1.0	3.5	0.81
13-Aug-93	85	1.0	3.5	0.43
14-Aug-93	86	1.0	3.5	0.55
15-Aug-93	87	1.0	3.5	0.51
16-Aug-93	88	1.0	3.5	0.64
17-Aug-93	89	1.0	3.5	0.41

Table 49. (continued).

Date	Time (days)	HRT (days)	Normal COD Load (g/L/day)	Std. Methane Production (L/L/day)
18-Aug-93	90	1.0	3.5	0.50
19-Aug-93	91	2.0	3.5	0.55
20-Aug-93	92	2.0	3.5	0.51
21-Aug-93	93	2.0	3.5	0.57
22-Aug-93	94	2.0	3.5	0.58
23-Aug-93	95	2.0	3.5	0.61
24-Aug-93	96	2.0	3.5	0.61
25-Aug-93	97	2.0	3.5	0.65
26-Aug-93	98	2.0	3.5	0.19
27-Aug-93	99	2.0	3.5	0.31
28-Aug-93	100	2.0	3.5	0.60
29-Aug-93	101	2.0	3.5	0.63
30-Aug-93	102	2.0	3.5	0.60
31-Aug-93	103	2.0	3.5	0.57
01-Sep-93	104	2.0	3.5	0.59
02-Sep-93	105	2.0	3.5	0.63
03-Sep-93	106	2.0	3.5	0.60
04-Sep-93	107	2.0	3.5	0.63
05-Sep-93	108	2.0	3.5	0.55
06-Sep-93	109	2.0	3.5	0.54
07-Sep-93	110	2.0	3.5	0.54
08-Sep-93	111	2.0	3.5	0.57
09-Sep-93	112	2.0	3.5	0.54
10-Sep-93	113	2.0	3.5	0.54
11-Sep-93	114	4.0	3.5	0.63
12-Sep-93	115	4.0	3.5	0.64
13-Sep-93	116	4.0	3.5	0.58
14-Sep-93	117	4.0	3.5	0.53
15-Sep-93	118	4.0	3.5	0.33
16-Sep-93	119	4.0	3.5	0.47
17-Sep-93	120	4.0	3.5	0.57
18-Sep-93	121	4.0	3.5	0.49
19-Sep-93	122	4.0	3.5	0.46
20-Sep-93	123	4.0	3.5	0.46
21-Sep-93	124	4.0	3.5	0.47
22-Sep-93	125	2.0	3.5	0.43
23-Sep-93	126	2.0	3.5	0.33
24-Sep-93	127	2.0	3.5	0.42
25-Sep-93	128	2.0	3.5	0.36
26-Sep-93	129	2.0	3.5	0.25
27-Sep-93	130	2.0	3.5	0.26
28-Sep-93	131	2.0	3.5	0.29
29-Sep-93	132	2.0	3.5	0.48
30-Sep-93	133	2.0	3.5	0.63
01-Oct-93	134	2.0	3.5	0.63

Table 49. (continued).

Date	Time (days)	HRT (days)	Nomial COD Load (g/L/day)	Std. Methane Production (L/L/day)
02-Oct-93	135	2.0	3.5	0.51
03-Oct-93	136	2.0	3.5	0.58
04-Oct-93	137	2.0	3.5	0.49
05-Oct-93	138	2.0	3.5	0.41
06-Oct-93	139	2.0	3.5	0.41
07-Oct-93	140	2.0	3.5	0.46
08-Oct-93	141	2.0	3.5	0.48
09-Oct-93	142	2.0	3.5	0.46
10-Oct-93	143	2.0	3.5	0.46
11-Oct-93	144	2.0	3.5	0.44
12-Oct-93	145	2.0	3.5	0.52
13-Oct-93	146	2.0	3.5	0.56
14-Oct-93	147	2.0	3.5	0.53
15-Oct-93	148	2.0	3.5	0.58
16-Oct-93	149	2.0	3.5	0.62
17-Oct-93	150	2.0	3.5	0.62
18-Oct-93	151	2.0	3.5	0.63
19-Oct-93	152	2.0	3.5	0.72
20-Oct-93	153	2.0	3.5	0.66
21-Oct-93	154	2.0	3.5	0.62
22-Oct-93	155	2.0	3.5	0.65
23-Oct-93	156	2.0	3.5	0.57
24-Oct-93	157	2.0	3.5	0.65
25-Oct-93	158	2.0	3.5	0.62
26-Oct-93	159	2.0	3.5	0.53
27-Oct-93	160	2.0	3.5	0.39
28-Oct-93	161	2.0	3.5	0.24
29-Oct-93	162	2.0	3.5	0.23
30-Oct-93	163	2.0	3.5	0.20
31-Oct-93	164	2.0	3.5	0.11
01-Nov-93	165	2.0	3.5	0.05
02-Nov-93	166	2.0	3.5	0.03

Table 50. Volatile acids data for the sucrose+ garnet test.

Date	Time from Start (days)	COD Load (g/L/day)	Volatile Acids (mg/L as acetic)
02-Jun-93	13	2.0	1,106
14-Jun-93	25	2.0	523
21-Jun-93	32	2.0	489
30-Jun-93	41	2.7	694
15-Jul-93	56	3.5	1,517
28-Jul-93	69	3.5	1,483
01-Sep-93	104	3.5	1,320
08-Sep-93	111	3.5	1,286
28-Sep-93	131	3.5	1,963

Table 51. Particle size analysis for the sucrose+ garnet test.

Date	Time from Start-up (days)	COD Load (g/L/day)	Average Diameter (arithmetic, μm)	Average Diameter (geometric, μm)
24-May-93	4	1.0	33	150
28-Jul-93	69	3.5	69	300
26-Aug-93	98	3.5	102	450
17-Sep-93	120	3.5	146	600
26-Oct-93	159	3.5	40	500

Table 52. Alkalinity and pH data for the sucrose + garnet test.

Date	Time (days)	COD Load (g/L/day)	Alkalinity (mg/L as CaCO ₃)	pH (units)
23-May-93	1	1.0	2,250	7.08
28-May-93	6	1.0	2,300	6.95
01-Jun-93	10	2.0	2,320	6.64
02-Jun-93	11	2.0	2,400	6.71
05-Jun-93	14	2.0	2,540	6.81
08-Jun-93	17	2.0	2,590	6.80
14-Jun-93	23	2.0	2,540	6.76
21-Jun-93	30	2.0	2,640	6.97
23-Jun-93	32	2.7	2,710	6.77
28-Jun-93	37	2.7	2,760	6.84
30-Jun-93	39	2.7	2,800	6.90
02-Jul-93	41	2.7	2,690	7.00
05-Jul-93	44	2.7	2,740	6.89
12-Jul-93	51	3.5	2,830	6.74
15-Jul-93	54	3.5	2,800	6.64
19-Jul-93	58	3.5	2,810	6.82
23-Jul-93	62	3.5	2,650	6.61
26-Jul-93	65	3.5	2,740	6.67
28-Jul-93	67	3.5	2,700	6.64
05-Aug-93	75	3.5	2,730	6.69
23-Aug-93	93	3.5	2,610	6.72
25-Aug-93	95	3.5	2,580	6.75
01-Sep-93	102	3.5	2,650	6.79
08-Sep-93	109	3.5	2,600	6.83
14-Sep-93	115	3.5	2,760	6.80
20-Sep-93	121	3.5	2,750	6.77
27-Sep-93	128	3.5	2,630	6.56
29-Sep-93	130	3.5	2,780	7.15
04-Oct-93	135	3.5	2,690	6.60
07-Oct-93	138	3.5	2,700	6.79
11-Oct-93	142	3.5	2,820	6.60
13-Oct-93	144	3.5	2,870	6.77

Table 53. Solids data for the sucrose+ garnet test.

Date	Time (days)	COD Load (g/L/day)	HRT (days)	MLSS (mg/L)	MLVSS (% of MLSS)	Effluent TSS (mg/L)	Effluent VSS (% of MLSS)	SRT (days)
24-May-93	4	1.0	2.0	17,800	57.6	4,770	57.0	7.5
02-Jun-93	13	2.0	2.0	10,290	64.2	1,405	64.4	14.6
14-Jun-93	25	2.0	2.0	8,580	71.6	3,385	62.9	5.8
21-Jun-93	32	2.0	2.0	6,740	75.4	1,095	74.7	12.4
30-Jun-93	41	2.7	1.5	6,280	78.6	593	79.0	15.8
15-Jul-93	56	3.5	1.0	8,270	83.2	718	80.6	11.9
28-Jul-93	69	3.5	1.0	9,980	85.9	1,140	81.9	9.2
09-Aug-93	81	3.5	1.0	8,640	89.1	1,118	87.7	7.9
17-Aug-93	89	3.5	1.0	5,310	83.5	1,798	84.3	2.9
24-Aug-93	96	3.5	2.0	5,200	86.2	2,130	85.9	4.9
01-Sep-93	104	3.5	2.0	5,910	85.0	2,225	84.5	5.3
08-Sep-93	111	3.5	2.0	5,020	85.6	2,435	85.7	4.1
17-Sep-93	120	3.5	4.0	6,930	84.9			
23-Sep-93	126	3.5	2.0	4,930	82.0	2,515	84.1	3.8
01-Oct-93	134	3.5	2.0			1,738	82.8	
06-Oct-93	139	3.5	2.0	7,040	84.1	1,290	75.9	12.1
11-Oct-93	144	3.5	2.0			1,005	76.3	
13-Oct-93	146	3.5	2.0			773	81.9	
15-Oct-93	148	3.5	2.0	11,170	84.8	405	76.5	61.1
25-Oct-93	158	3.5	2.0	12,600	84.9			

Table 54. COD data for the sucrose+sand test.

Date	Time from Start-Up (days)	HRT (days)	Influent COD (mg/L)	COD Load (g/L/day)	Effluent TOCD (mg/L)	TCOD Removal (%)	Effluent SCOD (mg/L)	SCOD Removal (%)
27-May-93	7	2.0	2,000	1.0	2,131	0.0	744	62.8
02-Jun-93	13	2.0	4,000	2.0	3,129	21.8	1,932	51.7
14-Jun-93	25	2.0	4,000	2.0	1,897	52.6	1,479	63.0
21-Jun-93	32	2.0	4,000	2.0	1,584	60.4	1,124	71.9
30-Jun-93	41	1.5	4,000	2.7	1,494	62.7	1,248	68.8
05-Jul-93	46	1.5	4,000	2.7	2,123	46.9	1,815	54.6

Table 55. Biogas data for the sucrose+ sand test.

Date	Time (days)	HRT (days)	Nominal COD Load (g/L/day)	Methane (% of total)	Std. Methane Production (L/L/day)
20-May-93	0	2.0	0.5		
21-May-93	1	2.0	0.5	60.38	0.13
22-May-93	2	2.0	1.0	60.38	0.07
23-May-93	3	2.0	1.0	60.38	0.08
24-May-93	4	2.0	1.0	61.36	0.04
25-May-93	5	2.0	1.0	62.35	0.08
26-May-93	6	2.0	1.0	63.33	0.08
27-May-93	7	2.0	1.0	61.26	0.22
28-May-93	8	2.0	1.0	59.19	0.20
29-May-93	9	2.0	2.0	57.12	0.20
30-May-93	10	2.0	2.0	55.05	0.17
31-May-93	11	2.0	2.0	52.97	0.18
01-Jun-93	12	2.0	2.0	50.90	0.19
02-Jun-93	13	2.0	2.0	48.83	0.19
03-Jun-93	14	2.0	2.0	46.76	0.13
04-Jun-93	15	2.0	2.0	47.56	0.20
05-Jun-93	16	2.0	2.0	48.37	0.24
06-Jun-93	17	2.0	2.0	49.17	0.26
07-Jun-93	18	2.0	2.0	49.58	0.25
08-Jun-93	19	2.0	2.0	49.99	0.25
09-Jun-93	20	2.0	2.0	50.41	0.28
10-Jun-93	21	2.0	2.0	50.82	0.26
11-Jun-93	22	2.0	2.0	51.23	0.27
12-Jun-93	23	2.0	2.0	51.64	0.31
13-Jun-93	24	2.0	2.0	52.06	0.27
14-Jun-93	25	2.0	2.0	52.47	0.25
15-Jun-93	26	2.0	2.0	52.88	0.26
16-Jun-93	27	2.0	2.0	50.18	0.28
17-Jun-93	28	2.0	2.0	47.47	0.29
18-Jun-93	29	2.0	2.0	44.77	0.17
19-Jun-93	30	2.0	2.0	42.06	0.23
20-Jun-93	31	2.0	2.0	43.53	0.26
21-Jun-93	32	2.0	2.0	45.00	0.26
22-Jun-93	33	1.5	2.7	46.48	0.32
23-Jun-93	34	1.5	2.7	47.95	0.36
24-Jun-93	35	1.5	2.7	49.42	0.41

Table 55. (continued).

Date	Time (days)	HRT (days)	Nominal COD Load (g/L/day)	Methane (% of total)	Std. Methane Production (L/L/day)
25-Jun-93	36	1.5	2.7	50.89	0.39
26-Jun-93	37	1.5	2.7	52.36	0.50
27-Jun-93	38	1.5	2.7	53.84	0.46
28-Jun-93	39	1.5	2.7	55.31	0.46
29-Jun-93	40	1.5	2.7	56.78	0.48
30-Jun-93	41	1.5	2.7	56.24	0.45
01-Jul-93	42	1.5	2.7	55.70	0.45
02-Jul-93	43	1.5	2.7	55.16	0.39
03-Jul-93	44	1.5	2.7	55.16	0.37
04-Jul-93	45	1.5	2.7	55.16	0.30
05-Jul-93	46	1.5	2.7	55.16	0.21
06-Jul-93	47	1.5	2.7	55.16	0.17
07-Jul-93	48	1.5	2.7	55.16	0.14

Table 56. Volatile acids data for the sucrose + sand test.

Date	Time from Start (days)	COD Load (g/L/day)	Volatile Acids (mg/L as acetic)
02-Jun-93	13	2.0	1,286
14-Jun-93	25	2.0	1,029
21-Jun-93	32	2.0	763
30-Jun-93	41	2.7	1,389

Table 57. Alkalinity and pH data for the sucrose + sand test.

Date	Time (days)	COD Load (g/L/day)	Alkalinity (mg/L as CaCO ₃)	pH (units)
23-May-93	1	1.0	1,870	7.08
28-May-93	6	1.0	1,900	7.08
01-Jun-93	10	2.0	2,130	6.59
02-Jun-93	11	2.0	2,460	6.72
05-Jun-93	14	2.0	2,150	6.76
08-Jun-93	17	4.0	2,210	6.79
14-Jun-93	23	2.0	2,240	6.69
21-Jun-93	30	2.0	2,080	7.02
23-Jun-93	32	2.7	1,950	6.68
28-Jun-93	37	2.7	1,790	6.86
30-Jun-93	39	2.7	1,780	6.90
02-Jul-93	41	2.7	1,800	6.83
05-Jul-93	44	2.7	1,870	6.76

Table 58. Solids data for the sucrose+ sand test.

Date	Time (days)	COD Load (g/L/day)	HRT (days)	MLSS (mg/L)	MLVSS (% of MLSS)	Effluent TSS (mg/L)	Effluent VSS (% of TSS)	SRT (days)
20-May-93	0	1.0	2.0	18,880				
24-May-93	4	1.0	2.0	10,450	58.6	4,920	61.1	4.1
02-Jun-93	13	2.0	2.0	8,810	66.7	1,655	65.9	10.8
14-Jun-93	25	2.0	2.0	7,230	74.7	720	68.1	22.0
21-Jun-93	32	2.0	2.0	7,190	78.2	688	74.4	22.0
30-Jun-93	41	2.7	1.5	6,370	82.9	698	83.5	13.6

Table 59. COD data for the sucrose+cationic polymer test.

Date	DAY (days)	HRT (days)	Influent		Effluent		TCOD	Effluent	SCOD
			COD (mg/L)	COD Load (g/L/day)	TCOD (mg/L)	Removal (%)	Removal (%)	SCOD (mg/L)	Removal (%)
18-Nov-93	6	2	2,000	1.0				400	80.0
22-Nov-93	10	1	2,000	2.0	762	61.9		620	69.0
02-Dec-93	20	1	2,000	2.0	678	66.1		520	74.0
07-Dec-93	25	1	2,000	2.0	851	57.5		550	72.5
17-Dec-93	35	1	3,000	3.0	1,508	49.7		324	89.2
06-Jan-94	55	1	4,000	4.0	795	80.1		84	97.9
14-Jan-94	63	1	6,000	6.0	1,410	76.5		366	93.9
24-Jan-94	73	1	8,000	8.0	2,236	72.1		224	97.2
28-Jan-94	77	1	8,000	8.0	2,060	74.3		252	96.9
08-Feb-94	88	1	8,000	8.0	2,197	72.5		316	96.1
18-Feb-94	98	1	8,000	8.0	1,607	79.9		58	99.3
28-Feb-94	108	1	10,000	10.0	1,835	81.7		176	98.2
07-Mar-94	115	1	14,000	14.0	7,806	44.2		5,009	64.2
12-Mar-94	120	1	8,000	8.0	3,933	50.8		1,450	81.9
18-Mar-94	126	1	8,000	8.0	1,695	78.8		320	96.0
28-Mar-94	136	1	10,000	10.0	1,506	84.9		286	97.1
04-Apr-94	143	1	12,000	12.0	3,179	73.5		234	98.1
14-Apr-94	153	1	14,000	14.0	1,955	86.0		350	97.5
21-Apr-94	160	1	17,000	17.0	5,698	66.5		1,943	88.6
28-Apr-94	167	1	17,000	17.0	8,435	50.4		4,744	72.1
05-May-94	174	1	20,000	20.0	13,564	32.2		9,766	51.2

Table 60. Biogas data for the sucrose+ cationic polymer test.

Date	Day	HRT (days)	Nominal COD Load (g/L/day)	Methane (% of total)	Std. Methane Production (L/L/day)
10-Nov-93	0	2	1		
11-Nov-93	1	2	1	69.39	0.04
12-Nov-93	2	2	1	69.39	0.05
13-Nov-93	3	2	1	69.39	0.02
14-Nov-93	4	2	1	69.39	0.12
15-Nov-93	5	2	1	69.39	0.13
16-Nov-93	6	2	1	69.39	0.15
17-Nov-93	7	2	1	69.54	0.21
18-Nov-93	8	2	1	69.68	0.22
19-Nov-93	9	1	2	69.55	0.24
20-Nov-93	10	1	2	69.42	0.33
21-Nov-93	11	1	2	69.28	0.29
22-Nov-93	12	1	2	69.15	0.30
23-Nov-93	13	1	2	69.02	0.28
24-Nov-93	14	1	2	69.02	0.34
25-Nov-93	15	1	2	69.02	0.27
26-Nov-93	16	1	2	69.02	0.34
27-Nov-93	17	1	2	69.02	0.33
28-Nov-93	18	1	2	69.02	0.23
29-Nov-93	19	1	2	69.02	0.51
30-Nov-93	20	1	2	69.17	0.31
01-Dec-93	21	1	2	69.32	0.43
02-Dec-93	22	1	2	69.47	0.36
03-Dec-93	23	1	2	69.62	0.35
04-Dec-93	24	1	2	69.77	0.35
05-Dec-93	25	1	2	69.92	0.42
06-Dec-93	26	1	2	70.07	0.49
07-Dec-93	27	1	2	70.22	0.33
08-Dec-93	28	1	3	70.37	0.45
09-Dec-93	29	1	3	69.81	0.55
10-Dec-93	30	1	3	69.26	0.63
11-Dec-93	31	1	3	68.70	0.58
12-Dec-93	32	1	3	68.14	0.68
13-Dec-93	33	1	3	67.59	0.69
14-Dec-93	34	1	3	67.03	0.67
15-Dec-93	35	1	3	66.47	0.60
16-Dec-93	36	1	3	65.92	0.82
17-Dec-93	37	1	3	65.36	0.70
18-Dec-93	38	1	3	64.80	0.63
19-Dec-93	39	1	4	64.25	0.79
20-Dec-93	40	1	4	63.69	0.85
21-Dec-93	41	1	4	63.13	0.88
22-Dec-93	42	1	4	62.58	0.86
23-Dec-93	43	1	4	62.02	0.90
24-Dec-93	44	2	4	62.15	0.94

Table 60. (continued).

Date	Day	HRT (days)	Nominal COD Load (g/L/day)	Methane (% of total)	Std. Methane Production (L/L/day)
25-Dec-93	45	2	4	62.27	1.05
26-Dec-93	46	2	4	62.40	1.08
27-Dec-93	47	2	4	62.53	1.05
28-Dec-93	48	2	4	62.66	1.03
29-Dec-93	49	2	4	62.78	1.49
30-Dec-93	50	2	4	62.91	1.10
31-Dec-93	51	2	4	63.04	1.11
01-Jan-94	52	2	4	63.17	1.17
02-Jan-94	53	2	4	63.29	1.18
03-Jan-94	54	2	4	63.42	1.23
04-Jan-94	55	1	4	63.55	1.24
05-Jan-94	56	1	4	63.68	0.97
06-Jan-94	57	1	4	63.80	1.09
07-Jan-94	58	1	4	63.93	1.10
08-Jan-94	59	1	5	63.52	1.23
09-Jan-94	60	1	5	63.11	1.38
10-Jan-94	61	1	6	62.69	1.52
11-Jan-94	62	1	6	62.28	1.65
12-Jan-94	63	1	6	61.87	1.55
13-Jan-94	64	1	6	61.46	1.60
14-Jan-94	65	1	6	61.05	1.58
15-Jan-94	66	1	8	60.63	1.93
16-Jan-94	67	1	8	60.22	2.12
17-Jan-94	68	1	8	59.24	2.19
18-Jan-94	69	1	8	58.26	2.17
19-Jan-94	70	1	8	57.28	1.99
20-Jan-94	71	1	8	55.93	1.88
21-Jan-94	72	1	8	54.59	2.43
22-Jan-94	73	1	8	55.06	2.00
23-Jan-94	74	1	8	55.54	2.16
24-Jan-94	75	1	8	56.01	2.22
25-Jan-94	76	1	8	56.00	2.14
26-Jan-94	77	1	8	55.99	2.16
27-Jan-94	78	1	8	56.78	2.36
28-Jan-94	79	1	8	56.10	2.25
29-Jan-94	80	1	8	55.82	2.25
30-Jan-94	81	1	8	55.55	2.22
31-Jan-94	82	1	8	55.28	2.17
01-Feb-94	83	1	8	55.55	2.13
02-Feb-94	84	1	8	55.81	2.30
03-Feb-94	85	1	8	56.08	2.04
04-Feb-94	86	1	8	56.35	2.30
05-Feb-94	87	1	8	56.62	2.33
06-Feb-94	88	1	8	56.18	1.76
07-Feb-94	89	1	8	55.74	1.82

Table 60. (continued).

Date	Day	HRT (days)	Nominal COD Load (g/L/day)	Methane (% of total)	Std. Methane Production (L/L/day)
08-Feb-94	90	1	8	56.23	2.35
09-Feb-94	91	1	8	56.73	2.22
10-Feb-94	92	1	8	57.22	2.13
11-Feb-94	93	1	8	57.72	2.26
12-Feb-94	94	1	8	57.69	2.19
13-Feb-94	95	1	8	57.66	2.37
14-Feb-94	96	1	8	57.63	2.19
15-Feb-94	97	1	8	57.60	2.24
16-Feb-94	98	1	8	57.57	2.29
17-Feb-94	99	1	8	57.54	2.05
18-Feb-94	100	1	10	57.51	2.28
19-Feb-94	101	1	10	57.48	2.67
20-Feb-94	102	1	10	57.45	2.88
21-Feb-94	103	1	10	57.42	2.95
22-Feb-94	104	1	10	57.39	2.77
23-Feb-94	105	1	10	57.36	2.58
24-Feb-94	106	1	10	57.33	2.72
25-Feb-94	107	1	10	57.30	2.80
26-Feb-94	108	1	10	57.28	2.77
27-Feb-94	109	1	10	57.25	2.68
28-Feb-94	110	1	14	57.22	2.69
01-Mar-94	111	1	14	57.19	3.57
02-Mar-94	112	1	14	57.16	3.89
03-Mar-94	113	1	14	57.13	3.92
04-Mar-94	114	1	14	56.75	3.58
05-Mar-94	115	1	14	56.37	3.36
06-Mar-94	116	1	14	55.99	3.01
07-Mar-94	117	1	8	55.61	2.50
08-Mar-94	118	1	8	55.24	1.91
09-Mar-94	119	1	8	54.86	1.70
10-Mar-94	120	1	8	54.48	2.71
11-Mar-94	121	1	8	54.10	0.58
12-Mar-94	122	1	8	53.72	1.53
13-Mar-94	123	1	8	54.62	1.66
14-Mar-94	124	1	8	55.52	1.81
15-Mar-94	125	1	8	56.42	1.47
16-Mar-94	126	1	8	57.32	2.49
17-Mar-94	127	1	8	57.18	2.04
18-Mar-94	128	1	10	57.04	2.18
19-Mar-94	129	1	10	56.91	2.18
20-Mar-94	130	1	10	56.77	2.19
21-Mar-94	131	1	10	56.64	2.67
22-Mar-94	132	1	10	56.50	2.91
23-Mar-94	133	1	10	56.30	2.91
24-Mar-94	134	1	10	56.10	2.97

Table 60. (continued).

Date	Day	HRT (days)	Nominal COD Load (g/L/day)	Methane (% of total)	Std. Methane Production (L/L/day)
25-Mar-94	135	1	10	55.90	2.88
26-Mar-94	136	1	10	55.71	2.82
27-Mar-94	137	1	10	55.51	2.82
28-Mar-94	138	1	10	55.31	2.60
29-Mar-94	139	1	12	55.11	2.76
30-Mar-94	140	1	12	54.91	3.09
31-Mar-94	141	1	12	54.71	3.49
01-Apr-94	142	1	12	54.52	3.34
02-Apr-94	143	1	12	54.32	3.63
03-Apr-94	144	1	12	54.12	2.98
04-Apr-94	145	1	12	53.92	2.62
05-Apr-94	146	1	14	53.50	3.36
06-Apr-94	147	1	14	53.08	3.50
07-Apr-94	148	1	14	52.66	3.93
08-Apr-94	149	1	14	52.24	2.27
09-Apr-94	150	1	14	51.81	3.08
10-Apr-94	151	1	14	51.39	3.17
11-Apr-94	152	1	14	50.97	1.92
12-Apr-94	153	1	14	51.62	3.92
13-Apr-94	154	1	14	52.26	3.68
14-Apr-94	155	1	17	52.91	3.75
15-Apr-94	156	1	17	51.66	4.22
16-Apr-94	157	1	17	50.42	4.46
17-Apr-94	158	1	17	49.17	4.21
18-Apr-94	159	1	17	47.93	4.08
19-Apr-94	160	1	17	49.67	4.26
20-Apr-94	161	1	17	51.42	4.39
21-Apr-94	162	1	17	51.32	3.99
22-Apr-94	163	1	17	51.21	4.38
23-Apr-94	164	1	17	51.11	3.99
24-Apr-94	165	1	17	51.01	3.94
25-Apr-94	166	1	17	50.91	3.76
26-Apr-94	167	1	17	50.80	3.76
27-Apr-94	168	1	17	50.70	3.66
28-Apr-94	169	1	17	49.22	3.48
29-Apr-94	170	1	17	47.74	3.41
30-Apr-94	171	1	20	46.26	3.13
01-May-94	172	1	20	44.78	3.23
02-May-94	173	1	20	43.31	3.04
03-May-94	174	1	20	41.83	3.36
04-May-94	175	1	20	40.35	2.22
05-May-94	176	1	20	40.35	2.51
06-May-94	177	1	20	40.35	2.50

Table 61. Volatile acids data for the sucrose+cationic polymer test.

Date	Time from Start (days)	COD Load (g/L/day)	Volatile Acids (mg/L as acetic)
22-Nov-93	10	2.0	497
02-Dec-93	20	2.0	377
07-Dec-93	25	2.0	351
17-Dec-93	35	3.0	206
06-Jan-94	55	4.0	51
14-Jan-94	63	6.0	163
24-Jan-94	73	8.0	137
28-Jan-94	77	8.0	77
08-Feb-94	88	8.0	283
18-Feb-94	98	8.0	34
28-Feb-94	108	10.0	51
07-Mar-94	115	14.0	3,754
12-Mar-94	120	8.0	1,123
18-Mar-94	126	8.0	206
28-Mar-94	136	10.0	446
04-Apr-94	143	12.0	69
14-Apr-94	153	14.0	197
21-Apr-94	160	17.0	1,594
28-Apr-94	167	17.0	3,643
05-May-94	174	20.0	5,500

Table 62. Particle size analysis for the sucrose+cationic polymer test.

Date	Time from Start-up (days)	COD Load (g/L/day)	Average Diameter (arithmetic, μm)	Average Diameter (geometric, μm)
08-Nov-93	0	1	31	100
22-Nov-93	14	2	141	300
07-Dec-93	29	4	76	765
06-Jan-94	59	4	186	1,054
21-Jan-94	74	8	415	2,358
18-Feb-94	102	10	313	2,185
12-Mar-94	124	8	153	969
04-Apr-94	147	12	216	661
02-May-94	175	20	250	900

Table 63. Alkalinity and pH for the sucrose+cationic polymer test.

Date	Time (days)	COD Load (g/L/day)	Alkalinity (mg/L as CaCO ₃)	pH (units)
15-Nov-93	6	1	1,200	7.02
18-Nov-93	9	1	1,230	6.95
21-Nov-93	12	2	1,370	6.89
29-Nov-93	20	2	1,400	6.95
02-Dec-93	23	2	1,440	7.03
14-Dec-93	35	3	1,400	6.85
03-Jan-94	55	4	1,300	7.15
06-Jan-94	58	4	1,220	6.90
07-Jan-94	59	5	1,400	6.85
11-Jan-94	63	6	1,680	6.82
14-Jan-94	66	6	1,700	6.88
16-Jan-94	68	8	1,870	6.85
18-Jan-94	70	8	2,130	6.85
19-Jan-94	71	8	2,340	6.90
22-Jan-94	74	8	2,540	6.89
24-Jan-94	76	8	2,810	6.93
25-Jan-94	77	8	2,940	6.85
28-Jan-94	80	8	2,900	6.97
30-Jan-94	82	8	2,880	6.88
08-Feb-94	91	8	2,790	6.84
12-Feb-94	95	8	2,950	6.92
17-Feb-94	100	8	2,900	6.90
18-Feb-94	101	8	2,860	6.85
19-Feb-94	102	10	3,100	7.01
28-Feb-94	111	10	3,140	6.98
01-Mar-94	112	14	3,020	7.01
04-Mar-94	115	14	2,800	6.90
06-Mar-94	117	8	3,340	6.71
11-Mar-94	122	8	3,320	6.90
12-Mar-94	123	8	3,400	6.95
13-Mar-94	124	8	3,360	6.95
18-Mar-94	129	8	3,420	7.06
21-Mar-94	132	10	3,300	7.13
23-Mar-94	134	10	3,270	7.06
28-Mar-94	139	10	3,210	7.03
04-Apr-94	146	12	3,400	7.11
07-Apr-94	149	14	3,360	7.17
11-Apr-94	153	14	3,310	7.05
13-Apr-94	155	14	3,390	7.13
18-Apr-94	160	17	3,450	7.14
25-Apr-94	167	17	3,560	6.54
26-Apr-94	168	17	3,590	6.79
28-Apr-94	170	17	3,520	6.86
02-May-94	174	20	3,500	6.42

Table 64. Solids analysis for the sucrose+cationic polymer test.

Date	Day	COD Load (g/L/day)	HRT (days)	MLSS (mg/L)	MLVSS (% of MLSS)	Effluent TSS (mg/L)	Effluent VSS (% of TSS)	SRT (days)
12-Nov-93	0	1	2	17,600	55.7			
15-Nov-93	3	1	2	5,940	55.9	703	61.4	15.4
22-Nov-93	10	2	1	7,620	59.4	263	74.4	23.1
02-Dec-93	20	2	1	9,280	67.4	260	67.3	35.7
07-Dec-93	25	2	1	9,760	65.8	373	71.2	24.2
17-Dec-93	35	3	1	7,760	74.0	1,213	79.7	5.9
06-Jan-94	55	4	1	10,660	83.3	814	79.5	13.7
14-Jan-94	63	6	1	11,210	84.0	1,203	81.2	9.6
24-Jan-94	73	8	1	14,080	86.9	2,320	83.0	6.4
28-Jan-94	77	8	1	14,380	86.9	1,980	80.1	7.9
08-Feb-94	88	8	1	14,320	86.9	2,048	83.8	7.3
18-Feb-94	98	8	1	17,630	89.0	1,623	85.7	11.3
28-Feb-94	108	10	1	23,580	89.4	1,680	86.0	14.6
07-Mar-94	115	14	1	17,920	90.2	3,295	86.2	5.7
12-Mar-94	120	8	1	13,990	90.4	2,660	87.4	5.4
18-Mar-94	126	8	1	15,360	89.9	1,615	84.2	10.2
28-Mar-94	136	10	1	21,030	90.5	1,475	79.7	16.2
04-Apr-94	143	12	1	25,640	90.7	3,010	85.1	9.1
14-Apr-94	153	14	1	25,820	91.1	1,590	87.6	16.9
21-Apr-94	160	17	1	23,230	91.7	3,860	90.0	6.1
28-Apr-94	167	17	1	24,390	90.5	3,840	88.3	6.5
05-May-94	174	20	1	20,500	89.5	3,950	88.5	5.2

Table 65. COD data for the sucrose+ polyDADM test.

Date	Time from Start-Up (days)	HRT (days)	Influent COD (mg/L)	COD Load (g/L/day)	Effluent TCOD (mg/L)	TCOD Removal (%)	Effluent SCOD (mg/L)	SCOD Removal (%)
18-Nov-93	6	2	2,000	1.0			557	72.2
22-Nov-93	10	1	2,000	2.0	1,574	21.3	733	63.4
02-Dec-93	20	1	2,000	2.0	902	54.9	703	64.9
07-Dec-93	25	1	2,000	2.0	1,315	34.3	944	52.8
17-Dec-93	35	1	2,000	2.0	797	60.2	671	66.5
06-Jan-94	55	1	3,000	3.0	1,376	54.1	1,262	57.9
14-Jan-94	63	1	3,000	3.0	1,692	43.6	1,250	58.3
24-Jan-94	73	1	4,000	4.0	2,325	41.9	1,804	54.9
28-Jan-94	77	1	4,000	4.0	2,933	26.7	2,133	46.7
08-Feb-94	88	1	3,000	3.0	2,069	31.0	1,580	47.3
18-Feb-94	98	1	3,000	3.0	1,917	36.1	880	70.7
28-Feb-94	108	1	3,000	3.0	1,835	38.8	771	74.3
07-Mar-94	115	1	4,000	4.0	1,918	52.1	1,328	66.8
12-Mar-94	120	1	4,000	4.0	2,205	44.9	1,376	65.6
18-Mar-94	126	1	4,000	4.0	2,065	48.4	1,251	68.7
28-Mar-94	136	1	5,000	5.0	2,687	46.3	1,576	68.5
04-Apr-94	143	1	5,000	5.0	2,387	52.3	1,676	66.5
14-Apr-94	153	1	5,000	5.0	2,654	46.9	1,478	70.4
21-Apr-94	160	1	6,000	6.0	3,043	49.3	1,889	68.5
28-Apr-94	167	1	6,000	6.0	2,883	52.0	1,143	81.0
05-May-94	174	1	8,000	8.0	3,990	50.1	3,400	57.5

Table 66. Biogas data for the sucrose+ polyDADM test.

Date	Day	HRT (days)	Nominal COD Load (g/L/day)	Methane (% of total)	Std Methane Production (L/L/day)
10-Nov-93	0	2	1		
11-Nov-93	1	2	1	67.53	0.00
12-Nov-93	2	2	1	67.53	0.00
13-Nov-93	3	2	1	67.53	0.06
14-Nov-93	4	2	1	67.53	0.09
15-Nov-93	5	2	1	67.53	0.11
16-Nov-93	6	2	1	67.53	0.11
17-Nov-93	7	2	1	68.78	0.14
18-Nov-93	8	2	1	70.03	0.14
19-Nov-93	9	1	2	69.69	0.16
20-Nov-93	10	1	2	69.35	0.19
21-Nov-93	11	1	2	69.01	0.19
22-Nov-93	12	1	2	68.67	0.22
23-Nov-93	13	1	2	68.33	0.23
24-Nov-93	14	1	2	68.19	0.24
25-Nov-93	15	1	2	68.06	0.20
26-Nov-93	16	1	2	67.92	0.14
27-Nov-93	17	1	2	67.78	0.22
28-Nov-93	18	1	2	67.65	0.23
29-Nov-93	19	1	2	67.51	0.24
30-Nov-93	20	1	2	67.94	0.23
01-Dec-93	21	1	2	68.37	0.29
02-Dec-93	22	1	2	68.79	0.22
03-Dec-93	23	1	2	69.22	0.20
04-Dec-93	24	1	2	69.65	0.18
05-Dec-93	25	1	2	70.08	0.28
06-Dec-93	26	1	2	70.50	0.38
07-Dec-93	27	1	2	70.93	0.30
08-Dec-93	28	1	2	71.36	0.25
09-Dec-93	29	1	2	70.60	0.23
10-Dec-93	30	1	2	69.84	0.28
11-Dec-93	31	1	2	69.07	0.24
12-Dec-93	32	1	2	68.31	0.29
13-Dec-93	33	1	2	67.55	0.28
14-Dec-93	34	1	2	66.79	0.27
15-Dec-93	35	1	2	66.03	0.24
16-Dec-93	36	1	2	65.26	0.24
17-Dec-93	37	1	2	64.50	0.30
18-Dec-93	38	1	2	63.74	0.25
19-Dec-93	39	1	3	62.98	0.33
20-Dec-93	40	1	3	62.22	0.38
21-Dec-93	41	1	3	61.45	0.37
22-Dec-93	42	1	3	60.69	0.31
23-Dec-93	43	1	3	59.93	0.25
24-Dec-93	44	2	3	59.84	0.32

Table 66. (continued).

Date	Day	HRT (days)	Nominal COD Load (g/L/day)	Methane (% of total)	Std Methane Production (L/L/day)
25-Dec-93	45	2	3	59.76	0.27
26-Dec-93	46	2	3	59.67	0.31
27-Dec-93	47	2	3	59.58	0.30
28-Dec-93	48	2	3	59.49	0.31
29-Dec-93	49	2	3	59.41	0.43
30-Dec-93	50	2	3	59.32	0.39
31-Dec-93	51	2	3	59.23	0.45
01-Jan-94	52	2	3	59.14	0.48
02-Jan-94	53	2	3	59.06	0.50
03-Jan-94	54	2	3	58.97	0.54
04-Jan-94	55	1	3	58.88	0.36
05-Jan-94	56	1	3	58.79	0.23
06-Jan-94	57	1	3	58.71	0.37
07-Jan-94	58	1	3	58.62	0.32
08-Jan-94	59	1	3	57.87	0.33
09-Jan-94	60	1	3	57.12	0.36
10-Jan-94	61	1	3	56.37	0.40
11-Jan-94	62	1	3	55.63	0.37
12-Jan-94	63	1	3	54.88	0.34
13-Jan-94	64	1	3	54.13	0.39
14-Jan-94	65	1	3	53.38	0.35
15-Jan-94	66	1	4	52.63	0.37
16-Jan-94	67	1	4	51.88	0.32
17-Jan-94	68	1	4	53.56	0.36
18-Jan-94	69	1	4	55.23	0.31
19-Jan-94	70	1	4	56.91	0.25
20-Jan-94	71	1	4	51.53	0.28
21-Jan-94	72	1	4	46.15	0.36
22-Jan-94	73	1	4	46.08	0.32
23-Jan-94	74	1	4	46.02	0.32
24-Jan-94	75	1	4	45.95	0.32
25-Jan-94	76	1	4	48.04	0.31
26-Jan-94	77	1	4	50.14	0.36
27-Jan-94	78	1	4	45.13	0.33
28-Jan-94	79	1	4	43.36	0.32
29-Jan-94	80	1	4	47.47	0.30
30-Jan-94	81	1	3	51.59	0.32
31-Jan-94	82	1	3	55.70	0.19
01-Feb-94	83	1	3	56.12	0.24
02-Feb-94	84	1	3	56.55	0.29
03-Feb-94	85	1	3	56.98	0.26
04-Feb-94	86	1	3	57.40	0.26
05-Feb-94	87	1	3	57.83	0.29
06-Feb-94	88	1	3	55.80	0.23
07-Feb-94	89	1	3	53.77	0.23

Table 66. (continued).

Date	Day	HRT (days)	Nominal COD Load (g/L/day)	Methane (% of total)	Std Methane Production (L/L/day)
08-Feb-94	90	1	3	55.77	0.26
09-Feb-94	91	1	3	57.77	0.26
10-Feb-94	92	1	3	59.77	0.30
11-Feb-94	93	1	3	61.77	0.29
12-Feb-94	94	1	3	61.60	0.46
13-Feb-94	95	1	3	61.42	0.26
14-Feb-94	96	1	3	61.24	0.42
15-Feb-94	97	1	3	61.06	0.43
16-Feb-94	98	1	3	60.88	0.39
17-Feb-94	99	1	3	60.70	0.42
18-Feb-94	100	1	3	60.52	0.43
19-Feb-94	101	1	3	60.34	0.52
20-Feb-94	102	1	3	60.16	0.44
21-Feb-94	103	1	3	59.98	0.44
22-Feb-94	104	1	3	59.80	0.46
23-Feb-94	105	1	3	59.63	0.45
24-Feb-94	106	1	3	59.45	0.42
25-Feb-94	107	1	3	59.27	0.44
26-Feb-94	108	1	3	59.09	0.43
27-Feb-94	109	1	3	58.91	0.43
28-Feb-94	110	1	4	58.73	0.42
01-Mar-94	111	1	4	58.55	0.39
02-Mar-94	112	1	4	58.37	0.58
03-Mar-94	113	1	4	58.19	0.41
04-Mar-94	114	1	4	57.87	0.59
05-Mar-94	115	1	4	57.55	0.60
06-Mar-94	116	1	4	57.23	0.60
07-Mar-94	117	1	4	56.91	0.58
08-Mar-94	118	1	4	56.59	0.60
09-Mar-94	119	1	4	56.27	0.65
10-Mar-94	120	1	4	55.95	0.69
11-Mar-94	121	1	4	55.63	0.66
12-Mar-94	122	1	4	55.31	0.71
13-Mar-94	123	1	4	55.79	0.68
14-Mar-94	124	1	4	56.26	0.67
15-Mar-94	125	1	4	56.73	0.66
16-Mar-94	126	1	4	57.21	0.75
17-Mar-94	127	1	4	56.56	0.58
18-Mar-94	128	1	5	55.91	0.67
19-Mar-94	129	1	5	55.26	0.62
20-Mar-94	130	1	5	54.61	0.58
21-Mar-94	131	1	5	53.96	0.67
22-Mar-94	132	1	5	53.32	0.73
23-Mar-94	133	1	5	53.44	0.76
24-Mar-94	134	1	5	53.56	0.72

Table 66. (continued).

Date	Day	HRT (days)	Nominal COD Load (g/L/day)	Methane (% of total)	Std Methane Production (L/L/day)
25-Mar-94	135	1	5	53.68	0.69
26-Mar-94	136	1	5	53.80	0.70
27-Mar-94	137	1	5	53.92	0.71
28-Mar-94	138	1	5	54.04	0.78
29-Mar-94	139	1	5	54.16	0.72
30-Mar-94	140	1	5	54.28	0.86
31-Mar-94	141	1	5	54.40	0.88
01-Apr-94	142	1	5	54.52	0.90
02-Apr-94	143	1	5	54.64	0.95
03-Apr-94	144	1	5	54.76	0.71
04-Apr-94	145	1	5	54.88	0.64
05-Apr-94	146	1	5	54.74	0.76
06-Apr-94	147	1	5	54.59	0.78
07-Apr-94	148	1	5	54.45	0.82
08-Apr-94	149	1	5	54.31	0.76
09-Apr-94	150	1	5	54.17	0.78
10-Apr-94	151	1	5	54.03	0.94
11-Apr-94	152	1	5	53.88	0.39
12-Apr-94	153	1	5	53.90	0.82
13-Apr-94	154	1	5	53.91	0.86
14-Apr-94	155	1	6	53.92	0.89
15-Apr-94	156	1	6	53.60	0.95
16-Apr-94	157	1	6	53.29	0.91
17-Apr-94	158	1	6	52.97	0.91
18-Apr-94	159	1	6	52.66	1.08
19-Apr-94	160	1	6	51.39	1.07
20-Apr-94	161	1	6	50.13	1.03
21-Apr-94	162	1	6	50.37	1.01
22-Apr-94	163	1	6	50.61	1.05
23-Apr-94	164	1	6	50.85	1.02
24-Apr-94	165	1	6	51.08	1.10
25-Apr-94	166	1	6	51.32	0.99
26-Apr-94	167	1	6	51.56	1.17
27-Apr-94	168	1	6	51.80	1.04
28-Apr-94	169	1	7	51.03	1.09
29-Apr-94	170	1	7	50.26	1.26
30-Apr-94	171	1	7	49.49	1.23
01-May-94	172	1	7	48.72	1.20
02-May-94	173	1	8	47.95	1.26
03-May-94	174	1	8	47.18	1.35
04-May-94	175	1	8	46.41	1.36
05-May-94	176	1	8	46.41	1.33
06-May-94	177	1	8	46.41	1.34

Table 67. Volatile acids data for the sucrose+ polyDADM test.

Date	Time from Start (days)	COD Load (g/L/day)	Volatile Acids (mg/L as acetic)
22-Nov-93	10	2.0	548
02-Dec-93	20	2.0	462
07-Dec-93	25	2.0	540
17-Dec-93	35	2.0	454
06-Jan-94	55	3.0	994
14-Jan-94	63	3.0	986
24-Jan-94	73	4.0	1,697
28-Jan-94	77	4.0	1,697
08-Feb-94	88	3.0	1,200
18-Feb-94	98	3.0	677
28-Feb-94	108	4.0	557
07-Mar-94	115	4.0	986
12-Mar-94	120	4.0	951
18-Mar-94	126	5.0	900
28-Mar-94	136	5.0	1,071
04-Apr-94	143	5.0	1,217
14-Apr-94	153	6.0	1,046
21-Apr-94	160	6.0	2,100
28-Apr-94	167	7.0	806
05-May-94	174	8.0	2,000

Table 68. Particle size analysis for the sucrose+ polyDADM test.

Date	Time from Start-up (days)	COD Load (g/L/day)	Average Diameter (arithmetic, μm)	Average Diameter (geometric, μm)
08-Nov-93	0	1	31	100
22-Nov-93	14	2	66	180
07-Dec-93	29	2	47	178
06-Jan-94	59	3	58	287
21-Jan-94	74	4	38	290
18-Feb-94	102	3	56	361
12-Mar-94	124	4	49	268
04-Apr-94	147	5	99	242
02-May-94	175	8	135	367

Table 69. Alkalinity and pH data for the sucrose + polyDADM test.

Date	Time (days)	COD Load (g/L/day)	Alkalinity (mg/L as CaCO ₃)	pH (units)
15-Nov-93	5	1	1,350	7.15
18-Nov-93	8	1	1,410	6.97
21-Nov-93	11	2	1,400	6.95
29-Nov-93	19	2	1,300	7.01
02-Dec-93	22	2	1,360	6.97
14-Dec-93	34	2	1,300	6.98
03-Jan-94	54	3	1,300	6.88
06-Jan-94	57	3	1,300	6.68
07-Jan-94	58	3	1,400	6.75
11-Jan-94	62	3	1,390	6.67
14-Jan-94	65	3	1,460	6.73
16-Jan-94	67	4	2,000	6.73
18-Jan-94	69	4	2,130	6.58
19-Jan-94	70	4	2,250	6.84
22-Jan-94	73	4	2,600	6.54
24-Jan-94	75	4	2,620	6.65
25-Jan-94	76	4	2,710	6.72
28-Jan-94	79	4	2,640	6.68
30-Jan-94	81	3	2,600	6.65
08-Feb-94	90	3	2,650	6.68
12-Feb-94	94	3	2,690	6.80
17-Feb-94	99	3	2,710	6.88
18-Feb-94	100	3	2,860	6.80
19-Feb-94	101	3	2,750	6.97
28-Feb-94	110	4	2,800	6.94
01-Mar-94	111	4	2,790	6.88
04-Mar-94	114	4	2,860	6.78
06-Mar-94	116	4	2,840	6.89
11-Mar-94	121	4	2,910	6.82
12-Mar-94	122	4	2,900	6.92
13-Mar-94	123	4	3,010	6.87
18-Mar-94	128	5	2,910	6.99
21-Mar-94	131	5	2,940	6.91
23-Mar-94	133	5	2,870	6.87
28-Mar-94	138	5	2,780	6.85
04-Apr-94	145	5	2,690	6.88
07-Apr-94	148	5	2,760	6.83
11-Apr-94	152	5	2,800	6.82
13-Apr-94	154	5	2,700	6.90
18-Apr-94	159	6	2,830	6.87
25-Apr-94	166	6	2,750	6.80
26-Apr-94	167	6	2,720	6.85
28-Apr-94	169	7	2,690	6.93
02-May-94	173	8	2,740	6.85

Table 70. Solids data for the sucrose+ polyDADM test.

Date	Time (days)	COD Load (g/L/day)	HRT (days)	MLSS (mg/L)	MLVSS (% of MLSS)	Effluent TSS (mg/L)	Effluent VSS (% of TSS)	SRT (days)
10-Nov-94	0	1	2	18,000	54.7			
15-Nov-93	5	1	2	7,440	54.7	263	85.7	36.1
22-Nov-93	12	2	1	7,370	61.3	1,150	62.0	6.3
02-Dec-93	22	2	1	6,350	71.2	340	68.4	19.4
07-Dec-93	27	2	1	5,250	71.2	450	77.8	10.7
17-Dec-93	37	2	1	6,020	79.6	228	69.9	30.1
06-Jan-94	57	3	1	8,010	86.1	167	71.6	57.7
14-Jan-94	65	3	1	7,490	86.1	505	80.2	15.9
24-Jan-94	75	4	1	9,850	87.5	660	83.7	15.6
28-Jan-94	79	4	1	9,920	86.2	953	83.7	10.7
08-Feb-94	90	3	1	9,600	87.0	825	76.7	13.2
18-Feb-94	100	3	1	9,190	86.7	1,145	84.5	8.2
28-Feb-94	110	3	1	9,420	87.1	1,080	85.4	8.9
07-Mar-94	117	4	1	11,020	88.5	693	84.9	16.6
12-Mar-94	122	4	1	11,490	89.3	890	86.5	13.3
18-Mar-94	128	5	1	9,240	87.9	905	85.4	10.5
28-Mar-94	138	5	1	8,320	89.0	1,205	86.9	7.1
04-Apr-94	145	5	1	9,400	89.0	810	82.8	12.5
14-Apr-94	155	6	1	8,070	89.7	1,185	87.1	7.0
21-Apr-94	162	6	1	7,180	87.9	1,455	85.2	5.1
28-Apr-94	169	7	1	6,800	88.0	1,940	85.0	3.6
05-May-94	176	8	1	7,400	89.0	1,840	86.1	4.2

Table 71. COD data for the sucrose+ferric chloride test.

Date	Time from Start-Up (days)	HRT (days)	Influent COD (mg/L)	COD Load (g/L/day)	Effluent TCOD (mg/L)	TCOD Removal (%)	Effluent SCOD (mg/L)	SCOD Removal (%)
18-Nov-93	6	2	2,000	1.0			817	59.2
22-Nov-93	10	1	2,000	2.0	897	55.2	811	59.5
02-Dec-93	20	1	2,000	2.0	1,085	45.8	825	58.8
07-Dec-93	25	1	2,000	2.0	907	54.7	854	57.3
17-Dec-93	35	1	2,000	2.0	1,303	34.9	1,161	42.0
06-Jan-94	55	1	2,000	2.0	1,384	30.8	1,327	33.7

Table 72. Biogas data for the sucrose+ferric chloride test.

Date	Time from Start-Up (days)	HRT (days)	Nominal COD Load (g/L/day)	Methane (% of total)	Std. Methane Production (L/L/day)
10-Nov-93	0	2	1.0		
11-Nov-93	1	2	1.0	64.15	0.04
12-Nov-93	2	2	1.0	64.15	0.00
13-Nov-93	3	2	1.0	64.15	0.01
14-Nov-93	4	2	1.0	64.15	0.06
15-Nov-93	5	2	1.0	64.15	0.03
16-Nov-93	6	2	1.0	64.15	0.09
17-Nov-93	7	2	1.0	62.10	0.10
18-Nov-93	8	2	1.0	60.05	0.08
19-Nov-93	9	1	2.0	59.40	0.09
20-Nov-93	10	1	2.0	58.74	0.10
21-Nov-93	11	1	2.0	58.09	0.03
22-Nov-93	12	1	2.0	57.43	0.05
23-Nov-93	13	1	2.0	56.78	0.07
24-Nov-93	14	1	2.0	57.44	0.25
25-Nov-93	15	1	2.0	58.10	0.07
26-Nov-93	16	1	2.0	58.76	0.13
27-Nov-93	17	1	2.0	59.42	0.04
28-Nov-93	18	1	2.0	60.08	0.09
29-Nov-93	19	1	2.0	60.74	0.10
30-Nov-93	20	1	2.0	62.10	0.09
01-Dec-93	21	1	2.0	63.46	0.28
02-Dec-93	22	1	2.0	64.82	0.13
03-Dec-93	23	1	2.0	66.18	0.12
04-Dec-93	24	1	2.0	67.53	0.16
05-Dec-93	25	1	2.0	68.89	0.22
06-Dec-93	26	1	2.0	70.25	0.09
07-Dec-93	27	1	2.0	71.61	0.12
08-Dec-93	28	1	2.0	72.97	0.18
09-Dec-93	29	1	2.0	72.07	0.11
10-Dec-93	30	1	2.0	71.16	0.16
11-Dec-93	31	1	2.0	70.26	0.08
12-Dec-93	32	1	2.0	69.35	0.04
13-Dec-93	33	1	2.0	68.45	0.21
14-Dec-93	34	1	2.0	67.55	0.09
15-Dec-93	35	1	2.0	66.64	0.04
16-Dec-93	36	1	2.0	65.74	0.10
17-Dec-93	37	1	2.0	64.83	0.06
18-Dec-93	38	1	2.0	63.93	0.12
19-Dec-93	39	1	2.0	63.03	0.06
20-Dec-93	40	1	2.0	62.12	0.15
21-Dec-93	41	1	2.0	61.22	0.11
22-Dec-93	42	1	2.0	60.31	0.18

Table 72. (continued).

Date	Time from Start-Up (days)	HRT (days)	Nominal COD Load (g/L/day)	Methane (% of total)	Std. Methane Production (L/L/day)
23-Dec-93	43	1	2.0	59.41	0.11
24-Dec-93	44	2	2.0	59.41	0.15
25-Dec-93	45	2	2.0	59.41	0.08
26-Dec-93	46	2	2.0	59.41	0.06
27-Dec-93	47	2	2.0	59.41	0.17
28-Dec-93	48	2	2.0	59.41	0.02
29-Dec-93	49	2	2.0	59.41	0.00
30-Dec-93	50	2	2.0	59.41	0.03
31-Dec-93	51	2	2.0	59.41	0.03
01-Jan-94	52	2	2.0	59.41	0.00
02-Jan-94	53	2	2.0	59.41	0.00
03-Jan-94	54	2	2.0	59.41	0.00
04-Jan-94	55	1	2.0	59.41	0.04
05-Jan-94	56	1	2.0	59.41	0.00
06-Jan-94	57	1	2.0	59.41	0.00
07-Jan-94	58	1	2.0	59.41	0.00

Table 73. Volatile acids data for the sucrose+ ferric chloride test.

Date	Time from Start-Up (days)	COD Load (g/L/day)	Volatile Acids (mg/L as acetic)
22-Nov-93	12	2.0	685
02-Dec-93	22	2.0	642
07-Dec-93	27	2.0	669
17-Dec-93	37	2.0	849
06-Jan-94	57	2.0	1,011

Table 74. Particle size analysis for the sucrose+ ferric chloride test.

Date	Time from Start-up (days)	COD Load (g/L/day)	Average Diameter (arithmetic, μm)	Average Diameter (geometric, μm)
08-Nov-93	0	1	31	100
22-Nov-93	14	2	66	223
07-Dec-93	29	2	42	204
06-Jan-94	59	2	53	160

Table 75. Alkalinity and pH for the sucrose+ ferric chloride test.

Date	Time (days)	COD Load (g/L/day)	Alkalinity (mg/L as CaCO_3)	pH (units)
15-Nov-93	6	1	1,400	7.04
18-Nov-93	9	1	1,380	6.86
21-Nov-93	12	2	1,340	6.81
29-Nov-93	20	2	1,320	6.82
02-Dec-93	23	2	1,300	7.01
14-Dec-93	35	2	1,410	6.77
03-Jan-94	55	2	1,300	6.87
06-Jan-94	58	2	1,260	6.75

Table 76. Solids data for the sucrose+ ferric chloride test.

Date	Day	COD Load (g/L/day)	HRT (days)	MLSS (mg/L)	MLVSS (% of MLSS)	Effluent TSS (mg/L)	Effluent VSS (% of TSS)	SRT (days)
12-Nov-93	0	1	2	17,880	54.3			
15-Nov-93	3	1	2	8,310	54.6	265	72.1	47.5
22-Nov-93	10	2	1	6,270	61.4	220	58.0	30.2
02-Dec-93	20	2	1	6,410	71.1	420	66.1	16.4
07-Dec-93	25	2	1	6,950	71.5	173	55.0	52.2
17-Dec-93	35	2	1	7,720	71.9	255	66.7	32.6
06-Jan-94	55	2	1	7,580	76.4	144	70.7	56.9

Table 77. COD data for the beef/glucose control test.

Date	DAY (days)	HRT (days)	Influent COD (mg/L)	COD Load (g/L/day)	Effluent TCOD (mg/L)	TCOD Removal (%)	Effluent SCOD (mg/L)	SCOD Removal (%)
24-Jan-94	7	2	2,000	1.0	873	56.4	686	65.7
28-Jan-94	11	1	2,000	2.0	1,196	40.2	937	53.2
08-Feb-94	22	1	2,000	2.0	1,693	15.4	767	61.7
18-Feb-94	32	2	5,500	2.8	2,803	49.0	1,938	64.8
28-Feb-94	42	2	4,000	2.0	2,510	37.3	1,835	54.1
07-Mar-94	49	1	2,000	2.0	1,853	7.4	788	60.6
12-Mar-94	54	1	2,000	2.0	1,667	16.7	837	58.2
18-Mar-94	60	1	2,000	2.0	1,207	39.7	764	61.8
28-Mar-94	70	1	3,000	3.0	1,533	48.9	1,039	65.4
04-Apr-94	77	1	3,000	3.0	1,488	50.4	803	73.2
14-Apr-94	87	1	4,000	4.0	2,336	41.6	1,415	64.6
21-Apr-94	94	1	4,000	4.0	1,981	50.5	1,300	67.5
28-Apr-94	101	1	4,000	4.0	1,695	57.6	820	79.5
05-May-94	108	1	6,000	6.0	3,240	46.0	1,580	73.7

Table 78. Biogas data for the beef/glucose control test.

Date	Day	HRT (days)	Nominal COD Load (g/L/day)	Methane (% of total)	Std. Methane Production (L/L/day)
17-Jan-94	0	2	1.0		
18-Jan-94	1	2	1.0	77.91	0.02
19-Jan-94	2	2	1.0	77.91	0.08
20-Jan-94	3	2	1.0	82.16	0.11
21-Jan-94	4	2	1.0	86.41	0.08
22-Jan-94	5	2	1.0	83.98	0.06
23-Jan-94	6	2	1.0	81.55	0.09
24-Jan-94	7	2	1.0	79.12	0.14
25-Jan-94	8	2	1.0	80.03	0.20
26-Jan-94	9	1	2.0	80.94	0.19
27-Jan-94	10	1	2.0	76.91	0.23
28-Jan-94	11	1	2.0	74.14	0.22
29-Jan-94	12	1	2.0	74.18	0.26
30-Jan-94	13	1	2.0	74.22	0.31
31-Jan-94	14	1	2.0	74.26	0.31
01-Feb-94	15	1	2.0	75.11	0.29
02-Feb-94	16	1	2.0	75.96	0.29
03-Feb-94	17	1	2.0	76.82	0.25
04-Feb-94	18	1	2.0	77.67	0.36
05-Feb-94	19	1	2.0	78.52	0.29
06-Feb-94	20	1	2.0	78.59	0.24
07-Feb-94	21	1	2.0	78.66	0.25
08-Feb-94	22	1	2.0	76.97	0.33
09-Feb-94	23	1	2.0	75.28	0.30
10-Feb-94	24	1	2.0	73.58	0.26
11-Feb-94	25	1	2.0	71.89	0.28
12-Feb-94	26	1	2.0	71.90	0.29
13-Feb-94	27	1	2.0	71.92	0.17
14-Feb-94	28	1	2.0	71.93	0.17
15-Feb-94	29	2	2.0	71.95	0.21
16-Feb-94	30	2	2.0	71.96	0.16
17-Feb-94	31	2	2.0	71.98	0.18
18-Feb-94	32	2	2.0	71.99	0.17
19-Feb-94	33	2	2.0	72.01	0.17
20-Feb-94	34	2	2.0	72.02	0.19
21-Feb-94	35	2	2.0	72.03	0.21
22-Feb-94	36	2	2.0	72.05	0.19
23-Feb-94	37	2	2.0	72.06	0.20
24-Feb-94	38	2	2.0	72.08	0.19
25-Feb-94	39	2	2.0	72.09	0.16
26-Feb-94	40	2	2.0	72.11	0.24
27-Feb-94	41	2	2.0	72.12	0.21
28-Feb-94	42	2	2.0	72.14	0.25
01-Mar-94	43	1	2.0	72.15	0.13
02-Mar-94	44	1	2.0	72.17	0.22

Table 78. (continued).

Date	Day	HRT (days)	Nominal COD Load (g/L/day)	Methane (% of total)	Std. Methane Production (L/L/day)
03-Mar-94	45	1	2.0	72.18	0.18
04-Mar-94	46	1	2.0	72.18	0.18
05-Mar-94	47	1	2.0	72.19	0.14
06-Mar-94	48	1	2.0	72.19	0.22
07-Mar-94	49	1	2.0	72.20	0.17
08-Mar-94	50	1	2.0	72.20	0.18
09-Mar-94	51	1	2.0	72.21	0.20
10-Mar-94	52	1	2.0	72.21	0.27
11-Mar-94	53	1	2.0	72.22	0.15
12-Mar-94	54	1	2.0	72.22	0.18
13-Mar-94	55	1	2.0	72.39	0.23
14-Mar-94	56	1	2.0	72.56	0.28
15-Mar-94	57	1	2.0	72.72	0.20
16-Mar-94	58	1	2.0	72.89	0.27
17-Mar-94	59	1	2.0	71.89	0.26
18-Mar-94	60	1	2.0	70.88	0.26
19-Mar-94	61	1	3.0	69.88	0.30
20-Mar-94	62	1	3.0	68.88	0.23
21-Mar-94	63	1	3.0	67.87	0.33
22-Mar-94	64	1	3.0	66.87	0.43
23-Mar-94	65	1	3.0	67.09	0.42
24-Mar-94	66	1	3.0	67.31	0.46
25-Mar-94	67	1	3.0	67.54	0.35
26-Mar-94	68	1	3.0	67.76	0.44
27-Mar-94	69	1	3.0	67.98	0.42
28-Mar-94	70	1	3.0	68.20	0.42
29-Mar-94	71	1	3.0	68.43	0.50
30-Mar-94	72	1	3.0	68.65	0.48
31-Mar-94	73	1	3.0	68.87	0.63
01-Apr-94	74	1	3.0	69.09	0.53
02-Apr-94	75	1	3.0	69.32	0.55
03-Apr-94	76	1	3.0	69.54	0.55
04-Apr-94	77	1	3.0	69.76	0.62
05-Apr-94	78	1	3.0	69.19	0.68
06-Apr-94	79	1	4.0	68.61	0.78
07-Apr-94	80	1	4.0	68.04	0.79
08-Apr-94	81	1	4.0	67.47	0.83
09-Apr-94	82	1	4.0	66.90	0.78
10-Apr-94	83	1	4.0	66.32	0.85
11-Apr-94	84	1	4.0	65.75	0.28
12-Apr-94	85	1	4.0	65.88	0.63
13-Apr-94	86	1	4.0	66.00	0.61
14-Apr-94	87	1	4.0	66.13	0.51
15-Apr-94	88	1	4.0	66.00	0.44
16-Apr-94	89	1	4.0	65.87	0.59

Table 78. (continued).

Date	Day	HRT (days)	Nominal COD Load (g/L/day)	Methane (% of total)	Std. Methane Production (L/L/day)
17-Apr-94	90	1	4.0	65.74	0.48
18-Apr-94	91	1	4.0	65.61	0.48
19-Apr-94	92	1	4.0	64.37	0.54
20-Apr-94	93	1	4.0	63.12	0.51
21-Apr-94	94	1	4.0	63.97	0.46
22-Apr-94	95	1	4.0	64.83	0.60
23-Apr-94	96	1	4.0	65.68	0.54
24-Apr-94	97	1	4.0	66.54	0.54
25-Apr-94	98	1	4.0	67.39	0.55
26-Apr-94	99	1	4.0	68.25	0.59
27-Apr-94	100	1	4.0	69.10	0.60
28-Apr-94	101	1	4.0	69.95	0.72
29-Apr-94	102	1	5.0	69.84	0.91
30-Apr-94	103	1	5.0	69.72	0.96
01-May-94	104	1	5.0	69.60	0.98
02-May-94	105	1	5.0	69.48	1.05
03-May-94	106	1	6.0	69.36	1.14
04-May-94	107	1	6.0	68.27	1.26
05-May-94	108	1	6.0	68.27	1.23
06-May-94	109	1	6.0	68.27	1.26

Table 79. Volatile acids data for the beef/glucose control test.

Date	Time from Start (days)	COD Load (g/L/day)	Volatile Acids (mg/L as acetic)
24-Jan-94	7	1.0	497
28-Jan-94	11	2.0	634
08-Feb-94	22	2.0	523
18-Feb-94	32	2.8	1,603
28-Feb-94	42	2.0	1,397
07-Mar-94	49	2.0	669
12-Mar-94	54	2.0	677
18-Mar-94	60	2.0	523
28-Mar-94	70	3.0	711
04-Apr-94	77	3.0	617
14-Apr-94	87	4.0	943
21-Apr-94	94	4.0	883
28-Apr-94	101	4.0	557
05-May-94	108	6.0	987

Table 80. Particle size analysis for the beef/glucose control test.

Date	Time from Start-up (days)	COD Load (g/L/day)	Average Diameter (arithmetic, μm)	Average Diameter (geometric, μm)
17-Jan-94	0	1	34	231
18-Feb-94	32	2	34	330
12-Mar-94	54	2	40	420
04-Apr-94	77	3	53	440
02-May-94	105	6	111	490

Table 81. Alkalinity and pH for the beef/glucose control test.

Date	Time (days)	COD Load (g/L/day)	Alkalinity (mg/L as CaCO ₃)	pH (units)
18-Jan-94	1	1	2,650	7.63
19-Jan-94	2	1	2,710	7.44
22-Jan-94	5	1	2,690	7.32
24-Jan-94	7	1	2,640	7.31
25-Jan-94	8	1	2,600	7.22
28-Jan-94	11	2	2,700	7.11
30-Jan-94	13	2	2,650	7.03
08-Feb-94	22	2	2,700	6.98
12-Feb-94	26	3	2,750	7.00
17-Feb-94	31	3	2,800	6.86
18-Feb-94	32	3	2,790	6.90
19-Feb-94	33	4	2,780	7.01
28-Feb-94	42	3	2,690	7.00
01-Mar-94	43	3	2,750	7.05
04-Mar-94	46	3	2,810	7.03
06-Mar-94	48	3	2,710	7.14
11-Mar-94	53	3	2,750	7.06
12-Mar-94	54	3	2,700	7.16
13-Mar-94	55	3	2,720	7.08
18-Mar-94	60	4	2,730	7.13
21-Mar-94	63	4	2,790	7.08
23-Mar-94	65	4	2,850	6.99
28-Mar-94	70	4	2,810	6.89
04-Apr-94	77	5	2,790	7.02
07-Apr-94	80	6	2,860	6.97
11-Apr-94	84	6	2,820	6.93
13-Apr-94	86	6	2,850	6.93
18-Apr-94	91	6	2,760	6.93
25-Apr-94	98	6	2,730	6.96
26-Apr-94	99	6	2,790	7.00
28-Apr-94	101	7	2,810	7.04
02-May-94	105	8	2,800	7.08

Table 82. Solids analysis for beef/glucose control test.

Date	Day	COD Load (g/L/day)	HRT (days)	MLSS (mg/L)	MLVSS (% of MLSS)	Effluent TSS (mg/L)	Effluent VSS (% of TSS)	SRT (days)
17-Jan-94	0	1	2	24,953	57.0			
24-Jan-94	7	1	2	7,460	57.0	233	52.7	69.3
28-Jan-94	11	2	1	8,210	61.0	418	51.5	23.3
08-Feb-94	22	2	1	6,740	63.4	1,053	70.8	5.7
18-Feb-94	32	2	2	5,600	77.5	803	71.4	15.1
28-Feb-94	42	2	2	8,560	82.3	715	73.8	26.7
07-Mar-94	49	2	1	6,800	83.4	763	80.0	9.3
12-Mar-94	54	2	1	6,290	83.2	552	81.2	11.7
18-Mar-94	60	2	1	6,510	83.8	438	74.3	16.8
28-Mar-94	70	3	1	6,390	83.9	488	73.9	14.9
04-Apr-94	77	3	1	6,290	84.9	640	77.8	10.7
14-Apr-94	87	4	1	3,720	81.2	755	79.8	5.0
21-Apr-94	94	4	1	4,550	82.5	663	84.6	6.7
28-Apr-94	101	4	1	6,480	82.0	888	83.0	7.2
05-May-94	108	6	1	6,900	83.1	925	82.3	7.5

Table 83. COD data for the beef/glucose+cationic polymer test.

Date	DAY (days)	HRT (days)	Influent COD (mg/L)	COD Load (g/L/day)	Effluent TCOD (mg/L)	TCOD Removal (%)	Effluent SCOD (mg/L)	SCOD Removal (%)
24-Jan-94	7	2	2,000	1.0	373	81.4	246	87.7
28-Jan-94	11	1	2,000	2.0	556	72.2	459	77.1
08-Feb-94	22	1	2,000	2.0	602	69.9	459	77.1
18-Feb-94	32	1	3,500	3.5	674	80.7	443	87.3
28-Feb-94	42	1	4,500	4.5	2,319	48.5	1,681	62.6
07-Mar-94	49	1	6,500	6.5	2,422	62.7	2,247	65.4
12-Mar-94	54	1	3,000	3.0	1,354	54.9	1,256	58.1
18-Mar-94	60	1	3,000	3.0	975	67.5	815	72.8
28-Mar-94	70	1	4,000	4.0	896	77.6	767	80.8
04-Apr-94	77	1	5,000	5.0	1,956	60.9	460	90.8
14-Apr-94	87	1	6,500	6.5	4,553	30.0	3,088	52.5
21-Apr-94	94	1	6,500	6.5	3,453	46.9	2,013	69.0
28-Apr-94	101	1	6,500	6.5	2,438	62.5	1,733	73.3
05-May-94	108	1	8,000	8.0	3,500	56.3	3,100	61.3

Table 84. Biogas data for the beef/glucose+ cationic polymer test.

Date	Day	HRT (days)	Nominal COD Load (g/L/day)	Methane (% of total)	Std. Methane Production (L/L/day)
17-Jan-94	0	2	1.0		
18-Jan-94	1	2	1.0	80.06	0.08
19-Jan-94	2	2	1.0	80.06	0.16
20-Jan-94	3	2	1.0	83.13	0.18
21-Jan-94	4	2	1.0	86.20	0.25
22-Jan-94	5	2	1.0	84.93	0.25
23-Jan-94	6	2	1.0	83.65	0.26
24-Jan-94	7	2	1.0	82.38	0.24
25-Jan-94	8	2	1.0	81.52	0.27
26-Jan-94	9	1	2.0	80.65	0.34
27-Jan-94	10	1	2.0	78.29	0.45
28-Jan-94	11	1	2.0	78.02	0.50
29-Jan-94	12	1	2.0	77.93	0.43
30-Jan-94	13	1	2.0	77.84	0.46
31-Jan-94	14	1	2.0	77.75	0.48
01-Feb-94	15	1	2.0	77.59	0.50
02-Feb-94	16	1	2.0	77.44	0.61
03-Feb-94	17	1	2.0	77.28	0.68
04-Feb-94	18	1	2.0	77.13	0.47
05-Feb-94	19	1	2.0	76.97	0.53
06-Feb-94	20	1	2.0	77.06	0.45
07-Feb-94	21	1	2.0	77.15	0.49
08-Feb-94	22	1	2.0	77.60	0.68
09-Feb-94	23	1	3.0	78.05	0.72
10-Feb-94	24	1	3.0	78.49	0.78
11-Feb-94	25	1	3.0	78.94	0.96
12-Feb-94	26	1	3.0	78.24	0.92
13-Feb-94	27	1	3.0	77.54	0.91
14-Feb-94	28	1	3.0	76.84	0.53
15-Feb-94	29	1	4.5	76.14	1.14
16-Feb-94	30	1	4.5	75.44	0.99
17-Feb-94	31	1	4.5	74.74	1.01
18-Feb-94	32	1	4.5	74.04	0.93
19-Feb-94	33	1	4.5	73.34	1.18
20-Feb-94	34	1	4.5	72.64	1.08
21-Feb-94	35	1	4.5	71.94	1.00
22-Feb-94	36	1	4.5	71.25	1.12
23-Feb-94	37	1	4.5	70.55	1.12
24-Feb-94	38	1	4.5	69.85	1.01
25-Feb-94	39	1	4.5	69.15	0.97
26-Feb-94	40	1	4.5	68.45	0.71
27-Feb-94	41	1	4.5	67.75	0.53
28-Feb-94	42	1	4.5	67.05	0.37
01-Mar-94	43	2	3.0	66.35	0.26
02-Mar-94	44	2	3.0	65.65	0.32

Table 84. (continued).

Date	Day	HRT (days)	Nominal COD Load (g/L/day)	Methane (% of total)	Std. Methane Production (L/L/day)
03-Mar-94	45	2	3.0	62.27	0.30
04-Mar-94	46	2	3.0	62.40	0.38
05-Mar-94	47	2	3.0	62.53	0.36
06-Mar-94	48	2	3.0	62.66	0.38
07-Mar-94	49	2	3.0	62.78	0.35
08-Mar-94	50	1	3.0	62.91	0.35
09-Mar-94	51	1	3.0	63.04	0.35
10-Mar-94	52	1	3.0	63.17	0.20
11-Mar-94	53	1	3.0	63.29	0.18
12-Mar-94	54	1	3.0	63.42	0.29
13-Mar-94	55	1	3.0	63.55	0.28
14-Mar-94	56	1	3.0	63.68	0.38
15-Mar-94	57	1	3.0	63.80	0.32
16-Mar-94	58	1	3.0	63.93	0.40
17-Mar-94	59	1	3.0	63.52	0.46
18-Mar-94	60	1	3.0	63.11	0.38
19-Mar-94	61	1	4.0	62.69	0.55
20-Mar-94	62	1	4.0	62.28	0.34
21-Mar-94	63	1	4.0	61.87	0.64
22-Mar-94	64	1	4.0	61.46	0.81
23-Mar-94	65	1	4.0	61.05	0.82
24-Mar-94	66	1	4.0	60.63	0.92
25-Mar-94	67	1	4.0	60.22	0.87
26-Mar-94	68	1	4.0	59.24	0.95
27-Mar-94	69	1	4.0	58.26	0.99
28-Mar-94	70	1	4.0	57.28	1.02
29-Mar-94	71	1	4.0	55.93	1.12
30-Mar-94	72	1	5.0	54.59	1.19
31-Mar-94	73	1	5.0	55.06	1.50
01-Apr-94	74	1	5.0	55.54	1.55
02-Apr-94	75	1	5.0	56.01	1.79
03-Apr-94	76	1	5.0	56.00	1.38
04-Apr-94	77	1	5.0	55.99	1.47
05-Apr-94	78	1	5.0	56.78	1.51
06-Apr-94	79	1	6.0	56.10	1.41
07-Apr-94	80	1	6.0	55.82	1.71
08-Apr-94	81	1	6.0	55.55	0.58
09-Apr-94	82	1	6.0	55.28	0.79
10-Apr-94	83	1	6.0	55.55	0.88
11-Apr-94	84	1	6.0	55.81	0.42
12-Apr-94	85	1	6.0	56.08	0.70
13-Apr-94	86	1	6.0	56.35	0.58
14-Apr-94	87	1	6.0	56.62	0.44
15-Apr-94	88	1	6.0	56.18	0.47
16-Apr-94	89	1	6.0	55.74	0.54

Table 84. (continued).

Date	Day	HRT (days)	Nominal COD Load (g/L/day)	Methane (% of total)	Std. Methane Production (L/L/day)
17-Apr-94	90	1	6.0	59.39	0.50
18-Apr-94	91	1	6.0	60.27	0.53
19-Apr-94	92	1	6.0	59.83	0.65
20-Apr-94	93	1	6.0	59.40	0.65
21-Apr-94	94	1	6.0	59.51	0.66
22-Apr-94	95	1	6.0	59.62	0.57
23-Apr-94	96	1	6.0	59.74	0.71
24-Apr-94	97	1	6.0	59.85	0.64
25-Apr-94	98	1	6.0	59.96	0.61
26-Apr-94	99	1	6.0	60.07	0.69
27-Apr-94	100	1	6.0	60.19	0.67
28-Apr-94	101	1	6.0	60.30	0.90
29-Apr-94	102	1	7.0	59.90	0.91
30-Apr-94	103	1	7.0	59.50	0.92
01-May-94	104	1	7.0	59.10	0.95
02-May-94	105	1	7.0	58.69	0.92
03-May-94	106	1	8.0	58.29	0.89
04-May-94	107	1	8.0	57.38	1.06
05-May-94	108	1	8.0	57.38	0.83
06-May-94	109	1	8.0	57.38	1.02

Table 85. Volatile acids data for the beef/glucose+ cationic polymer test.

Date	Time from Start (days)	COD Load (g/L/day)	Volatile Acids (mg/L as acetic)
24-Jan-94	7	1.0	103
28-Jan-94	11	2.0	240
08-Feb-94	22	2.0	291
18-Feb-94	32	3.5	274
28-Feb-94	42	4.5	1,269
07-Mar-94	49	3.0	1,723
12-Mar-94	54	3.0	1,011
18-Mar-94	60	3.0	634
28-Mar-94	70	4.0	86
04-Apr-94	77	5.0	334
14-Apr-94	87	6.0	1,971
21-Apr-94	94	6.0	1,371
28-Apr-94	101	6.0	1,183
05-May-94	108	8.0	2,200

Table 86. Particle size analysis for the beef/glucose+ cationic polymer test.

Date	Time from Start-up (days)	COD Load (g/L/day)	Average Diameter (arithmetic, μm)	Average Diameter (geometric, μm)
17-Jan-94	0	1	34	189
18-Feb-94	32	3	56	399
12-Mar-94	54	3	48	686
04-Apr-94	77	5	114	509
02-May-94	105	8	301	885

Table 87. Alkalinity and pH for the beef/glucose + cationic polymer test.

Date	Time from Start-Up (days)	COD Load (g/L/day)	Alkalinity (mg/L as CaCO ₃)	pH (units)
18-Jan-94	1	1	2,600	7.57
19-Jan-94	2	1	2,500	7.40
22-Jan-94	5	1	2,750	7.37
24-Jan-94	7	1	2,650	7.35
25-Jan-94	8	1	2,490	7.22
28-Jan-94	11	2	2,620	7.23
30-Jan-94	13	2	2,500	7.11
08-Feb-94	22	2	2,590	7.01
12-Feb-94	26	3	2,640	7.02
17-Feb-94	31	3	2,580	6.96
18-Feb-94	32	3	2,610	6.95
19-Feb-94	33	4	2,540	7.06
28-Feb-94	42	3	2,600	6.88
01-Mar-94	43	3	2,500	6.94
04-Mar-94	46	3	2,550	6.93
06-Mar-94	48	3	2,650	6.93
11-Mar-94	53	3	2,690	7.02
12-Mar-94	54	3	2,710	7.08
13-Mar-94	55	3	2,650	7.04
18-Mar-94	60	4	2,700	7.11
21-Mar-94	63	4	2,780	7.03
23-Mar-94	65	4	2,790	7.00
28-Mar-94	70	4	2,750	6.96
04-Apr-94	77	5	2,850	7.11
07-Apr-94	80	6	2,890	7.00
11-Apr-94	84	6	2,990	6.79
13-Apr-94	86	6	3,010	6.80
18-Apr-94	91	6	3,110	6.86
25-Apr-94	98	6	2,960	6.82
26-Apr-94	99	6	3,000	6.86
28-Apr-94	101	7	3,150	6.94
02-May-94	105	8	3,200	6.96

Table 88. Solids analysis for the beef/glucose+ cationic polymer test.

Date	Day	COD Load (g/L/day)	HRT (days)	MLSS (mg/L)	MLVSS (% of MLSS)	Effluent TSS (mg/L)	Effluent VSS (% of TSS)	SRT (days)
17-Jan-94	0	1	2	25,040	56.9			
24-Jan-94	7	1	2	12,830	56.3	233	53.8	115.2
28-Jan-94	11	2	1	13,240	58.7	245	48.9	64.9
08-Feb-94	22	2	1	10,750	65.6	355	56.3	35.3
18-Feb-94	32	3	1	10,170	71.7	395	62.3	29.6
28-Feb-94	42	4	1	4,550	76.5	750	73.7	6.3
07-Mar-94	49	3	2	8,610	81.7	408	60.7	56.8
12-Mar-94	54	3	1	10,940	84.3	232	63.0	63.1
18-Mar-94	60	3	1	11,760	85.2	300	65.9	50.7
28-Mar-94	70	4	1	12,210	84.0	305	62.4	53.9
04-Apr-94	77	5	1	11,400	83.8	1,788	81.4	6.6
14-Apr-94	87	6	1	7,550	83.1	1,230	80.7	6.3
21-Apr-94	94	6	1	9,830	84.6	1,263	82.8	8.0
28-Apr-94	101	6	1	11,830	85.0	868	82.0	14.1
05-May-94	108	8	1	12,000	85.1	1,121	81.9	11.1

Table 89. SMA test with the PAC-enhanced ASBR, day 158.

Time of Day (hr:min)	Time Elapsed (min)	Cumulative Gas (liters)	Cumulative Methane (% of total)	Cumulative Methane (liters)	Cumulative Methane (mL/g MLVSS)
02:01 PM	0	0.00	57.19	0.00	0.00
02:05 PM	4	0.13	57.60	0.07	0.26
02:07 PM	6	0.40	58.02	0.23	0.80
02:09 PM	8	0.74	58.43	0.43	1.49
02:11 PM	10	1.23	58.84	0.72	2.49
02:13 PM	12	1.66	58.39	0.97	3.37
02:15 PM	14	2.06	57.94	1.20	4.18
02:17 PM	16	2.42	57.49	1.41	4.90
02:19 PM	18	2.73	57.04	1.59	5.52
02:21 PM	20	3.02	56.58	1.75	6.10
02:23 PM	22	3.29	56.13	1.90	6.63
02:25 PM	24	3.54	55.68	2.04	7.11
02:27 PM	26	3.80	55.23	2.19	7.61
02:29 PM	28	4.06	54.20	2.33	8.11
02:31 PM	30	4.32	53.16	2.47	8.60
02:33 PM	32	4.56	52.13	2.59	9.04
02:35 PM	34	4.78	51.09	2.71	9.43
02:37 PM	36	5.01	50.06	2.82	9.84
02:39 PM	38	5.23	49.02	2.93	10.22
02:41 PM	40	5.45	47.99	3.04	10.59
02:43 PM	42	5.68	46.95	3.15	10.97
02:45 PM	44	5.90	45.92	3.25	11.32
02:47 PM	46	6.11	45.40	3.35	11.66
02:49 PM	48	6.32	44.88	3.44	11.99
02:51 PM	50	6.53	44.36	3.54	12.31
02:53 PM	52	6.75	43.84	3.63	12.65
02:55 PM	54	6.97	43.32	3.73	12.98
02:57 PM	56	7.19	42.80	3.82	13.31
02:59 PM	58	7.39	42.28	3.91	13.61
03:01 PM	60	7.60	41.76	4.00	13.92
03:03 PM	62	7.76	41.24	4.06	14.15
03:05 PM	64	7.94	40.72	4.14	14.41
03:07 PM	66	8.10	40.20	4.20	14.63
03:09 PM	68	8.28	40.04	4.27	14.88
03:12 PM	71	8.54	39.87	4.38	15.24
03:15 PM	74	8.79	39.71	4.48	15.59
03:18 PM	77	9.03	39.54	4.57	15.92
03:21 PM	80	9.27	39.38	4.67	16.25
03:25 PM	84	9.61	39.21	4.80	16.72
03:29 PM	88	9.96	39.05	4.94	17.19
03:33 PM	92	10.29	39.23	5.07	17.64
03:37 PM	96	10.64	39.40	5.20	18.12
03:41 PM	100	10.95	39.58	5.33	18.55

Notes: substrate = sucrose; MLVSS = 23,933 mg/L; F/M = 0.25.

Table 89. (continued).

Time of Day (hr:min)	Time Elapsed (min)	Cumulative Gas (liters)	Methane (% of total)	Cumulative Methane (liters)	Cumulative Methane (mL/g MLVSS)
03:46 PM	105	11.37	39.75	5.49	19.13
03:50 PM	109	11.68	39.93	5.62	19.56
03:55 PM	114	12.09	40.10	5.78	20.13
04:00 PM	119	12.49	40.28	5.94	20.69
04:05 PM	124	12.91	40.45	6.11	21.28
04:10 PM	129	13.33	40.63	6.28	21.87
04:15 PM	134	13.74	41.16	6.45	22.46
04:20 PM	139	14.14	41.70	6.62	23.03
04:25 PM	144	14.55	42.23	6.79	23.63
04:31 PM	150	15.04	42.76	7.00	24.36
04:37 PM	157	15.56	43.29	7.22	25.14
04:47 PM	167	16.37	43.83	7.57	26.37
04:53 PM	172	16.81	44.36	7.77	27.04
04:59 PM	178	17.28	44.89	7.98	27.77
05:02 PM	181	17.52	45.42	8.08	28.15
05:10 PM	189	18.14	45.95	8.37	29.14
05:21 PM	200	19.06	46.48	8.79	30.62
05:30 PM	209	19.80	47.01	9.14	31.82
05:41 PM	220	20.57	47.53	9.50	33.09
05:51 PM	230	21.33	48.06	9.87	34.35
06:00 PM	239	22.95	48.59	10.65	37.08
06:10 PM	249	23.72	49.12	11.02	38.39
06:20 PM	259	24.48	49.65	11.40	39.70
06:25 PM	264	24.82	50.18	11.57	40.29
06:31 PM	270	25.26	50.55	11.79	41.06
06:36 PM	275	25.62	50.92	11.97	41.69
06:41 PM	280	25.99	51.30	12.16	42.35
06:48 PM	287	26.51	51.67	12.43	43.28
06:54 PM	293	26.92	52.04	12.64	44.02
07:01 PM	300	27.42	52.41	12.90	44.93
07:08 PM	307	27.90	52.79	13.16	45.81
07:14 PM	313	28.31	53.16	13.37	46.57
07:23 PM	322	28.94	53.61	13.71	47.74
07:31 PM	330	29.51	54.05	14.02	48.81
07:38 PM	337	29.98	54.50	14.27	49.70
07:49 PM	348	30.70	54.95	14.67	51.07
07:55 PM	354	31.09	55.39	14.88	51.82
08:08 PM	367	31.95	55.84	15.36	53.48
08:19 PM	378	32.68	56.29	15.77	54.91
08:28 PM	387	33.25	56.74	16.09	56.03
08:35 PM	394	33.69	57.18	16.34	56.90
08:39 PM	398	33.93	57.63	16.48	57.38
08:46 PM	405	34.36	58.08	16.73	58.25
09:06 PM	425	35.60	58.54	17.45	60.77
09:11 PM	430	35.89	58.99	17.62	61.36

Table 89. (continued).

Time of Day (hr:min)	Time Elapsed (min)	Cumulative Gas (liters)	Methane (% of total)	Cumulative Methane (liters)	Cumulative Methane (mL/g MLVSS)
09:52 PM	471	38.20	59.62	18.99	66.13
09:59 PM	478	38.58	60.25	19.22	66.92
11:08 PM	547	41.49	61.02	20.98	73.07
11:16 PM	555	41.70	61.79	21.11	73.52
11:24 PM	563	41.89	62.03	21.23	73.93
11:37 PM	576	42.18	62.27	21.41	74.55
11:47 PM	586	42.40	62.51	21.55	75.03
11:56 PM	595	42.57	62.75	21.66	75.40
12:06 AM	605	42.77	62.99	21.78	75.84
12:17 AM	616	42.98	63.02	21.91	76.30
12:31 AM	630	43.25	63.05	22.08	76.89
12:48 AM	647	43.56	63.08	22.28	77.57

Table 90. SMA test with the PAC-enhanced ASBR, day 169.

Time of Day (hr:min)	Time Elapsed (min)	Cumulative Gas (liters)	Cumulative Methane (% of total)	Cumulative Methane (liters)	Cumulative Methane (mL/g MLVSS)
10:54 AM	0	0.00	57.86	0.00	0.00
10:56 AM	2	0.00	57.80	0.00	0.00
10:58 AM	4	0.00	57.74	0.00	0.00
11:00 AM	6	0.09	57.68	0.05	0.15
11:02 AM	8	0.33	57.62	0.19	0.57
11:04 AM	10	0.48	57.52	0.28	0.82
11:06 AM	12	0.58	57.43	0.33	0.99
11:08 AM	14	0.71	57.33	0.41	1.22
11:10 AM	16	0.78	57.23	0.45	1.33
11:12 AM	18	0.86	57.14	0.49	1.47
11:14 AM	20	0.94	57.04	0.54	1.61
11:16 AM	22	1.01	56.94	0.58	1.72
11:18 AM	24	1.07	56.85	0.61	1.83
11:20 AM	26	1.13	56.75	0.65	1.93
11:22 AM	28	1.17	56.71	0.67	1.99
11:24 AM	30	1.23	56.67	0.71	2.10
11:26 AM	32	1.28	56.63	0.73	2.18
11:28 AM	34	1.32	56.59	0.76	2.25
11:30 AM	36	1.35	56.54	0.77	2.30
11:32 AM	38	1.40	56.50	0.80	2.38
11:34 AM	40	1.45	56.46	0.83	2.47
11:36 AM	42	1.48	56.42	0.85	2.52
11:38 AM	44	1.51	56.36	0.86	2.57
11:40 AM	46	1.55	56.29	0.89	2.63
11:42 AM	48	1.59	56.23	0.91	2.70
11:44 AM	50	1.62	56.17	0.93	2.75
11:46 AM	52	1.66	56.10	0.95	2.82
11:48 AM	54	1.70	56.04	0.97	2.88
11:50 AM	56	1.79	55.98	1.02	3.03
11:52 AM	58	1.79	55.92	1.02	3.03
11:54 AM	60	1.82	55.85	1.04	3.08
11:56 AM	62	1.85	55.79	1.05	3.13
11:58 AM	64	1.88	55.69	1.07	3.18
12:00 PM	66	1.91	55.58	1.09	3.23
12:02 PM	68	1.95	55.48	1.11	3.30
12:04 PM	70	1.99	55.37	1.13	3.36
12:06 PM	72	2.01	55.27	1.14	3.40
12:10 PM	76	2.09	55.17	1.19	3.53
12:14 PM	80	2.16	55.06	1.23	3.64
12:18 PM	84	2.23	54.96	1.26	3.76
12:22 PM	88	2.28	54.85	1.29	3.84
12:27 PM	93	2.36	54.75	1.34	3.97
12:30 PM	96	2.44	54.66	1.38	4.10

Notes: substrate = acetate; MLVSS = 28,033 mg/L; F/M = 0.25.

Table 90. (continued).

Time of Day (hr:min)	Time Elapsed (min)	Cumulative Gas (liters)	Cumulative Methane (% of total)	Cumulative Methane (liters)	Cumulative Methane (mL/g MLVSS)
12:34 PM	100	2.49	54.57	1.41	4.18
12:38 PM	104	2.56	54.48	1.44	4.29
12:42 PM	108	2.60	54.38	1.47	4.36
12:46 PM	112	2.67	54.29	1.50	4.47
12:53 PM	119	2.77	54.20	1.56	4.63
01:00 PM	126	2.86	54.11	1.61	4.78
01:06 PM	132	2.96	54.02	1.66	4.94
01:12 PM	138	3.04	53.93	1.70	5.07
01:21 PM	147	3.20	53.84	1.79	5.32
01:28 PM	154	3.29	53.75	1.84	5.47
01:38 PM	164	3.43	53.77	1.91	5.69
01:43 PM	169	3.49	53.79	1.95	5.79
01:51 PM	177	3.59	53.82	2.00	5.95
01:59 PM	185	3.69	53.84	2.05	6.11
02:08 PM	194	3.81	53.86	2.12	6.30
02:15 PM	201	3.92	53.87	2.18	6.48
02:25 PM	211	4.06	53.89	2.25	6.70
02:39 PM	225	4.23	53.90	2.35	6.97
02:49 PM	235	4.37	53.91	2.42	7.20
02:55 PM	241	4.47	54.04	2.47	7.36
03:01 PM	247	4.55	54.17	2.52	7.49
03:08 PM	254	4.66	54.29	2.58	7.66
03:15 PM	261	4.75	54.42	2.63	7.81
03:22 PM	268	4.85	54.55	2.68	7.97
04:10 PM	316	5.57	54.49	3.07	9.14
04:20 PM	326	5.66	54.53	3.12	9.28
04:28 PM	334	5.76	54.58	3.18	9.45
04:36 PM	342	5.86	54.62	3.23	9.61
04:48 PM	354	6.02	54.67	3.32	9.87
04:56 PM	362	6.11	54.71	3.37	10.01
05:00 PM	366	6.22	54.75	3.43	10.19
05:10 PM	376	6.30	54.80	3.47	10.32
05:21 PM	387	6.43	54.84	3.54	10.53
05:31 PM	397	6.56	54.97	3.62	10.75
05:42 PM	408	6.72	55.10	3.70	11.01
05:49 PM	415	6.79	55.23	3.74	11.12
05:55 PM	421	6.88	55.36	3.79	11.27
06:04 PM	430	6.99	55.66	3.85	11.45
06:16 PM	442	7.12	55.96	3.93	11.67
06:31 PM	457	7.32	56.26	4.04	12.00
06:37 PM	463	7.40	56.56	4.08	12.14
06:48 PM	474	7.53	56.34	4.16	12.35
07:09 PM	495	7.80	56.12	4.31	12.81
07:30 PM	516	8.06	55.90	4.45	13.24
07:43 PM	529	8.53	55.49	4.72	14.02

Table 90. (continued).

Time of Day (hr:min)	Time Elapsed (min)	Cumulative Gas (liters)	Methane (% of total)	Cumulative Methane (liters)	Cumulative Methane (mL/g MLVSS)
08:51 PM	597	9.81	55.07	5.42	16.12
08:57 PM	603	9.90	54.66	5.47	16.27
09:06 PM	612	10.02	54.24	5.54	16.46
10:19 PM	685	10.96	53.83	6.05	17.97
10:29 PM	695	11.07	53.41	6.10	18.15
12:38 AM	824	12.43	54.08	6.84	20.32
12:56 AM	842	12.84	54.76	7.06	20.98
01:07 AM	853	13.02	55.43	7.16	21.28
01:22 AM	868	13.21	55.58	7.26	21.59
01:34 AM	880	13.36	55.74	7.35	21.84
01:49 AM	895	13.56	55.89	7.46	22.17
01:54 AM	900	13.62	56.04	7.49	22.27
02:06 AM	912	13.76	56.20	7.57	22.50
02:15 AM	921	13.87	56.35	7.63	22.69
04:17 AM	1,043	15.32	56.50	8.45	25.12
04:22 AM	1,048	15.38	56.66	8.48	25.22
04:29 AM	1,055	15.46	56.81	8.53	25.36
04:41 AM	1,067	15.62	57.13	8.62	25.63
04:45 AM	1,071	15.66	57.46	8.64	25.70
04:48 AM	1,074	15.69	57.78	8.66	25.75
04:52 AM	1,078	15.73	58.10	8.68	25.82
04:55 AM	1,081	15.76	58.43	8.70	25.87
07:07 AM	1,213	17.26	58.75	9.58	28.48
07:10 AM	1,216	17.30	59.08	9.60	28.55
07:13 AM	1,219	17.33	59.40	9.62	28.60
07:21 AM	1,227	17.44	59.72	9.69	28.80
08:39 AM	1,305	18.28	60.05	10.19	30.29
08:44 AM	1,310	18.33	60.37	10.22	30.38
09:26 AM	1,352	18.76	60.48	10.48	31.16
10:11 AM	1,397	19.23	60.59	10.77	32.00
10:39 AM	1,425	19.52	60.70	10.94	32.52
11:05 AM	1,451	19.81	60.81	11.12	33.05
11:16 AM	1,462	19.93	60.92	11.19	33.26
11:52 AM	1,498	20.31	61.03	11.42	33.95
01:10 PM	1,576	21.11	61.14	11.91	35.41
01:25 PM	1,591	21.28	61.25	12.01	35.72
01:52 PM	1,618	21.53	61.36	12.17	36.17
02:15 PM	1,641	21.76	61.47	12.31	36.59
02:23 PM	1,649	21.85	61.58	12.36	36.76
02:42 PM	1,668	22.04	61.69	12.48	37.10
02:54 PM	1,680	22.16	61.79	12.56	37.32
03:10 PM	1,696	22.31	61.90	12.65	37.60
06:28 PM	1,894	24.26	62.01	13.86	41.19
08:39 PM	2,025	25.47	62.12	14.61	43.42
12:56 AM	2,282	27.78	62.23	16.04	47.69

Table 90. (continued).

Time of Day (hr:min)	Time Elapsed (min)	Cumulative Gas (liters)	Methane (% of total)	Cumulative Methane (liters)	Cumulative Methane (mL/g MLVSS)
01:09 AM	2,295	28.35	62.34	16.40	48.75
01:11 AM	2,297	28.39	62.45	16.42	48.82
01:17 AM	2,303	28.47	62.56	16.47	48.97
01:21 AM	2,307	28.51	62.67	16.50	49.05
01:28 AM	2,314	28.59	62.78	16.55	49.20
07:20 AM	2,666	31.85	62.89	18.60	55.28
08:37 AM	2,743	32.54	63.00	19.03	56.58

Table 91. SMA test with the PAC-enhanced ASBR, day 228.

Time of Day (hr:min)	Time Elapsed (min)	Cumulative Gas (liters)	Cumulative Methane (% of total)	Cumulative Methane (liters)	Cumulative Methane (mL/g MLVSS)
09:18 AM	0	0.00	61.78	0.00	0.00
09:20 AM	2	0.00	61.78	0.00	0.00
09:22 AM	4	0.00	61.78	0.00	0.00
09:24 AM	6	0.00	61.78	0.00	0.00
09:26 AM	8	0.00	61.78	0.00	0.00
09:28 AM	10	0.00	61.78	0.00	0.00
09:30 AM	12	0.00	61.78	0.00	0.00
09:32 AM	14	0.00	61.78	0.00	0.00
09:34 AM	16	0.00	61.78	0.00	0.00
09:36 AM	18	0.00	61.78	0.00	0.00
09:38 AM	20	0.00	61.78	0.00	0.00
09:40 AM	22	0.00	61.78	0.00	0.00
09:42 AM	24	0.00	61.78	0.00	0.00
09:44 AM	26	0.00	61.78	0.00	0.00
09:46 AM	28	0.00	61.78	0.00	0.00
09:48 AM	30	0.00	61.78	0.00	0.00
09:50 AM	32	0.00	61.78	0.00	0.00
09:52 AM	34	0.33	61.51	0.20	0.98
09:54 AM	36	0.56	61.25	0.34	1.66
09:56 AM	38	0.73	60.98	0.45	2.16
09:58 AM	40	0.88	60.71	0.54	2.60
10:00 AM	42	1.02	60.45	0.62	3.00
10:02 AM	44	1.14	60.18	0.70	3.35
10:04 AM	46	1.27	59.91	0.78	3.73
10:06 AM	48	1.42	59.65	0.86	4.16
10:08 AM	50	1.50	59.38	0.91	4.39
10:10 AM	52	1.58	59.11	0.96	4.61
10:12 AM	54	1.68	58.85	1.02	4.90
10:14 AM	56	1.79	58.58	1.08	5.21
10:17 AM	59	1.91	58.31	1.15	5.55
10:20 AM	62	2.05	58.05	1.23	5.94
10:26 AM	68	2.30	57.78	1.38	6.63
10:30 AM	72	2.50	56.81	1.49	7.18
10:35 AM	77	2.70	55.85	1.61	7.73
10:40 AM	82	2.84	54.88	1.68	8.10
10:45 AM	87	3.00	54.35	1.77	8.52
10:50 AM	92	3.15	53.82	1.85	8.91
10:55 AM	97	3.30	53.29	1.93	9.30
11:00 AM	102	3.43	52.76	2.00	9.63
11:05 AM	107	3.57	52.24	2.08	9.98
11:10 AM	112	3.67	51.71	2.13	10.23

Notes: substrate = sucrose; MLVSS = 17,331 mg/L; F/M = 0.22.

Table 91. (continued).

Time of Day (hr:min)	Time Elapsed (min)	Cumulative Gas (liters)	Methane (% of total)	Cumulative Methane (liters)	Cumulative Methane (mL/g MLVSS)
11:13 AM	115	3.81	51.18	2.20	10.58
11:20 AM	122	3.97	50.65	2.28	10.97
11:29 AM	131	4.20	50.12	2.40	11.53
11:35 AM	137	4.32	49.59	2.46	11.90
11:43 AM	145	4.51	49.23	2.55	12.27
11:51 AM	153	4.77	48.88	2.68	12.88
12:08 PM	170	5.19	48.52	2.88	13.86
12:14 PM	176	5.35	48.16	2.96	14.23
12:29 PM	191	5.78	47.91	3.17	15.23
12:38 PM	200	6.02	47.66	3.28	15.78
12:52 PM	214	6.40	47.41	3.46	16.65
01:07 PM	229	6.78	47.16	3.64	17.51
01:11 PM	233	6.90	46.91	3.70	17.78
01:45 PM	267	7.75	46.51	4.10	19.69
02:06 PM	288	8.26	46.10	4.33	20.83
02:49 PM	331	9.20	46.25	4.77	22.91
02:58 PM	340	9.68	46.39	4.99	23.98
03:14 PM	356	9.73	46.27	5.01	24.10
03:20 PM	362	9.83	46.15	5.06	24.32
03:40 PM	382	10.26	46.56	5.26	25.28
03:45 PM	387	10.36	46.97	5.30	25.50
04:05 PM	407	10.83	47.65	5.53	26.57
04:11 PM	413	10.96	48.33	5.59	26.87
04:18 PM	420	11.12	48.33	5.67	27.24

Table 92. SMA test with the PAC-enhanced ASBR, day 283.

Time of Day (hr:min)	Time Elapsed (min)	Cumulative Gas (liters)	Cumulative Methane (% of total)	Cumulative Methane (liters)	Cumulative Methane (mL/g MLVSS)
01:46 PM	0	0.00	61.82	0.00	0.00
01:48 PM	2	0.00	61.11	0.00	0.00
01:53 PM	7	0.00	60.40	0.00	0.00
01:56 PM	10	0.00	59.69	0.00	0.00
02:00 PM	14	0.09	58.98	0.05	0.18
02:02 PM	16	0.44	58.28	0.26	0.89
02:04 PM	18	0.89	57.57	0.52	1.78
02:06 PM	20	1.31	56.86	0.76	2.61
02:08 PM	22	1.64	56.15	0.95	3.24
02:10 PM	24	1.87	55.22	1.07	3.68
02:13 PM	27	2.19	54.28	1.25	4.29
02:18 PM	32	2.65	53.34	1.50	5.13
02:22 PM	36	2.92	52.41	1.64	5.62
02:25 PM	39	3.12	51.47	1.74	5.98
02:29 PM	43	3.35	50.54	1.86	6.38
02:34 PM	48	3.60	49.32	1.99	6.81
02:42 PM	56	3.96	48.11	2.16	7.41
02:49 PM	63	4.27	46.89	2.31	7.92
02:55 PM	69	4.48	46.27	2.41	8.25
02:59 PM	73	4.62	45.66	2.47	8.47
03:04 PM	78	4.78	45.04	2.54	8.72
03:11 PM	85	4.98	44.43	2.63	9.03
03:19 PM	93	5.22	43.81	2.74	9.39
03:30 PM	104	5.53	42.86	2.87	9.85
03:33 PM	107	5.60	41.90	2.90	9.96
03:51 PM	125	6.04	40.95	3.08	10.58
03:54 PM	128	6.10	40.79	3.11	10.66
03:56 PM	130	6.15	40.64	3.13	10.73
04:06 PM	140	6.42	40.48	3.24	11.11
04:15 PM	149	6.65	40.33	3.33	11.43
04:22 PM	156	6.87	40.17	3.42	11.73
04:34 PM	168	7.16	39.73	3.54	12.13
04:49 PM	183	7.52	39.28	3.68	12.62
05:03 PM	197	7.84	38.88	3.80	13.05
05:19 PM	213	8.18	38.48	3.94	13.50
05:26 PM	220	8.27	38.07	3.97	13.62
05:34 PM	228	8.46	37.67	4.04	13.86
05:39 PM	233	8.58	37.54	4.09	14.02
05:47 PM	241	8.71	37.42	4.14	14.18
05:49 PM	243	8.71	37.29	4.14	14.18
05:55 PM	249	8.81	37.17	4.17	14.31
05:58 PM	252	8.89	37.04	4.20	14.41

Notes: substrate = sucrose; MLVSS = 24,295 mg/L; F/M = 0.22.

Table 92. (continued).

Time of Day (hr:min)	Time Elapsed (min)	Cumulative Gas (liters)	Methane (% of total)	Cumulative Methane (liters)	Cumulative Methane (mL/g MLVSS)
06:02 PM	256	8.98	36.91	4.24	14.53
06:10 PM	264	9.15	36.79	4.30	14.74
06:28 PM	282	9.47	36.66	4.42	15.15
06:45 PM	299	9.78	36.55	4.53	15.54
07:16 PM	330	10.25	36.45	4.70	16.12
07:23 PM	337	10.35	36.34	4.74	16.25
07:34 PM	348	10.47	36.23	4.78	16.40
07:44 PM	358	10.63	36.12	4.84	16.60
07:49 PM	363	10.69	36.01	4.86	16.67
07:57 PM	371	10.79	35.90	4.90	16.79

Table 93. SMA test with the GAC-enhanced ASBR, day 65.

Time of Day (hr:min)	Time Elapsed (min)	Cumulative Gas (liters)	Cumulative Methane (% of total)	Cumulative Methane (liters)	Cumulative Methane (mL/g MLVSS)
02:01 PM	0	0.00	57.13	0.00	0.00
02:05 PM	4	0.04	57.24	0.02	0.20
02:07 PM	6	0.17	57.34	0.10	0.86
02:09 PM	8	0.30	57.45	0.17	1.52
02:11 PM	10	0.42	57.55	0.24	2.12
02:13 PM	12	0.52	57.72	0.30	2.63
02:15 PM	14	0.62	57.88	0.36	3.14
02:17 PM	16	0.72	58.05	0.41	3.65
02:19 PM	18	0.81	58.21	0.47	4.12
02:21 PM	20	0.90	58.37	0.52	4.58
02:23 PM	22	0.98	58.54	0.57	4.99
02:25 PM	24	1.07	58.70	0.62	5.46
02:27 PM	26	1.15	58.87	0.67	5.87
02:29 PM	28	1.23	58.89	0.71	6.29
02:31 PM	30	1.30	58.91	0.75	6.65
02:33 PM	32	1.32	58.93	0.77	6.75
02:35 PM	34	1.44	58.95	0.84	7.38
02:37 PM	36	1.50	58.96	0.87	7.69
02:39 PM	38	1.57	58.98	0.91	8.05
02:41 PM	40	1.63	59.00	0.95	8.36
02:43 PM	42	1.70	59.02	0.99	8.73
02:45 PM	44	1.75	59.04	1.02	8.99
02:47 PM	46	1.82	58.94	1.06	9.35
02:49 PM	48	1.87	58.84	1.09	9.61
02:51 PM	50	1.93	58.75	1.13	9.92
02:53 PM	52	1.99	58.65	1.16	10.23
02:55 PM	54	2.04	58.55	1.19	10.49
02:57 PM	56	2.09	58.45	1.22	10.75
02:59 PM	58	2.15	58.35	1.25	11.06
03:01 PM	60	2.20	58.25	1.28	11.32
03:03 PM	62	2.25	58.16	1.31	11.57
03:05 PM	64	2.30	58.06	1.34	11.83
03:07 PM	66	2.35	57.96	1.37	12.09
03:09 PM	68	2.40	57.91	1.40	12.34
03:12 PM	71	2.47	57.86	1.44	12.70
03:15 PM	74	2.55	57.81	1.49	13.11
03:18 PM	77	2.62	57.75	1.53	13.46
03:21 PM	80	2.69	57.70	1.57	13.82
03:25 PM	84	2.78	57.65	1.62	14.28
03:29 PM	88	2.86	57.60	1.67	14.68
03:33 PM	92	2.95	57.37	1.72	15.14
03:37 PM	96	3.03	57.14	1.76	15.54
03:41 PM	100	3.11	56.91	1.81	15.95

Notes: substrate = sucrose; MLVSS = 9,450 mg/L; F/M = 0.25.

Table 93. (continued).

Time of Day (hr:min)	Time Elapsed (min)	Cumulative Gas (liters)	Cumulative Methane (% of total)	Cumulative Methane (liters)	Cumulative Methane (mL/g MLVSS)
03:46 PM	105	3.21	56.68	1.87	16.45
03:50 PM	109	3.29	56.45	1.91	16.85
03:55 PM	114	3.38	56.22	1.96	17.29
04:00 PM	119	3.46	55.99	2.01	17.69
04:05 PM	124	3.55	55.76	2.06	18.13
04:10 PM	129	3.63	55.53	2.10	18.53
04:15 PM	134	3.72	55.54	2.15	18.97
04:20 PM	139	3.80	55.54	2.20	19.36
04:25 PM	144	3.88	55.55	2.24	19.75
04:31 PM	150	3.99	55.55	2.30	20.29
04:37 PM	156.5	4.09	55.56	2.36	20.78
04:47 PM	166.5	4.24	55.56	2.44	21.51
04:53 PM	172	4.31	55.57	2.48	21.86
04:59 PM	178	4.42	55.37	2.54	22.39
05:02 PM	181	4.46	55.18	2.56	22.59
05:10 PM	189	4.57	54.98	2.62	23.12
05:21 PM	200	4.73	54.79	2.71	23.90
05:30 PM	209	4.87	54.59	2.79	24.57
05:41 PM	220	5.03	54.40	2.87	25.34
05:51 PM	230	5.17	54.20	2.95	26.01
06:00 PM	239	5.28	54.01	3.01	26.54
06:10 PM	249	5.42	53.81	3.08	27.20
06:20 PM	259	5.58	53.62	3.17	27.96
06:25 PM	264	5.66	53.42	3.21	28.34
06:31 PM	270	5.74	53.35	3.26	28.71
06:36 PM	275	5.81	53.27	3.29	29.04
06:41 PM	280	5.89	53.20	3.34	29.42
06:48 PM	287	5.98	53.12	3.38	29.84
06:54 PM	293	6.07	53.05	3.43	30.26
07:01 PM	300	6.18	52.98	3.49	30.78
07:08 PM	307	6.30	52.90	3.55	31.34
07:14 PM	313	6.39	52.83	3.60	31.76
07:23 PM	322	6.51	52.81	3.66	32.32
07:31 PM	330	6.64	52.80	3.73	32.92
07:38 PM	337	6.76	52.78	3.80	33.48
07:49 PM	348	6.94	52.76	3.89	34.32
07:55 PM	354	7.05	52.74	3.95	34.83
08:08 PM	367	7.27	52.73	4.07	35.85
08:19 PM	378	7.46	52.71	4.17	36.74
08:28 PM	387	7.61	52.69	4.24	37.43
08:35 PM	394	7.74	52.68	4.31	38.04
08:39 PM	398	7.82	52.66	4.36	38.41
08:46 PM	405	7.94	52.44	4.42	38.96
09:06 PM	425	8.30	52.22	4.61	40.63
09:11 PM	430	8.38	52.00	4.65	40.99

Table 93. (continued).

Time of Day (hr:min)	Time Elapsed (min)	Cumulative Gas (liters)	Methane (% of total)	Cumulative Methane (liters)	Cumulative Methane (mL/g MLVSS)
09:52 PM	471	9.11	52.24	5.03	44.35
09:59 PM	478	9.24	52.48	5.10	44.95
11:08 PM	547	10.50	52.85	5.76	50.80
11:16 PM	555	10.64	53.21	5.83	51.45
11:24 PM	563	10.74	53.37	5.89	51.92
11:37 PM	576	11.04	53.53	6.05	53.34
11:47 PM	586	11.22	53.70	6.15	54.19
11:56 PM	595	11.36	53.86	6.22	54.85
12:06 AM	605	11.54	54.02	6.32	55.71
12:17 AM	616	11.74	54.23	6.43	56.66
12:31 AM	630	11.98	54.45	6.56	57.81
12:48 AM	647	12.27	54.66	6.71	59.21

Table 94. SMA test with the GAC-enhanced ASBR, day 76.

Time of Day (hr:min)	Time Elapsed (min)	Cumulative Gas (liters)	Methane (% of total)	Cumulative Methane (liters)	Cumulative Methane (mL/g MLVSS)
10:54 AM	0	0.00	61.30	0.00	0.00
10:56 AM	2	0.35	61.30	0.21	1.27
10:58 AM	4	0.58	61.30	0.36	2.10
11:00 AM	6	0.61	61.30	0.37	2.21
11:02 AM	8	0.65	61.30	0.40	2.35
11:04 AM	10	0.68	61.28	0.42	2.46
11:06 AM	12	0.73	61.27	0.45	2.64
11:08 AM	14	0.76	61.25	0.47	2.75
11:10 AM	16	0.77	61.23	0.47	2.78
11:12 AM	18	0.84	61.22	0.51	3.04
11:14 AM	20	0.86	61.20	0.53	3.11
11:16 AM	22	0.90	61.18	0.55	3.25
11:18 AM	24	0.91	61.17	0.56	3.29
11:20 AM	26	0.96	61.15	0.59	3.47
11:22 AM	28	1.03	61.09	0.63	3.72
11:24 AM	30	1.05	61.03	0.64	3.79
11:26 AM	32	1.11	60.96	0.68	4.01
11:28 AM	34	1.12	60.90	0.69	4.05
11:30 AM	36	1.18	60.84	0.72	4.26
11:32 AM	38	1.20	60.78	0.73	4.33
11:34 AM	40	1.23	60.71	0.75	4.44
11:36 AM	42	1.29	60.65	0.79	4.65
11:38 AM	44	1.32	60.70	0.81	4.76
11:40 AM	46	1.36	60.74	0.83	4.91
11:42 AM	48	1.41	60.79	0.86	5.08
11:44 AM	50	1.43	60.84	0.87	5.16
11:46 AM	52	1.47	60.88	0.90	5.30
11:48 AM	54	1.51	60.93	0.92	5.44
11:50 AM	56	1.56	60.98	0.95	5.62
11:52 AM	58	1.59	61.03	0.97	5.73
11:54 AM	60	1.64	61.07	1.00	5.91
11:56 AM	62	1.68	61.12	1.03	6.06
11:58 AM	64	1.71	61.13	1.05	6.16
12:00 PM	66	1.76	61.15	1.08	6.34
12:02 PM	68	1.80	61.16	1.10	6.49
12:04 PM	70	1.84	61.18	1.12	6.63
12:06 PM	72	1.88	61.19	1.15	6.78
12:10 PM	76	1.97	61.20	1.20	7.10
12:14 PM	80	2.05	61.22	1.25	7.39
12:18 PM	84	2.13	61.23	1.30	7.68
12:22 PM	88	2.21	61.25	1.35	7.97
12:27 PM	93	2.31	61.26	1.41	8.33
12:30 PM	96	2.39	61.29	1.46	8.62

Notes: substrate = acetate; MLVSS = 14,130 mg/L; F/M = 0.25.

Table 94. (continued).

Time of Day (hr:min)	Time Elapsed (min)	Cumulative Gas (liters)	Cumulative Methane (% of total)	Cumulative Methane (liters)	Cumulative Methane (mL/g MLVSS)
12:34 PM	100	2.45	61.33	1.50	8.84
12:38 PM	104	2.56	61.36	1.57	9.23
12:42 PM	108	2.64	61.39	1.61	9.52
12:46 PM	112	2.74	61.42	1.68	9.89
12:53 PM	119	2.89	61.46	1.77	10.43
01:00 PM	126	2.98	61.49	1.82	10.75
01:06 PM	132	3.17	61.26	1.94	11.44
01:12 PM	138	3.30	61.03	2.02	11.91
01:21 PM	147	3.54	60.79	2.17	12.77
01:28 PM	154	3.67	60.56	2.24	13.24
01:38 PM	164	3.88	61.13	2.37	13.99
01:43 PM	169	3.98	61.71	2.43	14.35
01:51 PM	177	4.14	62.28	2.53	14.94
01:59 PM	185	4.31	62.86	2.64	15.57
02:08 PM	194	4.50	63.43	2.76	16.27
02:15 PM	201	4.64	63.67	2.85	16.80
02:25 PM	211	4.84	63.91	2.98	17.55
02:39 PM	225	5.12	64.14	3.16	18.61
02:49 PM	235	5.33	64.38	3.29	19.40
02:55 PM	241	5.48	64.42	3.39	19.97
03:01 PM	247	5.62	64.46	3.48	20.51
03:08 PM	254	5.79	64.49	3.59	21.15
03:15 PM	261	5.93	64.53	3.68	21.69
03:22 PM	268	6.08	64.57	3.77	22.26
04:10 PM	316	7.20	67.23	4.51	26.61
04:20 PM	326	7.37	67.43	4.63	27.28
04:28 PM	334	7.52	67.63	4.73	27.88
04:36 PM	342	7.68	67.83	4.84	28.52
04:48 PM	354	7.94	68.03	5.01	29.56
04:56 PM	362	8.08	68.22	5.11	30.12
05:00 PM	366	8.17	68.42	5.17	30.49
05:10 PM	376	8.39	68.62	5.32	31.38
05:21 PM	387	8.63	68.82	5.49	32.35
05:31 PM	397	8.89	69.16	5.66	33.41
05:42 PM	408	9.11	69.49	5.82	34.31
05:49 PM	415	9.25	69.83	5.91	34.88
05:55 PM	421	9.39	70.16	6.01	35.46
06:04 PM	430	9.58	70.20	6.15	36.25
06:16 PM	442	9.83	70.23	6.32	37.28
06:31 PM	457	10.15	70.27	6.55	38.61
06:37 PM	463	10.27	70.31	6.63	39.10
06:48 PM	474	10.50	70.88	6.79	40.06
07:09 PM	495	10.93	71.45	7.10	41.87
07:30 PM	516	11.35	72.02	7.40	43.64
07:43 PM	529	12.09	71.40	7.93	46.77

Table 94. (continued).

Time of Day (hr:min)	Time Elapsed (min)	Cumulative Gas (liters)	Methane (% of total)	Cumulative Methane (liters)	Cumulative Methane (mL/g MLVSS)
08:51 PM	597	13.12	70.79	8.66	51.09
08:57 PM	603	13.25	70.17	8.75	51.63
09:06 PM	612	13.47	69.55	8.91	52.54
10:19 PM	685	15.02	68.94	9.98	58.87
10:29 PM	695	15.23	68.32	10.13	59.72
12:38 AM	824	17.58	69.49	11.75	69.27
12:56 AM	842	18.09	70.65	12.10	71.38
01:07 AM	853	18.29	71.82	12.24	72.22
01:22 AM	868	18.55	71.83	12.43	73.32
01:34 AM	880	18.76	71.84	12.58	74.21
01:49 AM	895	19.31	71.85	12.98	76.54
01:54 AM	900	19.46	71.86	13.09	77.17
02:06 AM	912	19.76	71.86	13.30	78.44
02:15 AM	921	19.96	71.87	13.44	79.29
04:17 AM	1,043	22.12	71.88	15.00	88.45
04:22 AM	1,048	22.19	71.89	15.05	88.75
04:29 AM	1,055	22.29	71.90	15.12	89.17
04:41 AM	1,067	22.33	71.42	15.15	89.34
04:45 AM	1,071	22.52	70.94	15.28	90.14
04:48 AM	1,074	22.63	70.45	15.36	90.59
04:52 AM	1,078	22.74	69.97	15.44	91.05
04:55 AM	1,081	22.83	69.49	15.50	91.42
07:07 AM	1,213	24.15	69.01	16.42	96.81
07:10 AM	1,216	24.16	68.53	16.42	96.85
07:13 AM	1,219	24.17	68.05	16.43	96.89
07:21 AM	1,227	24.21	67.56	16.46	97.05
08:39 AM	1,305	24.49	67.08	16.64	98.16
08:44 AM	1,310	24.51	66.60	16.66	98.24
09:26 AM	1,352	24.64	66.60	16.74	98.75
10:11 AM	1,397	24.85	66.60	16.88	99.58

Table 95. SMA test with the GAC-enhanced ASBR, day 93.

Time of Day (hr:min)	Time Elapsed (min)	Cumulative Gas (liters)	Methane (% of total)	Cumulative Methane (liters)	Cumulative Methane (mL/g MLVSS)
11:11 AM	0	0.00	60.84	0.00	0.00
11:14 AM	3	0.63	60.87	0.38	1.93
11:16 AM	5	1.23	60.91	0.75	3.77
11:18 AM	7	1.48	60.94	0.90	4.54
11:20 AM	9	1.73	60.97	1.05	5.31
11:22 AM	11	1.98	61.01	1.21	6.07
11:24 AM	13	2.23	61.04	1.36	6.84
11:29 AM	18	2.75	61.07	1.68	8.44
11:32 AM	21	3.03	61.11	1.85	9.30
11:34 AM	23	3.20	61.14	1.95	9.83
11:36 AM	25	3.35	60.66	2.04	10.29
11:38 AM	27	3.50	60.18	2.13	10.74
11:40 AM	29	3.66	59.70	2.23	11.23
11:42 AM	31	3.83	59.22	2.33	11.73
11:45 AM	34	4.05	58.74	2.46	12.39
11:49 AM	38	4.31	58.26	2.61	13.15
11:55 AM	44	4.70	57.78	2.84	14.29
11:58 AM	47	4.89	57.29	2.95	14.84
12:02 PM	51	5.16	56.80	3.10	15.62
12:34 PM	83	7.03	56.32	4.16	20.95
12:36 PM	85	7.09	55.83	4.19	21.12
12:38 PM	87	7.20	55.34	4.25	21.42
12:40 PM	89	7.29	54.85	4.30	21.67
12:42 PM	91	7.40	54.36	4.36	21.98
12:44 PM	93	7.50	53.88	4.42	22.25
12:46 PM	95	7.60	53.39	4.47	22.52
12:48 PM	97	7.70	52.90	4.52	22.79
12:50 PM	99	7.79	53.02	4.57	23.03
12:52 PM	101	7.88	53.13	4.62	23.27
12:54 PM	103	7.98	53.25	4.67	23.54
12:56 PM	105	8.08	53.37	4.73	23.80
12:58 PM	107	8.18	53.49	4.78	24.07
01:00 PM	109	8.28	53.60	4.83	24.34
01:02 PM	111	8.38	53.72	4.89	24.61
01:07 PM	116	8.61	53.84	5.01	25.24
01:11 PM	120	8.79	53.96	5.11	25.72
01:18 PM	127	9.11	54.07	5.28	26.60
01:23 PM	132	9.32	54.19	5.39	27.17
01:26 PM	135	9.46	54.56	5.47	27.55
02:09 PM	178	11.23	54.94	6.44	32.43
02:12 PM	181	11.35	55.31	6.51	32.76
02:18 PM	187	11.61	55.57	6.65	33.49

Notes: substrate = sucrose; MLVSS = 16,546 mg/L; F/M = 0.16.

Table 95. (continued).

Time of Day (hr:min)	Time Elapsed (min)	Cumulative Gas (liters)	Methane (% of total)	Cumulative Methane (liters)	Cumulative Methane (mL/g MLVSS)
02:24 PM	193	11.84	55.82	6.78	34.14
02:28 PM	197	12.00	56.08	6.87	34.59
02:35 PM	204	12.28	56.33	7.02	35.38
02:42 PM	211	12.53	56.59	7.17	36.09
02:52 PM	221	12.92	56.84	7.39	37.20
02:55 PM	224	13.03	57.07	7.45	37.52
03:01 PM	230	13.22	57.31	7.56	38.07
03:12 PM	241	13.61	57.54	7.78	39.19
03:17 PM	246	13.91	57.77	7.96	40.07
03:22 PM	251	14.09	58.00	8.06	40.59
03:35 PM	264	14.51	58.24	8.30	41.82
03:42 PM	271	14.83	58.47	8.49	42.76
03:49 PM	278	15.10	58.87	8.65	43.56
04:01 PM	290	15.50	59.27	8.88	44.75
04:21 PM	310	16.14	59.66	9.27	46.67
04:28 PM	317	16.35	60.06	9.39	47.30
04:41 PM	330	16.72	60.23	9.61	48.42
04:47 PM	336	16.89	60.40	9.72	48.94
04:51 PM	340	17.00	60.57	9.78	49.27

Table 96. SMA test with the GAC-enhanced ASBR, day 113.

Time of Day (hr:min)	Time Elapsed (min)	Cumulative Gas (liters)	Methane (% of total)	Cumulative Methane (liters)	Cumulative Methane (mL/g MLVSS)
02:44 AM	0	0.00	70.35	0.00	0.00
02:46 AM	2	0.24	70.49	0.17	2.15
02:50 AM	6	0.87	70.63	0.61	7.81
02:52 AM	8	1.16	70.77	0.82	10.41
02:54 AM	10	1.26	70.92	0.89	11.32
02:56 AM	12	1.33	71.06	0.94	11.95
02:58 AM	14	1.37	71.20	0.97	12.31
03:00 AM	16	1.43	71.34	1.01	12.85
03:02 AM	18	1.48	71.48	1.05	13.31
03:04 AM	20	1.55	71.45	1.10	13.94
03:06 AM	22	1.61	71.42	1.14	14.49
03:08 AM	24	1.68	71.39	1.19	15.13
03:10 AM	26	1.74	71.36	1.23	15.67
03:12 AM	28	1.80	71.33	1.27	16.22
03:14 AM	30	1.86	71.30	1.32	16.76
03:16 AM	32	1.92	71.30	1.36	17.30
03:18 AM	34	1.98	71.31	1.40	17.85
03:20 AM	36	2.00	71.31	1.42	18.03
03:24 AM	40	2.12	71.32	1.50	19.12
03:26 AM	42	2.17	71.32	1.54	19.57
03:28 AM	44	2.22	71.33	1.57	20.03
03:30 AM	46	2.28	71.33	1.62	20.57
03:32 AM	48	2.34	71.34	1.66	21.12
03:35 AM	51	2.42	71.34	1.72	21.84
03:38 AM	54	2.50	71.13	1.77	22.57
03:42 AM	58	2.60	70.91	1.84	23.47
03:46 AM	62	2.70	70.70	1.92	24.37
03:50 AM	66	2.80	70.48	1.99	25.27
03:52 AM	68	2.89	70.27	2.05	26.07
03:59 AM	75	3.00	70.06	2.13	27.06
04:01 AM	77	3.10	69.84	2.20	27.95
04:04 AM	80	3.19	69.63	2.26	28.75
04:09 AM	85	3.33	69.35	2.36	29.98
04:16 AM	92	3.48	69.06	2.46	31.30
04:20 AM	96	3.59	68.78	2.54	32.27
04:31 AM	107	3.84	68.49	2.71	34.45
04:37 AM	113	3.98	68.14	2.80	35.67
04:39 AM	115	4.03	67.79	2.84	36.10
04:51 AM	127	4.31	67.43	3.03	38.51
04:58 AM	134	4.48	67.08	3.14	39.96
05:04 AM	140	4.64	66.88	3.25	41.33
05:13 AM	149	4.85	66.69	3.39	43.11

Notes: substrate = sucrose; MLVSS = 6550 mg/L; F/M = 0.25.

Table 96. (continued).

Time of Day (hr:min)	Time Elapsed (min)	Cumulative Gas (liters)	Methane (% of total)	Cumulative Methane (liters)	Cumulative Methane (mL/g MLVSS)
05:21 AM	157	4.97	66.49	3.47	44.13
05:30 AM	166	5.29	66.29	3.68	46.83
05:40 AM	176	5.53	66.10	3.84	48.85
05:47 AM	183	5.68	65.90	3.94	50.11
05:53 AM	189	5.81	65.78	4.02	51.20
06:03 AM	199	6.03	65.66	4.17	53.04
06:12 AM	208	6.23	65.54	4.30	54.71
06:23 AM	219	6.43	65.42	4.43	56.38
06:30 AM	226	6.58	65.30	4.53	57.62
06:35 AM	231	6.68	65.35	4.59	58.45
06:41 AM	237	6.78	65.41	4.66	59.29
06:47 AM	243	6.90	65.46	4.74	60.28
06:52 AM	248	6.99	65.51	4.80	61.03
07:02 AM	258	7.16	65.56	4.91	62.45
07:10 AM	266	7.31	65.62	5.01	63.70
07:18 AM	274	7.45	65.67	5.10	64.87
07:25 AM	281	7.58	65.80	5.18	65.96
07:45 AM	301	7.92	65.94	5.41	68.81
08:03 AM	319	8.27	66.07	5.64	71.75
08:16 AM	332	8.53	66.14	5.81	73.93
08:21 AM	337	8.61	66.22	5.86	74.61
08:39 AM	355	8.88	66.29	6.04	76.88
08:49 AM	365	9.03	66.37	6.14	78.15
08:57 AM	373	9.16	66.44	6.23	79.25
09:06 AM	382	9.31	66.52	6.33	80.52
09:15 AM	391	9.43	66.59	6.41	81.53
09:26 AM	402	9.60	66.70	6.52	82.97
09:34 AM	410	9.71	66.80	6.60	83.91
09:43 AM	419	9.85	66.91	6.69	85.10
09:49 AM	425	9.94	67.01	6.75	85.87
09:59 AM	435	10.08	67.12	6.84	87.06
10:03 AM	439	10.13	67.22	6.88	87.49
10:14 AM	450	10.29	67.21	6.98	88.86
10:22 AM	458	10.38	67.20	7.04	89.63

Table 97. SMA test with the GAC-enhanced ASBR, day 135.

Time of Day (hr:min)	Time Elapsed (min)	Cumulative Gas (liters)	Cumulative Methane (% of total)	Cumulative Methane (liters)	Cumulative Methane (mL/g MLVSS)
09:18 AM	0	0.00	63.63	0.00	0.00
09:20 AM	2	0.43	63.68	0.27	4.57
09:22 AM	4	1.00	63.73	0.64	10.64
09:24 AM	6	1.15	63.78	0.73	12.24
09:26 AM	8	1.20	63.83	0.76	12.77
09:28 AM	10	1.22	63.88	0.78	12.99
09:30 AM	12	1.24	63.94	0.79	13.20
09:32 AM	14	1.25	63.99	0.80	13.31
09:34 AM	16	1.25	64.04	0.80	13.31
09:36 AM	18	1.25	64.09	0.80	13.31
09:38 AM	20	1.26	64.14	0.80	13.41
09:40 AM	22	1.26	64.19	0.80	13.41
09:42 AM	24	1.26	64.24	0.80	13.41
09:44 AM	26	1.26	64.29	0.80	13.41
09:46 AM	28	1.26	64.34	0.80	13.41
09:48 AM	30	1.26	64.39	0.80	13.41
09:50 AM	32	1.33	64.45	0.85	14.17
09:52 AM	34	1.35	64.50	0.86	14.38
09:54 AM	36	1.39	64.55	0.89	14.81
09:56 AM	38	1.43	64.60	0.91	15.25
09:58 AM	40	1.45	64.65	0.93	15.46
10:00 AM	42	1.48	64.70	0.94	15.79
10:02 AM	44	1.52	64.75	0.97	16.22
10:04 AM	46	1.57	64.80	1.00	16.76
10:06 AM	48	1.61	64.85	1.03	17.19
10:08 AM	50	1.64	64.90	1.05	17.52
10:10 AM	52	1.68	64.96	1.07	17.95
10:12 AM	54	1.73	65.01	1.11	18.50
10:14 AM	56	1.78	65.06	1.14	19.04
10:17 AM	59	1.85	65.11	1.18	19.80
10:20 AM	62	1.90	65.16	1.22	20.34
10:26 AM	68	2.04	65.21	1.31	21.87
10:30 AM	72	2.14	65.08	1.37	22.96
10:35 AM	77	2.22	64.96	1.43	23.83
10:40 AM	82	2.30	64.83	1.48	24.69
10:45 AM	87	2.39	65.04	1.54	25.67
10:50 AM	92	2.47	65.26	1.59	26.54
10:55 AM	97	2.55	65.47	1.64	27.42
11:00 AM	102	2.62	65.68	1.69	28.18
11:05 AM	107	2.72	65.89	1.75	29.28
11:10 AM	112	2.80	66.11	1.81	30.16

Notes: substrate = sucrose; MLVSS = 4,987 mg/L; F/M = 0.22.

Table 97. (continued).

Time of Day (hr:min)	Time Elapsed (min)	Cumulative Gas (liters)	Cumulative Methane (% of total)	Cumulative Methane (liters)	Cumulative Methane (mL/g MLVSS)
11:13 AM	115	2.85	66.32	1.84	30.72
11:20 AM	122	2.98	66.53	1.92	32.16
11:29 AM	131	3.15	66.75	2.04	34.05
11:35 AM	137	3.26	66.96	2.14	35.50
11:43 AM	145	3.41	66.32	2.21	36.94
11:51 AM	153	3.58	65.69	2.32	38.82
12:08 PM	170	3.87	65.05	2.51	41.99
12:14 PM	176	3.96	64.41	2.57	42.96
12:29 PM	191	4.24	64.88	2.75	45.99
12:38 PM	200	4.39	65.36	2.85	47.62
12:52 PM	214	4.60	65.83	2.99	49.92
01:07 PM	229	4.80	66.31	3.12	52.13
01:11 PM	233	4.87	66.78	3.17	52.91
01:45 PM	267	5.40	66.47	3.52	58.81
02:06 PM	288	5.73	66.16	3.74	62.46
02:49 PM	331	6.27	66.45	4.10	68.45
02:58 PM	340	6.43	67.83	4.20	70.24
03:14 PM	356	6.68	67.73	4.37	73.07
03:20 PM	362	6.77	67.63	4.43	74.09
03:40 PM	382	7.05	67.59	4.62	77.25
03:45 PM	387	7.11	67.54	4.66	77.93
04:05 PM	407	7.38	67.82	4.85	80.98
04:11 PM	413	7.45	68.09	4.89	81.78
04:18 PM	420	7.54	68.09	4.96	82.80

Table 98. SMA test with the GAC-enhanced ASBR, day 190.

Time of Day (hr:min)	Time Elapsed (min)	Cumulative Gas (liters)	Cumulative Methane (% of total)	Cumulative Methane (liters)	Cumulative Methane (mL/g MLVSS)
01:46 PM	0	0.00	63.94	0.00	0.00
01:48 PM	2	0.00	64.01	0.00	0.00
01:53 PM	7	1.19	64.09	0.76	5.89
01:56 PM	10	1.25	64.16	0.80	6.19
02:00 PM	14	1.25	64.24	0.80	6.19
02:02 PM	16	1.26	64.31	0.81	6.24
02:04 PM	18	1.33	64.38	0.85	6.59
02:06 PM	20	1.41	64.46	0.90	6.99
02:08 PM	22	1.50	64.53	0.96	7.44
02:10 PM	24	1.58	64.58	1.01	7.84
02:13 PM	27	1.69	64.62	1.08	8.39
02:18 PM	32	1.91	64.67	1.23	9.49
02:22 PM	36	2.05	64.71	1.32	10.19
02:25 PM	39	2.16	64.76	1.39	10.74
02:29 PM	43	2.31	64.80	1.49	11.49
02:34 PM	48	2.51	64.47	1.61	12.49
02:42 PM	56	2.83	64.15	1.82	14.08
02:49 PM	63	3.09	63.82	1.99	15.37
02:55 PM	69	3.28	64.14	2.11	16.31
02:59 PM	73	3.42	64.46	2.20	17.00
03:04 PM	78	3.59	64.79	2.31	17.85
03:11 PM	85	3.81	65.11	2.45	18.96
03:19 PM	93	4.05	65.43	2.61	20.17
03:30 PM	104	4.39	64.86	2.83	21.88
03:33 PM	107	4.47	64.29	2.88	22.28
03:51 PM	125	4.94	63.72	3.18	24.61
03:54 PM	128	5.01	63.51	3.23	24.95
03:56 PM	130	5.06	63.31	3.26	25.20
04:06 PM	140	5.35	63.10	3.44	26.62
04:15 PM	149	5.60	62.90	3.60	27.83
04:22 PM	156	5.79	62.69	3.72	28.76
04:34 PM	168	5.98	62.49	3.84	29.68
04:49 PM	183	6.19	62.29	3.97	30.69
05:03 PM	197	6.50	62.12	4.16	32.18
05:19 PM	213	6.87	61.95	4.39	33.96
05:26 PM	220	7.01	61.78	4.48	34.63
05:34 PM	228	7.20	61.61	4.59	35.53
05:39 PM	233	7.32	61.58	4.67	36.10
05:47 PM	241	7.48	61.56	4.77	36.87
05:49 PM	243	7.52	61.53	4.79	37.06
05:55 PM	249	7.64	61.51	4.87	37.63
05:58 PM	252	7.70	61.48	4.90	37.91

Notes: substrate = sucrose; MLVSS = 10,775 mg/L; F/M = 0.22.

Table 98. (continued).

Time of Day (hr:min)	Time Elapsed (min)	Cumulative Gas (liters)	Methane (% of total)	Cumulative Methane (liters)	Cumulative Methane (mL/g MLVSS)
06:02 PM	256	7.77	61.45	4.95	38.25
06:10 PM	264	7.96	61.43	5.06	39.15
06:28 PM	282	8.34	61.40	5.30	40.95
06:45 PM	299	8.71	61.39	5.52	42.71
07:16 PM	330	9.31	61.37	5.89	45.56
07:23 PM	337	9.39	61.36	5.94	45.94
07:34 PM	348	9.53	61.57	6.03	46.60
07:44 PM	358	9.69	61.78	6.12	47.37
07:49 PM	363	9.75	61.99	6.16	47.65
07:57 PM	371	9.87	62.20	6.24	48.23

Table 99. SMA test with the GAC-enhanced ASBR, day 195.

Time of Day (hr:min)	Time Elapsed (min)	Cumulative Gas (liters)	Cumulative Methane (% of total)	Cumulative Methane (liters)	Cumulative Methane (mL/g MLVSS)
05:03 AM	0	0.00	66.98	0.00	0.00
05:05 AM	2	0.00	67.67	0.00	0.00
05:07 AM	4	0.10	68.37	0.07	0.67
05:09 AM	6	0.10	69.06	0.07	0.67
05:13 AM	10	0.11	69.75	0.07	0.73
05:15 AM	12	0.12	70.45	0.08	0.80
05:17 AM	14	0.12	71.14	0.08	0.80
05:19 AM	16	0.13	70.74	0.09	0.87
05:21 AM	18	0.15	70.33	0.10	1.01
05:23 AM	20	0.17	69.93	0.12	1.15
05:25 AM	22	0.19	69.53	0.13	1.29
05:30 AM	27	0.22	69.13	0.15	1.49
05:35 AM	32	0.30	68.72	0.21	2.03
05:39 AM	36	0.33	68.32	0.23	2.23
05:41 AM	38	0.35	67.60	0.24	2.37
05:45 AM	42	0.39	66.88	0.27	2.63
05:49 AM	46	0.44	66.17	0.30	2.95
06:02 AM	59	0.51	65.45	0.35	3.41
06:10 AM	67	0.51	64.73	0.35	3.41
06:28 AM	85	0.52	64.01	0.35	3.47
06:39 AM	96	0.70	63.30	0.47	4.59
06:49 AM	106	0.80	62.58	0.53	5.21
06:53 AM	110	0.84	61.86	0.56	5.45
07:01 AM	118	1.91	59.56	1.21	11.82
07:03 AM	120	2.08	57.26	1.31	12.80
07:05 AM	122	2.22	54.96	1.38	13.57
07:08 AM	125	2.49	52.66	1.53	14.99
07:10 AM	127	2.60	50.36	1.59	15.55
07:13 AM	130	2.70	49.36	1.64	16.03
07:18 AM	135	2.83	48.37	1.70	16.66
08:01 AM	178	3.51	47.37	2.02	19.85
08:11 AM	188	3.82	46.27	2.17	21.27
08:15 AM	192	4.30	45.17	2.39	23.42
08:23 AM	200	4.87	44.07	2.64	25.92
08:29 AM	206	5.11	42.98	2.75	26.94
08:33 AM	210	5.22	41.88	2.79	27.40
08:36 AM	213	5.40	40.78	2.87	28.13
08:39 AM	216	5.48	39.68	2.90	28.44
08:45 AM	222	5.56	39.26	2.93	28.75
08:52 AM	229	5.67	38.84	2.98	29.17
09:05 AM	242	5.88	38.42	3.06	29.97

Notes: substrate = acetate; MLVSS = 8,500 mg/L; F/M = 0.15.

Table 99. (continued).

Time of Day (hr:min)	Time Elapsed (min)	Cumulative Gas (liters)	Methane (% of total)	Cumulative Methane (liters)	Cumulative Methane (mL/g MLVSS)
09:10 AM	247	6.00	38.00	3.10	30.42
09:21 AM	258	6.16	38.00	3.16	31.02
09:25 AM	262	6.22	38.00	3.19	31.24
09:37 AM	274	6.41	38.00	3.26	31.95
09:42 AM	279	6.52	38.00	3.30	32.36
09:45 AM	282	6.60	38.00	3.33	32.65
09:48 AM	285	6.60	38.00	3.33	32.65
09:55 AM	292	6.70	38.00	3.37	33.03

Table 100. SMA test with the garnet-enhanced ASBR, day 83.

Time of Day (hr:min)	Time Elapsed (min)	Cumulative Gas (liters)	Cumulative Methane (% of total)	Cumulative Methane (liters)	Cumulative Methane (mL/g MLVSS)
02:44 AM	0	0.00	63.65	0.00	0.00
02:46 AM	2	0.00	63.22	0.00	0.00
02:50 AM	6	0.00	62.78	0.00	0.00
02:52 AM	8	0.00	62.34	0.00	0.00
02:54 AM	10	0.00	61.91	0.00	0.00
02:56 AM	12	0.00	61.47	0.00	0.00
02:58 AM	14	0.24	61.04	0.15	1.70
03:00 AM	16	0.25	60.60	0.15	1.77
03:02 AM	18	0.32	60.17	0.20	2.26
03:04 AM	20	0.40	60.39	0.24	2.82
03:06 AM	22	0.48	60.60	0.29	3.38
03:08 AM	24	0.58	60.82	0.35	4.08
03:10 AM	26	0.67	61.03	0.41	4.72
03:12 AM	28	0.75	61.25	0.46	5.28
03:14 AM	30	0.81	61.46	0.49	5.71
03:16 AM	32	0.86	61.65	0.52	6.07
03:18 AM	34	0.92	61.84	0.56	6.49
03:20 AM	36	0.97	62.03	0.59	6.85
03:24 AM	40	1.06	62.22	0.65	7.50
03:26 AM	42	1.11	62.40	0.68	7.86
03:28 AM	44	1.15	62.59	0.70	8.15
03:30 AM	46	1.19	62.78	0.73	8.44
03:32 AM	48	1.23	62.97	0.75	8.73
03:35 AM	51	1.28	63.16	0.79	9.10
03:38 AM	54	1.34	63.11	0.82	9.53
03:42 AM	58	1.42	63.06	0.87	10.12
03:46 AM	62	1.49	63.01	0.92	10.63
03:50 AM	66	1.56	62.96	0.96	11.14
03:52 AM	68	1.62	62.91	1.00	11.58
03:59 AM	75	1.71	62.86	1.06	12.23
04:01 AM	77	1.75	62.81	1.08	12.52
04:04 AM	80	1.84	62.76	1.14	13.18
04:09 AM	85	1.93	62.69	1.19	13.83
04:16 AM	92	2.00	62.63	1.24	14.34
04:20 AM	96	2.04	62.56	1.26	14.63
04:31 AM	107	2.13	62.49	1.32	15.28
04:37 AM	113	2.18	62.51	1.35	15.64
04:39 AM	115	2.20	62.54	1.36	15.78
04:51 AM	127	2.31	62.56	1.43	16.58
04:58 AM	134	2.38	62.58	1.48	17.09
05:04 AM	140	2.44	62.41	1.51	17.52
05:13 AM	149	2.53	62.23	1.57	18.17

Notes: substrate = sucrose; MLVSS = 7200 mg/L; F/M = 0.25.

Table 100. (continued).

Time of Day (hr:min)	Time Elapsed (min)	Cumulative Gas (liters)	Methane (% of total)	Cumulative Methane (liters)	Cumulative Methane (mL/g MLVSS)
05:21 AM	157	2.61	62.06	1.62	18.75
05:30 AM	166	2.71	61.88	1.68	19.46
05:40 AM	176	2.79	61.71	1.73	20.04
05:47 AM	183	2.85	61.53	1.77	20.46
05:53 AM	189	2.91	61.30	1.80	20.89
06:03 AM	199	3.00	61.07	1.86	21.53
06:12 AM	208	3.08	60.83	1.91	22.09
06:23 AM	219	3.18	60.60	1.97	22.79
06:30 AM	226	3.26	60.37	2.02	23.35
06:35 AM	231	3.32	60.43	2.05	23.77
06:41 AM	237	3.37	60.49	2.08	24.12
06:47 AM	243	3.41	60.55	2.11	24.40
06:52 AM	248	3.44	60.60	2.13	24.61
07:02 AM	258	3.52	60.66	2.18	25.18
07:10 AM	266	3.58	60.72	2.21	25.60
07:18 AM	274	3.65	60.78	2.25	26.09
07:25 AM	281	3.71	60.30	2.29	26.51
07:45 AM	301	3.87	59.83	2.39	27.62
08:03 AM	319	4.07	59.35	2.51	29.00
08:16 AM	332	4.18	59.32	2.57	29.76
08:21 AM	337	4.21	59.28	2.59	29.96
08:39 AM	355	4.33	59.25	2.66	30.79
08:49 AM	365	4.41	59.22	2.71	31.33
08:57 AM	373	4.47	59.19	2.74	31.75
09:06 AM	382	4.54	59.15	2.78	32.23
09:15 AM	391	4.61	59.12	2.83	32.70
09:26 AM	402	4.70	59.03	2.88	33.32
09:34 AM	410	4.77	58.94	2.92	33.80
09:43 AM	419	4.84	58.84	2.96	34.27
09:49 AM	425	4.88	58.75	2.98	34.55
09:59 AM	435	4.96	58.66	3.03	35.09
10:03 AM	439	4.99	58.57	3.05	35.29
10:14 AM	450	5.07	58.72	3.10	35.84
10:22 AM	458	5.11	58.87	3.12	36.11